Resource Adequacy, Risk, and Resilience in Low-Carbon Energy System Planning: *Methods, Tools, and Metrics*

FINAL REPORT

Prepared for CSIRO under the Australian Research in Power Systems Transition (AR-PST)

Tim Kopka, Muhammad Yasirroni, Pablo Apablaza, Bastian Moya, Sleiman Mhanna, Pierluigi Mancarella

The University of Melbourne

June 2026

Acknowledgements

This research has been conducted under the Australian Research in Power Systems Transition (AR-PST) initiative. The authors gratefully acknowledge the funding and support from the Commonwealth Scientific and Industrial Research Organisation (CSIRO) and the continuous feedback from AEMO and CSIRO. We kindly thank Leon Kwek (AEMO), Dean Sharafi (AEMO), Biswajit Bala (CSIRO), Thomas Brinsmead (CSIRO), Ghulam Mohy-ud-din (CSIRO), John Ward (CSIRO), Yunqi Wang (CSIRO), Liam Landman (GHD), and Christian Schaefer (GHD) for their valuable support and feedback during the development of this project.

Executive Summary

As the supply side of Australian power systems becomes more weather-dependent and energy-constrained due to the growing integration of variable renewable energy (VRE) and energy-limited resources (ELR), current resource adequacy (RA) frameworks risk becoming unfit for purpose. This is partly due to their reliance on deterministic parameters, average-focused metrics, and simplified operational representations of system components that are becoming increasingly dominant, such as energy storage systems (ESS) and distributed energy resources (DER).

Simultaneously, reliability risks are becoming increasingly concentrated in infrequent yet high-impact weather-related events, rather than in isolated component failures under normal conditions. Growing exposure to extreme weather, such as heatwaves and thunderstorms, increases the likelihood of common-mode failures, thereby requiring a fundamental transformation in the methodologies used to evaluate adequacy and resilience.

Advancing RA frameworks in this context requires a clear understanding of the limitations inherent in current assumptions and methodologies, followed by targeted enhancements that, for example, reflect the constraints and operational decisions of ELR and elucidate the impact of weather on the system operation. In line with the CSIRO–AR-PST roadmap, this project addresses these pressing research needs through three primary pillars: the development of an open-source reliability assessment toolkit, the establishment of realistic modelling guidelines for ELR, and the definition of systematic practices for designing scenarios to evaluate system resilience. These developments are supported by extensive evidence, in particular a range of case studies conducted within the Australian East Coast Power System / National Electricity Market (NEM).

This research in Stage 5 of the *Power System Planning* topic for the Australian Research in Power Systems Transition (AR-PST) initiative was centred around five complementary tasks, as shown in Figure 0.1, with key findings and planning implications synthesised in Table 0.1. Following this, a comprehensive summary of the main findings for each task is provided.

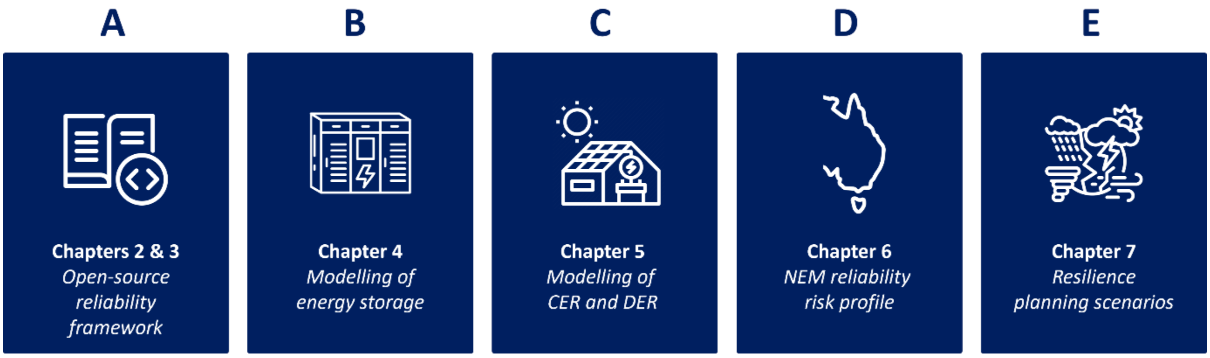

Figure 0.1: Overview of research tasks A - E of Stage 5 of the Power System Planning research of the AR-PST initiative and corresponding chapters in this report.

Table 0.1: Overview of key findings, relevant tasks and chapters, corresponding figures and tables, as well as planning implications.

<table>
<tr><th>Key findings</th><th>Tasks</th><th>Chapters</th><th>Key figures and tables</th><th>Planning implications</th></tr>
<tr><td>Reliability levels of the NEM become sensitive to storage operation approximations post-2030, and assumptions about state of charge, charging behaviour, and dispatch incentives materially change the estimated reliability risk.</td><td>B, D</td><td>4, 6</td><td>Figure 4.7
Figure 4.8</td><td rowspan="2">Storage operation uncertainty (i.e. lack of knowledge of storage operation behaviour in the future) should be explicitly represented in adequacy studies. This may be achieved by assessing adequacy across multiple approximations. Furthermore, operational measures to influence storage behaviour should be considered for ensuring adequacy in the future NEM.</td></tr>
<tr><td>Storage operation assumptions impact the distribution, timing, and drivers of reliability events. This sensitivity of adequacy outcomes to storage operation indicates opportunity for operational measures to ensure reliability.</td><td>B, D</td><td>4, 6</td><td>Figure 4.9
Figure 6.5
Figure 6.9</td></tr>
<tr><td>DER coordination, even at lower compliance levels, may be fundamental for ensuring reliability in the NEM, particularly after 2030.</td><td>C, D, E</td><td>5, 6, 7</td><td>Figure 5.6
Figure 6.6
Figure 7.17
Figure 7.19</td><td rowspan="2">The National CER roadmap [1] and related initiatives should support the effective implementation of enhanced DER coordination to maximise the visibility and controllability of customer energy resources. Universal consumer participation may not necessarily be required to realise system-level reliability improvements.</td></tr>
<tr><td>Demand side participation (DSP) may provide valuable hedging against storage operation uncertainty. DSP can defer storage depletion, support critical periods, and reduce the spread of resource adequacy estimates under storage operation assumptions.</td><td>C</td><td>5</td><td>Figure 5.10</td></tr>
<tr><td>While average resource adequacy levels may remain acceptable for the NEM under the 2024 Integrated System Plan (ISP) Optimal Development Path, there are specific weather years, outage combinations, and operational behaviours that can produce materially higher risks, highlighting the importance of an extended and tail-focused resource adequacy assessment.</td><td>D</td><td>6</td><td>Figure 6.3
Figure 6.5</td><td rowspan="2">Multi-metric reliability risk frameworks should become standard practice. Complementing average with tail risk metrics such as Conditional Value at Risk (CvaR) may prove valuable in capturing the full risk profile. This can help to identify necessary measures to prepare the system against average as well as tail risk events (e.g. through evaluating investments explicitly against their reduction in CVaR), to ensure reliability in a weather-dependent, energy-limited future NEM.</td></tr>
<tr><td>After increased shutdown of thermal generation post-2030, reliability risks increasingly arise from low renewable availability and storage depletion events, rather than from peak demand periods alone. In particular, load shedding events can become longer, larger, and harder to anticipate with traditional peak load-only resource adequacy approaches.</td><td>D</td><td>6</td><td>Figure 6.5
Figure 6.7
Figure 6.8</td></tr>
<tr><td>Historical extreme events in the NEM have been reviewed to identify multiple risk driver classes, including heatwaves, windstorms, hailstorms, and flash floods.</td><td>E</td><td>7</td><td>Table 7.2</td><td rowspan="3">Weather-driven resilience events should be assessed in tandem with traditional adequacy studies, as their impacts may pose large risk in a highly weather-dependent power system. The resilience-scenario workflow developed in this work may provide guidelines to translate hazard drivers into modelling parameters affecting generation, storage, transmission, and renewable availability.</td></tr>
<tr><td>Heatwave events may present primarily as a capacity constraint rather than a long-duration energy drought problem, suggesting that increased system flexibility through storage and demand response may serve as an effective resilience measure.</td><td>E</td><td>7</td><td>Figure 7.15Figure 7.14
Figure 7.17</td></tr>
<tr><td>Extended VRE droughts may be particularly sensitive to storage operation approximations, however increased levels of demand response may reduce uncertainty.</td><td>E</td><td>7</td><td>Figure 7.18
Figure 7.19</td></tr>
</table>

Open-source toolkit and datasets for assessing reliability and resilience

Task A developed an open-source modelling and data-parsing toolkit to assess resource adequacy, operability, and resilience in a future NEM dominated by weather-dependent and energy-limited resources. The central contribution of this task is a transparent, reproducible set of modelling packages that enables researchers, industry stakeholders, and practitioners to conduct extensive reliability and resilience studies in the NEM.

The toolkit converts public ISP and *Inputs, Assumptions, and Scenarios Report* (IASR) data into structured models of the Australian east-coast power system for planning studies. It supports both probabilistic adequacy assessments and more detailed operational analysis, allowing testing of different modelling assumptions. The open-source toolkit is built around four complementary packages and an integrated repository that orchestrates their use. Figure 0.2 presents the overarching architecture of the developed modelling suite.

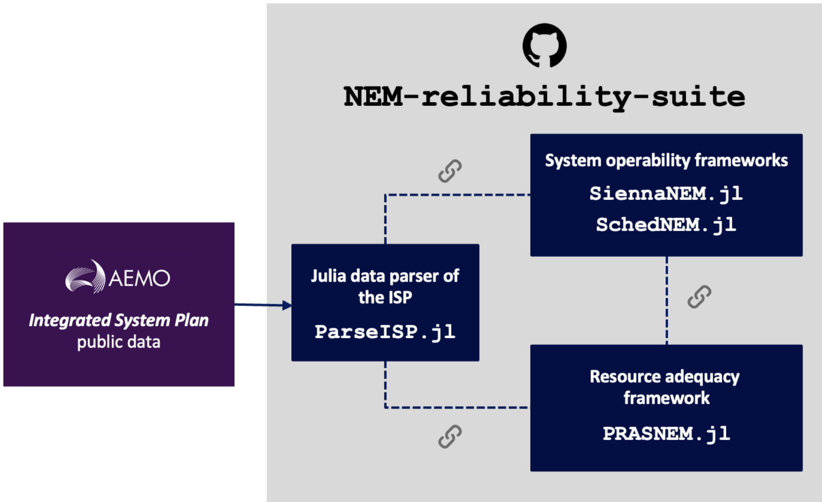

Figure 0.2: General overview of the NEM reliability suite architecture.

ParseISP.jl provides the data-parsing layer. It extracts and structures ISP and IASR data into datasets suitable for planning and reliability modelling, including conventional and renewable generation, storage, transmission, DER, demand, and hydro inflows.

PRASNEM.jl provides the probabilistic resource adequacy layer. It uses the Probabilistic Resource Adequacy Suite (PRAS) simulation engine to perform sequential Monte Carlo simulations of infrastructure outages. This enables efficient creation and evaluation of a large set of outage and weather combinations, from which probabilistic resource adequacy metrics, such as unserved energy and event-level statistics, can be derived.

SiennaNEM.jl provides a more detailed production-cost and operational modelling layer. It supports economic dispatch and unit commitment formulations, with operational constraints such as ramping, minimum up/down times, renewable curtailment, storage operation, and network transfer limits.

SchedNEM.jl, as an alternative to SiennaNEM.jl, provides a lightweight, flexible, and faster operational system scheduling framework. It is designed to bridge the gap between large-scale adequacy runs and detailed operational representation. It provides a rolling-horizon dispatch that considers energy storage constraints and limited foresight, demand response, and inter-temporal component scheduling, making it particularly useful for testing storage and DER behaviour under different assumptions.

Time-sequential resource adequacy assessment with storage and operability considerations

Task B studies how the operation and representation of storage facilities impact resource adequacy assessments as storage becomes increasingly widespread and a relevant contributor to system reliability. Unlike conventional firm generation, storage systems cannot contribute to resource adequacy purely through their installed capacity. Their contribution depends on whether sufficient energy is available during critical periods, whether they have been charged in advance, how they respond to different market signals, and the degree of operator foresight and risk aversion regarding future system conditions.

This makes storage operation a critical modelling assumption for modern power systems and an emerging risk factor for future resource adequacy studies. If storage is assumed to preserve energy for reliability events or high demand periods, it may appear to provide substantial firming value. However, if the same resource is operated according to economic principles under limited foresight, it might begin critical operating periods with a lower-than-expected state of charge, potentially contributing less to reliability.

To assess such uncertainty, Task B develops a storage modelling framework that enables the comparison of approximations to storage operations. In this task, three assumptions are considered: A1, ‘high energy’ operation (i.e., a state of charge reserved for peak load periods); A2, ‘derated energy’ operation; and A3, ‘economic’ operation. These cases emulate a spectrum of plausible storage behaviours: ‘High energy’ represents a simplified storage operation under reliability obligations, potentially through capacity market accreditation, thereby representing an adequacy-optimistic dispatch. ‘Derated energy’ includes AEMO’s principles taken in reliability studies of the NEM, which balances the optimistic simplified dispatch with reduced energy capacity levels. ‘Economic operation’ simulates storage behaviour based on energy arbitrage, a commercially driven operation with no capacity obligation. Importantly, all these approaches remain approximations of the actual realised operation, as real operation is shaped by heterogeneous actors and may be driven by various other factors (such as different levels of risk-aversion, or financial contracts and obligations).

The first key finding in this task is that storage operation assumptions become increasingly relevant as storage emerges as a dominant part of the resource mix. Before 2030, as shown in Figure 0.3, the differing assumptions between storage modelling approximations have a relatively limited effect on resource adequacy metrics (the expected value and the 95%-CVaR of the unserved energy, respectively). After 2030, as thermal capacity retires and storage systems make up a larger share of the capacity mix, such an extended range of assumptions could begin to materially affect reliability studies.

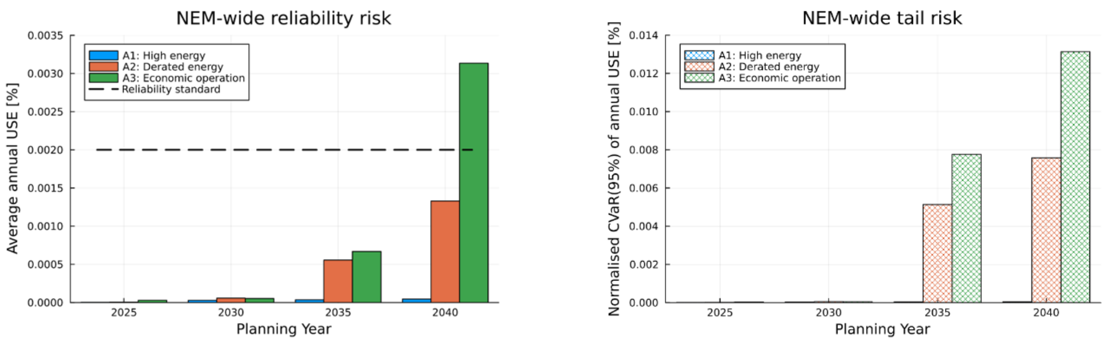

(a) Average annual unserved energy

(b) Average annual unserved energy of 5% worst-case events

Figure 0.3: NEM reliability risk profile (USE, CVaR$_{95\%}$) under storage modelling approximations (note the different scales)

As a consequence, differing approximations about storage operations might underestimate reliability risks. For example, under the high energy (high state-of-charge) assumption, storage is kept as full as possible and discharged primarily during peak-demand periods to avoid unserved energy, resulting in low USE levels. Under the derated energy modelling assumption, reliability risk increases but remains limited and within the standard. Under an economically driven operation, however, the expected unserved energy rises materially after 2030 and could exceed the reliability standard in later years under the assumptions of the study.

Moreover, storage operations could affect not only the average level of unserved energy but also influence the longer tail of the reliability risk distribution. For example, a subset of storage assumptions yields shortfall events of smaller magnitude and potentially more manageable. An economically driven operation produces a more dispersed distribution with more pronounced tails, as shown in Figure 0.3(b). This indicates that planning decisions based only on average USE may overlook important changes in the severity and variability of reliability risk.

Overall, these results highlight a direct link between reliability planning assumptions and operations that are closer to real-time. If reliability planning studies assume an adequacy-oriented storage behaviour, but market incentives lead storage to discharge earlier or later, or to maintain lower states of charge, a system dominated by storage may require more frequent operational interventions than expected at the planning stage. Conversely, if storage is expected to provide reliability support, market design, reliability obligations, capacity mechanisms, or operational tools may be needed to align storage behaviour with resource adequacy needs.

Regarding the modelling choice, the findings of this task (and confirmed by the following tasks) underscore that operational representation in reliability planning should be carefully handled. Models that simplify storage behaviour in a way that may not be reflected in real operation (e.g. the 'high energy' approximation in an energy-only market setting such as the NEM), may be especially unfit to capture the actual underlying risk. While the 'economic operation' approximation of this report is our best approach and suggestion for representing system operation at this stage, further work is needed to benchmark and compare modelling assumptions. Utilising multiple operational approximations may be the most suited approach to capture adequacy risk in planning models.

As a complementary result, Figure 0.4 presents the full probability distribution of reliability events with material impacts on unserved energy. For instance, under the 'derated energy' approximation, the risk distribution is concentrated around lower-magnitude events, suggesting a limited impact on system reliability. In contrast, the 'economic' operation approximation exhibits a more dispersed distribution with a longer tail, indicating a greater likelihood of reliability events with higher magnitude.

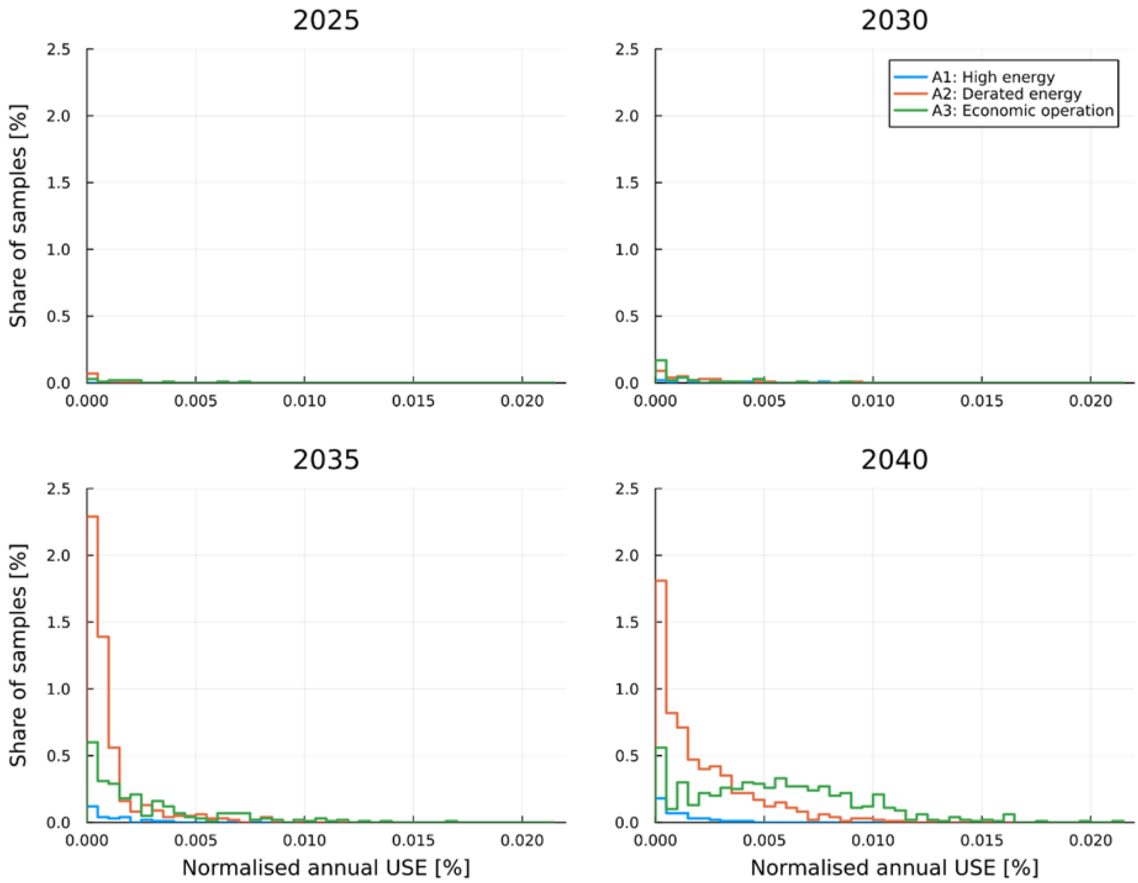

Figure 0.4 Distribution of annual USE per sample across the different underlying planning years, as well as storage operation assumptions.

Overall, the analysis of the full distribution shows that assumptions about storage operations at the planning stage can materially reshape the reliability risk profile. In particular, assumptions that storage behaviour can be represented as a highly "predictable" asset by single-model approximations become increasingly difficult to justify as storage penetration rises. This issue is further amplified as, in practice, storage operators increasingly rely on automated bidding algorithms, *"autobidders"*, which follow specific commercial principles, making storage behaviour more dispersed, revenue-oriented, and difficult to anticipate from a system adequacy perspective.

Therefore, these results suggest that future resource adequacy studies in storage-rich systems should explicitly account for **uncertainty in storage behaviour**. This dimension, as shown in Figure 0.5, should be considered alongside established sources of uncertainty, such as stochastic generation and transmission infrastructure outages, as well as weather-driven variability in load and renewable generation.

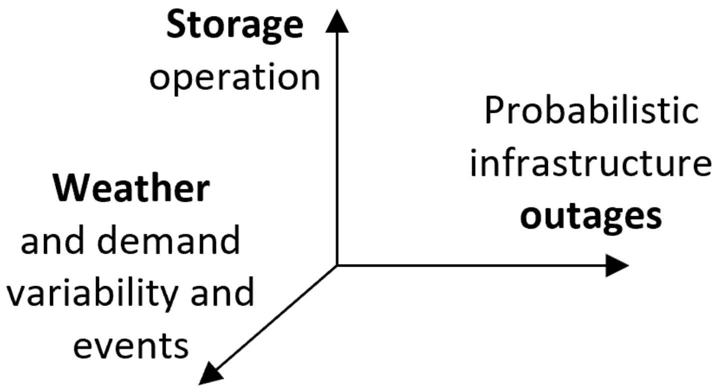

Figure 0.5: Stylised representation of dimensions of fundamental uncertainties for adequacy assessments in weather-dependent systems dominated by storage.

Benefits, opportunities, and risks associated with CER and DER for resource adequacy

Task C assessed how consumer energy resources (CER) and distributed energy resources (DER) could contribute to resource adequacy in a future NEM in which these assets constitute a significant share of the resource mix. This task advanced understanding of the opportunities, benefits, and risks associated with DER for resource adequacy, as well as the modelling choices needed to realistically study their contribution. The focus is on DER with material relevance at the system-operation level, including rooftop PV, electric vehicles (EV), distributed storage aggregated through virtual power plants (VPPs), and demand-side participation.

This analysis is motivated by a central planning challenge: as the NEM transitions toward higher shares of VRE, storage, and DER, resource adequacy will increasingly depend not only on installed capacity, but also on whether flexible resources are visible, coordinated, available, and operationally aligned with system needs. DER can provide a material reliability contribution, but it depends on the type of technology, location, energy availability, consumer willingness to participate, network constraints, and the extent to which resources can be coordinated and respond during critical periods.

The work first reviewed the contribution mechanisms of different DER classes, summarised as follows:

- **Distributed generation**, especially rooftop PV, can reduce net demand, but its contribution to resource adequacy is weather-dependent and may be limited during critical periods with low solar availability. In addition, distributed generation can present operational risks if units disconnect unexpectedly during voltage or frequency disturbances.
- **Distributed storage** can provide support to resource adequacy by shifting energy, but its value depends strongly on whether it is operated independently for local purposes or coordinated through aggregators or VPPs.
- **Demand flexibility**, including EV charging reduction, load shifting, and demand-side participation, can help in reducing system stress during periods of peak load, but its contribution highly depends on consumer willingness to participate

A key insight from the literature is that *DER observability* and *controllability* (broadly grouped as *coordination*) are fundamental to unlocking the value of DER for resource adequacy. Without these features, DER may contribute to local supply or support peak load shaving but may not necessarily respond during critical periods with a system-level contribution. As power systems transition toward being VRE-dominated, reliability incidents may not always coincide with traditional peak demand; instead, they may occur during combinations of high demand, low renewable availability, outages, and depleted storage. Consequently, DER must receive appropriate operational signals, whether through markets, aggregators, reliability mechanisms, or operational instructions, to provide support when the system is under stress.

The review of modelling practices found no broad consensus on how DER are represented in adequacy assessments. System operators worldwide use a range of methods. Some implicitly incorporate DER into demand traces; some model demand response as supply-side capacity; and others explicitly represent flexible technologies such as EVs, heat pumps, distributed batteries, and industrial demand response, with operational constraints.

Building on this review, the work under this task developed a DER modelling framework aligned with AEMO data availability and the broader adequacy workflow developed in the project. The main modelling developed is characterised as follows.

- **Rooftop PV** is represented by generation profiles, with network effects already reflected in traces collected from AEMO's publicly available data. The aggregated traces are explicitly represented and included across all cases.
- **EV flexibility** is modelled as time-varying load, with charging profiles sourced from the ISP as an upper bound. Uncontrolled EV charging is included in the base load, and EV flexibility is explicitly enabled in the sensitivity studies, by allowing reduction of EV load of either 25% or 50% of the EV charging demand to capture low- and high-compliance scenarios.
- **VPPs** are represented as aggregated embedded storage at a subregional granularity and explicitly added to the supply-side system with 50% and 100% capacity, representing different levels of VPP coordination.
- **Demand-side participation** (demand response) was modelled as a constant, price-responsive load-reduction capacity across differentiated price bands, and added with either 50% and 100% capacity compliance, and a daily energy limit on the reliability response to avoid unrealistic behaviour.

This modelling enabled the case studies in this task to test how different DER technologies and coordination levels affect both average reliability outcomes and exposure to tail risks.

The case study assessed the resource adequacy of the NEM between 2025 and 2040 under the resource buildout for the 2024 ISP *Step Change* scenario. Specific operational conditions were selected to test adequacy under different weather and demand scenarios, including a low renewable availability year with high demand. The *supply-side-only* case included utility-scale resources, interconnectors, and rooftop PV, assuming fixed EV charging, no VPP units and no demand-side participation. DER coordination options (EV flexibility, added VPP storage, or enabled DSP) were then introduced individually and in combination to evaluate their incremental contribution to adequacy.

The results show that **supply-side resources alone may be insufficient to maintain adequacy in later planning years,** particularly after 2030, as thermal capacity retires and the system becomes increasingly dependent on VRE and storage. As shown in Figure 0.6, average unserved energy increases strongly across the planning horizon, while the tail risk in the worst 5% of cases rises even more sharply. This indicates that adequacy risk is not only increasing on average, but also becoming more concentrated in severe outage and low-renewable-availability conditions.

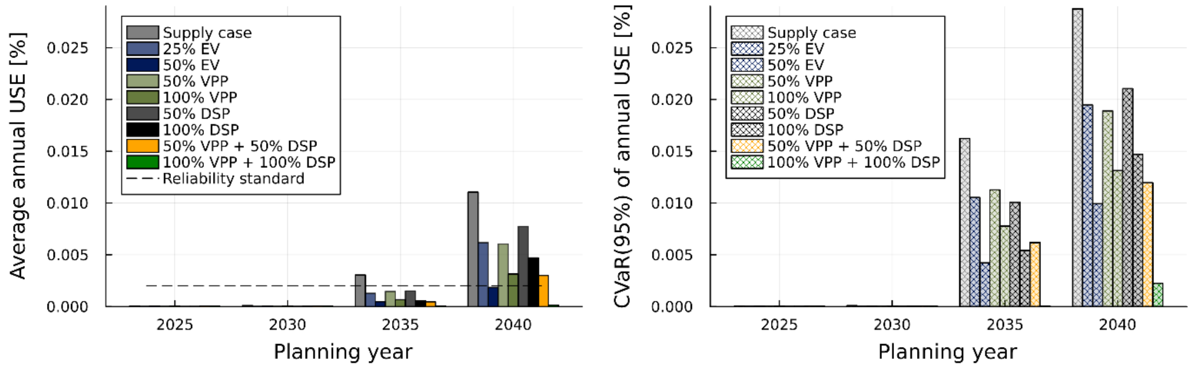

Figure 0.6: NEM-wide average risk (left) and tail risk (right) results of the supply-only-case compared to different DER coordination scenarios across the planning years.

Across all the different DER coordination cases, demand-side flexibility materially reduces both average and tail adequacy risk, with the largest benefits emerging in the post-2030 period. The relative changes shown in Figure 0.7 highlight that EV flexibility, VPP coordination, and DSP can all contribute meaningfully, even when consumer participation or compliance is partial. A key takeaway is that **even modest levels of flexible DER in the NEM may deliver substantial reliability value**, suggesting that full coordination of all DER is not necessarily required for system-level adequacy benefits to emerge.

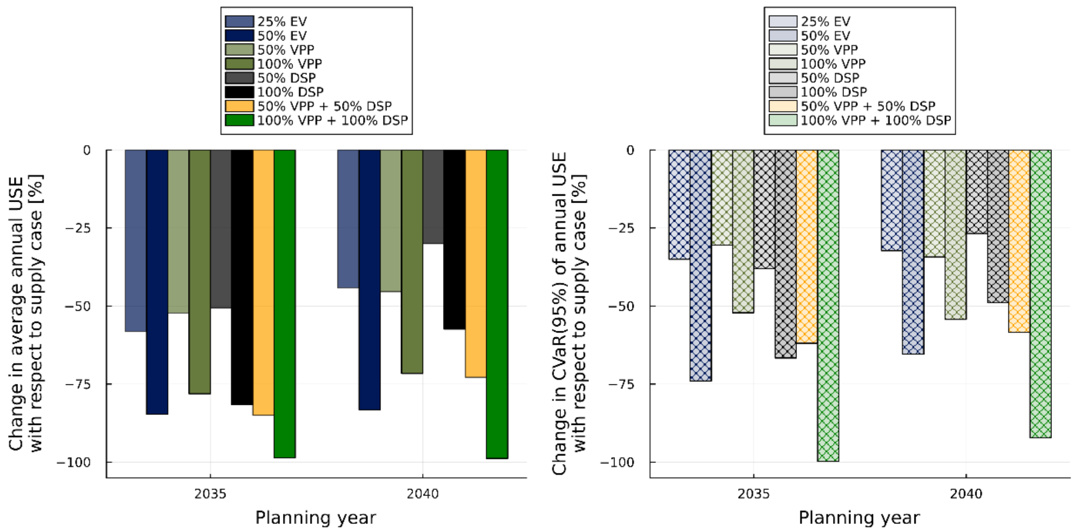

Figure 0.7: Relative change in adequacy metrics values with added demand flexibility for the planning years 2035 and 2040. Note that the relative change is not shown for the earlier years due to the lower number of underlying risk events.

The technology-specific case studies show that EV flexibility can provide strong adequacy support through relatively simple load reduction during critical periods, without requiring more sophisticated vehicle-to-grid (V2G) mechanisms. VPPs also reduce adequacy risk, but their contribution is more sensitive to energy availability and storage operating assumptions, as illustrated in Figure 0.8: The risk reduction due to VPP coordination reduces when applying the ‘derated energy’ or ‘economic operation’ approximations. Contrary to this, demand-side participation (DSP; i.e., price-responsive load reduction, as defined by AEMO) appears particularly valuable for hedging against uncertainty in storage operations. When enabling price-responsive demand response at lower price bands (in the ‘economic operation’), DSP can improve adequacy additionally by preserving storage for later critical periods. This suggests that while VPPs may provide broader market benefits, their reliability contribution depends strongly on whether sufficient energy is available during critical periods, especially in low-VRE weather years.

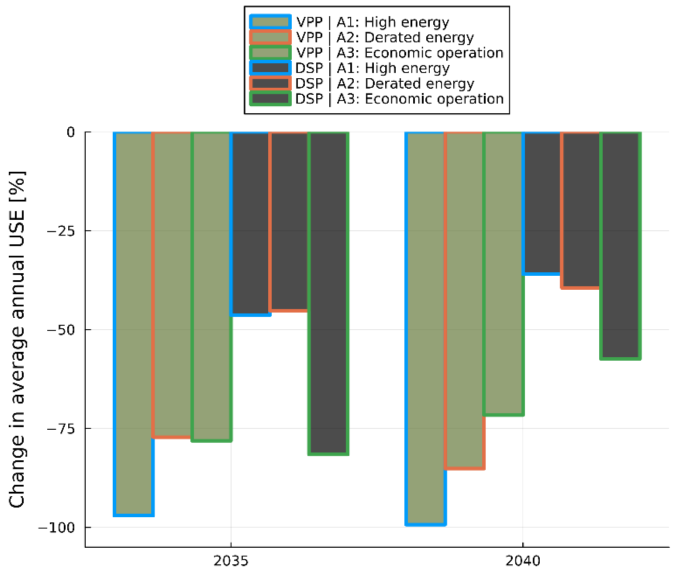

Figure 0.8: Relative change in average annual USE from 100% VPP or 100% DSP coordination, as represented under different operational approximations for energy storage systems.

Furthermore, **DER coordination may be especially valuable in weather years with low VRE availability.** As shown in Figure 0.9, all demand side resources (EV flexibility, VPP coordination, DSP enablement) effectively reduce the extended tail in the assessed weather year. However, even though the added capacity of VPPs is significantly greater than of EV flexibility and DSP, their reliability contribution depends strongly on whether sufficient energy is available during critical periods, especially in low-VRE weather years. This suggests that while VPPs may provide broader market benefits, their reliability contribution depends strongly on whether sufficient energy is available during critical periods, especially in low-VRE weather years. On the other hand, DSP appears particularly valuable for mitigating tail reliability risks, serving as an effective hedge for rare events.

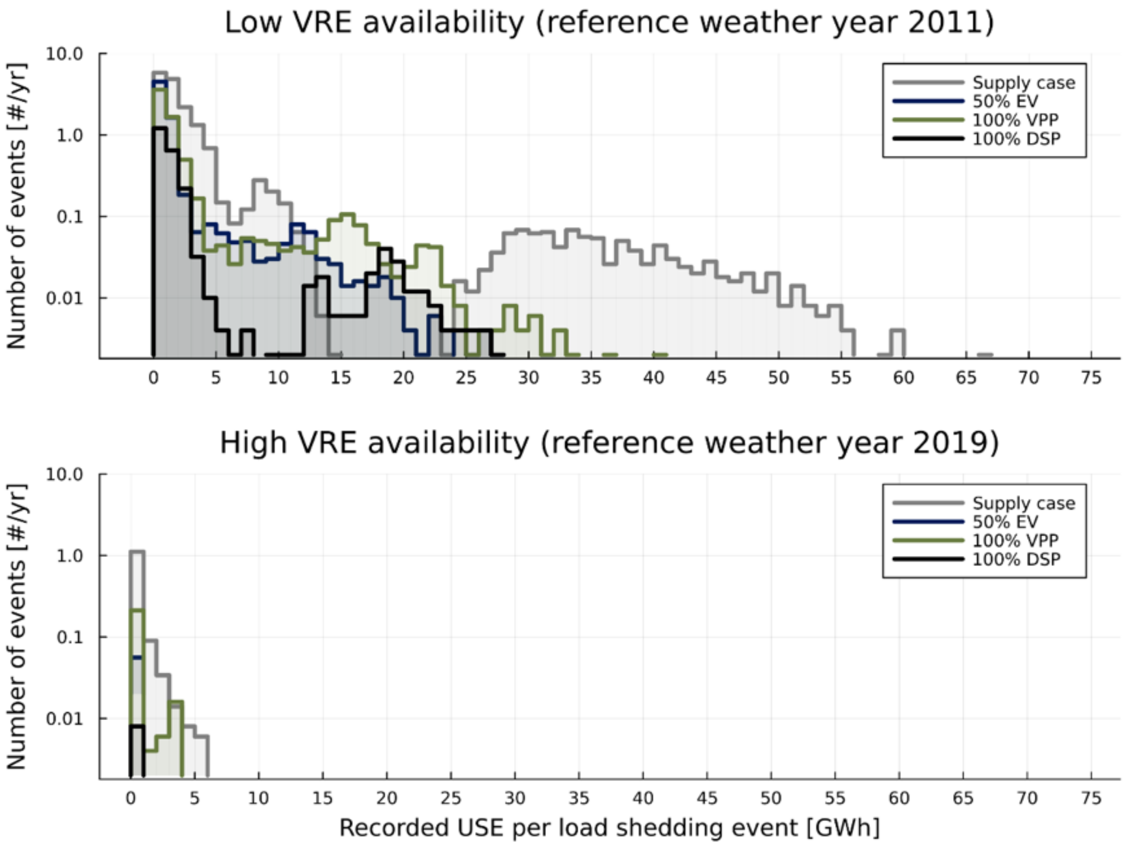

Figure 0.9: Distribution of unserved energy (USE) events in planning year 2040 with different levels of DER penetrations and two different weather years under storage operation assumption "A3: Economic Operation". The y-axis is on a logarithmic scale.

Overall, the results for this task suggest that any degree of coordinated demand flexibility, including reduction of EV charging, VPP coordination, or DSP, may become a relevant contribution for maintaining reliability in a weather-dependent and storage-dominated NEM.

Reliability risk profile of the Australian National Electricity Market

As coal-fired generation retires and the NEM transitions towards a system dominated by VRE and storage, the underlying factors influencing reliability risks are undergoing a fundamental transformation. Conventional adequacy frameworks, which are based on practices that evaluate peak demand periods and installed firm capacity, are insufficient to characterise a system in which weather variability and strategies for storage operation, rather than installed capacity alone, determine resource adequacy.

Task D consolidates developments from previous tasks to provide a structured and transparent characterisation of the NEM's reliability risk profile through 2040. The methodological approach integrates the developed operability frameworks, in particular *SchedNEM*.jl, with the adequacy engine, *PRASNEM*.jl, drawing data from public ISP sources via *ParseISP*.jl.

The NEM-wide reliability is initially assessed through a 'base case' scenario. The 'base case' uses the projected infrastructure buildout from the 2024 ISP *Step Change* scenario, including developments for generation, transmission, storage, and DER, across the planning horizon 2025-2040. The assessment considers 13 historical reference weather scenarios (2011 to 2023), both demand traces provided by the ISP (defined by their respective probability of exceedance (POE) of 10% and 50%), and 100 outage samples representing thermal generator and transmission line outages. Distributed PV and VPPs are explicitly modelled within the framework. In addition, three alternative approximations for storage operations are evaluated to examine how storage scheduling assumptions influence adequacy outcomes and reliability risks.

In first place, **the NEM meets the reliability standard on average, but the reliability risk profile shows important changes in both its shape and the magnitude of events**. Under the expected ISP infrastructure buildout, the NEM complies with the reliability standard on an annual-average basis across the 2025-2040 planning horizon, as shown in Figure 0.10.

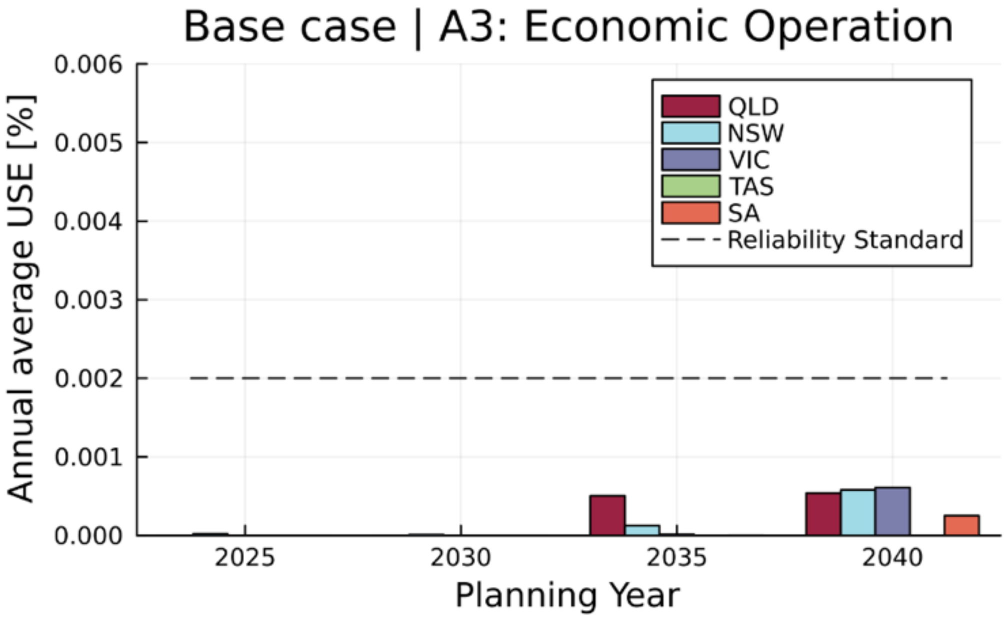

Figure 0.10: Annual normalised average unserved energy by NEM region in the base case.

However, **the underlying reliability risk is increasingly weather-driven**: some weather scenarios, modelled through historical weather years, are well above the standard, while others show almost no unserved energy (Figure 0.11). As a matter of fact, system reliability after 2030 depends on weather conditions in ways it did not in a thermal-dominated system, and resource adequacy measured only via average metrics masks and dilutes a much wider distribution of risk.

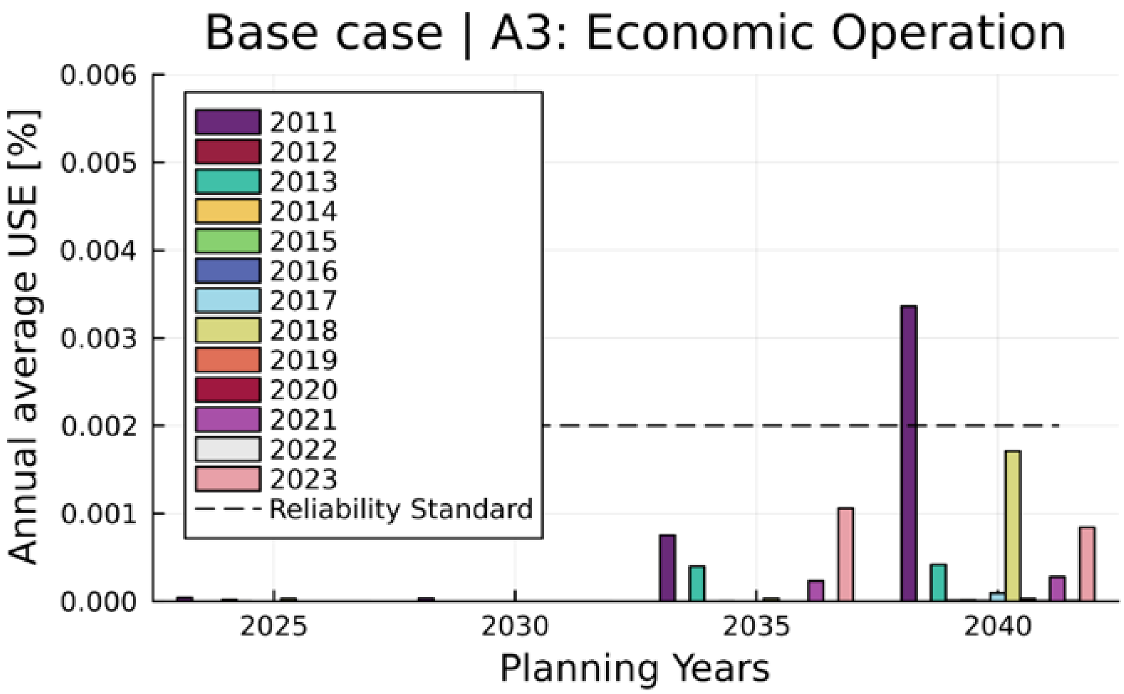

Figure 0.11: NEM-wide normalised average unserved energy (USE) per reference year in the base case.

Load-shedding events could become longer, larger and more frequent, and tail risks could grow faster than the average. Across magnitude, duration and frequency of reliability events, tail metrics rise more steeply than averages, particularly after 2030 (Figure 0.12). Moreover, the tail of event durations grows more pronounced, signalling that average adequacy metrics alone are increasingly unsuitable for a storage- and weather-dominated system. These changes are driven by the underlying resource mix and demand traces, which represent a system that responds more sensitive to weather conditions than the current thermal dominated NEM.

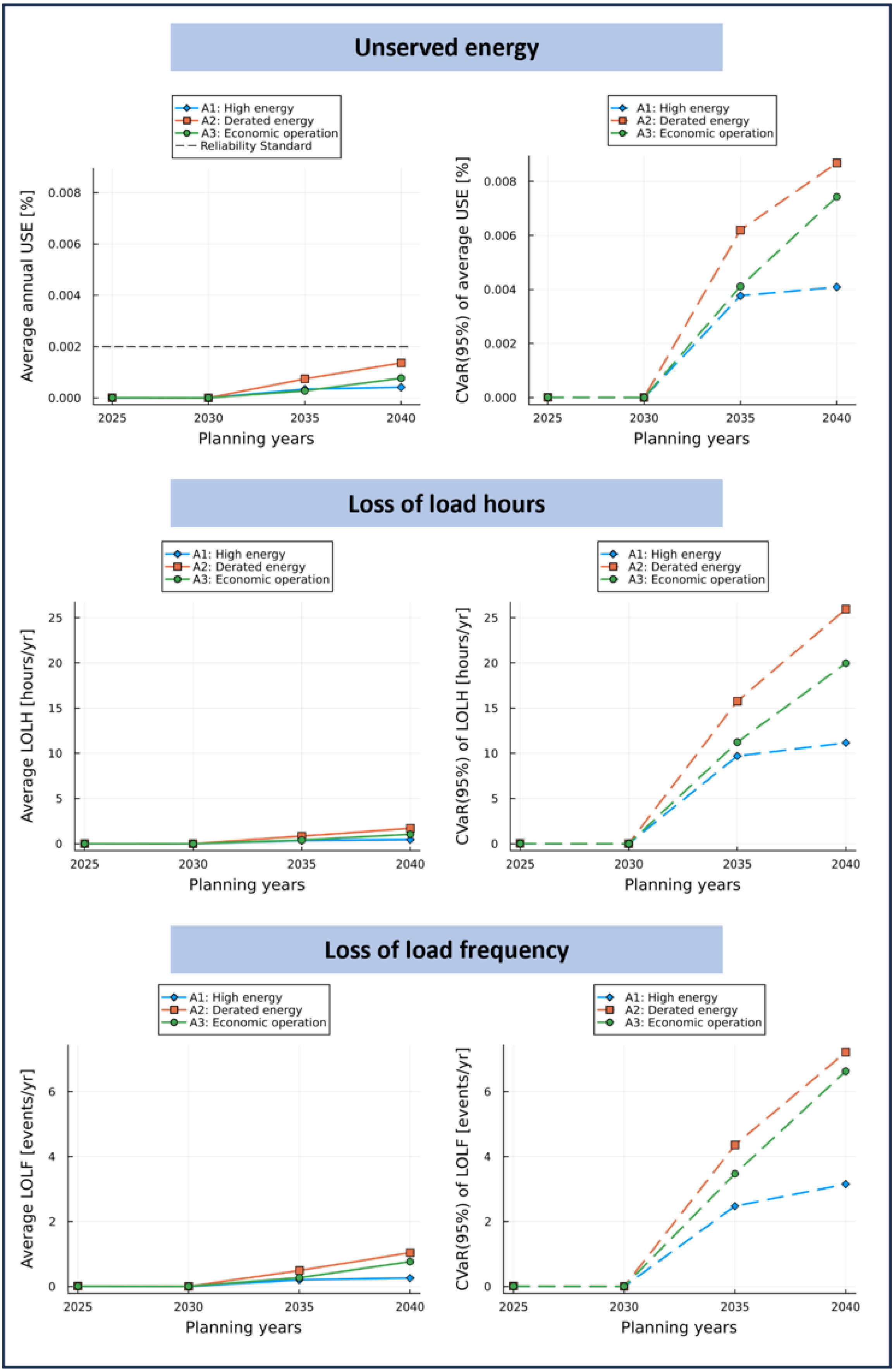

Figure 0.12: NEM-wide reliability risk measured across all weather-demand reference traces.

Storage operation assumptions are becoming a first-order source of uncertainty in resource adequacy. The three storage approximations under study diverge materially in both the magnitude and timing of risk events. Under a derated energy operation (A2) assumption, events cluster around high residual-demand periods; under economic operation (A3), which reflects an energy-only market with imperfect foresight, events align more strongly with periods of preceding low state of charge (Figure 0.13).

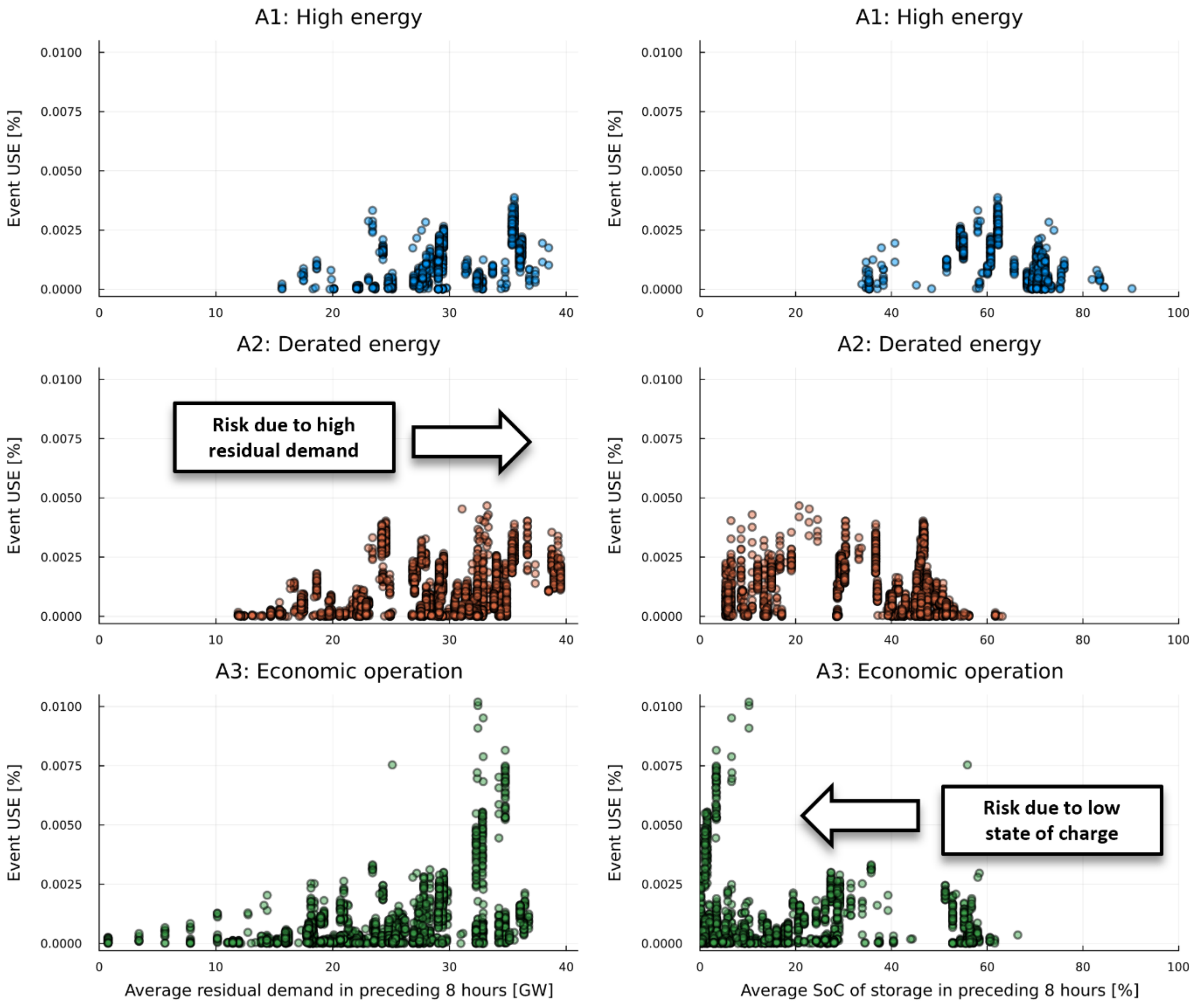

Figure 0.13: Distribution of risk events with recorded unserved energy (USE) in 2040 across the NEM under the three different storage operation approximations introduced in chapter 4.

Start times for shortfall events also exhibit a notable shift, moving from predominantly evening peaks in 2025 and 2030 toward morning peaks and late-night hours as storage state of charge becomes a binding constraint (Figure 0.14). As these differences are strongly driven by storage operating behaviour, no single storage representation should be assumed to fully capture future system adequacy outcomes. Instead, a range of storage operation approximations may be required to adequately characterise the range of potential reliability risks.

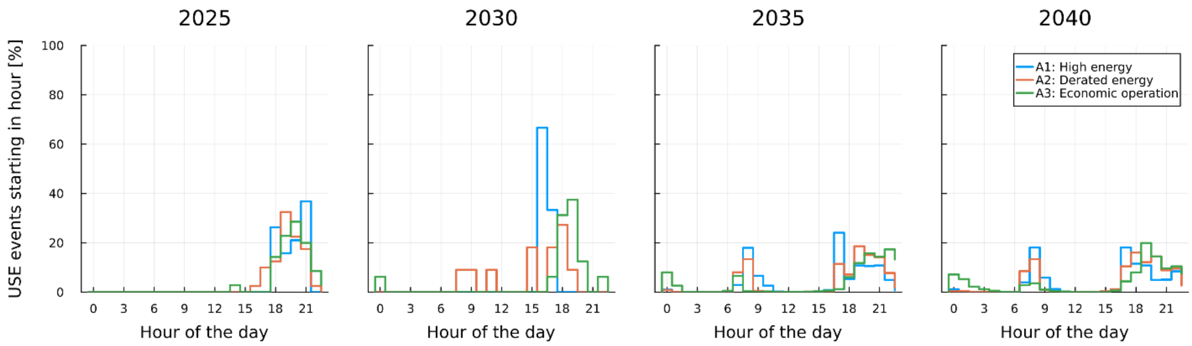

Figure 0.14: Distribution of start time of observed load shedding events across all weather-demand reference years, as well as under different storage operation approximations.

Peak demand is no longer the only risk driver. Periods with high net demand remain a central risk in 2035 and 2040, supporting traditional planning focus on peaks, as observed in Figure 0.15. However, an increasing share of USE events occurs at residual demand levels as low as 60% of the annual peak. This reinforces recent theoretical findings and practical observations that adequacy frameworks focused exclusively on peak load conditions may overlook material reliability risks that emerge during lower-demand periods. Consequently, reliability assessments and mitigation measures should extend throughout the full daily cycle, including nighttime and low-VRE conditions.

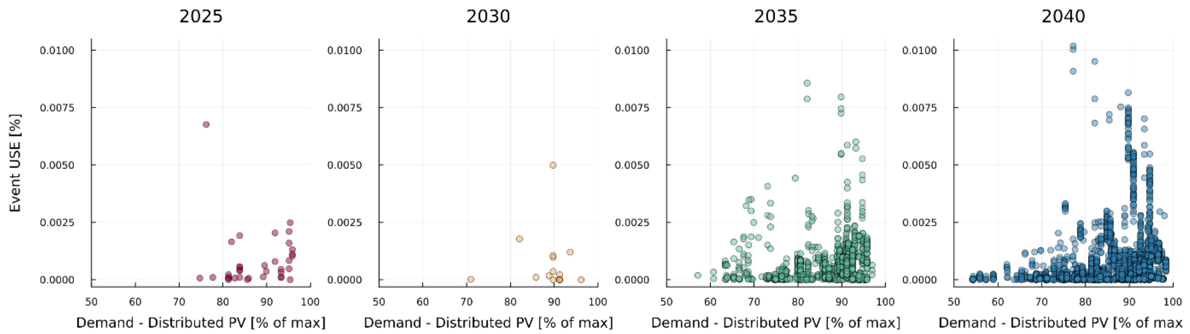

Figure 0.15: Distribution of event-level unserved energy (USE) with respect to underlying demand minus distributed PV generation at the start of the event, under the economic operation storage approximation.

In summary, the post-2030 NEM is likely to be characterised by weather-driven and storage-dependent reliability risks, with outcomes becoming increasingly sensitive to operational and regulatory decisions. Robust system planning, therefore, requires adequacy assessments across a range of assumptions for storage operating regimes, reliability frameworks that extend beyond assessing peak-demand periods, and recognition that policy settings, particularly those shaping storage incentives and behaviour, can directly influence system reliability. The main actionable insights from the reliability risk profile of the NEM can be summarised as follows:

- Employ a range of plausible approximations to storage operations in adequacy assessments. No single representation of the storage operating regime captures all implications for system reliability, and comparing different operating assumptions helps identify the range of possible reliability outcomes and the required mitigation measures.
- Expand the assessment to determine mitigation and operational measures under reliability frameworks beyond peak-demand periods. Reliability risks could increasingly emerge during

early mornings, nighttime hours, and periods of moderate demand, requiring more flexible operational triggers and potential intervention capabilities.

- Treat storage operating regimes as a policy and market design issue. Mechanisms such as capacity obligations, visibility of state-of-charge (SoC), or minimum SoC requirements might reduce the exposure and materialisation of tail risks while also improving the confidence of stakeholders in resource adequacy assessments.

Scenario design for resilience studies and system stress testing

As the east coast Australian power system becomes increasingly dominated by weather-dependent VRE and energy-limited resources, the traditional reliability planning framework may become insufficient to characterise emerging weather risks. While reliability assessments evaluate system performance under foreseeable operating conditions, they do not address extreme events that exceed conventional planning criteria.

As thermal generation retires and the NEM becomes increasingly dependent on weather-driven resources, reliability risks are becoming concentrated in infrequent yet high-impact weather-related events, such as heatwaves, windstorms, droughts, and their compound effects, rather than in isolated component failures. These extreme events can trigger common-mode failures across multiple asset types and geographic regions simultaneously. A unified planning framework integrating both reliability and resilience perspectives is therefore essential.

To establish this integrated approach, the work under Task E reviews definitions and current practices for both reliability and resilience planning across international standards and system operators. This review highlighted that while reliability planning is well-established and mandatory, resilience planning remains nascent and inconsistently applied. For a future NEM dominated by weather-dependent resources, both perspectives are necessary.

To understand resilience challenges specific to Australia, we conducted a comprehensive survey of historical extreme events affecting the east coast power system. This survey identified multiple risk driver classes, including heatwaves, windstorms, hailstorms, and flash floods, and their impacts on specific hazards as shown in Table 0.2.

Table 0.2: Reviewed historical extreme events in the NEM

Hazard	*Driver*			
	Heat wave	**Windstorm**	**Hailstorm**	**Flash flood**
High Ambient Temperature	SA-02/17			
High Front Wind Speed	VIC-02/24	SA-09/16	NSW-10/24	
Smog	VIC-01/07			
Hail		SA-09/16	NSW-10/24	
Lightning	TAS-02/15	SA-09/16	QLD-11/25	
Flood		SA-09/16		QLD-02/22
Bush Fire	NSW-01/20			
Low Wind Speed	SA-02/17			
Drought	NSW-06/07			

Based on this evidence, the work under Task E developed a structured methodology to represent external risk drivers in resilience studies. The framework translates *exogenous* weather hazards into *endogenous* system parameters through three sequential stages: (1) data collection and hazard quantification, (2) driver determination and input parametrisation, and (3) integration into operational and adequacy models. The framework explicitly distinguishes between drivers (underlying hazard conditions), triggers (instantaneous outage initiators), and events (cascading consequences), enabling transparent, evidence-based scenario design. An overview of the framework is presented in Figure 0.16:.

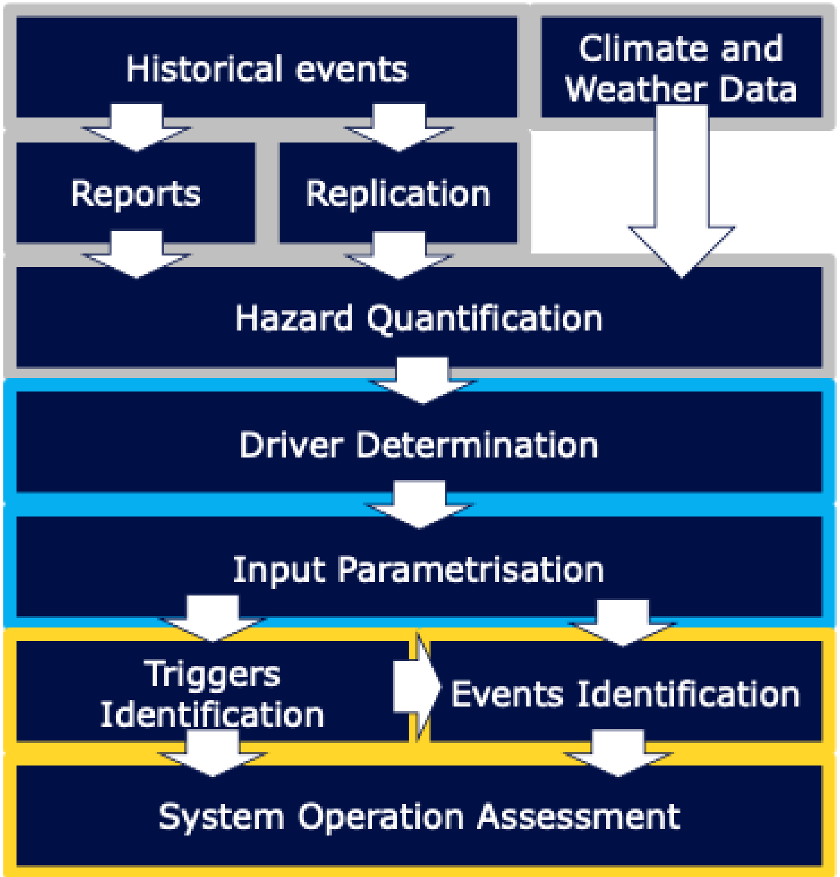

Figure 0.16: Overview of the proposed workflow for the design of scenarios to assess system resilience.

To demonstrate the practical applicability of this methodology, we conducted a detailed resilience case study focused on an extreme heatwave scenario in 2040 for the Australian east coast. We collected high-resolution meteorological data from the European Centre for Medium-Range Weather Forecasts Reanalysis v5 (ERA5) and the Australian Community Climate and Earth System Simulator Coupled Model 2 (ACCESS-CM2) with sufficient spatial granularity to represent realistic geographic variation across the NEM's renewable energy zones. The applied spatial granularity is shown in Figure 0.17. Rather than applying a uniform derating, spatially resolved parametrisation functions are developed for transmission lines, thermal generators, wind turbines, and solar PV, reflecting component-specific thermal sensitivities.

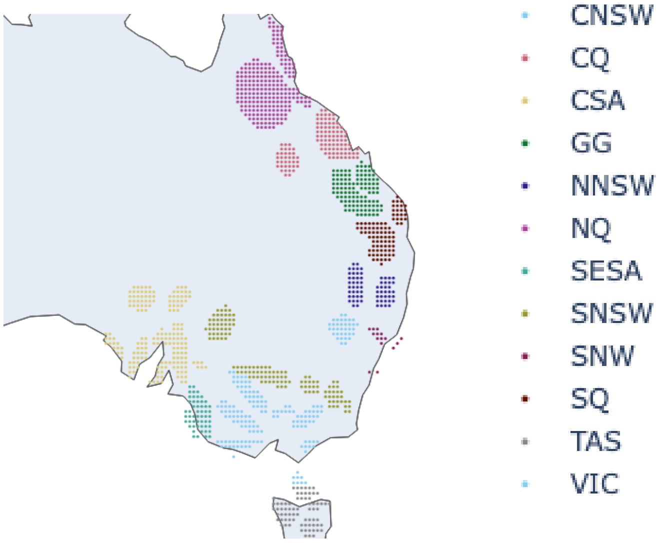

Figure 0.17: Temperature measurement mesh points inside renewable energy zones in the dataset, assigned to the nearest node in the 2024 ISP 12 bus network representation.

After applying the component-level parametrisations onto the relevant heatwave week in 2040, we observed resilience-related compound derating of up to 10 GW on the NEM-wide generation mix at peak temperatures. The derating across the technologies is shown in Figure 0.18.

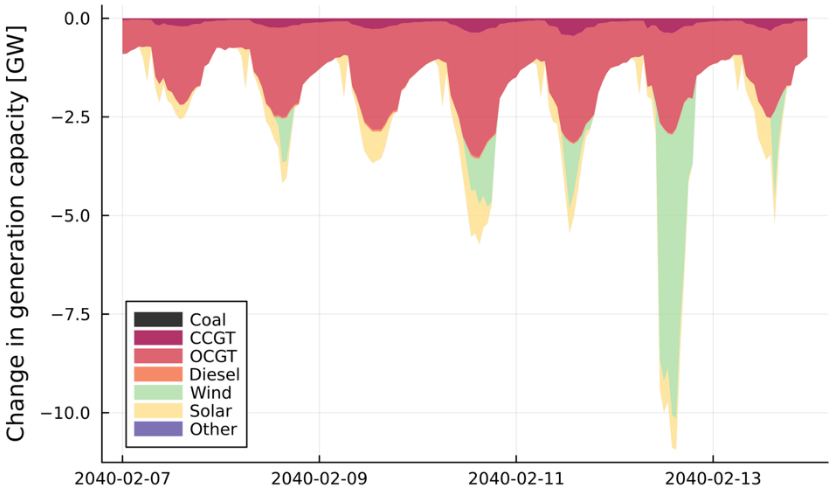

Figure 0.18: Potential derating in NEM-wide generation capacity driven by an extreme heatwave in 2040 by type of generation, considering external climate and weather forecasts, systematic component level impact parametrisation, as well as input reference weather traces.

To further characterise the risk introduced by deratings across different system components, and to identify the most relevant metrics for capturing the specific risk of an extreme heatwave, we compare average and tail metrics, as shown in Figure 0.19. The comparison reveals that the change in tail risk is concentrated in an increase in magnitude rather than in duration or frequency, suggesting that the **heatwave in this work presents a capacity constraint problem, where there is missing capacity for two to three hours, rather than a long-duration energy drought**. This also implies that CVaR USE, as an energy-based metric, is best suited to capturing the tail risk of extreme hot-day events.

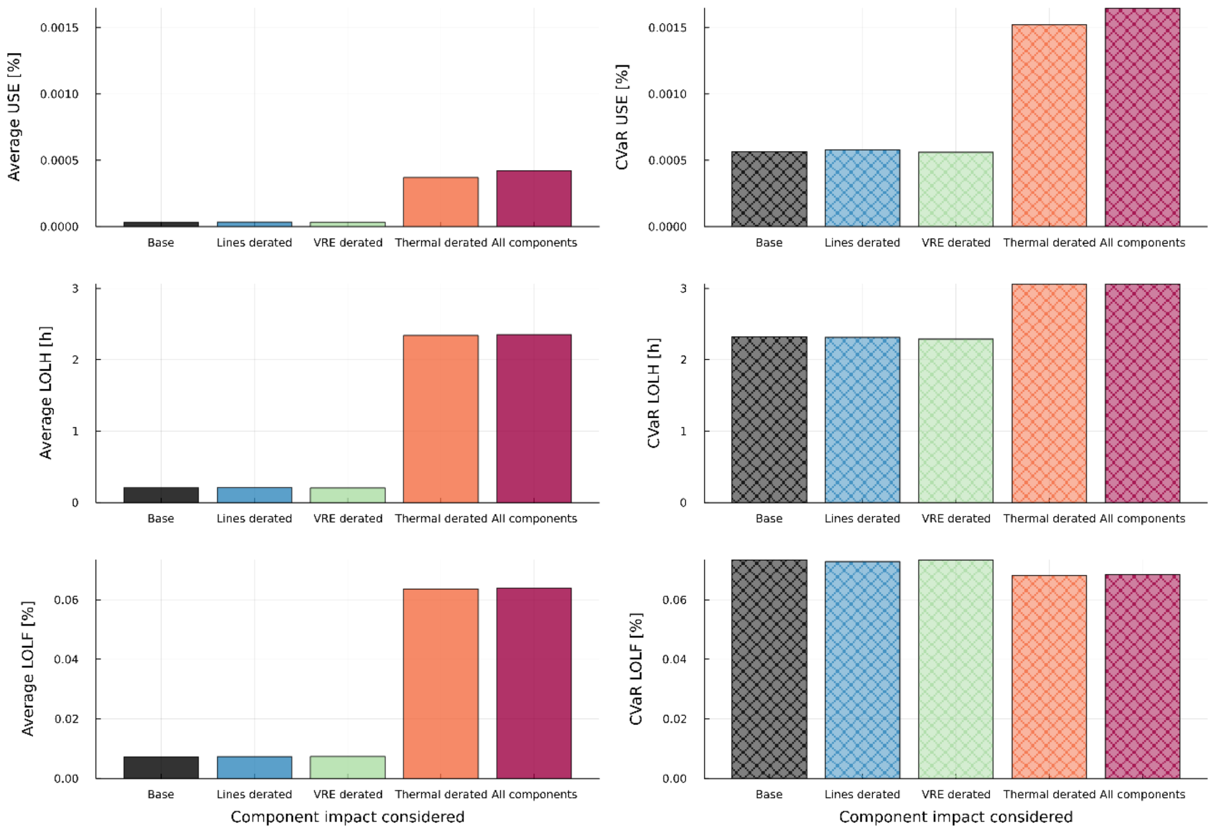

Figure 0.19: Comparison of NEM-wide average (left) and tail (right) metrics of unserved energy (USE), loss of load hours (LOLH) and loss of load frequency (LOLF) across 1500 outage samples for the extreme heatwave derating in 2040, under the storage operation approximation of economic operation. The Conditional Value at Risk (CvaR) is calculated with respect to the 95th percentile. The energy results are normalised for the three-month simulation period (January – March).

A second key finding from Figure 0.19 is that the potential derating of thermal generation may trigger a condition of lack of available capacity during a narrow time window. Although we can see significant capacity derating of wind farms in Figure 0.18, no significant change in risk due to VRE derating was observed in Figure 0.19 to the different time period of the derating (and therefore different underlying demand conditions). While this observation may be strongly dependent on the specific event studied, it suggests that resilience against heatwaves may be best addressed through flexible capacity that helps increase available capacity during peak operational demand. This flexibility can take the form of storage and demand response, as well as operational measures that respond during critical hours. This finding is supported by a sensitivity case, assuming 100% VPP coordination, where the unserved energy risk in this period is prevented by shifting VRE energy into the critical period, highlighting the fundamental role of storage even under resilience scenarios.

Complementary to the heatwave analysis, and representing an increasing intrinsic system stressor, we examined system resilience to an extended period of low VRE availability. Figure 0.20 presents the NEM-wide average and CvaR USE metrics observed under the described low-VRE period.

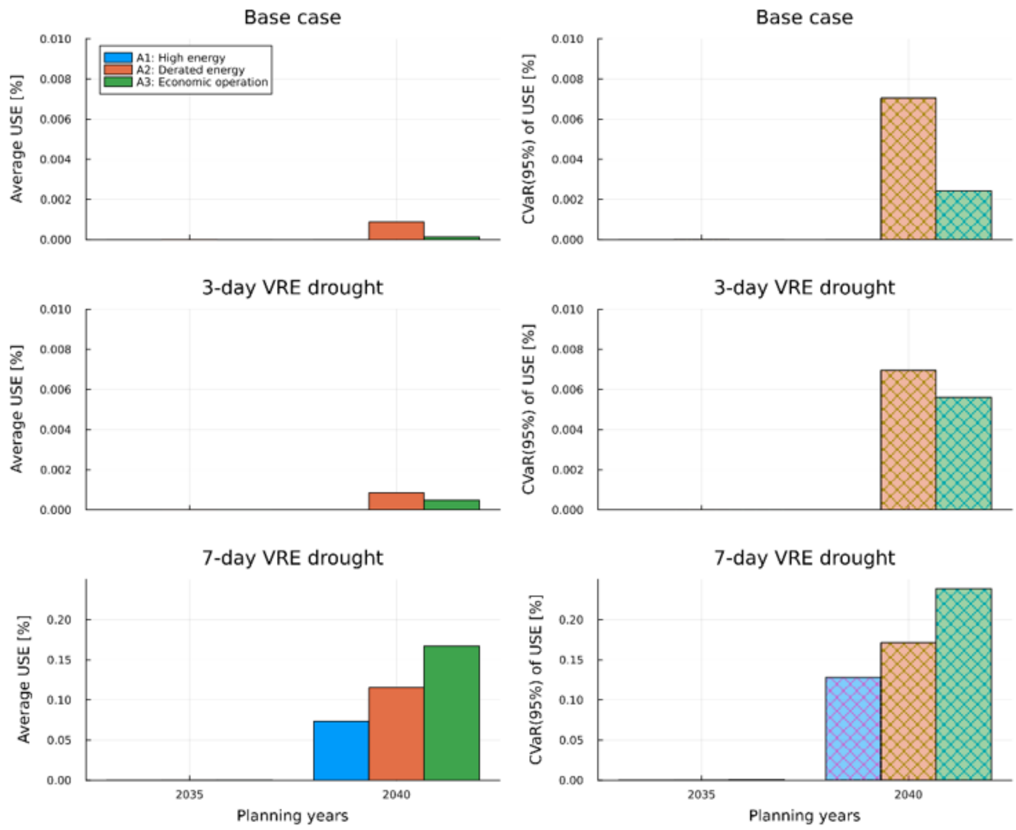

Figure 0.20: Average NEM-wide unserved energy risk (left) and NEM-wide tail risk (right) with increasing duration of VRE drought, under different storage operation assumptions. Note the different scale in the 7-day drought scenario. Unserved energy is normalised with respect to total demand in the simulated horizon (June – August).

Based on the results of Figure 0.20, we found that VRE drought risk may be highly sensitive to storage operation assumptions, with tail risk being even more dispersed across storage operation approximations. In particular, the analysis shows that exposure to VRE drought risk emerges highest under the 2040 resource mix, where higher storage penetration and retirements of thermal generation leave the system potentially more vulnerable to weather conditions.

While a 3-day VRE drought in the NEM could have a limited effect on average USE, a more severe 7-day event significantly increases adequacy risk, with the extent of that increase depending strongly on how storage operation is represented. Under the 'high-energy' assumption, material reliability risk only emerges during the most extreme drought conditions. In contrast, the 'derated-energy' and 'economic-operation' storage approximations reveal more substantial adequacy risks under more moderate droughts. Tail-risk metrics diverge even more strongly between storage assumptions, however demand-side participation may be able to reduce this uncertainty. These results highlight the importance of explicitly accounting for uncertainty in storage operations when assessing system resilience to prolonged energy-constrained events.

Glossary

AEMC	Australian Energy Market Commission
AEMO	Australian Energy Market Operator
AR-PST	Australian Research in Power Systems Transition
BESS	Battery energy storage systems
CER	Consumer energy resources
CSIRO	Commonwealth Scientific and Industrial Research Organisation
DER	Distributed energy resources
DNSP	Distribution network service provider
DR	Demand response
DSP	Demand-side participation
ECMC	Energy and Climate Change Ministerial Council
EENS	Expected energy not supplied, *equivalent to EUE*
ELCC	Effective load carrying capability
ELR	Energy-limited resources
ENS	Energy not supplied
ESS	Energy storage systems
ESOO	Electricity Statement of Opportunities
EUE	Expected unserved energy, *equivalent to EENS*
EV	Electric vehicle
FOR	Forced outage rate
GPG	Gas-powered generators
HP	Heat Pump
IASR	Inputs, Assumptions and Scenarios Report
ISP	Integrated System Plan
ISON	International System Operator Network
LOLE	Loss-of-load expectation
LOLH	Loss-of-load hours
LOLP	Loss-of-load probability
NEM	National Electricity Market
NLR	National Laboratory of the Rockies
NSMS	Non-sequential Monte Carlo simulation
PHES	Pumped hydro energy storage
ParseISP	Parser of the Integrated System Plan
PRAS	Probabilistic Resource Adequacy Suite
POE	Probability of exceedance
PV	Photovoltaic
RA	Resource adequacy
REZ	Renewable energy zone
RY	Reference year (i.e. historical year)
SMCS	Sequential Monte Carlo simulation
SME	Subject matter expert
VPP	Virtual power plant
VRE	Variable renewable energy

Table of Contents

1 Introduction

1.1 Research context

Australia is rapidly transitioning towards energy systems dominated by substantial variable renewable energy (VRE) and energy-limited resources (ELR), such as energy storage systems (ESS) and distributed energy resources (DER).

This transition introduces new risk factors that could fundamentally change the systems' risk profiles, challenging the underlying assumptions and suitability of existing reliability planning frameworks. As the resource mix becomes increasingly weather-dependent and energy-constrained, current approaches and tools for assessing resource adequacy[1], built on assumptions of average conditions, deterministic parameters, and simplified representations of system behaviour, such as storage operation under perfect foresight are no longer sufficient to capture their energy-limited nature.

At the same time, reliability risks are increasingly concentrated in rare yet high-impact, compounded weather-driven events, rather than in single-component failures. As the exposure to extreme weather, such as heatwaves, thunderstorms, and droughts, might intensify, supply infrastructure becomes more susceptible to common-mode failures. This new landscape underscores the need for a fundamental evolution in how resource adequacy (RA) and system resilience are assessed, to inform a resource mix that can withstand adverse operating conditions across a widening range of risk factors.

Advancing resource adequacy assessment in this context requires first identifying the shortcomings of existing approaches and their underlying assumptions to then determining targeted methodological improvements for RA procedures. This, in turn, would enable a more robust evaluation of the extent to which energy-limited resources, such as ESS and DER can contribute to an optimal resource mix that alongside VRE, can reliably replace ageing conventional generation. This remains a highly complex task, as the market-driven operation of ESS and DER does not necessarily fully align with the operational assumptions of current RA frameworks.

In line with the CSIRO–AR-PST research roadmap, this project addresses critical resource adequacy challenges to determine the impacts and merits of flexible, energy-constrained technologies in achieving a reliable resource mix. Core contributions of the project include developing an open-source toolkit for studying reliability in systems with deep penetration of VRE and ELR, the identification of modelling steps to realistically assess their contribution to adequacy and determining suitable metrics to quantify reliability risks that power systems could face in the coming years.

The resulting insights and tools assist stakeholders, in identifying and addressing potential deficiencies within Australia's current power system reliability framework. Furthermore, the project outcomes offer technical evidence to underpin future methodological enhancements, ultimately promoting timely investment and the operation of an appropriate mix of variable, storage, and firm resources to ensure system reliability.

---

[1] Resource adequacy encompasses the long-term planning perspective of reliability: Resource adequacy studies the potential risks to supply infrastructure and whether there will be sufficient available resources to meet electricity demand. In Australia, this is also often referred to as reliability – in contrast to security, which is an operational requirement for supplying demand.

1.2 Objectives of the research project

This stage of research under the AR-PST roadmap aligns with the resource adequacy component within the broader domain of power system planning. The objectives of this research are guided by the original roadmap[2] projects outlined below.

A. Develop an open-source modelling and implementation framework, including models and datasets, to efficiently perform resource adequacy and resilience studies of the NEM with system operability considerations (*Planning roadmap – Research project* **R2S1P1**).

B. Investigate the methodological and modelling steps for developing a time-sequential framework for resource adequacy and resilience assessments with operability considerations, addressing the complexities of temporal variation in renewable output and the management of energy storage (*Planning roadmap – Research project* **R3S4P1**).

C. Propose a planning-oriented model for integrating and assessing the role of CER and DER in resource adequacy and resilience assessment frameworks (*Planning roadmap – Research projects* **R3S4P2**, **R5S3P2**).

D. Analyse the changing reliability risk profile of the NEM across various scenarios through relevant metrics, addressing an ultra-deep penetration of VRE, energy storage and DER/CER (*Planning roadmap – Research projects* **R3S1P1**, **R3S3P2**).

E. Determine the methodological steps, relevant drivers and assumptions for developing suitable scenarios to plan for resilience under deep penetration of VRE, storage and DER (*Planning roadmap – Research projects* **R1S2P1**, **R3S2P1**).

Table 1.1 reports each Stage 5 research task's contribution to the AR-PST research roadmap, alongside cumulative progress to date. Roadmap activities that have not progressed across Stages 1 to 5 are excluded.

[2] L. Zhang, S. Püschel-Løvengreen, G. Liu, R. Laird, and P. Mancarella. Australia's Global Power System Transformation Research Roadmap. Topic 4: "Planning". https://www.csiro.au/-/media/EF/Files/GPST-Roadmap/Topic-4-Planning-Report.pdf

Table 1.1 Total progress for the research activities at the end of this project stage. The reported percentages reflect progress achieved during this stage and cumulative progress across all stages. Roadmap activities that have not progressed across Stages 1 to 5 are excluded.

RESEARCH PROGRAMME (R)	STREAM (S)	CODE	PROJECT (P)	Total FTE	Completed FTE	Contribution of Stage 5 to roadmap	Cumulative roadmap progress	Stages involved
1. Long-term Uncertainty	Scenario development for planning studies	**R1S1P3**	Modelling long-term uncertainty in power system planning with the consideration of HILP events (adequacy and security) and critical operation conditions	3	0.45	Not progressed	15%	**2**
	Climate change impact on individual power system components performance	**R1S2P1**	Modelling of climate change for power system planning purposes (different types of events, spatio-temporal representation, probabilities, correlation, etc.)	1	0.2	20% *(Task E)*	20%	**5**
2. Power System Operation	Steady-state operation modelling	**R2S1P1**	Modelling the steady-state operation of the system considering the trade-off between computational efficiency and model precision	2	0.8	20% *(Task A)*	40%	**3&5**
3. Reliability and Resilience	Reliability and resilience metrics	**R3S1P1**	Developing new metrics to quantify the benefits to reliability and resilience associated with the investment in new system assets	1	0.3	*30% (Task D)*	*30%*	**5**
	Impact of climate change	**R3S2P1**	Assessing the reliability and resilience of power system considering the impact of climate change and extreme weather conditions on its infrastructure/components	4	0.4	10% *(Task E)*	10%	**5**
	Credible and non-credible contingencies	**R3S3P2**	Profiling power system risks under various contingencies and indistinct events for future low-carbon grid with high penetration of IBR/DERs	2	0.4	20% *(Task D)*	20%	**5**
		R3S3P3	Modelling the impacts and benefits of other infrastructure and sector coupling (e.g., gas, hydrogen) on power system reliability and resilience	2	1.2	Not progressed	60%	**3&4**
	DER/IBR response to different events	**R3S4P1**	Modelling and analysing the impact on planning from IBR (including and in particular batteries) response to credible contingencies and high impact low probability (HILP) events	4	0.4	10% *(Task B)*	10%	**5**
		R3S4P2	Modelling and analysing the impact on planning from DERs and distribution network assets response to credible contingencies and high impact low probability (HILP) events	2	0.4	20% *(Task C)*	20%	**5**
4. Decision Making	Metrics, objectives and risk modelling of different stakeholders	**R4S1P1**	Modelling competing objectives, sources of risk, and risk appetite of different stakeholders in power system planning. Determination of metrics to value cost and risk	4	1	Not progressed	25%	**2**
		R4S2P2	Modelling investment flexibility in power system planning decision making by enhancing the decision structure and the representation of scenario trees	2	1	Not progressed	50%	**2**
	Methodologies for decision-making under uncertainty	**R4S2P3**	Methodologies and tools to incorporate the assessment of non-network solutions value streams in the network expansion problem	1	0.2	Not progressed	20%	**3**
	Interdependence	**R4S3P1**	Modelling investment decisions (including demand response) at distribution network level and determining the methodologies to integrate them in power system planning	1	0.3	Not progressed	30%	**4**
5. Distributed Energy Systems	Multi-energy systems	**R5S1P1**	Modelling the impact and flexibility embedded in the interactions between power systems and other energy systems for planning studies	3	1.2	Not progressed	40%	**2,3 & 4**
	Distributed energy markets and demand-side flexibility	**R5S2P1**	Identifying the sources and availability of demand side flexibility, quantifying its aggregated profile, and determining its representation in power system planning	2	0.8	Not progressed	40%	**3 & 4**
		R5S2P2	Modelling distributed energy systems (e.g., DERs, VPPs) operation and determining data requirement to represent their operation for planning studies	1	0.25	Not progressed	25%	**3**
	Distributed energy resources impact	**R5S3P1**	Modelling the impact of high DERs penetration on power system planning	2	0.4	Not progressed	20%	**4**
		R5S3P2	Modelling and analysing the contribution of DERs to system reliability (security and adequacy) and resilience.	3	0.9	10% *(Task C)*	30%	**3 & 5**

1.3 Research relevance for Australia

This research project supports Australia's energy transition by laying the foundations for a new generation of models, tools, and capabilities to assess the resource adequacy and operability of future Australian power systems. The project examines the changing reliability risk profile of the East Coast Australian Electricity System, and studies risk factors, operational strategies, and weather events that could lead to critical operating conditions relevant to AEMO, the AEMC and other stakeholders involved in reliability planning.

More broadly, the project develops and delivers advanced open-source tools, planning models that account for the energy-constrained nature of ESS, CER, and DER, and methods to support the development of resilience-oriented scenarios. Ultimately, this project contributes with technical evidence and practical recommendations to enable the effective design of a reliable system dominated by VRE, ESS, DER, and CER. The outcomes of the project will directly help address key technical constraints of different technologies that might otherwise hinder the integration of renewables, CER, and DER or drive up the costs of the Australian energy transition, supporting a more reliable and cost-effective path to decarbonisation.

The highlighted aspects of the project closely relate to the current Australian context, particularly concerning the key priorities for reliability planning outlined in the latest iterations of the ISP[3] and ESOO[4], the discussions initiated by the AEMC regarding updates to the reliability standard for the 2028-2032[5] period, the operability challenges caused by imperfect foresight on storage operations recently detailed in the 2026 draft ISP[6], and the updated research agenda of AEMO and the ISON[7] within the planning domain for 2026. Furthermore, this research aims to inform and deepen stakeholders' understanding, including AEMO, AEMC, ECMC, and DNSPs, of potential shortcomings in Australia's current power system reliability framework. It also intends to contribute technical evidence to support future methodological improvements, facilitating timely investment in and the operation of an appropriate mix of resources across generation, transmission, and distribution systems to guarantee system reliability.

1.4 Report structure

This report is divided into eight main chapters, summarised as follows:

a. **Chapter 2** presents the overarching context of resource adequacy assessments in electric power systems, covering standard probabilistic analysis procedures, the applicable metrics, and their respective contexts of use. The chapter concludes with a summary of the current state of resource adequacy assessments, highlighting existing gaps and ongoing challenges in this field.

[3] AEMO, "Draft 2026 Integrated System Plan", Dec. 2025. Available: https://www.aemo.com.au/consultations/current-and-closed-consultations/draft-2026-isp-consultation.

[4] AEMO, "2025 WEM Electricity Statement of Opportunities". Jul. 2025. Available: https://www.aemo.com.au/energy-systems/electricity/wholesale-electricity-market-wem/wem-forecasting-and-planning/wem-electricity-statement-of-opportunities-wem-esoo

[5] AEMC, "2026 Reliability Standard and Settings Review," Nov. 2025. Available: https://www.aemc.gov.au/market-reviews-advice/2026-reliability-standard-and-settings-review

[6] AEMO, "Draft 2026 ISP Appendix A4. System operability". Dec. 2025. Available: https://www.aemo.com.au/-/media/files/major-publications/isp/draft-2026/a4-system-operability.pdf

[7] ISON, "System Operator Priorities", Dec. 2025. Available: https://www.aemo.com.au/-/media/files/initiatives/international-system-operator-collaboration/system-operator-priorities-report-2026.pdf

b. **Chapter 3** provides a description and contextual overview of the open-source toolkit developed for this research project to conduct reliability and operability studies using models of the National Electricity Market.

c. **Chapters 4 and 5** address the modelling challenges of energy storage systems and distributed energy resources for resource adequacy, the prospective contributions they may offer toward ensuring reliability, and the potential risks posed to system adequacy if their models in RA frameworks are highly stylised with respect to their time-dependent and market-driven behaviours.

d. **Chapter 6** consolidates all methodological and modelling developments from the previous chapters to construct a risk profile for the East Coast Australian Power System. It reports on potential risks not identified by existing approaches to assessing RA, as well as risk drivers and potential mitigation measures ensure system reliability.

e. **Chapter 7** presents a methodological and modelling framework for designing extreme event scenarios within the Australian context. The framework is based on the principles of stress testing and parametric modelling to evaluate system resilience, and explains

f. **Chapter 8** concludes with the project's main findings and insights.

2 Assessment of reliability risks in electric power systems

Reliability is defined by CIGRE [2] as a “measure of a power system to deliver electricity to all points of consumption and receive electricity from all points of supply within accepted standards and in the amount desired”. For a more detailed, engineering-focused categorisation, the concept of reliability has been divided into its planning and operational dimensions, which are further distinguished into the two main sub-properties of “**adequacy**” and “**security**”, respectively.

Regarding the long-term planning aspect of reliability, *resource adequacy* is defined in [2] as “the ability of a power system to meet the power and energy demands of its consumers within technical constraints, accounting for both scheduled and unscheduled outages of system components”. Specifically, “scheduled” outages refer to planned maintenance periods for assets such as generators, substations, and transmission circuits. “Unscheduled” outages refer to credible contingencies, including equipment faults, the loss of a circuit, or a generator failure, among others.

For a system to be considered *adequate*, it must be planned so that all necessary components across the electricity supply chain, including generation, transmission, and distribution, can meet the expected demand while maintaining sufficient generation and network reserves to handle outages over a specified planning horizon. This horizon typically spans around a decade, reflecting the time required for assessments, regulatory approvals, and the construction of large-scale infrastructure.

The identification of risk factors threatening the supply adequacy of electric power systems and the associated infrastructure requirements is intrinsically linked to adequacy assessments. Fundamentally, adequacy assessments evaluate whether the system's current and future technology mix is sufficient to meet expected demand while allowing for reserves. These assessments also help identify potential resource shortages across different time scales [3].

Utilities and system operators perform forward-looking resource adequacy assessments to determine risk factors, quantify their effects and identify an appropriate mix of infrastructure. Historically, these assessments have been conducted under two broad paradigms: deterministic and probabilistic. The following subsections briefly outline these approaches. More broadly, this chapter outlines adequacy assessment methodologies in their current practice, with emphasis on a broad set of metrics, as well as emerging and desirable practices as power systems transition toward high penetrations of VRE and ELR.

2.1 Deterministic resource adequacy assessments

Deterministic adequacy assessments evaluate whether the existing technology mix can provide a capacity margin above the peak system demand, typically based on a single forecast. This capacity margin is commonly referred to as a “planning reserve margin” (PRM), which sets a fixed amount of capacity required above the system peak demand [4].

In its simplest form, deterministic adequacy studies and standards might stylise the adequacy analysis by focusing solely on mitigating the risk of capacity shortfalls during peak load times. As a result, they could fail to capture key chronological dependencies that are increasingly important in power systems with high penetration of VRE and ELR, including the management of energy storage state of charge, the temporal availability of demand response, and intra-hour and inter-hour variability in wind and solar generation. These chronology-related challenges, particularly those arising from energy storage and distributed energy resources to ensure resource adequacy, are explored in greater detail in Chapters 4 and 5.

2.2 Probabilistic resource adequacy assessments

While deterministic criteria and standards have been developed to account for component failures with some degree of stochasticity, they nonetheless rest on fundamentally deterministic frameworks that presume complete knowledge of system events. The principal limitation is that such deterministic criteria neither acknowledge nor account for the probabilistic characteristics of power systems, including customer demand, component failures, and more recently, and perhaps importantly, weather variability. As outlined in [4], historically recognised probabilistic aspects of electric power systems include:

- (a) Forced outage rates of generation units are known to be a function of the size and type of units. Therefore, a fixed percentage reserve (capacity margin) cannot ensure a consistent level of risk.
- (b) The failure rate of a transmission line is a function of its length, materials, location, and environmental conditions. Consequently, a steady risk of supply interruption cannot be ensured by constructing a minimum number of circuits.
- (c) Most planning and operational decisions are based on load and renewable generation forecasting. These methodologies cannot predict demands and renewable generation outputs with absolute precision, and inherent uncertainties are present within the forecasts.

To address the stochastic nature of power systems, methodologies for evaluating resource adequacy have evolved into probabilistic approaches. Furthermore, as temporal and spatial relationships become increasingly complex and uncertain, these techniques have become indispensable for assessing resource adequacy (RA) [5]. Rather than yielding a single deterministic result, probabilistic methods establish a framework for integrating and evaluating a wider array of scenarios and conditions (e.g., unit outages, generation and demand profiles, resource availability) within the analysis, thereby generating a spectrum of potential events with associated likelihoods.

Probabilistic resource adequacy assessments can be structured into three principal stages:

(1) Modelling uncertainty in demand, DER and large-scale resources. This process includes the development of consumption, DER and variable generation output profiles as well as component availability (e.g. outages and scheduled maintenance of system components)
(2) Assessing the system's capacity adequacy across multiple operating conditions.
(3) Calculating resource adequacy metrics, which provide a statistical quantification of reliability risks and estimate the contribution of supply-side resources to overall adequacy.

As depicted in Figure 2.1—inspired by the one presented in [6] and adapted for the Australian context—these stages are sequential and interdependent, with each phase requiring specific inputs to produce its respective outputs. The figure provides a high-level summary of the procedures essential to conducting a comprehensive adequacy evaluation in power systems.

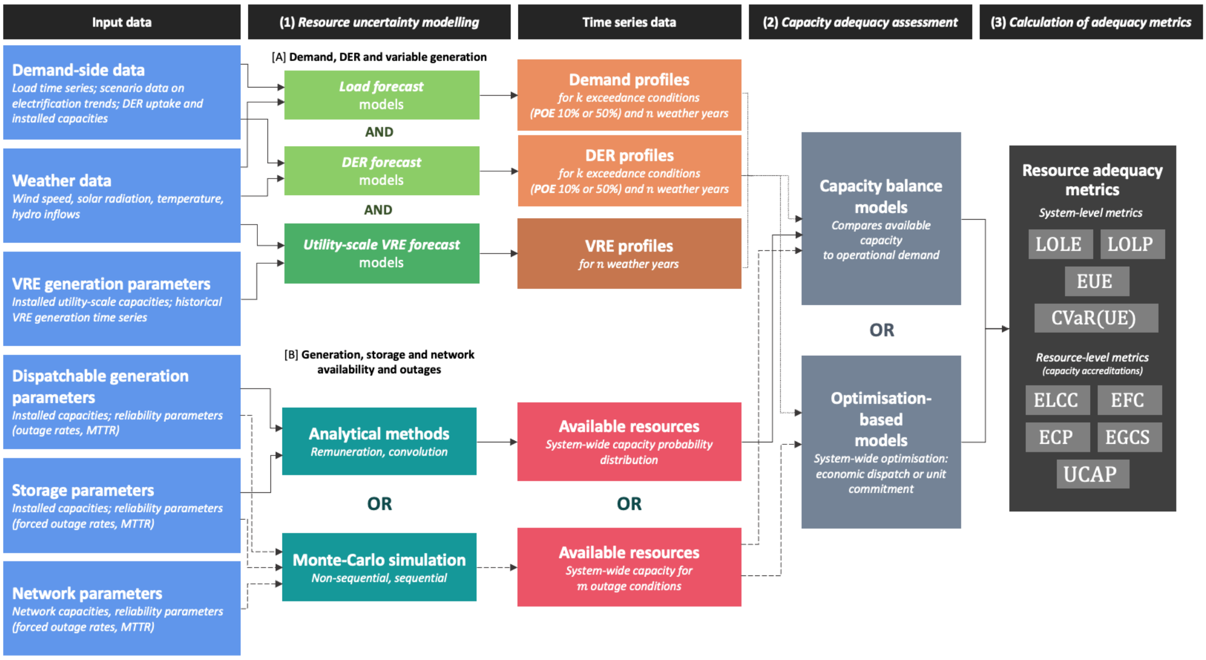

Figure 2.1: Input data requirements, sequential steps and method-selection decision points for the design and execution of probabilistic resource adequacy assessments.

As shown in Figure 2.1, inputs to the adequacy assessment processes should include historical weather and demand-side data (e.g. a characterisation DER uptake and electrification trends), technical and reliability parameters (e.g. installed capacities, forced outage rates, mean time to repair, maintenance schedules) of the resource fleet (e.g. generation, storage) as well as a characterisation of the network, including interconnections and potential relevant economic parameters of the system under study.

(1) <u>Modelling uncertainty in the demand-side, large-scale renewables and resource availability</u>

The described inputs are used for the first stage of the adequacy assessment, which consists of modelling uncertainty in the system's resources.

This stage is typically divided into two independent modelling parts, given the nature of the resources under assessment:

- **[A]** demand-side resources, consumption and variable (renewable) generation
- **[B]** characterisation of resource availability and outages in generation, storage and the network.

Importantly, the method for characterising uncertainty in demand-side resources, consumption and variable generation (that is part [A]) should be able to capture the correlations between supply and demand and the weather. In the usual practice, this method is usually independent of the method used to characterise the availability and failures of resources in the system (part [B]).

Regarding [A], a wide variety of long-term forecast models for consumption, distributed resources and renewable generation produce time-series data. Such time series characterise the variability and uncertainty of these resources over the horizon of the adequacy assessment and at the required temporal and spatial resolution. As a practical example, in the Australian RA assessment for the east-coast power system [7], all profile time series are developed at half-hour resolution with state-level spatial granularity. Demand and distributed generation profiles are typically developed for 10% and

50% probability of exceedance (POE)[8] and for at least 10 weather years, while VRE (wind and solar) time series are also for at least 10 weather years.

In [B], time series for resource availability are developed via analytical techniques or by simulation. As a general practice, RA frameworks generate randomised unit *outage schedules*, which characterise resource failures that might threaten system reliability. The two major classes of methods to model unit outages, analytical and simulation, can be described as follows [6], [9]:

- **Analytical techniques:** These methods use mathematical models of the system and probability theory to estimate the probability distributions of available capacity and forced outage rates for a group of units, which are then used to generate a system-level availability distribution. For example, convolution methods [10] calculate the system-wide capacity distribution by aggregating unit-level availability probabilities. Importantly, significant assumptions are frequently necessary to simplify the problem and develop an analytical model of the system, which may reduce the significance of the results.
- **Simulation (Monte Carlo) techniques:** Monte Carlo sampling[9] allows modelling unit outages consistent with each unit's outage rates and time-to-repair statistics. These techniques, divided into non-sequential (NSMS) and sequential (SMCS), use *time-to-failure* and *time-to-repair* parameters to generate a randomised, chronologically ordered outage time series for each asset. The outage time series represents the unit's forced outage rate: in each time slice, a unit is either fully available or partially or fully unavailable.

After the time-series data for load, renewable generation, and component availability are generated, they serve as inputs to the model used for the capacity adequacy assessment.

(2) <u>Capacity adequacy assessment</u>

At this stage, two major methods for assessing RA are distinguished: *capacity balance models* and *optimisation-based models*. As outlined by the different types of arrows in Figure 2.1, the selection of an appropriate methodology for performing the RA assessment is inherently contingent on the specific approach employed in (1) to obtain the time series that models resource availability uncertainties.

- **Capacity balance models** compare the available capacity in the system with respect to the demand. Depending on the approach to modelling component failures (convolution, NSMS or SMCS), the methodological steps for computing the capacity balance differ. For convolution-based failures, the probability of available capacity in each time slice is convolved with the operational demand time series. For MCS-based, each slice of operational demand is compared against the capacity availability time series (whether non-sequential or sequential),

---

[8] *Probability of exceedance* (POE) – POE is the likelihood a maximum or minimum demand forecast will be met or exceeded. A 10% POE maximum demand forecast, for example, is expected to be exceeded, on average, one year in 10, while a 90% POE maximum demand forecast is expected to be exceeded nine years in 10 [8].

[9] In the domain of Monte Carlo simulation there exist *(i) non-sequential* (also referred to as *random*) and *(ii) sequential* (also referred to as *chronological*) procedures. Importantly, non-sequential MCS represent time-independent snapshots that ignore time correlation. In the context of modern electric power systems, where chronological dependencies have higher prevalence, sequential Monte Carlo sampling is becoming the standard practice as resource availability time series incorporate the temporal correlation of resource availability and are supported by both capacity balance and optimisation-based models.

producing measurements of the frequency and magnitude of (unserved energy) events in the system

- **Optimisation-based models** typically comprise unit commitment (UC) and economic dispatch (ED). Each VRE, demand, and component availability time series is fed into an optimisation problem, with explicit temporal constraints (ramp rates, minimum up- and down-time for generators, storage, and DER operations, etc.). Given their sequential nature, these models can only be fed with outage schedules produced by SMCS. As with capacity balance models, USE measurements emerge as outputs of the optimisation model. These measurements then feed the metric calculation stage.

(3) Calculation of adequacy metrics

As described, both types of models for assessing RA—capacity balance and optimisation— produce measurements for periods that present capacity shortfalls. These measurements can include the count of event-periods[10] with capacity shortfalls (or more specifically, the count of hours, days or years where such shortfalls happen) as well as the magnitude and duration of every unserved energy event.

This collection of measurements, which together form a probability density function when a sufficiently large number of measurements are computed, is subsequently utilised to derive probabilistic metrics that facilitate the estimation, quantification and summary of reliability risks. Among the metrics commonly used for these purposes are *loss-of-load expectation* (LOLE), *loss-of-load probability* (LOLP), *loss-of-load hours* (LOLH), and *expected unserved energy* (EUE). The forthcoming Section 2.3 offers a comprehensive review of established and emerging metrics for assessing reliability risks as well as recommendations for their usage.

2.2.1 On the suitability of probabilistic methods for assessing resource adequacy

The previous section outlined three techniques for modelling resource availability uncertainties—convolution, NSMS, and SMCS—and two approaches for calculating RA metrics at the system level—capacity balance and optimisation. While all these methods are established, the pronounced temporal couplings characteristic of new technologies in modern electric power systems require consideration by practitioners when selecting appropriate methodologies. The choice will depend on each method's ability to accurately capture temporal dependencies—such as state of charge, ramping, and service availability—and inter-unit dependencies, including spatial correlations and common-mode failures. Consideration should be given to:

- Convolution and the NSMS model the availability of units, assuming temporal independence of the states of units in the system. This precludes representing time-coupled processes, such as energy-limited resources, demand response, and network constraints. These approaches are therefore best suited to capacity-limited systems dominated by thermal generation. Risk

[10] An event-period is defined as a period of time (defined with respect to a chosen temporal resolution), in which, at some point, system resources are insufficient to meet demand, and, therefore, unserved energy occurs. An event-period can be any event-hours, event-days, event-years. The resolution of the event determines how the occurrence, persistence and frequency of the event are quantified. For a visual explanation of event-periods, refer to [11].

may be misrepresented when temporal dynamics (e.g., high penetration of ESS) materially affect supply resources and their availability. Importantly:

  - Convolution provides an exact analytical capacity distribution for the system, but scales poorly as system size and component heterogeneity increase.
  - NSMS improves scalability through unit-level sampling, yet remains non-chronological.

- Sequential MCS is widely regarded as essential [6] when temporal dynamics and operational flexibility can materially contribute to adequacy assessments. SMCS preserves the chronological evolution of system states, enabling explicit modelling of ELR and intertemporal constraints across time and assets. This allows SMCS to capture correlated outages, weather-driven variability, and prolonged stress events that may increasingly drive adequacy risks.
- SMCS with optimisation-based operational models allows adequacy metrics to be evaluated under high-fidelity operational and network constraints, including storage dispatch and interconnector limits. However, computational requirements scale significantly with sampling depth.

2.3 Metrics for assessing resource adequacy

In the context of resource adequacy studies, metrics quantify and summarise the risk of having insufficient supply-side resources to meet demand, in other words, the risk of load shedding. The following summarises how RA metrics are applied at the planning level.

- Resource adequacy metrics quantify the likelihood, magnitude or duration of supply inadequacy events across a spectrum of anticipated operating conditions that a particular jurisdiction (region, state, country) may face.
- In system planning processes, adequacy metrics inform **reliability standards**. If an adequacy assessment determines that the metric underpinning the standard exceeds a predefined threshold (typically set by policy), corrective actions must be taken to keep it below that threshold.
- At the planning scale, these corrective actions may include commissioning new infrastructure (e.g., additional investments) and postponing the decommissioning of existing facilities (e.g., delaying the closure of a thermal power plant).

The subsequent sections provide an overview of metrics for assessing resource adequacy, including metrics established in different jurisdictions, emerging metrics that could better complement adequacy assessments by reflecting the evolving nature of reliability risks, and metrics used to quantify the individual contributions of technologies.

2.3.1 Deterministic resource adequacy metrics

Deterministic metrics seek to establish, based on a single-system forecast, the margins of power capacity and energy available in the system during specific times, such as peak demand or concurrent periods. Table 2.1 provides an overview of these metrics.

Table 2.1: Summary of deterministic resource adequacy metrics.

<table>
<tr><th>Deterministic metric</th><th>Definition</th><th>Additional considerations</th><th>Advantages</th><th>Disadvantages</th></tr>
<tr><td>Planning reserve margin PRM</td><td>Difference between the total installed generation capacity and the expected peak load, divided by the peak load</td><td>Supply sources are derated, representing the likelihood of availability at peak times.</td><td rowspan="2">Simple calculation and definition

Simulation is not required.</td><td rowspan="2">Ignores system operating conditions.

Could be inappropriate when the proportion of variable generation is significant in the system.

It requires that installed capacity does not vary greatly from year to year.</td></tr>
<tr><td>Hourly energy reserve margin ERM</td><td>Sets a reserve margin of energy at specific time periods</td><td>Extends the PRM, allowing an enforcement of power and energy adequacy, particularly for storage systems.</td></tr>
</table>

Deterministic metrics are simple to understand, require minimal computational time, and can be calculated based on limited system data. However, their application, such as in the calculation of the PRM, reduces the RA assessment to evaluating system-wide shortfalls only at the expected peak load, failing to account for chronological and intertemporal behaviours.

Importantly, deterministic metrics are not inherently indicative of resource adequacy risks. Although a system with reasonably high margins is likely to encounter fewer adequacy issues than one with lower margins [9], the PRM and ERM do not characterise the ***probabilistic distribution of events*** that drive the adequacy risk itself, particularly their expected frequency, duration, or magnitude.

2.3.2 Probabilistic resource adequacy metrics

Probabilistic metrics are derived from the probability distribution of specific event measurements in the system (e.g., the probability distribution of event counts, durations, or magnitudes), thereby providing a more detailed overview of adequacy risks than deterministic metrics. Probabilistic metrics can be divided into two main groups:

- <u>*Loss-of-load*</u> metrics present information on the **frequency** and **duration** of shortfall events. Importantly, they do not describe the magnitude of the energy shortfall. That is, how many MWh are not being supplied on a specific shortfall event.
- <u>*Energy-centric*</u> metrics capture the **magnitude** of energy shortfalls, usually measured in expected MWh not supplied per year, but not the duration or frequency of events when that loss of load happens.

The main advantage of using probabilistic metrics is that load shedding *risk* is evaluated on a range of events rather than a single one. This means that a probabilistic assessment remains a more comprehensive way to perform a full adequacy evaluation. When using a probabilistic approach, the risk of load shedding is evaluated across all hours of the day rather than only during relevant peak conditions. Table 2.2, based on the content of [3], provides an overview of established probabilistic resource adequacy metrics.

Table 2.2: Summary of probabilistic resource adequacy metrics.

Probabilistic metric	Definition	Information provided	Measure unit	Advantages	Disadvantages
Loss of load expectation *LOLE*	Average number of event-periods per year. *Event-periods* refer to any time-period length (user defined).	Event frequency	Time periods with event/year	Simple definition. Makes it possible to compare systems of different sizes.	The depth (magnitude) of the events are not quantified. It may depend on decisions made by the system operator (definitions of event-periods).
Loss of load hours *LOLH*	Average event-hours per year simulated samples (LOLE for event-hours).	Event duration; event frequency	Hours with event/year *e.g. 3 event-hour/10 years*		
Loss of load days *LOLD*	Average event-days per year across simulated samples (LOLE for event-days).	Event duration; event frequency	Days with event/year *e.g. 1.5 event-day/10 years*		
Loss of load years *LOLY*	Average event-years per study horizon across simulated samples (LOLE for event-years).	Event duration; event frequency	Years with event/study horizon *e.g. 1 event-year/15 years*		
Loss of load probability *LOLP*	Total number of event-periods, divided over the total number of periods sampled.	Event likelihood	Unitless (%)		The depth and duration of the failure are not quantified.
Loss of load frequency *LOLF*	Average number of adequacy events[11] per study horizon.	Event frequency	Events/year		
Expected unserved energy *EUE*	Average load not served per year across simulated samples.	Event magnitude (energy)	MWh/year *e.g. 20 MWh/year*	It is not possible to directly compare systems of different sizes. This limitation can be mitigated by normalising EUE by the total energy consumption.	Quantifies the energy not supplied. Offers the possibility of assigning an economic value to outages, allowing a cost-benefit analysis.
Normalised expected unserved energy *nEUE*	Average load not served per year across simulated samples, normalised with respect to the total system energy consumption	Event magnitude	Unitless (%)		

The technical literature recognises that reliance on a single metric in resource adequacy assessments does not provide a complete characterisation of adequacy risks [3], [12], [13]. As power systems transition, both adequacy metrics and the reliability standards derived from them should similarly evolve to reflect a broader set of risk dimensions and characteristics of possible events. Important consideration should be taken to the following aspects:

- Metrics presented in Table 2.2 are not interchangeable. When used jointly, they offer distinct and complementary insights into the characterisation of resource adequacy risks.

[11] An *adequacy event* is defined as a contiguous set of hours with a shortfall (unserved energy). Each event is considered as a separate occurrence. For example, a LOLF of 3 events/year means the system experiences three separate loss-of-load events per year, regardless if each lasts one hour or several days.

- For example, LOLF characterises the expected **yearly frequency** of loss-of-load events, while EUE captures their expected **magnitude**. Together, such metrics provide a richer understanding of system performance than any single indicator in isolation.
- Most used adequacy metrics quantify the ***average risk***—such as the expected frequency, duration, or magnitude of load-shedding events. As a result, they do not explicitly allow the quantification of the impacts of extreme risks (and therefore operating conditions) that could drive higher levels of unserved energy or longer events.
- In Australia, long-term resource adequacy processes for the NEM are guided by a reliability standard based on the normalised EUE (nEUE), an energy-centric metric. This metric is recognised as being more robust in a context of high ELR penetration, providing information on the magnitude of events (quantifying energy in its non-normalised form, EUE). However, a recent study has proposed [12] that (i) complementing it with metrics associated with the frequency of events and (ii) equipping the analysis with a focus on the tail of the distribution of UE is highly desirable.

2.3.3 Tail metrics for assessing adequacy of supply

As discussed in the previous section, reliance on single metrics and expected values can skew the resource adequacy analysis, particularly as durations and magnitudes of events become less predictable or less normally distributed due to increasing dependence on weather, ELR and growing exposure to extreme climate events.

In this regard, an assessment of the entire distribution of possible unserved energy events becomes necessary to take timely actions at the planning scale. Below are points that aim to enrich the reasoning behind this discussion. Subsequently, this section presents metrics that have been proposed in the technical literature to develop an extended understanding of reliability risks.

- The primary *risk factor* in systems dominated by thermal generation were outages of system components. This means that any resulting load shedding events due to insufficient capacity were likely to be relatively small in duration and magnitude (for example, on the order of the size of one generator's nameplate capacity) [12].
- As systems transition towards VRE, DER and ELR-dominated, load-shedding events may be much different in magnitude, duration, frequency, timing and predictability. The increased dependence on weather could start concentrating resource adequacy risks into a limited number of specific weather events, but with larger impacts–such as *dunkelflaute* periods.
- As a result of the previous points, in the past it was sufficient to employ metrics and set reliability standards based, for example, on the LOLE–the expected number of days per year with a loss-of-load event.
- However, for example, two systems under assessment might have the same LOLE of 1 day in 10 years. Still, one might experience a severe, system-wide outage with 50% of the load lost on that day, whereas the other might have only a minor, short outage [14].
- To address this potential bias, in recent years, it has been widely recommended to complement the analysis with metrics that also capture the details of the probability distribution of these measurements [12]. This does not necessarily mean that reliability

standards (which are informed by specific metrics) should be set only by non-average metrics. Rather, additional metrics should be employed by planners to help them identify potentially more extreme risks and their consequences, establishing multi-criteria assessments.

- The previous point is supported by the fact that, for example, in very skewed probability distributions, the average value can be relatively small–almost insignificant, but extremely high values can occur as well (that is, the so-called *tail*). This type of effect, which can easily occur in power systems, can be ***masked or ignored by metrics or standards*** if only average values (or even standard deviations) are evaluated. Figure 2.2 illustrates this effect [4].

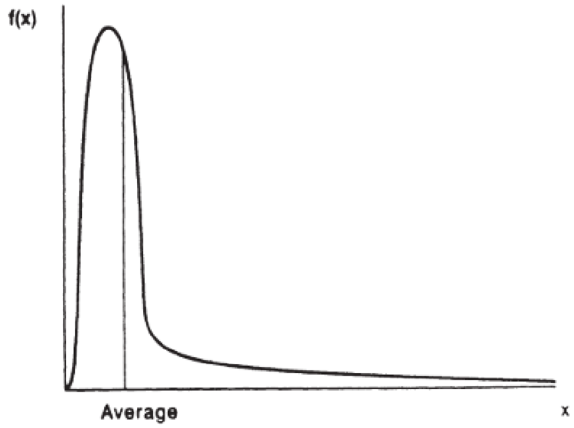

Figure 2.2: Example of highly skewed probability density distribution.

Tail metrics

As discussed, capturing information from the entire probability distribution could provide valuable insights for decision makers. When hundreds of thousands of simulation results are synthesised into a single number (the *average*), extreme values can be hidden or diluted, concealing risks at first glance but not materially mitigating them. For example, recent research [13] showcases that even while it is possible to maintain a constant EUE, the value of tail metrics can increase significantly.

In this context, a significant part of the debate around the innovations required in resource adequacy methods for modern power systems [12], [15] is the incorporation of metrics that better reflect the risks at the "tail" of the probability distributions, suggesting multi-metric analysis. As a matter of fact, tail-end events could have disproportionate effects if they were to materialise, even though their probability is low compared to other, less impactful events.

The literature and extensive technical reviews have advocated for the use of two functions that could contribute to better characterising these *tail* risks: (1) the "**percentile**", also referable to as **"Value-at-Risk**" in RA contexts, and (2) the *Conditional Value-at-Risk*, the so-called "**CVaR**." It is important to note that **these two are not metrics per se**, but rather functions (such as the expected value function) that are applied to the probability distribution of different measurements, and which together allow to construct a metric that characterises the tail. Table 2.3 summarises their definitions and the insights they might provide.

Table 2.3: Overview of functions to construct tail metrics for assessing resource adequacy.

Function to build a tail metric	Technical definition	Information provided	Measure unit
α-Percentile / Value-at-Risk *$P_{\alpha\%}$; $VaR_{\alpha\%}$*	The percentile, or equivalently the Value-at-Risk, defines the threshold of a probability distribution for a given resource adequacy measurement such that α% of outcomes lie below this value. Values below the threshold represent the α% of events (e.g., the unserved energy value not exceeded in 95% of simulated years).	Threshold value of which α% of measurements lie below.	Same as the input probability distribution
Conditional Value-at-Risk *$CVaR_{\alpha\%}$*	The CVaR function computes the average value of an adequacy measurement across outcomes that exceed the α-th percentile/ *$VaR_{\alpha\%}$* of a probability distribution. It quantifies the expected severity of tail-end events (e.g., the average unserved energy of the worst 5% (i.e, the higher UE) of simulated events when α = 95%).	Average value of the worse (100-α)% measurements.	Same as the input probability distribution

Tail metrics: *Understanding their application and value*

When conducting a probabilistic adequacy assessment, following the high-level steps outlined in Figure 2.1, planners typically obtain multiple system performance measurements from each simulation run. These measurements may include, for example, the total energy not supplied (ENS) over a year, the total number of hours with capacity shortfalls measured in event-hours, and the number of days with supply inadequacy events, expressed in event-days within a one-year horizon.

By performing a sufficiently large number of simulations under diverse operating conditions (generated through systematic sampling, as detailed in Section 2.2) these measurements will eventually converge to stable probability distributions, as illustrated in Figure 2.3, which presents illustrative distributions for:

- **UE (unserved energy or energy not supplied):** The total energy not supplied to the system during the year evaluated, measured in MWh
- **H (event-hours):** The total duration of supply shortfalls within the year, expressed as the number of hours in which unserved energy occurs (event-hours).
- **D (event-days):** The total number of days within the year during which at least one supply inadequacy event occurs, expressed in event-days.

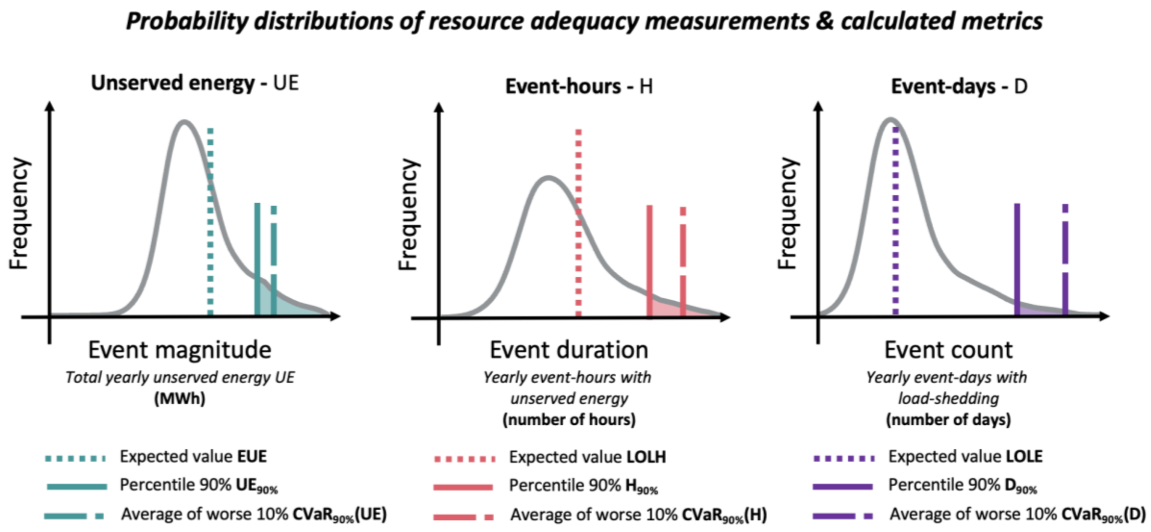

Figure 2.3: Illustrative example of multiple probability distribution of resource adequacy measurements and related average and tail metrics.

Adequacy assessments typically summarise these empirical probabilistic distributions through their expected (average) values, which correspond to the most widely used resource adequacy metrics. For instance, the mean of the UE distribution yields the Expected Unserved Energy (EUE). Likewise, the average of the distribution of event-hours, H, defines the Loss of Load Hours (LOLH), while the mean of the distribution of event-days, D, corresponds to the Loss of Load Expectation (LOLE).

In practice, these widely adopted metrics synthesise each probability distribution into a single average value, as illustrated by the dotted segments in Figure 2.3. Although such averages provide a compact and intuitive summary of system risk, they do not fully disclose the potentially broader spectrum of risk. In particular, the right-hand tail of the distributions, highlighted with lighter shading, contains the most severe realisations: years with the largest volumes of unserved energy or the most supply interruptions, measured in hours and days.

In fact, assessing the *tail risk* involves analysing and subsequently providing quantitative metrics that represent the outcomes of the "worst" conditions a system could experience. Conceptually, this involves asking: ***if the worst (100−α) % of system conditions were to occur, what level of impact would the system experience?*** This is answered by the Conditional Value-at-Risk ($CVaR_\alpha$), which measures the average outcome within the most severe (100−α) % of the distribution. Complementarily, the Value-at-Risk function identifies the threshold value VaR_α below which α% of outcomes lie, defining an exact bound between acceptable and extreme conditions.

As shown, tail metrics offer a powerful means of broadening the resource adequacy analysis by exposing high-impact events, thus enabling a more explicit characterisation of risk. Still, as highlighted in [12], it is important to understand that in systems with significant storage other energy-limited resources (e.g. demand response), both the duration and the severity of adequacy events depend strongly on how these resources are scheduled and optimised within the simulation framework employed. Therefore, the information tail metrics provide is strongly linked to the assumptions on the operating behaviours of these resources.

Finally, tail risk metrics can be applied in practice in two key ways. First, a tail metric reliability standard may complement an average reliability standard, resulting in a multi-metric system reliability criteria.

This has been explored in recent literature [16] and has historically been employed by the Belgian system operator Elia [17]. Second, reliability investment decisions for specific projects (e.g. transmission line expansion) may be evaluated based on changes in tail risk. A project that provides limited reduction in average risk may be justified by its benefits for tail events. This can be assessed through scenario comparison (with and without the investment) or by basing capacity accreditation on tail metrics (e.g. CVaR). Capacity accreditation approaches across different risk metrics are presented in the following section.

2.3.4 Metrics for assessing resource contribution to adequacy (capacity accreditation)

Resource adequacy metrics are the primary outputs of adequacy assessments, providing a quantitative view of system risk by capturing the size, frequency, duration, and timing of loss-of-load events. While these metrics characterise the adequacy of the system, or specific regions of a system, capacity accreditation focuses on the contribution of individual resources, or classes of resources, to improving overall adequacy. This contribution is commonly quantified through the Effective Load Carrying Capability (ELCC) or related approaches that determine the extent to which a resource can reduce system shortfall risk.

Table 2.4 summarises, based on [3], the key metrics used to assess resource-specific contributions, highlighting their purpose and interpretation in adequacy studies. As a complement, Figure 2.4 provides a conceptual illustration of the four probabilistic metrics used to assess resource contributions. The illustration considers introducing distributed energy storage (DES) as a new resource and the loss-of-load frequency (LOLF) as the resource adequacy metric to establish the baseline (LOLF of the system without DES). However, this approach can be followed under any average or tail risk metric described above, effectively quantifying the resource contribution towards the selected reliability metric.

Table 2.4: Metrics for assessing the contribution of resources to the system-level adequacy.

Computation method	**Resource contribution metric**	**Information provided and definition**
Probabilistic methods	Effective Load Carrying Capability *ELCC*	Amount by which the system load must increase when a resource (e.g. a battery storage system) is added to the system to maintain the same adequacy level.
	Equivalent Firm Capacity *EFC*	Amount of firm, fully reliable capacity needed (e.g. a fully reliable gas turbine) to replace the resource under assessment (e.g. distributed energy storage) while maintaining the same system adequacy level.
	Equivalent Conventional Power/Capacity *ECP/ECC*	Amount of capacity from a conventional dispatchable generating technology (e.g., a gas turbine) needed to replace the resource under assessment (e.g. distributed energy storage) while maintaining the same system adequacy level.

		The process for calculating the ECP is equivalent to the EFC, with the difference that the ECP procedure considers outages, derates and operational limitations for the resource under assessment.
	Equivalent Generation Capacity Substituted *EGCS*	Amount by which certain resource (e.g. energy storage systems or demand response) can displace conventional generation. This metric quantifies the capability of the resource to displace existing generation capacity when added to the system.
Capacity-based methods	Unforced Capacity *UCAP*	Amount of physical generating capacity available after accounting for a unit's forced outage rate (FOR).

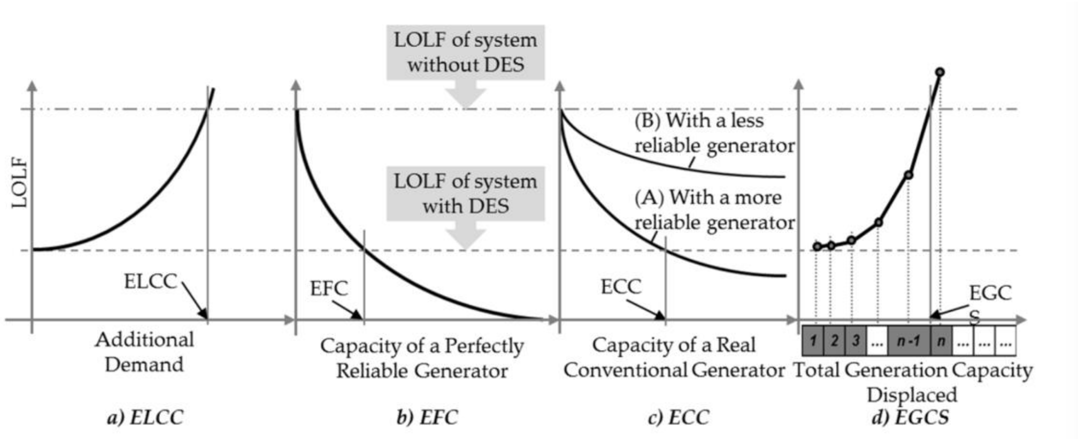

Figure 2.4: Conceptual illustration of the definition of metrics for capacity accreditation. Extracted from [18].

2.4 Key takeaways: Challenges and gaps for resource adequacy assessments and planning

This chapter outlined current methodological practices and metrics for resource adequacy (RA) and highlighted why innovation is necessary as power systems transition. The following points synthesise the key challenges and structural shifts that could justify the need for evolution, providing a summarised background for the upcoming chapters that aim to build upon these gaps.

- **RA methods should adapt to weather-driven, technology-diverse systems.** Australian power systems increasingly rely on variable renewables, distributed resources, and energy-limited technologies, all of which are heavily influenced by weather. There is a broad consensus that RA methods need to evolve; current simulation frameworks**,** behavioural assumptions, and metrics might not be fully fit for purpose [12], [19], [20], [21]. Fundamental questions lie in *how to effectively improve* these frameworks and *what implications* this could have for the optimal future resource mix. *[See Chapters 4,5 and 6]*
- **Energy adequacy needs to be assessed.** Australia is one of the world leaders in shares of DER and ESS, requiring adequacy assessments consider a component for energy adequacy. In fact, energy capacities are now much more limited (even for gas turbines, as fuel supply may become constrained), constantly varying, and driven, in most cases, by market drivers, which are not fully

captured in existing RA models. Improved methods are needed to represent this new class of risks and ultimately identify an optimal mix of different proportions of firm, variable and storage capacity to ensure power and energy adequacy. *[See Chapters 4,5 and 6]*

- **Multi-metric frameworks should become standard practice.** RA assessments relying on single metrics might not capture all reliability risks in power systems that are constantly evolving. Multi-metric approaches would measure how often, how long, and how severe adequacy events are and raise alerts for extreme risks. Naturally, as metrics inform decisions, an assessment across multiple metrics would allow identifying individual technologies and the mix of resources that is better equipped across various dimensions of adequacy (e.g., a mix that it robust across event frequency, magnitude and duration). *[See Chapter 6]*
- **Flexibility from energy-limited and demand-side resources requires proper characterisation.** Utility-scale and distributed storage, electric vehicles, heating and cooling systems, electrolysers, and data centres are becoming more widespread and increasingly signal-responsive participants in the system. Their ability to contribute to adequacy depends on where they are located, how they operate over time, their technical constraints, and the incentives they face. Capturing this flexibility realistically—through data, modelling, and behavioural assumptions—is essential if planners are to harness its reliability and economic potential. *[See Chapters 4 and 5]*
- **Stress testing for extreme, correlated weather events should complement probabilistic RA.** High-impact, low-probability events—such as prolonged VRE droughts or severe weather-related disruptions—can expose vulnerabilities that average-based metrics and standard sampling techniques may dilute or hide. Such events should be explicitly modelled in adequacy studies. Systematic stress-testing frameworks and parametrised scenario analysis can help identify hazards and thresholds, reveal fragile operating points of the system, and inform mitigation strategies, thereby strengthening regulatory preparedness beyond what standard probabilistic assessments alone might provide. *[See Chapter 7]*

3 Open-source toolkit for assessing and studying resource adequacy

A critical factor in ensuring the success and accuracy of adequacy assessments is the use of data and software tools with suitable capabilities to evaluate risks within the region and the specific study context. Under this premise, a substantial portion of this research project is dedicated to developing and deploying open-source software tools to generate datasets and build models to assess resource adequacy in the National Electricity Market.

The software developments under this project are consolidated into a suite of fully open-source tools intended for industry practitioners, researchers, and professionals at large. This suite, accessible at https://github.com/ARPST-UniMelb, comprises four independent packages: **ParseISP.jl**, **PRASNEM.jl**, **SiennaNEM.jl**, and **SchedNEM.jl**, which are interoperated via the **NEM-reliability-suite**, also available at the link provided. Overall, these tools facilitate the generation of datasets and models of the East Coast Australian power system for conducting adequacy and operability analyses. An overview of each package is provided below.

3.1 Parser of the Integrated System Plan (ParseISP.jl)

ParseISP.jl stands for Parser of the Integrated System Plan (ISP). It is a data-parsing toolkit written in the Julia programming language that generates datasets for planning and reliability studies of the Australian East Coast Electricity System, based on AEMO's workbooks for the 2024 ISP and the Inputs, Assumptions and Scenarios Report (IASR) [22]. ParseISP allows the generation of datasets containing technical parameters for conventional and renewable generation, transmission, storage, and distributed energy resources, as well as hourly-granularity generation traces of utility-scale and distributed solar, wind, and hydro inflows and electricity demand. The open-source package can be accessed at https://github.com/ARPST-UniMelb/PISP.jl.

3.2 PRAS model of the NEM (PRASNEM.jl)

PRASNEM.jl is the modelling framework for conducting large numbers of time-sequential operational simulations of the NEM under various outage scenarios. It is built upon the Probabilistic Resource Adequacy Suite (PRAS) [23], which is developed and maintained by the National Laboratory of the Rockies (NLR, former NREL), USA. PRAS is a dedicated adequacy assessment engine that performs highly efficient sequential Monte Carlo sampling of infrastructure outages whilst tracking the state of charge of storage devices in the system. PRASNEM.jl provides the features and interface to enable these effective adequacy studies of the NEM**.** The open-source package can be accessed at https://github.com/ARPST-UniMelb/PRASNEM.jl. The main capabilities of the modelling framework PRASNEM.jl are:

- Creating detailed PRAS models of the NEM, based on data generated by ParseISP.jl. This includes representing static parameters such as capacity limits of generators, storage devices, and transmission lines, failure and repair rates, as well as time series of VRE production, water inflows into hydro reservoirs, and demand.
- Updating PRAS models of the NEM to enable custom adequacy studies, including by updating storage dispatch assumptions, as further detailed in Chapter 4.

- Providing functions to analyse and process results from PRAS simulations of the NEM, including aggregation by state, as well as synthesising event-level details.

3.3 Sienna model of the NEM (SiennaNEM.jl)

SiennaNEM.jl is a modelling framework for detailed system operation studies through optimising production cost modelling (PCM), written in the *Julia* programming language [24]. It is grounded in the Sienna modelling framework [25] and supplied with datasets via ParseISP.jl. It is designed to perform detailed scheduling analysis of the Australian east-coast electricity system by enabling the construction and solution of economic dispatch (ED) and unit commitment (UC) models.

The framework accommodates a large number of technical constraints, including ramping and minimum online and offline times of generators, time-coupled operation of energy-limited resources and options for managing renewable generation outputs. The PCM optimisation problem is formulated using *JuMP* [26] and can be extended with other optimisation formulations. It also provides post-processing, data analysis, and visualisation capabilities to deliver high-quality insights from model outputs. SiennaNEM.jl benefits from Sienna's broader modelling ecosystem, allowing users to extend the provided base for the east-coast Australian electricity system to perform studies using other Sienna features. The open-source package can be accessed at https://github.com/ARPST-UniMelb/SiennaNEM.jl.

3.4 Operational time-sequential framework of the NEM (SchedNEM.jl)

SchedNEM.jl is an optimisation-based power system scheduling framework, designed to perform efficient system scheduling with inter-temporal constraints required for capturing storage and DER operational details. The core of the tool is a fast and flexible cost minimisation optimisation setup in the programming language *Julia* [24] using the optimisation package *JuMP* [26]. The open-source tool can be found here: https://github.com/ARPST-UniMelb/SchedNEM.jl.

While SiennaNEM.jl is equipped with extensive scheduling capabilities and detailed operational representation, SchedNEM.jl is designed to be lightweight, fast, and easily customisable, with a specific focus on core operational constraints. In the context of this work, such characteristics allow SchedNEM.jl to be used as a complement to PRASNEM.jl, allowing to capture a greater number of operational details relevant for assessing resource adequacy, including storage operation and unit commitment. Specific capabilities of SchedNEM.jl are:

- SchedNEM enables users to set up a unit commitment optimisation model based on a PRAS system model (for example generated by PRASNEM). Additional parameters such as costs or technical constraints are taken from the data generated by ParseISP.jl. The formulation allows to represent various technical constraints such as generation limits and ramping constraints, inter-temporal storage energy conservation, and demand response constraints.
- The objective function of the optimisation framework is to minimise system operation costs for a given horizon (which includes generator production and commitment costs, as well as load shedding costs). The main decision variables include generator outputs and commitment status, storage operation decisions, and interconnector flows. In order to speed up computations, the binary unit commitment variables can be relaxed linearly, in line with [27]. The full mathematical formulation of SchedNEM.jl can be found in 9A.2.

- The model is designed for performing efficient rolling horizon simulations, with updating key parameters in each iteration, which is embedded in one function to allow intuitive handling of the package. The core setup is to create a JuMP model first, which is then iteratively updated from the PRAS parameters (e.g. VRE availability and demand), carrying forward the unit commitment status and storage levels.
- Furthermore, SchedNEM includes capacities to read out key results, as well as to visualise scheduling outcomes of the optimisation to allow detailed investigation and understanding of operational details.

3.5 NEM reliability suite

The **NEM-reliability-suite** is a code repository that integrates the described packages. It contains the scripts that, from a user perspective, coordinate the developments described above to generate datasets and run case studies. Its objective is to provide examples of use and transparent code to enable the replication of studies conducted within this project. Figure 3.1 summarises the package management architecture within the NEM-reliability-suite.

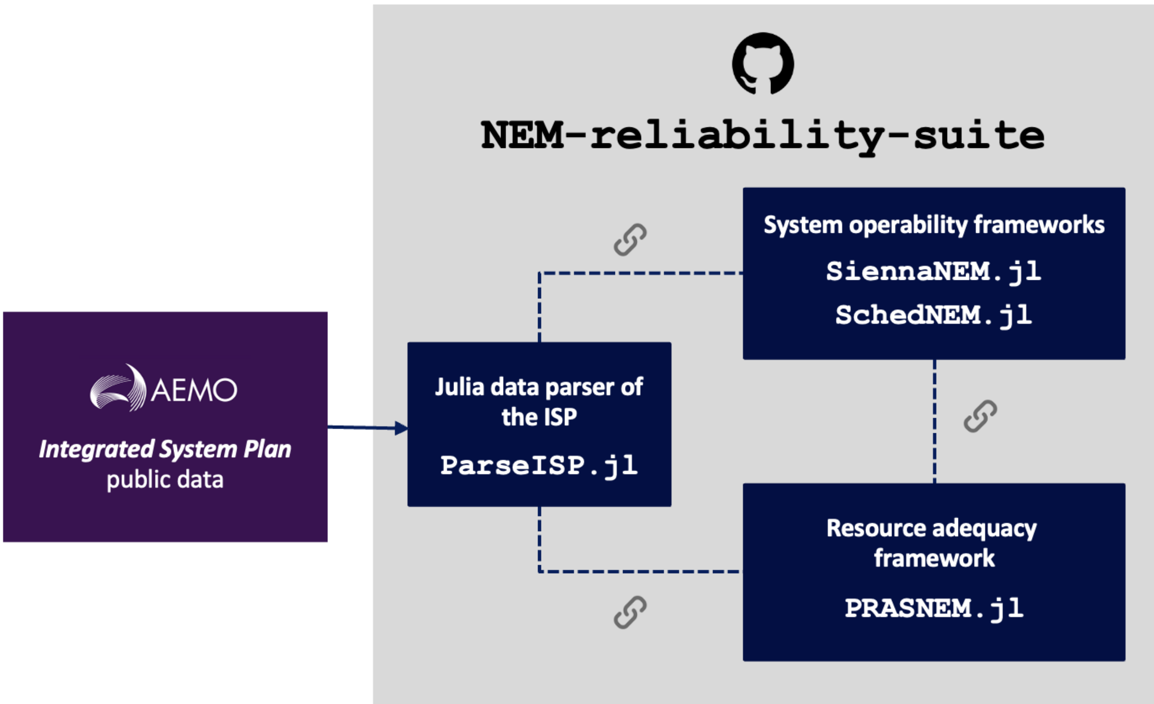

Figure 3.1: General overview of the NEM reliability suite architecture.

4 Energy storage for adequacy of supply

Energy storage, in general, encompasses technologies that can store energy for use at a later time. In the context of resource adequacy, storage systems are typically classified either by size (distributed or large-scale) or by storage duration (short-duration or long-duration).

Large-scale storage includes technologies connected to transmission systems that directly participate in the electricity market. This includes utility-scale batteries and pumped hydro storage systems, which can contribute to adequacy by charging from large-scale renewable energy and are therefore typically included explicitly as supply resources [28]. On the other hand, distributed storage units located in the distribution system, including behind-the-meter installations, may not have direct access to market resources and may be limited by distribution network constraints. Therefore, their operation may be captured within the demand traces without the potential to participate in the market and hence without access to large-scale generation for charging [18].

The duration of a storage describes how long a fully charged storage unit would be able to discharge at its maximum power, i.e. describing the ratio between energy and power capacity [29]. Although the distinction is not mutually exclusive, a common one is to group storage with up to 6 hours of duration as short-duration storage (mainly battery energy storage systems, BESS), compared with long-duration storage, which typically includes pumped hydro energy storage (PHES)[12] [29]. However, other researchers argue to differentiate at the 10-hour mark or more [30]. With regards to adequacy, the general distinction is insightful since short-duration storage might be fully depleted within a specific loss of load event [31], while long-duration storage is limited rather across multiple risk days and potentially even seasons [32].

Numerous studies demonstrate the value of all types of storage for adequacy of supply [33], and therefore storage has been included in various adequacy evaluations in the literature [34]. Already in 2005, Bagen and Billinton [28] show that storage can contribute to adequacy of supply in systems with variable renewable energy (VRE). Since then, various papers have addressed the challenge to quantify the potential of storage to support adequacy of supply. This task is not straightforward, since storage (without energy inflows) is not able to serve demand *in isolation* and can only support adequacy by shifting energy supply from other sources in time [35].

Looking at distributed units, the contribution of storage to adequacy of supply mainly stems from reducing (peak) demand. While this can be effective in supporting adequacy, its overall contribution may be limited by the fact that it can lead to periods with sustained high demand if it is operated to shift demand from the peak to time periods just before or after the peak period [36]. Furthermore, if connected to distributed solar generation, contribution to adequacy might be limited by the amount of solar PV energy available on days with critical peak demand if this is the sole charging opportunity [18].

From the perspective of large-scale storage, the possibility of charging from large-scale energy generation through the market enables storage units to increase the level of adequacy of supply of a given system. This has been observed in modelling when adding battery storage to a system with PV generation [37], [38], wind generation [39], [40] and multiple technologies [41]. Here, the contribution

[12] Hydro power stations might have additional natural inflows, which increase their contribution to adequacy of supply since they allow operation as generators in the traditional sense.

of storage lies in shifting the excess energy from these generators from times of abundance of generating capacity to critical periods in which the generators themselves might be limited (e.g. low wind). Therefore, when considering generation investments, storage can unlock additional adequacy contribution of the technologies, which means that investments for adequacy should always be considered as a portfolio rather than the different technologies separately [5], [42]. Otherwise, if investments are only considered for selected technologies separately, the marginal contribution to adequacy would decline with additional capacity. For example, if increasing levels of wind power generation are added to a given system, the risk shifts to periods of low wind production, and adding more wind power generation is less beneficial for adequacy than adding storage to shift wind power to the critical hours. This has been observed throughout the literature [43], [44], [45].

Furthermore, the value of the contribution of storage to adequacy of supply is dependent on the evaluated adequacy metric. Sun et al [37] notice that adding storage to a system shifts the timing and the frequency of loss of load events, and highlight that multiple adequacy metrics are needed to fully capture the benefits of storage to adequacy of supply. Along the same lines, Liu et al. [45] demonstrate that the capacity credit of storage might not increase if a frequency-based metric is used instead of an energy-based metric. Therefore, it is important to evaluate adequacy under multiple metrics to fully understand the risk and benefits of storage.

In general, the contribution of storage to adequacy is fundamentally defined by its capacity and energy available to discharge in critical periods. There are a range of factors, that can be roughly grouped into exogenous factors such as equipment failures and weather conditions, as well as operational factors such as profit oriented discharging, that may leave energy levels of storage lower than optimal for adequacy. While exogenous factors are typically included in adequacy assessments (e.g. AEMO models storage outages in the ESOO [7]), operational factors remain largely neglected across the industry and academia. In the following, the effect of imperfect operation on the contribution of storage to adequacy of supply is explored in detail, before modelling approaches are discussed and compared with industry standards.

4.1 Literature review on the effect of imperfect operation

To support resource adequacy, the theoretically best strategy is to charge a storage unit whenever possible and only discharge to avoid loss of load events. This charging strategy is commonly assumed for adequacy contribution calculations across the literature [23], [32]. However, the actual charging behaviour of storage might be imperfect with regards to adequacy purposes, leading to reduced state of charge of storages in the lead up to potential critical periods compared to optimal operation under perfect foresight. In general, it is assumed that critical periods would eventuate in a high-enough incentive for storage to discharge [46]. However, if the critical period is not anticipated beforehand, storage might not be able to operate in an adequate-supporting manner.

We therefore define ***imperfect operation*** and ***imperfect energy levels*** in this work as any storage operation and its corresponding energy levels which deviate from a purely adequacy-oriented operation, i.e. not keeping the highest technically possible state of charge during normal system operation (in the absence of load shedding). Therefore, *imperfect* is considered purely from a reliability point of view, acknowledging that the perfect adequacy operation might not be “perfect” for economic cost-minimising objectives.

The main reason for a lower state of charge of storage units than desired for adequacy purposes is scheduled market participation of storage units: If a storage unit is discharging due to market incentives with not enough knowledge or incentives to have energy available for a critical period, its contribution to adequacy will be reduced [44], [47], [48].

We have identified the following drivers of imperfect energy levels which have been described across the literature. An overview of the drivers, as well as potential modelling approaches can be found in Table 4.1.

1) **Unknown outages:** Imperfect foresight of future random outages may limit the contribution of storage to adequacy. Dratsas et al [38] study this effect by simulating market participation of storage units before sampling outages of thermal generators. The authors observe that lack of knowledge of future system conditions results in higher loss of load levels and therefore lower storage contribution to adequacy of supply, especially for storage units with shorter durations.

2) **Unanticipated weather conditions:** In a renewables-based system, imperfect foresight might also arise from unanticipated weather conditions, which limit storage contribution to adequacy. Boegheim [44] illustrates this through a case study of NEM conditions, modelling the dispatch of a pumped-hydro power plant ahead of low VRE conditions. The author observes significant unserved energy when restricting modelled foresight of future weather conditions.

3) **Misaligned risk and price incentives:** Perfect operation from an adequacy point of view is aimed at minimising load shedding, hence operating storage units risk-averse, disregarding potential economic operation costs and prices in the market. However, risk-neutral independent storage operators are not faced with the impact of load shedding events, therefore focusing on price incentives. Therefore, high prices during charging periods may also reduce the adequacy support of storage, as recently observed on 24 August 2025 in the South-Western Interconnected System (SWIS) in Western Australia. Due to high prices and uncertain future price and lack of reserve conditions, storage units were charged to only approximately 50% ahead of a high system peak in the evening, prompting the system operator to force storage units to increase state of charge [49].

4) **Early discharging to secure profits:** Analysis of real battery operation in the NEM by Grover [50] shows that during a recent high-price event, battery storage units tended to discharge early to avoid forgoing profit opportunities, resulting in less available storage energy later. This has also been observed by Yang et al [51], who analysed storage operation against perfect foresight and noted large discrepancies in storage operation, particularly due to early or limited discharging during high-price periods.

5) **Limited lookahead horizon:** The impact of a limited foresight length on storage operation has been described by Stephen et al [32] as well as Guerra et al [52]. The authors observe a large decline in adequacy contribution when storage dispatch is modelled without long-term foresight, which is especially critical for long-duration energy storage.

6) **Insufficient forecast data quality:** However, the forecast quality of longer-term foresight may also limit system adequacy, as observed by Sun et al [37], highlighting that longer foresight is not always beneficial for adequacy. In a NEM case study, Prakash et al [53] describe the

limiting factor of foresight quality in the context of price development and battery rebidding, which they observe has increased significantly in recent years.

7) **Misaligned discharging objective:** Short-duration storage discharge objectives during an energy shortfall may be misaligned with adequacy metrics or goals. Gonzato et al [31] investigate the discharging behaviour of a single short-duration storage unit during a shortfall. Through illustrative studies, they show that depending on the storage operation objective (e.g. minimise peak, minimise length), different adequacy results may be obtained due to discharging behaviour. This is especially the case for non-energy metrics such as LOLH and LOLE, which has also been observed by Dratsas et al when comparing perfect foresight with other adequacy-aware methods [44]. This is particularly critical for short-duration storage, which may be energy-limited during the critical periods itself.

8) **Uncoordinated discharge of multiple storage units:** In systems with multiple heterogeneous storage units, imperfect discharging strategies become even more critical. Edwards et al [54] investigate different strategies of short-duration storage units and note that misaligned discharging could lead to scenarios where, in case of shortfall, not all capacity may be available even though sufficient energy is stored. This challenge has also observed by other authors across the literature [55], [56].

9) **Provision of system services or reserves:** If storage provides system services or reserves, this can influence its operation and therefore its ability to mitigate loss of load [57]. For example, if a storage unit is providing upward reserve, it must maintain a headroom to respond, effectively reducing its maximum state of charge.

Under real conditions, large-scale short-duration storage discharging strategies are diverse, as can be observed in the Australian NEM. As Grover [50] describes, whilst diverse discharging strategies mean that various storage units operate somewhat complementarily, their operation can adapt quickly and operators change their discharging strategies dynamically based on other storage operation. Similarly, Yang et al [51] analyse storage operation against perfect foresight and note large discrepancies in both storage operation and profits. This highlights the need for accurate representation of storage operation in adequacy studies. In the following, modelling approaches to address imperfect operation are presented.

4.1.1 Modelling Approaches in the Literature

Storage operation could be somehow included in traditional convolution-based adequacy assessments by considering historical operation patterns (see e.g. [58], [59]). However, since probabilistic sequential Monte Carlo based approaches are better suited to capture time-sequential storage and DER operation, and are established across literature and industry [5], [6], [34], we focus on storage representation in this method.

In sequential MC adequacy assessments, common approaches for storage modelling are **perfect foresight** (e.g. [37], [39], which is also the most common in industry; see below), as well as **greedy management** (charging whenever possible, discharging only when needed) (e.g. [23], [32], [42], [56], [60]). However, as mentioned above, these approaches focus on adequacy-aware operation and do not capture imperfect operation, leading to overestimates. To address imperfect adequacy contribution of storage with regard to operation, multiple different methods are proposed in the literature.

Determining storage operation before changing system conditions (**expectation dispatch**) could address limited knowledge of future states within adequacy modelling. This approach is proposed, for example, by Zhou et al [36] who consider distributed storage operation with peak load minimisation, then apply the storage schedule to the net-load curve before determining outages via Monte Carlo sampling. A similar approach is employed by Stephen et al [32], who optimise storage to minimise net-load peaks before sampling outages.

To further introduce market based imperfect operation of storage, a **market-based dispatch** can be employed before sampling system conditions. This approach is used, for example, by Liu et al [45], who calculate the optimal system dispatch in a unit commitment least cost problem, before passing the net-load curve to the Monte Carlo sampling. Multiple further works in the literature determine the storage schedule based on minimum system cost optimisation [18], [44], [45], [61]. While profit driven operation of actors could be additionally implemented for example via complementarity [62], or agent-based modelling [63], the desire to evaluate a comprehensive set of scenarios limits this application due to computational complexity.

Additionally, to represent a limited foresight length, **rolling horizon** optimisation can be employed. Stephen et al [32] implement this by comparing a 24-hour rolling horizon with 1-hour steps approach with the *greedy management* or *expectation dispatch* modelling. Rolling horizon dispatch is also proposed by Sun et al [37], who perform a rolling horizon optimisation with 24-hour steps and combine perfect foresight (of outages) within the day with imperfect lookahead for hours 24-36 within the simulation. Addressing forecast data quality, the authors further propose using **forecast errors** when determining the system dispatch. The authors specifically employ imperfect solar power production for scheduling the system, including storage within hybrid plants. Whilst the rolling horizon scheduling can be powerful in representing limited knowledge of the future, its implementation within adequacy assessments is limited by its computational complexity due to potentially many optimisation runs [32].

Considering the potential misalignment of the discharging objective of the storage unit with the adequacy metric, Gonzato et al [31] suggest that modellers should explicitly and transparently describe the selected storage operation. This is particularly relevant for assessments of non-energy-based metrics such as duration of shortfalls (LOLH).

To address the discharge of multiple storage units, multiple heuristic approaches have been proposed. Evans et al [55] propose a mathematical optimal approach to discharge storages based on their potential longest discharging time first in every timestep. This approach is implemented in the adequacy assessment engine PRAS [23]. However, to simulate imperfect and uncoordinated discharging, other approaches could be employed. Edwards et al [54] propose to dispatch storages *proportional to their energy levels,* which aims at providing equal discharging so that no storage is depleted first. Alternatively, Zachary et al [56] propose to discharge heterogeneous storage units based on roundtrip efficiency to maximise available energy at any time.

An overview of the drivers of imperfect operation of storage and potential modelling approaches can be found in Table 4.1. The next sections will address details of modelling specifically with regards to balancing storage operation and capturing long-duration storage, before reviewing current industry practice.

Table 4.1: Drivers of imperfect storage operation and proposed modelling approaches.

Category	**Driver of imperfect operation**	**Potential modelling approach**
Uncertainty	Unknown outages [44]	***Expectation dispatch*** [32] Determine adequacy-driven operation before sampling system conditions
	Unanticipated weather conditions [64]	
Markets	Misaligned risk and price incentives [49], [53]	***Market-based dispatch*** [44] Determine profit-driven operation before sampling system conditions
	Early discharge to secure profits [50]	
Forecasting	Limited lookahead horizon [32]	***Rolling horizon*** [32] Limit lookahead of storage optimisation
	Insufficient forecast data quality [37]	***Forecast errors*** [37] Use erroneous forecasts for dispatch
Coordination	Misaligned discharge objective [31]	*Explicitly describing discharging objectives (e.g. min peak, min duration)*
	Uncoordinated discharge of multiple units [54]	***Proportional dispatch*** [54] Dispatch storages based on state of charge
Services	Provision of system services or reserves [57]	*Explicit modelling of reserve requirements* [18]

4.1.2 Balancing conservative and optimistic storage operation for adequacy

Whilst the above approaches can address specific aspects of imperfect storage operation, the modelling choice can significantly influence modelling results, which could potentially reflect a very conservative view compared to the optimistic assessment using perfect foresight or greedy management. This has been described by Stephen et al [32] and can be clearly observed by looking at the state of charge of the battery across different samples (see Figure 4.1). Here the authors describe the largely different state of charge when using rolling horizon (bottom), compared to greedy management (middle) or expectation dispatch (top).

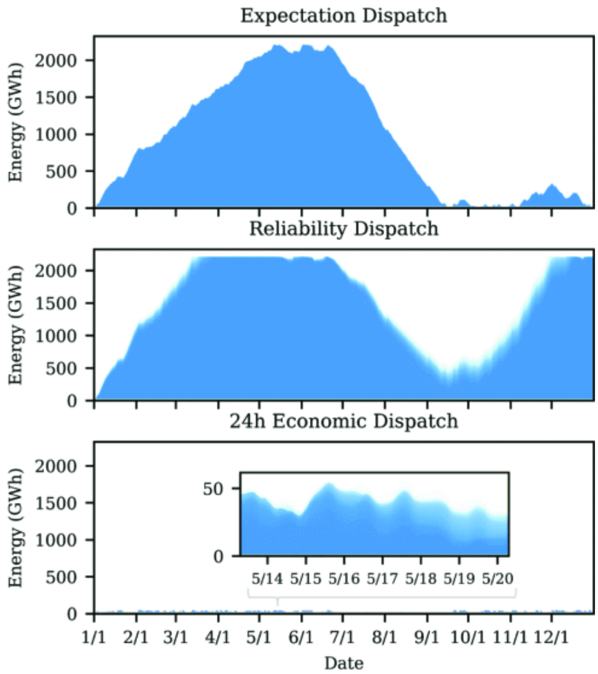

Figure 4.1: State of charge of storage under different operation assumptions. Note that "reliability dispatch" corresponds to the greedy management described above, and "24h Economic Dispatch" results from a rolling horizon with 24 hour window. The bottom figure includes a zoomed in section to show the energy levels which are consistently low across the whole year. Taken from Stephen et al [32].

While an expectation dispatch can help address imperfect storage operation, it might be overly pessimistic for storage operation, due to the modelled inability to react to changing system conditions. In a market context, critical hours are expected to result in high prices to which storage would react in real-time if allowed by the market rules. For example, in the Australian NEM, storage units regularly perform rebidding based on updated market expectation [53].

This has been described by Dratsas et al [44] and can be seen in Figure 4.2. Whilst the market-based expectation dispatch (labelled "fixed schedule") exhibits the highest levels of loss of load hours, perfect foresight and greedy management show the "optimistic" adequacy-aware operation results. To find a more realistic adequacy operation, the authors propose **real-time redispatch,** which they present as a combination of expected dispatch (with adequacy or market-oriented objective based on a parameter), as well as a contribution of storage to respond to randomly sampled thermal generation outages.

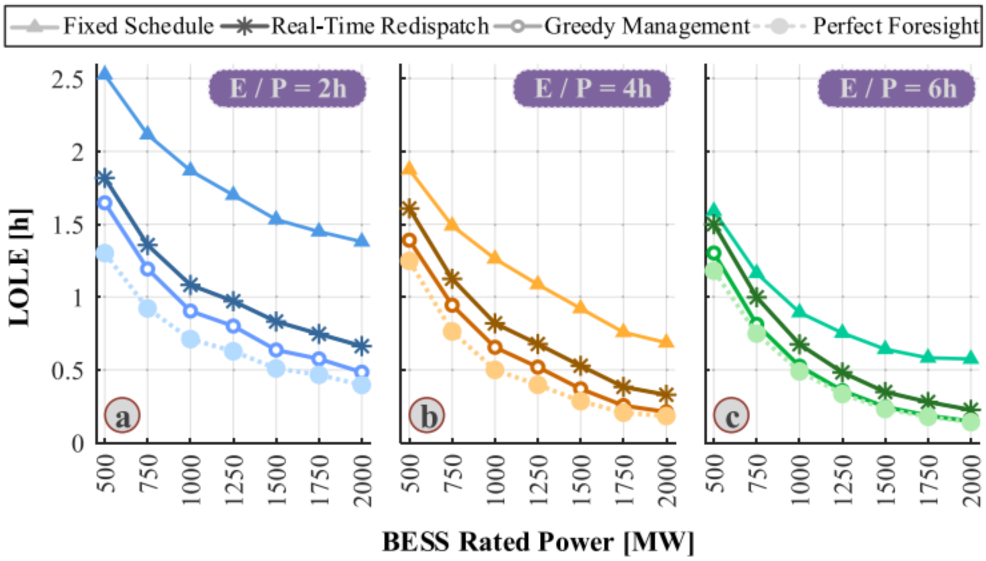

Figure 4.2: Comparison of different storage operation modelling and its impact on adequacy results. Note that "fixed schedule" corresponds to "expectation dispatch" with cost minimisation objective. Taken from Dratsas et al [44].

In Figure 4.2, note that the difference between perfect foresight and greedy management arises only because of the adequacy metric: if an energy-based metric had been chosen, these would exhibit the same adequacy levels. This highlights again the importance of using multiple metrics to properly capture the impact of storage [37].

Two further methods aim to capture storage operation in a trade-off between adequacy-focused operation and expectation dispatch, if capacity markets and non-performance penalties are present. To include anticipatory storage operation for adequacy, Kim et al [65] propose a stochastic-dynamic-optimisation approach in which storage operation is optimised based on price expectations and LOLP levels in future time-steps, with penalties for non-performance in reliability events. With similar considerations regarding reliability-aware operation, Qi et al [47] propose a storage operation modelling algorithm for reliability that considers strategic capacity withholding in normal market operation but includes capacity market calls (i.e. redispatch) when shortfalls arise. Whilst these methods are advanced in storage scheduling, they are computationally intensive and therefore only limitedly compatible with MC sampling.

4.1.3 Long duration storage considerations

As can be seen in Figure 4.1, seasonal patterns might be missed if the foresight length of storage is reduced. However, since hydro power stations and other long-duration storages might anticipate the seasonal risk periods, these patterns need to be included in adequacy modelling.

In general, if the whole simulation horizon is simulated at once (e.g. a whole year), seasonal risk would be captured by long-duration storage dispatch [32]. This is also regularly done in adequacy assessments (e.g. [44], [45], [61]). However, this may be overly optimistic, given uncertainty and limited knowledge of future system conditions [32], [37].

On the other hand, a *rolling horizon* approach with long-term lookahead might be most realistic to capture long-duration storage dispatch. There is extensive research on hydro-power scheduling under uncertainty, including considering decision-dependent uncertainty (DDU) via stochastic dual dynamic programming (SDDP) [66]. However, including detailed scheduling under uncertainty with long foresight horizons is not feasible for extensive adequacy assessments due to the high computational burden [52]. Therefore, approximations are necessary. Guerra et al [52] describe different approaches in the literature to dispatch long-duration storage under a rolling horizon optimisation, namely extended optimisation horizons, pre-determined end volume targets, assigning stored energy value and variable time step optimisation. They observe an increase of capacity credit of 14% - 34% when implementing these different scheduling assumptions, compared to no additional long-duration storage considerations, showcasing the need for nuanced modelling of long-duration storage.

Overall, longer foresight is required for the dispatch of long-duration storage in adequacy assessments [32]. However, no best practice methodology has been identified in the literature. The differences in dispatch approaches can also be seen in the following overview of industry approaches of storage operation.

4.1.4 Industry approaches for storage operation

The common approach by system operators and planners around the world to include storage in their adequacy assessments is based on perfect foresight operation, in combination with additional long-duration storage constraints. An overview of selected system operators can be found in Table 4.2. While this overview is non exhaustive, it can provide some insight into different approaches and the current state of adequacy modelling in industry.

Table 4.2: Overview of practices of selected system operators and planners around the world.

Country (Organisation)	**Report**	**Storage penetration level (% total installed power capacity)**	**Short-duration storage modelling**	**Dispatch horizon**	**Additional long-duration storage considerations**	**Risk drivers explicitly addressed**	**Additional imperfect foresight constraints**
Europe (ENTSO-E)	European Resource Adequacy Assessment (ERAA) [67]	BESS 2% Hydro 17% (2025) [68]	Perfect foresight	Daily - weekly	Reservoir level limits	Forecasting (limited foresight length)	-
United Kingdom (NESO)	Resource Adequacy in the 2030s [69]	BESS 12% Hydro 5% (2025) [68]	Perfect foresight	2 days	Uncertain future pathways	Forecasting (limited foresight length)	-
Ireland (Eirgrid)	All-Island Resource Adequacy Assessment (AIRAA) [70]	BESS 7% Hydro 5% (2025) [70]	Perfect foresight	Daily - Weekly	Pre-optimised energy targets	Forecasting (limited foresight length)	-
Germany (BNzAg)	Versorgungs-sicherheit Strom Bericht 2025 [71]	BESS 1% Hydro 5% (2025) [68]	Perfect foresight	Year	No	-	-
Belgium (Elia)	Adequacy and Flexibility Study 2026-2036 [72]	BESS 1% Hydro 4% (2025) [73]	Perfect Foresight	Weekly	No	-	-
USA/Canada West (WECC)	Western Assessment of Resource Adequacy (WARA) [58]	BESS 5% Hydro 23% (2024) [74]	*Historical hourly distributions of storage dispatch*	N/A	N/A	*Historical behaviour may capture markets, forecasting, coordination and services*	-

USA/Texas (ERCOT)	NERC Long-term reliability assessment [75]	BESS 8% Hydro <1% (2024) [75]	*0% capacity credit (will be changed to ELCC in the future)*	N/A	N/A	N/A	N/A
USA/East (PJM)	2025 PJM Effective Load Carrying Capability and Reserve Requirement Study [76]	BESS 3% Hydro 1% (2026/27) [76]	Greedy management *(Discharge longest duration first, charge proportionally to capacity)*	Hourly	No	-	-
Indonesia	Indonesian Electricity Company planning reports (RUPTL [77]) and Indonesia's National Energy Plan (RUKN [78])	BESS 0% Hydro 0% (2025) [77]	Static constant schedule in hybrid with PV setup for future developments	N/A	N/A	-	-
Chile	Chilean Power Generators Bulletin [79] Chilean Law (Decree 70) [80]	BESS 5% Hydro 19%	Fixed capacity credits depending on duration	N/A	LOLE is calculated assessing various hydrological traces	-	-
Australia/NEM (AEMO)	NEM Electricity Statement of Opportunities (ESOO) [7]	BESS 10% Hydro 10% *(WEM for reference: BESS 18%, Hydro 0%* (2025) [81]	Perfect foresight	Weekly	Pre-optimised energy targets	-	Energy capacity derating of short-duration storage

In the continental **European** adequacy assessment, ENTSO-E considers the contribution of storage to adequacy of supply through the European Resource Adequacy Assessment [67]. Short-duration storage is modelled with perfect foresight, whilst long-duration storage in the form of pumped-hydro energy storage (PHES) is subject to additional reservoir limits to ensure seasonality.

In the **United Kingdom's** resource adequacy assessment [69], short-duration storage operates within a two-day horizon with perfect foresight, whilst long-duration storage is managed through providing the model with multiple future pathways. This approach incentivises the optimisation model to avoid full discharge over the two-day scheduling horizon.

In **Ireland and Northern Ireland** [70], system operators include storage through optimising its operation with perfect foresight. Long-duration storage is pre-optimised to obtain weekly energy targets, which then serve as soft constraints within the short-term dispatch module.

The **German** national resource adequacy report [71] optimises storage operation over the entire outage sampling year, thereby capturing perfect foresight of both short-duration and long-duration storage.

The **Belgian** system operator Elia is also considering storage with perfect weekly foresight within its adequacy studies [72]. Long-duration storage is not explicitly mentioned.

In **North America**, the North American Electric Reliability Corporation (NERC) compiles annual resource adequacy reports based on various regional assessments [75]. Reliability is generally assessed using planning reserve margins, though recently extended to probabilistic metrics such as expected unserved energy (EUE) and loss of load hours (LOLH).

In the **American western interconnection (WECC)** [58], adequacy assessment employs a convolution-based method that probabilistically combines resource availability and demand to quantify "demand at risk". Long- and short-duration storage is included based on historical operation distributions at hourly resolution, which is then matched against the hourly demand distribution.

Within the **eastern connection in the US, PJM** [76] assesses adequacy using hourly sequential Monte Carlo sampling with storage operated under "greedy management". Discharging is modelled only in case of shortfall based on storage size, whilst storage is charged whenever possible at rates proportional to storage capacity.

For the **Texas** power system, resource adequacy is assessed through sequential Monte Carlo simulations using the software SERVM [75], which doesn't document its internal storage operation publicly. However, ERCOT currently assigns a 0% reliability contribution to battery energy storage for planning reserve margin purposes.

Indonesia currently has no grid-scale energy storage systems. Future storage operation remains speculative and depends on modelling assumptions. In resource adequacy and planning studies, the system planner PLN considers storage either as standalone units or as hybrid plants with solar PV generation [77]. In hybrid plants, storage is modelled to flatten solar PV output, making the combined power output follow a constant baseload profile. Standalone plants are considered to operate as peak shavers

In **Chile**, resource adequacy is assessed through a capacity margin approach. Within this, the regulatory framework [82] formalises the capacity contribution of utility-scale battery storage through a duration-based recognition scale. Under this methodology, firm capacity credits are tiered to reflect their contribution to resource adequacy: 1-hour systems receive a 36% credit, 2-hour 65%, 3-hour 85% and 4-hour 98%. Full 100% recognition is reserved for long-duration storage of 5 hours or more.

In **Australia,** AEMO considers storage in its key NEM adequacy modelling report, the Electricity Statement of Opportunities (ESOO) [7]. Long-duration storage is first optimised to obtain weekly energy targets to capture seasonal uncertainty. Subsequently, within weekly intervals, short-duration storage is optimised to operate with perfect foresight. To address imperfect foresight of battery storage, derating is applied to the energy capacity of the storage units (-50% for <1.5h storage, -25% for 1.5h to 3.5h storage, -10% for 3.5h to 7.5h storage).

Across these jurisdictions, a diverse range of storage operation modelling approaches is evident. Most assessments employ perfect foresight for short-duration storage, though with varying time horizons (from two days to one year). Long-duration storage is typically managed through additional constraints or pre-optimisation to capture seasonal patterns. However, the treatment of imperfect foresight varies significantly: whilst some jurisdictions apply derating factors (Australia), others rely on historical distributions (WECC), and some do not yet formally recognise storage contributions (ERCOT). The heterogeneity in approaches and the predominant absence of imperfect operation modelling underscore both the technical complexity of realistic storage representation and the lack of consensus on best practice methodology, highlighting the critical need for advanced and transparent storage modelling assumptions in adequacy assessments.

4.2 Research questions

To systematically evaluate the effects of imperfect storage operation for system reliability and resource adequacy, we are investigating the following research questions:

1. What methodology allows capturing the uncertainty associated with energy storage operation in adequacy assessments?
2. How large is the risk related to the uncertainty of storage operation in a system with high storage penetration?
3. How does reliability risk change with increasing penetrations of storage in a transitioning system?

These research questions guide the development of the methodology, case study setup, and insights in this chapter, which are discussed below.

4.3 Modelling approach for energy storage

Building on the insights from the literature review, the storage modelling approach adopted in this work focuses on explicitly representing the (i) *imperfect foresight of storage* units and their (ii) *responses to evolving system conditions*. As discussed above, both aspects must be modelled to appropriately balance the trade-off between overly optimistic and overly conservative treatment of storage operation.

Within the scope of this project, the representation of storage operations is implemented by integrating the modelling frameworks for time-sequential scheduling and sampling of system conditions in a three-stage procedure. The detailed mathematical modelling and all parameters are described in Appendix 9A.2, and the full source code can be accessed in the *NEM-reliability-suite*. The setup with respect to storage operation is summarised in Figure 4.3, and described in detail in the following:

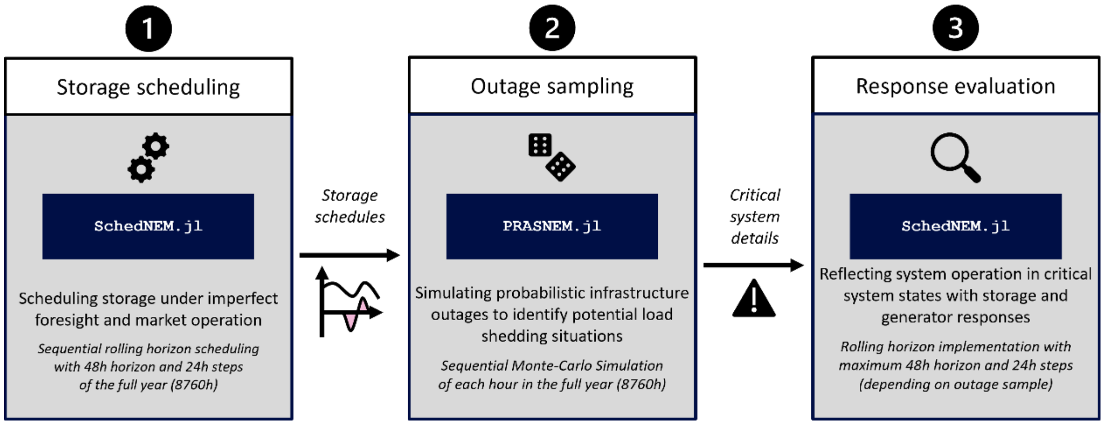

Figure 4.3: Overview of the proposed methodology for capturing storage operation within the adequacy framework.

1. **Storage scheduling under imperfect foresight**
   To reflect a market-based system operation, the first stage employs the system scheduling framework *SchedNEM* that has been developed for this project. This generates realistic storage charging and discharging profiles for each day, based on expected generator availability and VRE production traces. By deriving storage dispatch schedules explicitly

without knowledge of potential outage situations and to minimise system costs, the results reflect a stylised market environment in which storage operation is determined with imperfect foresight and based on price expectations. Because the methodology relies on storage scheduling separate to outage sampling, we derate the storage power capacity by the forced outage rate.

2. **Probabilistic infrastructure outage sampling**
   The second stage incorporates the storage schedules from stage one and evaluates system performance under probabilistic infrastructure outages. This is performed by employing PRASNEM.jl with the underlying adequacy engine PRAS. While storage dispatch is kept fixed in this stage, sequential probabilistic outage sampling of generation, storage and network infrastructure is performed to identify critical system states that may lead to unserved energy.

3. **Response simulation in critical system situations**
   To accurately capture the response of storage and other units in critical system events, the third stage employs the time-sequential operation framework of *SchedNEM*. This stage takes the critical situations identified in stage two and re-simulates them with flexible storage and generator schedules to enable reactive dispatch.

With this methodology, we approximate a representation of imperfect storage operation by specifically capturing the following risk drivers identified in the literature review (see Table 4.1):

- **Uncertainty:** Storage schedules are determined in stage one without knowledge of realised system conditions as simulated in stages two and three. This results in storage operation based on expected conditions and allows capturing potentially lower energy reserves than desired for system reliability.
- **Forecasting:** The scheduling of storage is performed in a rolling horizon setup to reflect the potentially limited lookahead of its operation. Additionally, this methodology allows errors to be introduced into the underlying data that inform scheduling, reflecting forecast data quality issues.
- **Markets:** The cost-based optimisation framework for scheduling storage in stages one and three operation enables simulation of market-oriented storage operation based on price arbitrage.

Overall, these three stages allow more realistic operational details of storage to be captured whilst maintaining computational tractability and efficiency by avoiding simulation of all possible system states with the same operational detail. Whilst stages one and three employ *SchedNEM* to capture complex inter-temporal constraints and may be computationally intensive, the use of *PRAS* in stage two with lower operational representation to identify potentially critical conditions enables a high number of probabilistic samples. Table 4.3 provides an overview of how the proposed methodology may be able to capture the risk drivers that have been identified above. While we focus our case study on a subset of all risk-drivers to demonstrate the risk related to approximating imperfect storage operation, the full methodology framework may be used to capture all identified risk-drivers explicitly.

Table 4.3: Overview of capability of modelling aspects to address the identified risk drivers

		Baseline		Proposed methodology				
		Greedy dispatch	**Perfect foresight**	**Expectation dispatch**	+ market-based	+ rolling horizon	+ response simulation	**Represented in this work**
Uncertainty	Unknown outages			X	X	X	X	X
	Unanticipated weather conditions			X	X	X	X	
Markets	Misaligned price incentives				X	X	X	
	Early discharge to secure profits				X	X	X	X
Forecasting	Limited lookahead horizon	X				X	X	X
	Insufficient forecast data quality			X	X	X	X	
Coordination	Misaligned discharge objective	X	X				X	
	Uncoordinated discharge of multiple units	X		X	X	X	X	X
Services	Provision of system services or reserves	X	X	X	X	X	X	(x)

We emphasise that this methodology ***remains a simplified approximation of storage operation***, as is inherently the case for any modelling framework. However, it may provide a more realistic representation of market-based storage behaviour, leading to adequacy outcomes that differ from the more idealised approximations commonly adopted in academia and industry. Accordingly, the objective of this analysis isTable 0.8 not to predict actual storage operations, but rather to assess the uncertainty and adequacy risks associated with alternative storage operations under an evolving resource mix.

4.4 Case study parameters

To understand the implications of approximating storage operation when assessing resource adequacy, we compare three storage behaviour assumptions:

1. **High energy**: Storage units maintain state-of-charge levels as high as possible to maximise availability during critical periods. This approximation, adopted, for example, by PJM in its adequacy assessment studies [76], reflects storage operation under adequacy-oriented incentives such as capacity or reliability schemes. This approximation is embedded within the PRAS heuristic dispatch.
2. **Derated energy**: This follows the same heuristic as the *High* energy strategy, maintaining state-of-charge levels as high as possible. However, to approximate limited storage foresight, a derating is applied to the energy capacity of storage systems, particularly BESS and VPPs. This derating is based on factors used in AEMO's adequacy assessment, the ESOO [7]. Storage units with less than 1.5 hours of duration, as well as VPPs, are reduced to operating at 50% of their energy capacity. Units with less than 3.5 hours of duration are derated by 25% energy capacity, and units with less than 7.5 hours are derated by 10%. Larger storage units are not derated in energy capacity.
3. **Economic operation**: This approximation is implemented through the workflow described in Figure 4.3. This approach assumes that storage units make operating decisions based on economic signals under limited foresight.

A summary of the three approaches is shown in Figure 4.4 Figure below.

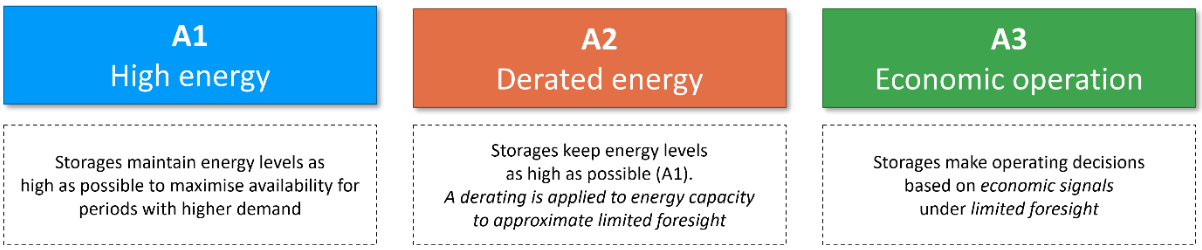

Figure 4.4: Overview of the three different storage operation approximations compared. A3 is based on the adequacy assessment framework developed in this report.

We apply the three storage operation strategies presented to evaluate the resource adequacy of Australia's east coast power system (NEM) using the 12-subregion network representation adopted in the 2024 ISP [83]. The analysis considers the expected infrastructure deployments under the *Step Change* scenario Optimal Development Path (ODP) for the planning horizon 2025–2040, which exhibits a progressive transition towards high penetrations of energy-limited and weather-dependent resources, as summarised in Table 4.4.

Table 4.4: Installed capacity as a percentage of peak demand for the base case scenario, based on the 2024 ISP Step Change scenario [83].

Base case capacity **- Integrated System Plan NEM**				
Year	***2025***	***2030***	***2035***	***2040***
Firm capacity (%)	85%	53%	31%	28%
Storage (incl. VPP) (%)	20%	53%	75%	91%
VRE (%)	127%	206%	245%	235%
Hydro (incl. PHES) (%)	20%	22%	25%	22%

We consider demand-side flexibility in the form of aggregated storage units (VPPs) that are approximated to operate following the same operation regime as utility-scale storage. Importantly, other forms of demand response are not considered in this case. This is to isolate and specifically understand the effects of storage operation (see the detailed DER analysis in Chapter 5 below).

We evaluate adequacy using 500 randomly selected outage samples across generation and transmission assets, as well as two weather-year reference traces from the 2024 ISP traces. The weather years used for this study are selected based on average VRE availability to capture renewable generation variability:

1. A high VRE energy scenario (reference weather trace of the year 2019 with peak demand of 50% probability of exceedance (POE))
2. A low VRE energy scenario (reference weather trace of the year 2011 with peak demand of 10% POE).

We note that although the high VRE scenario has the highest overall energy availability among the provided reference traces, the adequacy risk is concentrated during low VRE periods in winter.

4.5 Insights and Results

4.5.1 Implications of different storage operation approximations

To analyse and understand the storage operation under the three different approximate models, Figure 4.5 presents the average state of charge of each short- and medium-duration unit, including VPPs, for a given planning year.

The high-energy model assumes storage units remain as fully charged as possible, whereas the derated-energy model assumes they operate at lower state-of-charge levels depending on their storage duration. In contrast, the economic-operation model approximation results in lower average state-of-charge levels for storage units across all durations.

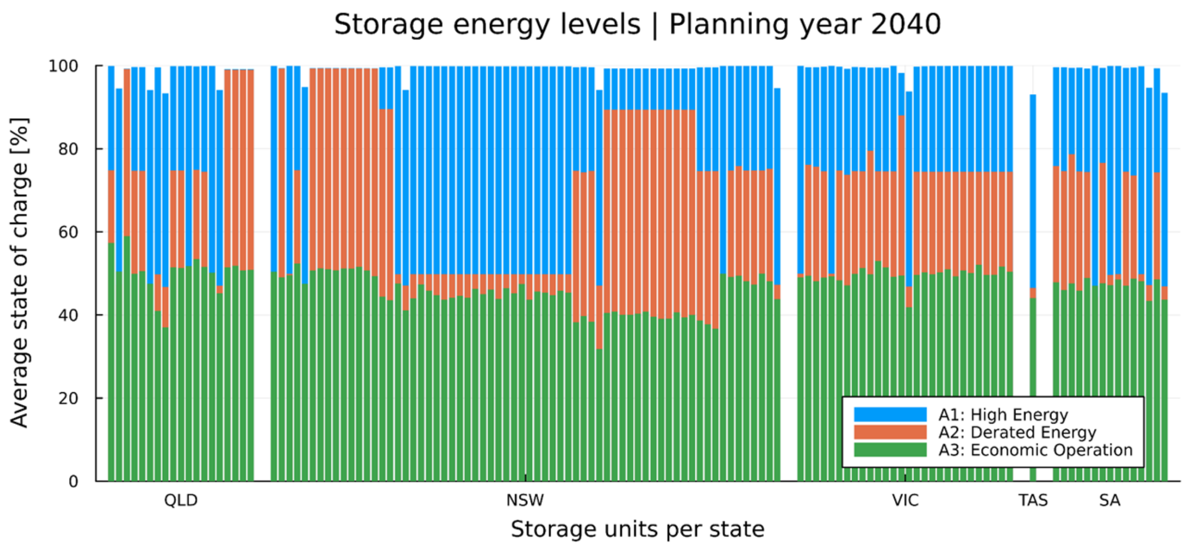

Figure 4.5: Average energy levels of short-duration storage units (BESS and VPP) across the NEM in 2040 under the three storage operation approximations.

While the average state of charge across the storage operation assumptions reveals significant differences in the dispatch, these differences are also reflected in the daily charging and discharging profiles shown in Figure 4.6. Assumptions A1 and A2 do not exhibit clear average daily operating patterns, consistent with the objective of maintaining storage units as fully charged as possible for adequacy purposes. In contrast, A3 operates in an economically driven manner, charging during daytime and discharging during evening peak and nighttime hours.

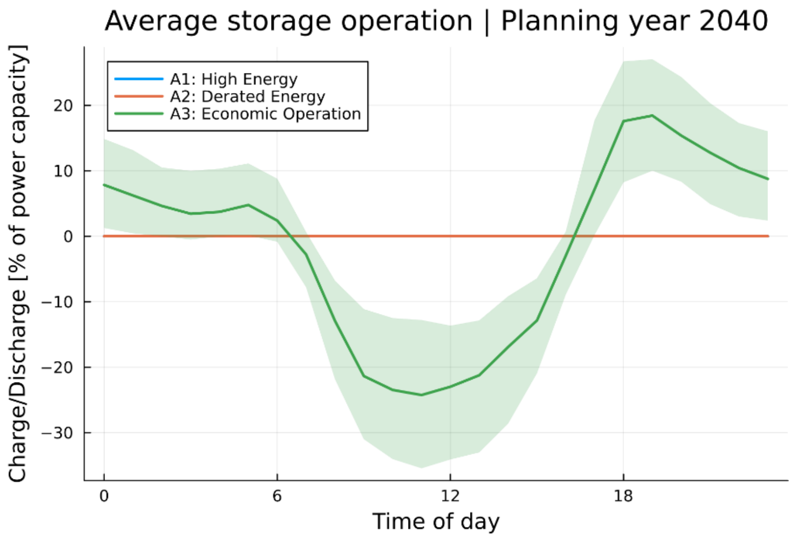

Figure 4.6: Storage operation across the day, as observed in the schedule for planning year 2040 under the three different storage operation approximations (A1 and A2 both are overlapping). While the lines show the median operation across all days, the shaded areas show the interquartile range (25%-75% of the daily values).

Overall, we observe that the proposed storage approximation (A3) yields a significantly different storage dispatch from the adequacy-oriented storage operation heuristics in PRAS (A1 and A2). This highlights the significant uncertainty associated with the underlying representation of storage operations in adequacy assessments. In the following section, we investigate how different approximations of storage operations affect resource adequacy outcomes as the capacity mix evolves.

4.5.2 Reliability risk due to storage operational approximations and assumptions

Figure 4.7 presents the results of the NEM-wide reliability risk assessment under the three storage operation approximations, based on the case study parameters described above, over the planning horizon 2025-2040. This figure presents the average annual unserved energy (USE) for the system and simulation settings described in Section 4.3.

Under the *high energy* assumption (A1), the system exhibits adequacy levels both within and well below the reliability standard. For example, in the simulation setting considered, the achieved USE in 2040 is 0.000045%, which is 44 times lower than the reliability standard of 0.002% USE. Such a result suggests that if all storage units operate with perfect or near-perfect foresight and can fully realise their energy capacity to supply during periods of high demand, the NEM would maintain adequate supply margins throughout the assessment period.

Under the *derated energy* assumption (A2), unserved energy levels increase after 2030; however, average system USE remains within the reliability standard. This indicates that approximating storage operational constraints by limiting the state of charge (energy capacity derating) materially affects the estimation of system adequacy, although the system may still retain sufficient adequacy margins under this assumption.

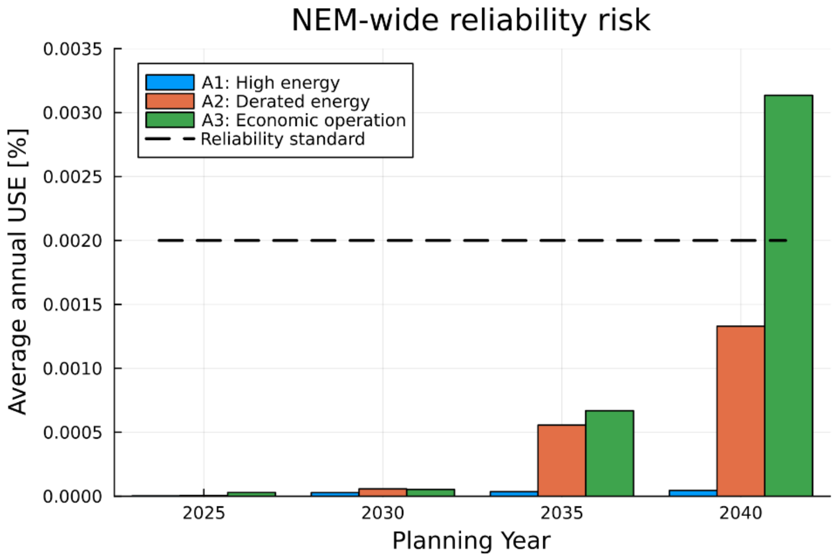

Figure 4.7: Average annual unserved energy (USE) for four selected planning years and the three system operation approximations, based on 500 outage samples and two reference weather years of high and low average VRE availability. USE is aggregated across the whole NEM and normalised by the total annual demand.

The impact of selecting a specific storage operation approximation becomes particularly evident when assessing the *economic operation* (A3) model. Under this representation, as shown in Figure 4.7, system adequacy deteriorates after 2030, with an observed annual USE exceeding 0.003% in 2040.

Together with the results obtained under assumptions A1 and A2, this result demonstrates that **as storage becomes a dominant component of the resource mix after 2030, adequacy outcomes become increasingly sensitive to the operational representation of storage adopted.** The divergence in annual USE levels among the three approximations highlights that the assumptions used to model the operation of energy storage facilities can materially influence reliability assessment outcomes.

This finding has important implications across both **planning** and **operational** timescales. Under a wide range of plausible storage operating assumptions, reliability risks may be either under- or overestimated. For example, comparing cases A1 and A3 shows that, under A1, the observed USE levels could suggest that the system remains within the reliability standard, whereas under A3, assuming a more economically driven representation of storage operation may reveal emerging reliability risks.

Consequently, at the planning timescale, adopting assumptions aligned with A1, for example, could lead to underinvestment in firm capacity, network augmentations, or other reliability resources. Such mischaracterisation of adequacy risk may increase the likelihood of corrective operational measures, including operator interventions and load shedding.

To assess the implications of the storage operation assumptions for the wider risk profile, we examine the average tail risk across the 5% worst-case scenarios with respect to annual USE, as shown in Figure 4.8. Comparing the different storage operation algorithms, we note that while the adequacy estimation of the average risk becomes inherently more *volatile* as storage penetration grows, tails may become even more dispersed across storage approximations. Additionally, the *high energy* approximation, most optimistic in terms of storage operation for adequacy, may not even reveal the potential tail risk at all.

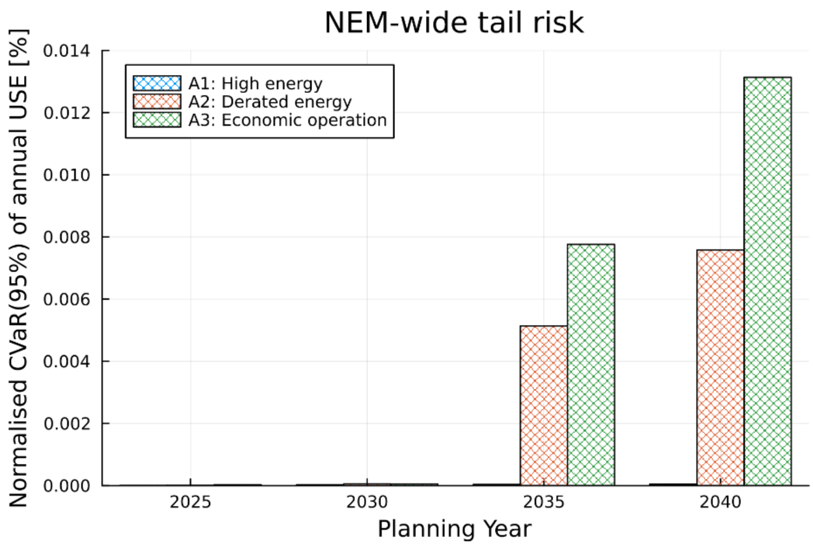

Figure 4.8: NEM-wide tail risk with respect to unserved energy (USE) for selected planning years and three different storage operation approximations, based on 500 outage samples and two reference weather years of high and low average VRE availability.

The key message is that resource adequacy levels are, on average, sensitive to storage-operation approximations, but this sensitivity may be even more pronounced in tail-risk events. As storage penetration increases and becomes a dominant part of the resource mix, the choice of storage operation model therefore materially influences not only mean adequacy outcomes but also the distribution of extreme USE observations in adequacy assessments. To prepare against this spread, and uncertainty in the tail risks, a broader set of metrics may be required to assess adequacy risk comprehensively, alongside potential policy measures to hedge within both planning and operation.

A broader set of metrics, combined with the use of a set of approximations for storage operations within the same assessment, will be essential **for anticipating and quantifying the inherent risks associated with forecasting storage behaviour** in storage- and renewables-dominated systems. This will enable system operators and planners to account for the uncertainty introduced by different storage representations when making investment and operational decisions. A multi-metric assessment of the reliability risk of the NEM under the context of the storage approximations is presented in chapter 6.

4.5.3 Impacts of storage operation approximations on the full risk distribution and change in risk profile

After analysing metrics quantifying average and tail risks, we now investigate the extended probability distributions of annual unserved energy across the storage operation approximations under study. In the results, under assumption *A2: Derated energy*, the distribution of unserved energy samples shows concentration in smaller events, suggesting more manageable load shedding events. In contrast, *A3: Economic operation* exhibits a more uniform distribution of events with a more pronounced and larger tail, indicating greater variability in reliability events.

A key takeaway is that the differences extend beyond higher levels of load shedding; **the reliability risk distributions themselves become less predictable under different assumptions about storage operations**. Hence, different storage approximations may produce fundamentally different risk distribution profiles, even under identical weather and outage conditions, highlighting the strong influence of storage behaviour on adequacy outcomes. This divergence is, therefore, not merely a matter of magnitude but reflects a qualitative **change in** the nature of adequacy risk, that is, the **'*risk profile*', driven by the heterogeneous ways in which storage may respond to evolving system conditions**.

Moreover, the differences observed in the shapes of risk distribution suggest that assumptions of "predictable" storage behaviour may no longer hold in systems with high storage penetrations. As storage becomes a larger and more influential component of the resource mix of the NEM beyond 2030, its operational behaviour becomes increasingly fundamental to both system operation and long-term resource adequacy. Prior to this transition, different storage operation approximations may still produce relatively similar adequacy results; however, as storage penetration increases, adequacy outcomes become progressively more sensitive to how storage behaviour is represented.

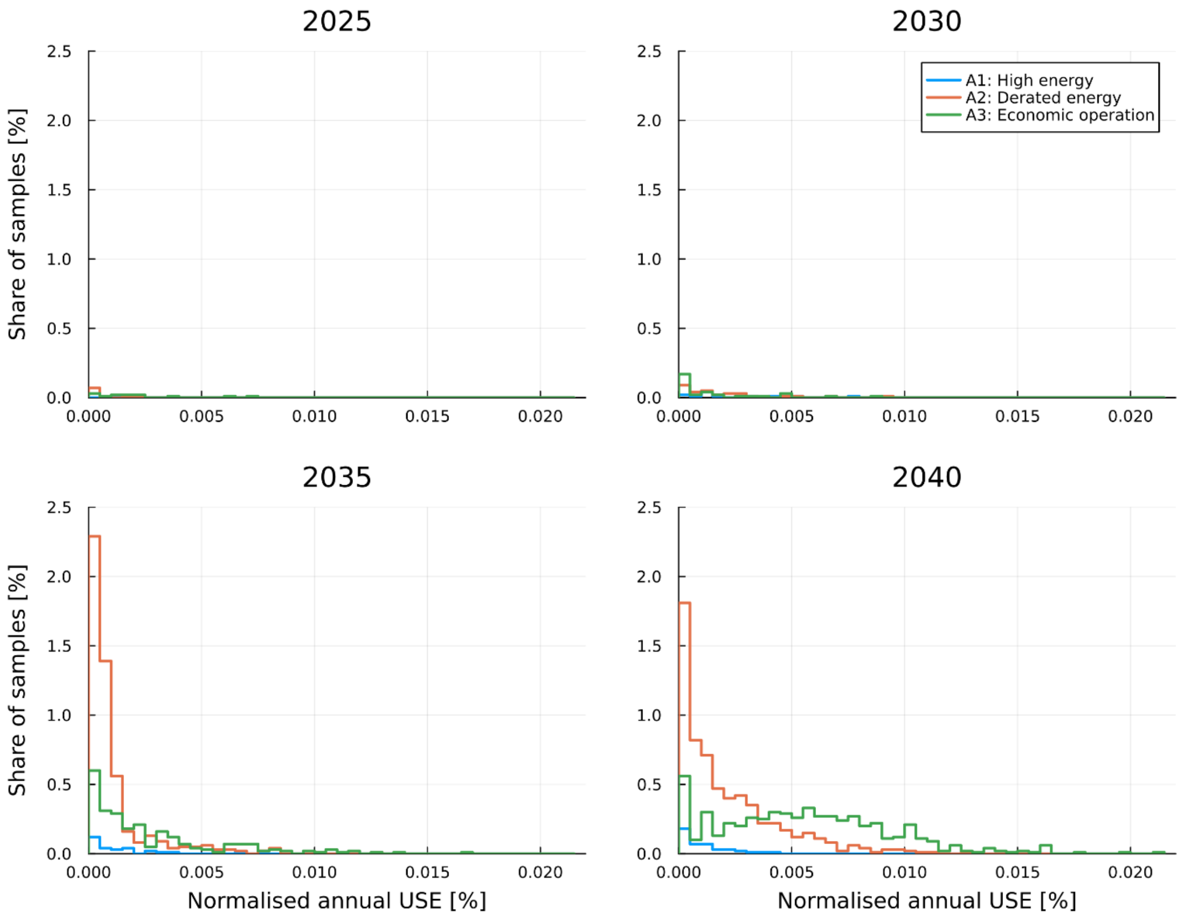

Figure 4.9: Distribution of annual USE per sample across the different underlying planning years, as well as storage operation assumptions.

Further details on the NEM reliability risk profile, including event-level analyses under different storage operation approximations, are presented in the consolidated reliability risk assessment in Chapter 6.

4.6 Key findings

The following points summarise the key findings of this chapter, highlighting the implications of approximations in storage operations for resource adequacy assessment in storage- and renewables-rich power systems.

- **Storage operation will become a first-order driver of resource adequacy after 2030**, as firm capacity retires and power systems worldwide, including the Australian National Electricity Market, increasingly rely on energy-limited resources to firm renewable generation.
- **The contribution of storage systems to resource adequacy is highly conditional on their operating behaviour**: it is strongly tied to a broad range of factors, including current state of charge, charging opportunities, market signals, operator foresight as well as risk aversion, and the ability to preserve energy ahead of critical periods.
- **Storage operation assumptions at the planning stage can reshape the full reliability risk distribution**, affecting not only the expected magnitude of unserved energy events but also their spread, skewness, and tail size; therefore, no single storage approximation proves to be sufficient, and adequacy assessments should aim to test multiple plausible storage behaviours within the same framework.
- **Storage behaviour uncertainty should be treated as a fundamentally new dimension of risk in resource adequacy assessments for modern power systems**. Such a dimension should be added to already well-established probabilistic generation and transmission outages, demand variability, and weather-driven renewable availability.
- **Addressing this uncertainty in practice may require higher planning margins** (e.g., additional headroom and reserves), potentially stronger operational intervention or monitoring capabilities, and updates to reliability metrics (e.g., to explicitly characterise tail-event risks) and policy frameworks to proactively provide hedging mechanisms across both planning and operational timescales.

5 Distributed energy resources

Distributed energy resources (DER) are in the broadest sense "a group of flexible technologies that are connected to distribution systems" [84]. Various definitions exist across the literature and industry, encompassing different technologies such as distributed generation, storage, and demand flexibility [84]. A subcategory of DER are consumer energy resources (CER), which are technologies "behind-the-meter" on consumer sites [85]. For this work and to guide the literature review, we differentiate DER into three key categories that exhibit different characteristics for adequacy of supply:

1. **Distributed generation:** Distributed generation encompasses any type of electricity generation connected to the distribution system, including small-scale wind, gas, or hydro generation plants [86]. In Australia, the largest distributed generation source is distributed solar photovoltaic (PV) generation, which already represents the largest aggregated installed capacity of any technology in the NEM [87] and is expected to continue growing [83].
2. **Distributed storage:** Distributed storage may include batteries with direct access to the network (e.g. community batteries) or could include customer owned storage "behind-the-meter". Therefore, distributed storage is commonly considered in synergy with other customer-located technologies such as distributed PV [18] or might also be aggregated within demand response modelling [36].
3. **Demand flexibility:** Demand flexibility refers to any temporary changes to demand [88] and can encompass multiple aspects, such as price informed load shifting and reliability motivated load changes. Across the literature, this is also referred to as demand-side management (DSM) [89], [90], [91], or demand-side participation (DSP) [7]. A specific form of demand flexibility is demand response (DR), which broadly considers the reaction of demand. A recent review defines it as "the actions of customer-sited energy resources, located downstream of metering points, to *voluntarily, actively, and temporarily* adjust their electricity production and/or consumption in response to signals (e.g., commands, prices, measurements)" [85]. Different types of demand response are relevant in the context of adequacy of supply [92]:

    - *Shaping*: Medium- to long-term permanent demand changes due to price response or behavioural campaigns.
    - *Shifting*: Short-term energy consumption changes from critical periods to times of higher energy availability.
    - *Load reduction*: Reducing energy consumption in critical periods without the need to repay in later periods. This is currently the model used by AEMO to represent demand-side participation within their adequacy assessment [7].

    Demand flexibility refers to the abstract concept of a change in the electricity demand, and can be provided by any flexible technology "behind the meter" [85], which may include electric vehicles (EVs) [93], heating- and cooling demand [94], or other smart loads.

In the following, we outline the potential contribution of DER to adequacy of supply, aligned with these categories, and summarise literature insights. Afterwards, modelling approaches from academic literature and industry practices are described.

5.1 Literature review of DER contributions to adequacy of supply

The potential contributions of DER to adequacy of supply have been assessed across the literature, e.g. [18], [36], [88], [89], [90], [94], [95], [96]. The specific contribution of DER to the adequacy of supply depends on the technology [84], the location in the network [95], and the operating mode assumed [18].

It should be noted that distribution system reliability often includes the evaluation of metrics such as *system average interruption duration index (SAIDI)* or *system average interruption frequency index (SAIFI)* [97], [98], which describe the average power unavailability duration or frequency at customer locations. These metrics are relevant for assessing distribution systems. However, in the context of adequacy of supply, the focus is laid on the ability of the whole system to supply demand even after equipment failures, and therefore on large-scale events rather than individual consumer experiences [4].

Considering **distributed generation,** larger penetrations can support adequacy of supply by avoiding reliance on large-scale transmission buildouts [99], and by supporting potential islanded operations [97], [100]. However, as described by Khashei et al [101], distributed solar has also been observed to trip unexpectedly during critical events. This means that during critical periods following unexpected outages, if grid parameters such as voltage and frequency deviate, distributed generation may potentially disconnect unexpectedly, thereby exacerbating the problem rather than continuing to deliver energy during critical events. Furthermore, as pointed out by Zhang et al [18], the underlying energy availability (e.g. solar irradiation) on critical days might also limit its contribution to adequacy of supply.

Regarding **distributed storage** two key operating modes define its contribution to adequacy of supply: coordinated/integrated operation or distributed/independent operation [18]. Coordinated operation describes a dispatch which is visible to the market, where multiple distributed units are coordinated via an aggregator. Independent operation describes an operational regime where each unit is scheduled without coordination and is therefore not able to react to the market and the wider system. A coordinated dispatch of distributed storage (e.g. [18], [36]), may contribute to adequacy to a similar extent as large-scale storage, with imperfect operation being a key limitation (see Chapter 4). This is for example also considered by Qi et al [47] who include coordinated distributed storage in their category of “generalised energy storage (GES)”.

However, when distributed/independent control of distributed storage is assumed, its contribution to adequacy of supply may be limited due to the inability to be scheduled following market conditions [18], or uncoordinated charging and discharging, which could lead to suboptimal miscoordination [55].

The difference between the two operation strategies is illustrated in Figure 5.1 for a case study in the UK. Under integrated control, the capacity credit of distributed storage could increase linearly with larger penetrations. In contrast, under independent control, the capacity credit saturates faster with greater storage uptake. This difference arises due to fact that independent control can only leverage distributed generation for scheduling and is not able to operate optimally with respect to the large-scale generation. Therefore, the lack of solar irradiation on critical days limits the adequacy contribution of distributed storage under independent control.

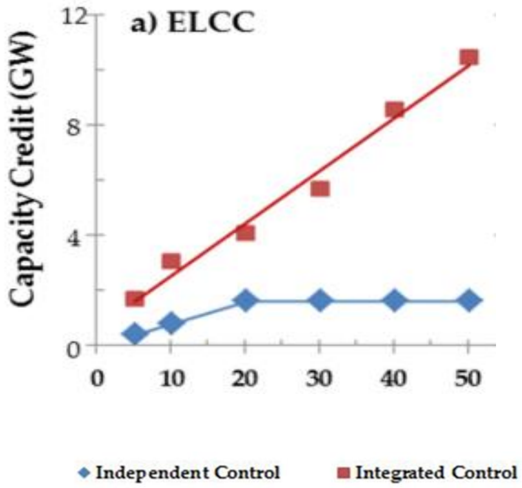

Figure 5.1: Saturation of contribution to adequacy of supply of distributed storage, depending on operation mode. Taken from Zhang et al [22].

The contribution of **demand flexibility and demand response (DR)** to adequacy of supply is intuitive: it reduces the demand that needs to be served by available supply during critical periods and can therefore reduce unserved load [88] and investment needs in generation capacity [94], [102]. Similar to storage, a synergy with renewable variability has been described for demand response, for example with high wind penetration [94], [103]. Additionally, DR is regularly considered in combination with storage since it provides similar benefits to the system [34].

In capacity limited systems, the most critical periods are at peak times [4], which means that reducing the peak demand directly increases adequacy of supply [89]. However, if some demand needs to be repaid — for example due to heating and cooling requirements — the contribution of demand response to adequacy of supply may be limited [36], [91]. This can be seen in Figure 5.2, which shows different demand response profiles to reduce peak demand. Under certain conditions, the peaks could be flattened (due to DR), but lengthened due to payback requirements. Therefore, whilst all payback scenarios show a reduction in expected energy not served (EENS / EUE), indicating an increase in adequacy levels, accurate representation of realistic payback is essential for adequacy assessments.

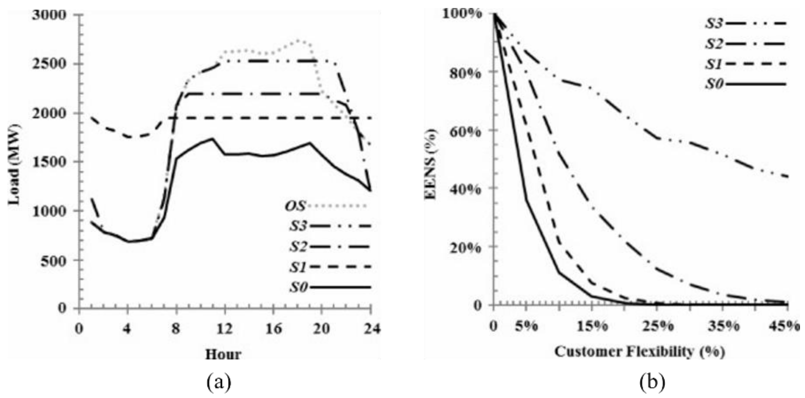

Figure 5.2: (a) Different demand response profiles with load payback parameters (increasingly constrained in payback amount and time from S0 to S3) and (b) the resulting reduction in expected energy not supplied (EENS). Reproduced from Zhou et al [85].

On the other hand, pre-charging may also play a crucial role in the contribution of demand response to adequacy of supply [104]. This means that demand might be able to increase consumption before forecasted critical times. Pacco et al [90] model this for the European continental system and observe a decrease of 4–21% in expected energy not served (EENS) due to this additional demand flexibility.

Furthermore, apart from scheduled demand response to static signals such as peak times, it may contribute to adequacy during sudden contingency periods [105]. However, also here the payback or duration of the call matters. For example Wildstein et al [105] describe how participant overrides may reduce the contribution to adequacy by more than half for events lasting 3–4 hours. Additionally, a limiting factor might be the uncertainty around its availability in critical periods due to uncertain consumer behaviour and preferences: Earle et al [106] observe decreases in the effective load-carrying capability (ELCC) of demand response by 20–30% when increasing the distribution of demand response availability.

Whilst all the above technologies may contribute to adequacy of supply, their contribution may be inherently limited by network constraints in the distribution system to which the resources are connected. Therefore, for accurate evaluation of adequacy of supply with DER, potential network constraints need to be considered in the aggregation of DER [107].

5.1.1 The role of asset coordination

As described above, the contributions of DER to supply adequacy rely on coordination schemes (for example, via virtual power plants). Without effective coordination, the anticipated benefits are unlikely to be achieved (see, for example, Figure 5.1). We identified two key mechanisms that highlight the benefits of coordination for DER contribution to adequacy of supply:

1) **Unlocking optimal dispatch of heterogeneous technologies:** As described for storage, uncoordinated discharging of heterogeneous storage units might lead to higher amounts of unserved energy, since some energy might not be available due to capacity limitations [54], [55]. Since DER aggregate various distributed technologies which can have many different configurations, optimal dispatching is especially important to unlock the full potential.
2) **Signalling critical periods:** While a distributed scheduling of DER may contribute to adequacy by reducing peak demand, risk periods might also arise at times outside of peak demand, if there is also a lower amount of VRE available to supply the demand [5]. Therefore, signalling critical periods of the system for DER scheduling is crucial to unlock a larger contribution to adequacy of supply. Zhang et al [18] describe an example of this, comparing an independent operation mode of distributed storage with an integrated (coordinated) approach in which storage has knowledge of critical periods in the system.

5.1.2 Summary of DER contributions

Overall, distributed energy resources can contribute to adequacy of supply in various ways and are critical to represent in adequacy assessments to accurately capture the risk profile. An overview can be found in Table 5.1. Coordination of the technologies is crucial for materialising these adequacy contributions. Note that this is merely one attempt of categorising DER for adequacy of supply; other categorisations are also possible. For example, Sperstad et al [96] review flexibility services of DER based on their capacity contribution (i.e. the power supply to the grid) or the mode of support for reliability (preventive, corrective, restorative). This highlights the number of underlying technologies and considerations that may play a role when analysing DER in the context of adequacy of supply.

Table 5.1: Overview on contribution mechanisms of DER to adequacy of supply and potential limitations

Technology	Support mechanism / operating mode	Potential risk factors	Relevant studies
Distributed generation (DG)	Emergency support	Energy availability, unknown tripping behaviour of DG, network constraints	[18], [97], [99], [100], [101], [108]
	Energy supply	Energy availability (e.g. solar irradiation), network constraints	
Demand response *(incl. distributed storage)*	Energy shifting	Imperfect operation, network constraints	[108]
	Scheduled load reduction/shifting	Payback constraints, uncertain availability, network constraints	[36], [89], [91]
	Emergency support	Inefficient coordination, payback constraints, uncertain availability, network constraints	[105], [106]

5.2 Methodological approaches to incorporate DER to assessments of adequacy of supply

As highlighted above, incorporating DER into adequacy assessments is important for developing an accurate picture to inform investment decisions. Selecting the appropriate modelling approach may be determined by the desired aspects to capture in the adequacy assessment: Is DER solely operated to reduce peak demand, is the focus laid on its response to system events, or is DER dispatched simultaneously with the other system resources to increase system efficiency? All these aspects play a role in the future low-carbon power system, and transparent modelling design is essential to understand adequacy risks appropriately. In the following, approaches to represent DER are reviewed, first within the academic literature and subsequently in the context of modelling of system planners and operators around the world.

5.2.1 Academia

Various modelling approaches for distributed energy resource management and optimisation are described across the literature, as reviewed by Morales-Espagna et al [109] and Wagner et al [110]. Practically, three fundamental modelling approaches are typically pursued for capturing distributed energy sources and demand flexibility: DER are incorporated into demand traces [36], modelled as specific DER source [90], or considered as aggregated generation or storage technology [18] within adequacy assessments.

Distributed generation such as rooftop solar PV may be explicitly included in specific distribution system modelling with detailed network modelling [99], [108]. If network constraints are disregarded or simplified assumptions are taken, a common approach is to consider aggregate energy generation [18]. Due to the large number of devices, explicitly modelling outages of distributed generation is commonly disregarded; however, it may become more important given common mode failures [101].

Modelling **distributed storage** is also addressed through aggregated storage devices [18], [99]. Whilst the representation of storage in adequacy modelling is established, the main modelling consideration for distributed storage is whether the units are operating decentralised or aggregated to participate in upstream system scheduling. Zhang et al [18] propose an "independent" operation by pre-optimising operation for self-consumption with distributed generation, or by performing peak-clipping operation in critical periods, before sampling system conditions. The authors compare this to an "integrated" operation, where the aggregated storage is fully optimised within the wider system. Distributed storage is also commonly included in modelling of storage in adequacy assessments, aggregated for example as "generalised energy storage" [47] or virtual power plants, which may also include other forms of demand response. Regardless of the operational mode, imperfect operation may be addressed with similar approaches as for storage (e.g. market-based dispatch before sampling system conditions and/or limiting scheduling foresight), as discussed in Chapter 4.

Demand flexibility is generally modelled similarly to distributed storage. For example, Qi et al [95] include demand flexibility as "virtual energy storage", and Zhou et al [36] use the same method to model demand response and energy storage for adequacy of supply. However, multiple key modelling differences from distributed storage have been described in the literature:

1) **Inverse storage**: Demand response may "discharge" before "charging", which could be performed by shifting demand via smart appliances. This is for example proposed in the modelling by Goransson et al [111] which Zeherran and Shill [104] extend to also include "pre-charging", i.e. shifting of demand to earlier times. Whilst both propose a detailed mixed integer programming (MIP) model, Pacco et al [90] apply this within an resource adequacy study of Europe and compare the complex MIP model with more simplified approaches. The authors note that a simplified LP approach was needed for the MC simulation and highlight that demand flexibility might be overestimated within the results.
2) **Time-varying energy and power capacity**: Changing DER conditions — for example, how many electric vehicles (EVs) are plugged into a charger at a given time — may limit the power and energy capacity of demand response over the course of the day, compared static large-scale storage [112].
3) **Load shifting limitations**: The load shifting potential may be restricted due to consumer preferences. For example, to keep the temperature in a building within acceptable limits, heating/cooling might not be post-/preponed more than a few hours. This might be implemented by restricting load shifting in time or by limiting the number of calls.
    a. A payback time limit of one hour is for example implemented by Zhou et al [36], who describe a significantly reduced capacity credit from payback time limitations. This is also considered in other studies with for example 24h payback [94], or only few hours [112].

   b. A limit on the number of calls per time-period (e.g. x calls per year) might be implemented [113].

4) **Reduced or no payback**: Some part of the load might not have to be served if it is too expensive (e.g. industrial loads), thereby effectively reducing the payback amount [36], [111]. This is the most straightforward form of demand response; however, its implications need to be carefully considered, since it is equivalent to a very flexible firm generator and might therefore significantly influence adequacy results [36].

Furthermore, operating decisions for demand response may also be taken on a system level or at decentralised unit level. Therefore, coordination and availability of demand response are additional parameters to consider. This has already been reflected by the Danish system operator Energinet, which has started defining reserve requirements with minimum availability limits [114] to explicitly allow demand response to participate in system reserves.

Additionally, large loads, such as data centres, may also provide load shifting or load reduction services [88], [115], and might require additional specific parameters. However, since this is only recently becoming relevant for power systems, the literature on large loads for adequacy is limited at this stage.

Finally, the impact of networks on the contribution of DER to adequacy of supply may be represented by calculating nodal aggregations of DER with underlying grid constraints to maximise flexibility or by imposing network wide constraints on the aggregated DER operation [116]. While the former may result in a higher contribution of DER due to optimised network performance, the latter approach might be preferred if future coordination levels are uncertain.

5.2.2 Industry

In the following, we are reviewing multiple industry practices for including DER into adequacy assessment modelling. There are many different approaches of modelling taken, which are roughly differentiated into load adjustments, dedicated demand response modelling, and supply/generation modelling, see Table 5.2. While these categories are not necessarily mutually exclusive, they may provide better understanding of the general approach.

Of the studied modelling approaches, the most comprehensive approach of the reviewed operators is taken by Elia (Belgium) [72], since it considers EVs, HPs and distributed storage operation as partially uncoordinated and non-responsive and partially market oriented, thereby aiming at representing a large heterogeneity in DER operation.

Table 5.2: Overview of DER modelling in adequacy frameworks of selected system operators.

Country (Organisation)	Report	DER in (inelastic/ unresponsive) demand	Demand response	DER in supply modelling	Additional constraints / payback
Europe (ENTSO-E)	ERAA, Methodology Appendix 2 [67]	Rooftop PV, Distributed batteries, EVs, HPs (non-price sensitive share)	Demand Side Response (DSR): Optimise a share of consumer	Explicit industry DSR included as “generation” with high marginal cost	EV and HP load shifted only within time-windows (no reduction).

			batteries, EVs and HPs		Industry DSR with maximum activation time per day
United Kingdom (NESO)	Resource Adequacy in the 2030s [69]	Time of use tariff impact reflected in demand change profiles	DSR: DSR markets and dynamic demand-shifting. Capacity constant + variable	-	Payback/shifting within 4 hours. Daily maximum energy limit (2 hours at full capacity).
Ireland (Eirgrid) Northern Ireland (Soni)	All-Island Resource Adequacy Assessment (AIRAA) [70]	Demand flexibility from EVs and HPs included in the electricity demand profiles, reducing peak demand	-	Demand side units (DSU): Run hour limited or not, dispatched as generators	For run hour limited DSU: Daily activation limit of 2-3 hours (5 in Northern Ireland)
Germany (BNzAg)	Versorgungs-sicherheit Strom Bericht 2025 [71]	-	DR and distributed storage optimised with technology specific parameters and time-varying capacity	Load reduction based on price, but limited by yearly activation	Max payback time windows, max delay for payback start, max shifted energy. Annual load reduction limited by hours
Belgium (Elia)	Adequacy and Flexibility Study 2026-2036 [72]	Part of the demand from EV, HP and other loads added to demand profile. Part of distributed storage is included as static profile.	Market oriented EVs, HPs and distributed storage dispatch are fully optimised, subject to varying capacity limits	-	Minimum energy demand served per day
USA/Texas (ERCOT)	NERC Long-term reliability assessment [75]	Rooftop PV, EVs and large loads	*Unknown*	Aggregated DERs considered as generation	*Unknown*
USA/East (PJM)	2025 PJM Effective Load Carrying Capability and Reserve	Distributed storage + solar to minimise peak, uncoordinated EV charging and heating/cooling	Demand resources dispatched before storage discharge	-	No

	Requirement Study [76]				
Chile	Chilean law[82]	Distributed PV (residential, up to 300 kW)	-	Small and medium size PV (up to 9 MW)	No
Australia (AEMO)	ESOO [7]	Rooftop PV, batteries, embedded demand flexibility	Demand Side Participation (DSP): Last resort before load shedding	Virtual Power Plants (VPP) included as generation	Maximum daily energy limits for reliability response of DSP

In the **continental-wide European adequacy assessment** [67], ENTSO-E uses the category of "Demand Side Responses" (DSR) to include demand response within the modelling. Of "out-of-market batteries" (OOMBs), electric vehicles (EVs) and heat pumps (HPs), the input data defines a specific share as price-responsive. While the non-price response parts are included in the demand traces, the price-responsive share is optimised within the adequacy assessment with specific constraints based on the technology. While OOMBs are fully optimised as aggregated battery, EVs and HPs are optimised to shift their demand within specific time-windows of the day (e.g. at night, or within the afternoon). Additionally, ENTSO-E is also differentiating industrial DSR to be price responsive and acting as a "generator" with higher marginal costs within the optimisation.

In the **United Kingdom**, the system operator NESO differentiates three different demand side flexibility options [69]. First, daily peak-shaving caused by time-of-use tariffs is considered and included in the demand traces. Second, a demand-side response market is modelled with a constant power limit at a high price just below load shedding. Whilst half of the potential is purely reduced demand, the other half is included with payback within four hours, and there is a daily limit on shifted energy. Third, NESO considers a level of "dynamic demand-shifting" modelled to be flexible within four hours, with hourly varying shifting potential and a daily limit. Distributed generation and distributed storage are not specifically addressed.

In **Ireland and Northern Ireland** [70], demand flexibility is included in the residential electricity demand traces and reduces peak demand. Flexible demand from electric vehicles is considered to be an emergency measure and not explicitly included in the adequacy assessment. However, demand side units (DSU) from the capacity market are considered on the supply side, which may include demand reduction or distributed generation. These units are grouped into "run hour limited" and "non-run hour limited", which the larger share being run hour limited by 2-3 hours daily activation limit (5 hours in Northern Ireland).

In **Germany** [71], the adequacy modelling includes load reduction, as well as load shifting. Whilst load reduction is only limited by the amount of hours per year, load shifting is characterised by load payback window, maximum delay, and maximum energy. These parameters are defined for specific technologies, and the potential is included with varying capacities across the year.

In **Belgium** [72]**,** the system operator Elia considers different operation methods for EVs and HPs: no flexibility, decentralised operation, and market-optimised operation. All three groups are included with specific percentages defined in the scenarios. Whilst group 1 and 2 are added as static timeseries onto the load, market-optimised operation is explicitly modelled within the assessment with varying power capacity availability and a daily minimum energy constraint to ensure the energy is delivered. Furthermore, distributed storage is also considered partially decentralised operated (static timeseries) and partially optimised within the market, adhering to storage operation constraints.

In **Western North America** (WECC) [58], the adequacy assessment is based on probabilistic convolution of demand and supply availability. Whilst DER are described to be included in the demand forecast, no specific modelling is applied.

In **Texas** [75]**,** ERCOT includes rooftop PV, EV loads and large loads within the demand traces used for the adequacy assessment. Additionally, demand-side management (DSM) is described for emergency management; however, the detailed modelling is not specified. Further DERs are mentioned but remain limited and are modelled as generation if registered at the markets.

In the **Eastern USA** [76], PJM considers a number of DER within load forecasting, such as distributed storage in connection with distributed solar to minimise peak consumption, heating and cooling, as well as (uncoordinated) EV charging. Additionally, demand resources are considered within the adequacy assessment with varying hourly capacity (full trace in summer, based on 24h trace in winter). These resources are dispatched after unlimited generation, however before discharging limited duration resources (such as storage), without payback or further constraints.

The **Chilean** regulation [80] categorises DER into two tiers: residential units and medium-scale distributed generation (PMGD). Behind-the-meter residential systems (up to 300 kW) are modelled as "negative demand," subtracted from the total system load. PMGD projects (up to 9 MW) are treated as supply-side resources, with their capacity credit determined by statistical performance during peak hours. Under recent reforms, any PMGD solar PV project paired with storage can now opt for fixed-capacity credits based on the storage duration.

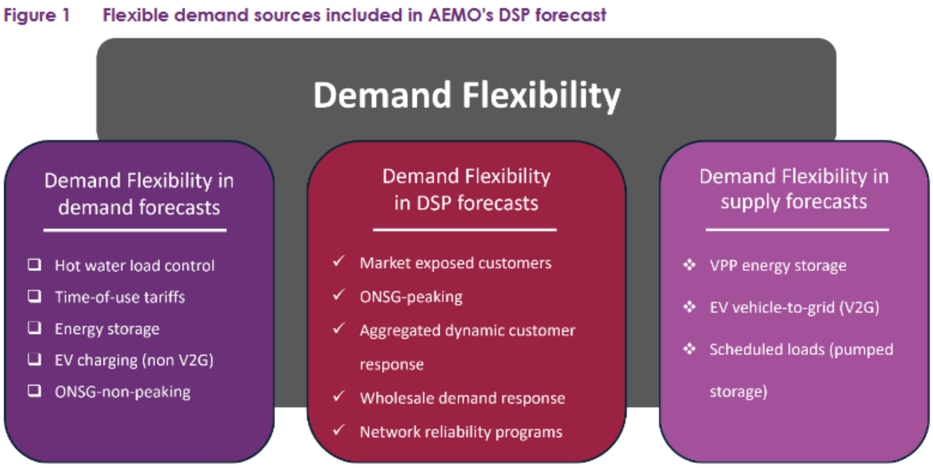

Figure 5.3: AEMO differentiation of demand flexibility into supply, demand and "DSP" categories. Screenshot from 2025 ESOO Appendix 3 [9].

AEMO considers DER in multiple ways in its key adequacy modelling report Electricity Statement of Opportunities (ESOO) [7]. Distributed generation such as rooftop PV and small-scale generation sources is directly considered to be contributing to adequacy of supply and is explicitly included with varying availability according to the weather traces. Demand flexibility is in general differentiated in three categories (see Figure 5.3). Whilst some technologies are reflected in the demand forecasts directly, and coordinated resources modelled on the supply side (operating as “Virtual Power Plants” (VPP)), a category of “Demand Side Participation” (DSP) is used to reflect demand response operation as a last resort before load shedding. No explicit payback constraints are considered; however, a daily energy maximum limit is applied to demand response due to reliability signals.

5.3 Research questions

To investigate the role of DER in supporting adequacy, and potential limitations that may limit adequacy results, we are studying the following research questions:

1. What are the benefits of DER coordination for resource adequacy in a changing underlying supply mix?
2. How does DER coordination shape the adequacy risk profile?

5.4 DER modelling in this work

The modelling of DER in this work is focused on explicitly representing key technologies in the adequacy framework to evaluate their contribution to system adequacy, and the benefits associated with enabling the coordination of demand side resources. Specifically, we model rooftop PV, electric vehicles (EV), embedded aggregated storage (as virtual power plants, VPPs), and demand-side participation (DSP). In the literature review of academic and industry sources, no clear “best practice” has been identified due to the diversity of technologies, locations, and regulatory considerations. Therefore, our modelling builds upon AEMO’s data availability, and aims to provide transparent parameters for investigating DER coordination of different technologies.

Even if DER has been coordinated (e.g. by providing a signal), in practice there may be instances where not all units respond at their nameplate capacity, and instead a lower aggregate response is observed. We refer to this as **compliance factor**, which is explicitly considered in this work because this reduction in response may affect system adequacy outcomes. A schematic overview of the distinction between coordination and compliance and their role within total demand is presented in Figure 5.4.

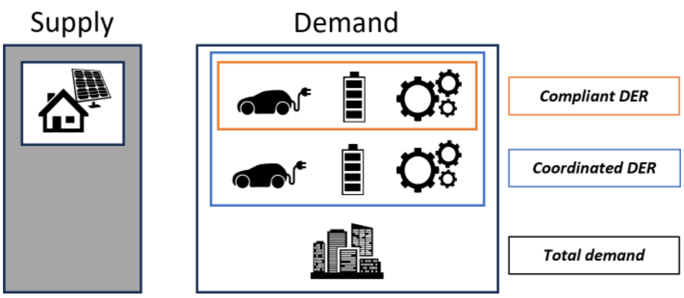

Figure 5.4: Schematic overview of DER representation and classification in this work.

Since DER require a detailed representation of operational parameters, their full modelling is primarily included in the time-sequential operational tool *SchedNEM* and can be utilised in the full adequacy chain described in Section 4.3. Additionally, a simplified representation is provided in PRASNEM for efficient and rapid adequacy assessments and evaluation of DER.

We first establish a base case **'supply-side' scenario** that assesses system adequacy from all utility-scale resources, including transmission and rooftop PV. This case therefore evaluates the ability of these resources to meet a strictly *inflexible demand*, including fixed EV charging without VPP nor DSP support.

This scenario and the assessed baseline reliability are then compared against cases which are individually representing key sources of DER coordination that may reduce the amount of unserved energy. These are shown in Table 5.3, and explained below:

1. Since part of the demand includes **EV charging,** and it may be disconnected to support reliability in critical periods, we explicitly reconstruct the charging profiles from the 2024 ISP *EV workbook,* aggregated by subregion. We consider these hourly charging values as an "upper bound" of potential reduction in EV charging. This reduction in load is priced just under the maximum market price, in order to consider this as a measure of last resort before instructing load shedding.
2. Demand flexibility from aggregated embedded storage units may support adequacy by shifting underlying demand. These storage units are modelled through **VPPs** as sub-regional aggregated storage units, in line with ISP representation, whose capacities are extracted from AEMO's projections provided in the 2024 ISP [22]. These VPPs are assumed to operate in line with utility-scale storage units, and are therefore subject to imperfect foresight (as outlined in chapter 4).
3. Demand response may also react to price and reliability signals, supporting system adequacy in critical periods. Therefore, **demand side participation (DSP)**, as described by AEMO, is represented as a constant demand reduction capacity either at defined price bands (300, 500, 1000, or 7500 AUD), or at just below the price of load shedding for the respective reliability response band, with corresponding capacities obtained from the ISP data [22]. Additionally, a maximum daily energy cap at full capacity of 3h is applied to the reliability response band of DSP to avoid an unrealistic use of this resource and consumer overrides, which is aligned with observations of demand response data in California [105].

In practice, nonetheless, since demand flexibility relies on a high number of individual responses, the actual observed behaviour may show significantly lower response of reported capacities than anticipated, especially in peak periods. This is represented in this work as a ***compliance factor***, which is used to parametrise this challenge. We investigate multiple levels of compliance of the different technologies:

1. For **EV charging**, we consider a low compliance case of 25%, and a high compliance case of 50% of charging reduction at any time.
2. For **VPP**, compliance is modelled as 50% or 100% of the forecasted aggregated storage capacity.
3. For **DSP**, compliance is considered as 50% and 100% of the forecasted capacity.

It is worth noting that higher compliance factors are considered for VPP and DSP flexibility, since the reported capacities in the ISP already account for a reduced level of compliance, while in the case of EV charging, capacity data is representing full forecasted capacity levels. Compliance factors may also be interpreted in terms of “rolling reduction”. For instance, in the case of EV flexibility, it could be represented by a given car experiencing reduced charging once every four hours (25% compliance factor) or two hours (50% compliance factor). Table 5.3 provides an overview of the technologies and compliance cases is considered in this work.

Table 5.3: Overview of modelling representation of the DER technologies.

	Rooftop PV	EV charging reduction	Aggregated embedded storage (VPP)	Demand side participation (DSP)
Modelling representation	Aggregated generation profile at sub-regional nodes. Network constraints considered within traces as provided by AEMO.	Load reduction with time-varying capacity priced at just below market price cap	Storage units aggregated at sub-regional nodes	Constant load reduction capacity at different price bands. Maximum energy limit of 3h on reliability response band.
Compliance factors considered	*N/A*	25% or 50%	50% or 100%	50% or 100%

This explicit representation and modelling of DER coordination using different levels of compliance is aimed at assessing the role of DER for reliability in an increasingly weather-dependent system which is dominated by energy-limited resources.

5.5 Case study and parameter assumptions

In line with the analysis of storage operation assumptions, the studies are based on two reference weather years which follow from the ISP traces [83]. These are characterised by low and high average VRE availability across the year, combined with high and medium demand, respectively. These are weather reference year 2011 with demand 10% POE, and weather reference year 2019 with demand 50% POE. For both of the considered weather years, we evaluate 500 infrastructure outage samples.

The adequacy of the NEM for resource and DER capacity buildout is evaluated based on the *2024 ISP Step Change* scenario, for planning years of 2025 to 2040. The installed capacities considered are listed in Table 5.4.

Table 5.4: Installed capacity as percentage of peak demand in the respective planning year.

Base case - Integrated System Plan NEM 24				
Year	**2025**	**2030**	**2035**	**2040**
Firm capacity (%)	85%	53%	31%	28%
Distributed energy resources				
Electric vehicle (EV) charging peak (%)	0%	2%	4%	5%
Virtual power plants (VPP) (%)	2%	10%	22%	33%
Demand side participation (DSP) in summer (%)	3%	4%	4%	4%

To evaluate and represent the role that DER coordination may play for ensuring reliability, and complementing supply side adequacy, we systematically evaluate the potential of DER to provide adequacy support by adding the different technologies individually with the different compliance factors outlined above. Finally, we evaluate a combination of VPP and DSP flexibility with different compliance factors.

The sensitivities of lower compliance factors of the different technologies are especially important given the updated forecasts of coordinated DER capacities in the Draft 2026 ISP [117], which are significantly reduced compared to 2024 ISP projections, as shown in Figure 5.5 below.

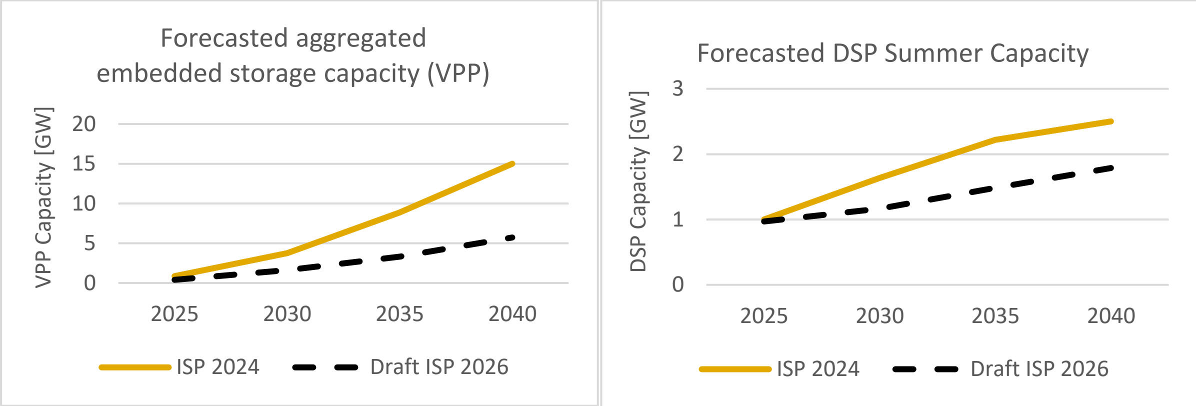

Figure 5.5: Forecasts of VPP and DSP capacity in the 2024 ISP [83], compared with the revision in the 2026 Draft ISP [117].

5.6 Insights and Results

An overview of the adequacy results across all DER coordination cases can be found in Figure , which shows the NEM-wide average and tail risk based on unserved energy, based on the underlying operational approximation of economic operation (A3) for DER and storage resources in the system, i.e. utilising the full workflow and DER representation developed for this work.

First, considering only the reliability levels provided by supply side resources: A strong increase in average unserved energy levels can be seen across the different planning years as thermal capacity retires and is replaced by VRE and storage capacity. The results exhibit significantly higher unserved energy levels than the reliability standard, given the supply side investments in line with ISP projections. We observe that the tail risk (in the worst 5% of the cases) increases even stronger than the average risk, highlighting the exposure of the system to specific outage conditions in critical periods which elevate the supply side adequacy risk.

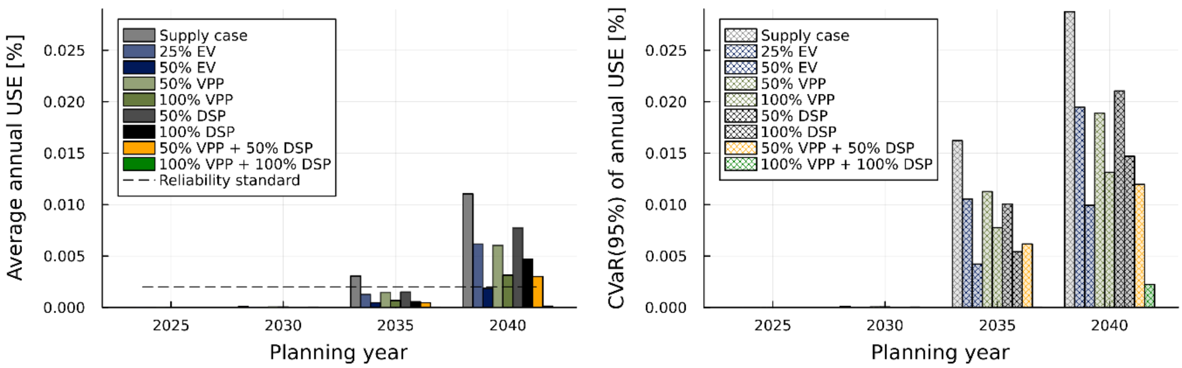

Figure 5.6: NEM-wide average risk (left) and tail risk (right) results of the supply case compared to all DER coordination scenarios across the planning years.

Compared to this supply case, the benefits of DER coordination *across all compliance scenarios* can be clearly observed in a reduction of both average and tail risk, especially in the years post 2030. Figure 5.7 shows the relative benefits of the different DER technologies with respect to the base supply-side case in the resource mixes of the planning years in which DER coordination is essential for providing reliability. In the following, we discuss the implications of the individual DER technologies.

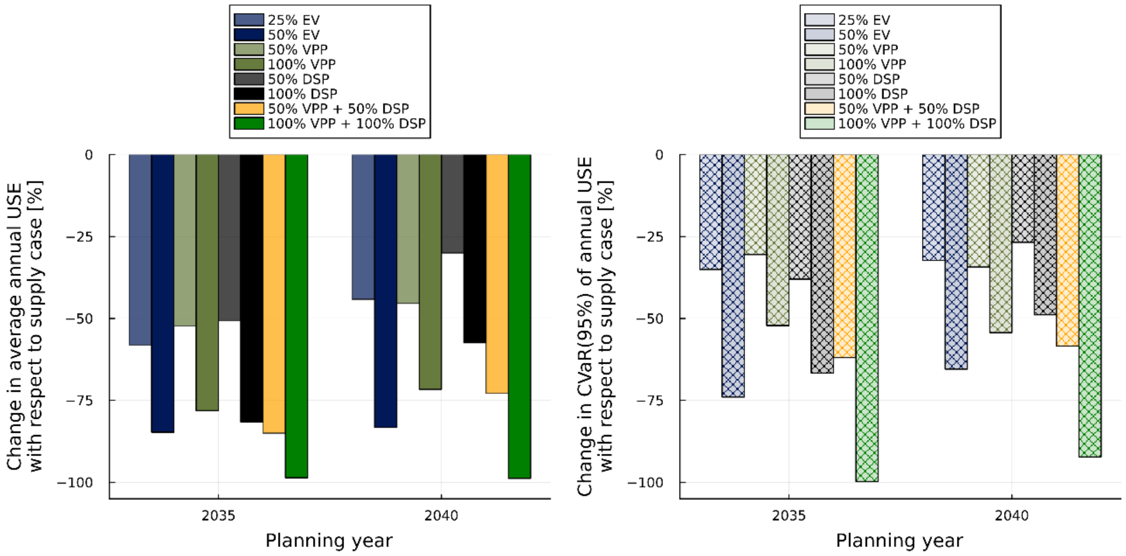

Figure 5.7: Relative change in adequacy metrics with added demand flexibility for the planning years 2035 and 2040. Note that the relative change is not shown for the earlier years due to the lower number of underlying risk events.

Looking at the potential of **EV charging reduction** for supporting reliability in critical periods (modelled as time-varying capacity priced at just below market cap price), the results demonstrate that electrification may provide substantial benefits to the entire system. While electrification – here in form of electric vehicles - increases overall electricity demand, the underlying source of increased demand may create flexibility opportunities that can directly offset the impact of the increased demand in terms of reliability.

Even modest levels of EV flexibility—such as 25% compliance—can deliver meaningful adequacy benefits. This relatively low penetration may correspond to not serving individual vehicles only every four hours, suggesting that substantial system benefits may already be realised without requiring all vehicles to participate or frequent load reduction events. A potentially important message from these results is that relatively complex vehicle-to-grid (V2G) operation may not be necessary to realise substantial adequacy benefits. Simple charging reduction during critical periods may already provide strong adequacy support.

However, it should be noted that a limitation of this analysis is that the charging profiles are differentiated only between weekday and weekend patterns. More detailed understanding of actual EV charging behaviours—including seasonal variations, time-of-day preferences, and location-specific patterns—would be valuable for refining these estimates.

Looking at the benefits provided by DER coordination through **VPPs** (represented as aggregated storage capacity under compliance factors of 50% and 100%), we observe that adequacy benefits are similar to the EV results, despite significantly higher capacity being installed. This suggests that whilst VPPs may provide benefits to the market — such as avoiding the need to run peaking plants and potentially reducing wholesale prices — its adequacy contribution is fundamentally limited by the availability of energy to shift during critical periods.

Furthermore, VPP operation may be characterised by the same *imperfect operation* as utility-scale storage units as described in chapter 4, which adds a second layer of uncertainty to the contribution of VPP to adequacy in the future resource mix. The difference in the VPP benefit to adequacy with respect to the different operational representation in shown in Figure 5.8. The results show that while assuming the *A1: High energy* operation, for all storage units, VPP coordination may effectively reduce the adequacy risk almost entirely (which already is low given the operation of the other storage units in the system). However in the derated and the economic operation case, the benefit is reduced (VPP units are derated in energy by 50% regardless the duration in line with AEMO assumptions[7]).

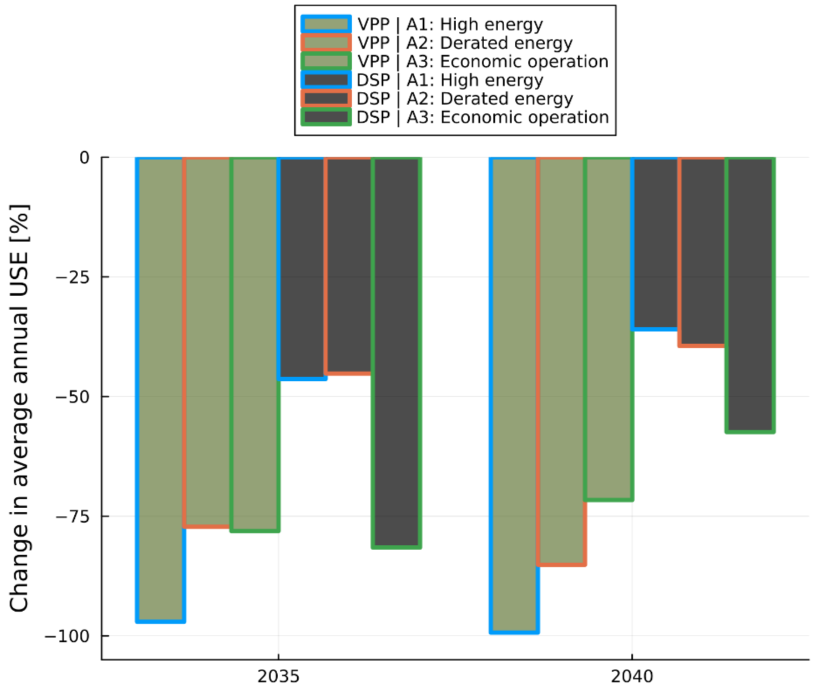

Figure 5.8: Change in average annual USE from 100% VPP or 100% DSP coordination, as represented under different operational approximations A1 – A3, as introduced in chapter 4. Results of earlier planning years not depicted due to insufficient USE event sample size.

Furthermore, even with substantial capacity, the ability of VPP to support the system during critical events depends on having sufficient energy available to shift. This becomes particularly evident in the underlying weather years, where the key risk emerges when energy availability is generally low. This can be observed when looking at the distribution of events when load shedding was recorded across the adequacy assessment, as depicted in Figure 5.9. In the low VRE availability weather year, we can see that VPPs are able to effectively shift the tail events, however not reducing the number of events observed. This indicates that under the modelling assumptions of this work, VPPs are providing energy to the events but are not as effective in reducing the frequency of the severe shortfall events compared to DSP (even though the installed VPP capacity is more than 8x the capacity of DSP).

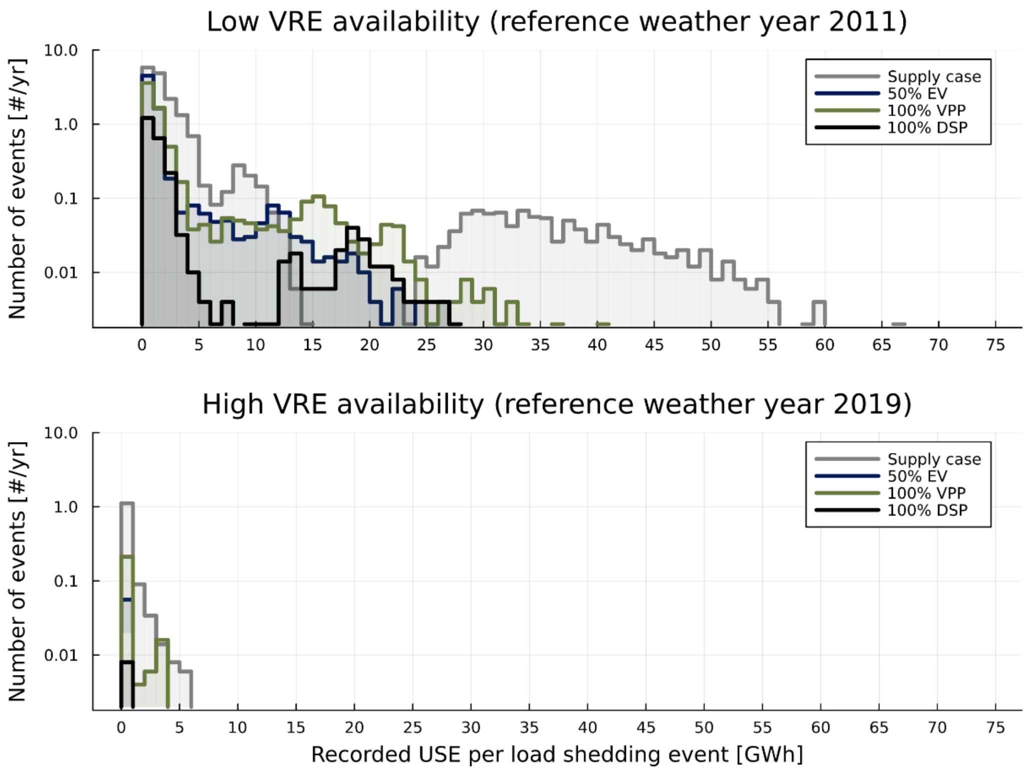

Figure 5.9: Distribution of unserved energy (USE) events in planning year 2040 with different levels of DER penetrations and two different weather years under storage operation assumption "A3: Economic Operation". Note the logarithmic scale on the y-axis.

Comparing these weather years, we can observe that the **DSP load reduction** is very effective at shifting and reducing the tail, which is especially crucial in the low VRE availability year. This effect is also reflected in the adequacy metric results, as shown in Figure 5.6: DSP coordination (modelled as price-responsive load reduction capacity) is less effective in reducing *average* adequacy risk compared to EV load reduction and VPP coordination (due to lower installed capacity), however the reduction in tail risk is more closely correlated across the technologies. **This suggests that demand flexibility in the form of DSP may be especially crucial for tail risk mitigation.**

On the other hand, the full potential of DSP may only be reflected in adequacy assessments when with different price bands are operationally considered. This can be seen in Figure , where there is a significant difference observed across the different operational representation within the adequacy assessment. While *A1* and *A2* are based on the PRAS dispatch engine (which reflects current industry practice at PJM [76]), which dispatches demand side resources heuristically as last response, after exhausting all available hydro and storage units. However, as *A3* is based upon an economic dispatch with price visibility and inter-temporal scheduling, DSP in lower price bands may be activated earlier, effectively deferring storage discharging to later periods. This interaction between price sensitive demand side response and storage discharging therefore leads to a greater reduction in adequacy levels. Therefore, activating this demand side resources already at lower prices may provide even stronger benefits than just as a last resort measure, which may be achieved through increased market exposure of flexible demand, e.g. through dynamic pricing schemes.

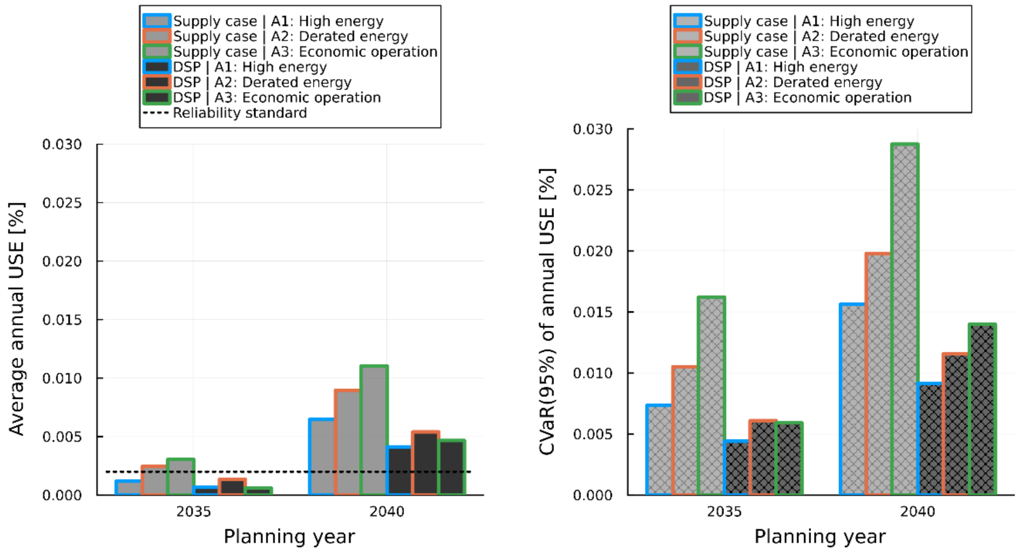

Figure 5.10: NEM-wide average risk (left) and tail risk (right) with respect to annual unserved energy (USE) across different operational approximations.

Additionally, the results with DSP coordination against the impact of operational representation in the supply case can be seen in Figure 5.10. Here, we observe that while the adequacy results of the supply case are increasingly diverging across storage operation representation with increased storage and VRE penetration (in grey), adding DSP to the resource mix (black) reduces the spread across the operational representations, both in average and tail risk results.

This finding suggests that **DSP may provide additional hedging against operational uncertainty of storage**, since DSP activation can complement storage operation across a wider range of system conditions. There is therefore a strong reason to introduce operational details to find the right balance of investments. DSP coordination at lower prices (e.g. enabled through increased market exposure) has even stronger benefits for adequacy, suggesting that **priority should be placed on enabling price sensitivity in demand-side resources**. However, this also needs to be captured by adequacy assessment methodologies to actively inform decision making.

Finally, regarding the cases of **lower compliance** across the different DER technologies, see Figure 5.7, we observe that already half of the full potential may provide significant adequacy benefits, and may be sufficient to reach adequacy levels in earlier years, as first significant thermal generation is retiring. However, towards ultra-high penetrations of VRE and storage (as in 2040), higher compliance factors might be needed to ensure reliability under the buildout assumptions in the *2024 ISP Step Change* scenario.

Furthermore, given that multiple DER technologies may be available at the same time, a combination of VPP and DSP with low compliance factors may already provide significant benefits, as can be seen in Figure 5.6 especially in the storage dominated system post 2030. Therefore, given the high degree of uncertainty around DER adoption and coordination, the key message should be that any degree of demand flexibility - even solely EV load reduction in critical periods – may be essential for ensuring adequacy in a weather-dependent system dominated by storage.

5.7 Key findings

The following points summarise the key insights and recommendations considering DER coordination of various technologies and its implications for reliability in an increasingly weather-dependent, energy-limited NEM power system.

- Overall, in line with various other recent reports such as the National Electricity Market Reliability & Security Report FY2025 [118], our results suggest that while DER coordination levels are highly uncertain, there is **strong evidence of the benefits of DER coordination for reliability** by reducing demand in critical periods in the future NEM.
- As thermal generation retires post 2030, the **reliability of the future system is highly sensitive to both DER uptake and coordination** levels. All three DER categories examined—electric vehicle load reduction, VPP coordination, and DSP enablement—can deliver significant adequacy benefits in a future resource mix, even under lower compliance factors.
- While coordinated demand response in the form of DSP represents only approximately 4% of peak capacity across the assessment period, it can play an essential role in ensuring adequacy within a storage-dominated system. Importantly, **DSP may provide effective hedging against the impact of storage operation uncertainty on adequacy results**.
- **Overall, DER coordination can effectively shift and reduce tail risk** while simultaneously reducing expected risk. This concentrates remaining risk to extended periods characterised by low VRE availability and high residual demand.
- To ensure reliability in the future NEM, the National CER roadmap [1] and related initiatives must support the effective implementation of enhanced DER coordination to maximise the visibility and controllability of customer energy resources.

6 Reliability risk profile of the National Electricity Market

This chapter builds upon the previous described developments for capturing storage operation and modelling DER. The goal is to consolidate different emerging relevant adequacy risk drivers and support technologies and provide a structured methodology to assess the reliability risk profile of the NEM.

6.1 Methodology overview

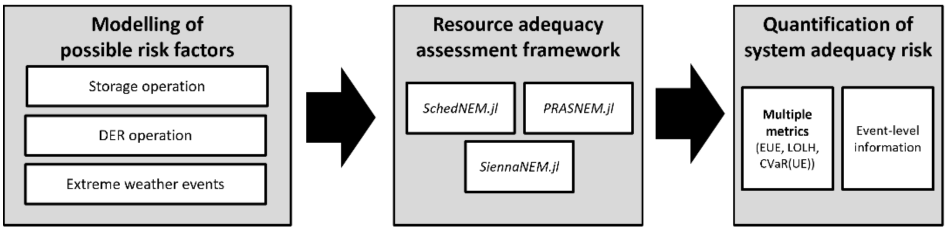

Figure 6.1: Schematic overview of the methodology applied for systematic assessments of the reliability risk profile of the future NEM

To understand the reliability risk profile of the NEM during the energy transition, we apply the open-source modelling framework described above to provide a full characterisation of adequacy risk under ISP scenario projections, storage operation modelling addressing imperfect foresight, and explicit DER representation. A schematic overview is presented in Figure 6.1.

Specifically, the methodology uses *ParseISP.jl* to access and consolidate all necessary data sources from public ISP data into a comprehensive data format that serves as the foundation for subsequent studies. This includes various weather years and demand traces, as well as the buildout scenarios developed in the development pathways. This data is then translated into the operability frameworks of *SiennaNEM.jl* and *SchedNEM.jl* to capture the time-sequential operational details of the system under various technology constraints. Complementarily, the adequacy framework *PRASNEM.jl* provides the computational efficiency and performance to evaluate the system under various outage conditions. The methodology builds upon the three stages described in Chapter 4.

The analysis of the reliability risk profile is built upon the following approach:

1. **Characterising the risk** events and the full risk profile under multiple metrics
2. **Highlighting risk drivers** and correlations, as well as the implications of storage operation approximations

These perspectives on adequacy are designed to provide a comprehensive picture of the reliability risk profile of the National Electricity Market in the energy transition over the next decades. Furthermore, all underlying modelling code is provided in the *NEM-reliability-suite*, *SchedNEM.jl*, and *PRASNEM.jl* to enable reproducibility and empower stakeholders to employ and test different assumptions.

6.2 Case study parameters

To obtain a comprehensive picture of the risk profile of the changing system, we assess adequacy risk in a *'base case'* scenario across all 13 available reference weather years (2011-2023), as well as both demand levels provided (POE 10% and POE 50%). We apply 100 outage samples of thermal generators and transmission lines, therefore resulting in 2600 samples per planning year, with hourly granularity across the whole year. The buildout of the installed capacities is based upon the *2024 ISP Step Change* scenario, with the installed capacities as in Table 6.1. Because VPPs are forecasted as a significant share of installed capacity, we include their buildout in the analysis, noting that this storage capacity may also be provided by large-scale batteries, with an increasing uptake forecasted in the recent 2026 Draft ISP [117].

Table 6.1: Installed capacities across the different planning years as percentage of peak demand. The buildout is based upon the 2024 ISP Step Change scenario.

Base case capacity **- Integrated System Plan NEM**				
Year	***2025***	***2030***	***2035***	***2040***
Firm capacity (%)	85%	53%	31%	28%
Storage (incl. VPP) (%)	20%	53%	75%	91%
VRE (%)	127%	206%	245%	235%
Hydro (incl. PHES) (%)	20%	22%	25%	22%

When assessing the results across multiple weather-demand reference years, we are applying the weighting across the demand traces as outlined in the 2025 NEM Electricity Statement of Opportunities (ESOO) [7], namely 30.4% for POE 10% and 39.2% for POE 50%, effectively reducing the overall average risk, assuming a weight of 30.4% for the POE 90% cases which are not provided in the ISP and not explicitly assessed, assuming no unserved energy events. These demand weights are applied for the results below for the average metrics. Following this reasoning, when calculating tail metrics such as VAR and CVaR, we assume a third run of the same number of samples with no underlying adequacy risk events (i.e. the 90% demand trace).

6.3 Insights and results

As outlined above, the results are focused to first provide an overall characterisation of the risk profile, followed by insights about underlying risk drivers, and finally concluded with a discussion of planning and operational measures for ensuring adequacy in a transitioning power system.

6.3.1 Characterising the changing risk profile

The overall average risk under the operational assumption of *A3: economic operation* is presented in Figure 6.2 distinguished by region and in Figure 6.3 with respect to the underlying reference weather year. We observe that on average across all weather years, the system complies with the reliability standard, even with the fundamental shift in underlying capacity beyond planning year 2030. This is expected since the ISP buildout is designed to expand the system to adhere to the reliability standard. Looking at Figure 6.3, we note that some years are above the reliability standard, while other years showcase close to no unserved energy, which follows expectations, as also described in the 2024 ISP [119], but also reinforces that reliability in the future system is increasingly dependent on underlying weather conditions as thermal generation retires post 2030.

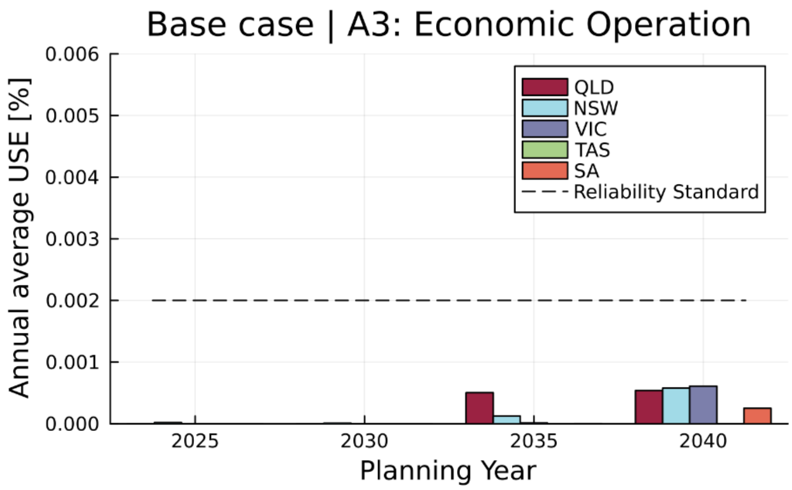

Figure 6.2: Annual normalised average unserved energy by NEM region in the base case.

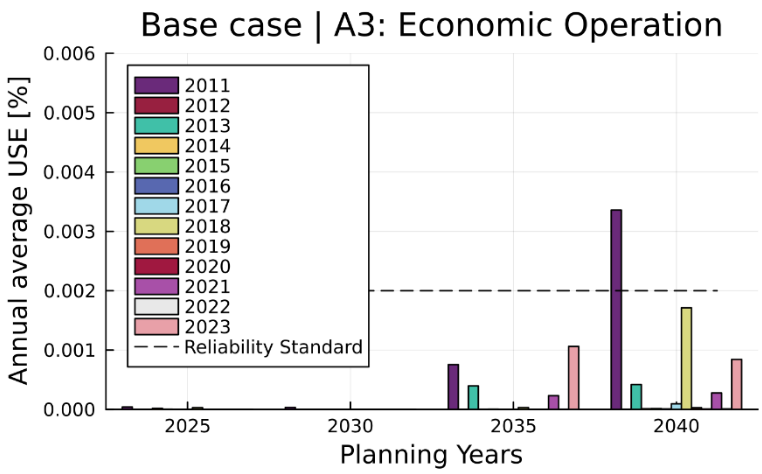

Figure 6.3: NEM-wide normalised average unserved energy (USE) per reference year in the base case.

While these base results provide a core understanding of the risk profile, we now investigate the underlying risk first on a sample level by looking at overall risk metrics, followed by an analysis of event level details.

Complementary risk metric results

As described in Chapter 2, the adequacy risk in an energy-limited and weather dependent power system may be needed to assess with multiple complementary metrics. To characterise the changing risk, we determine the magnitude, duration, and frequency of the risk, across all the samples, with respect to the average as well as tail metrics. An overview of the NEM-wide reliability risk across the four planning years can be found in Figure 6.4.

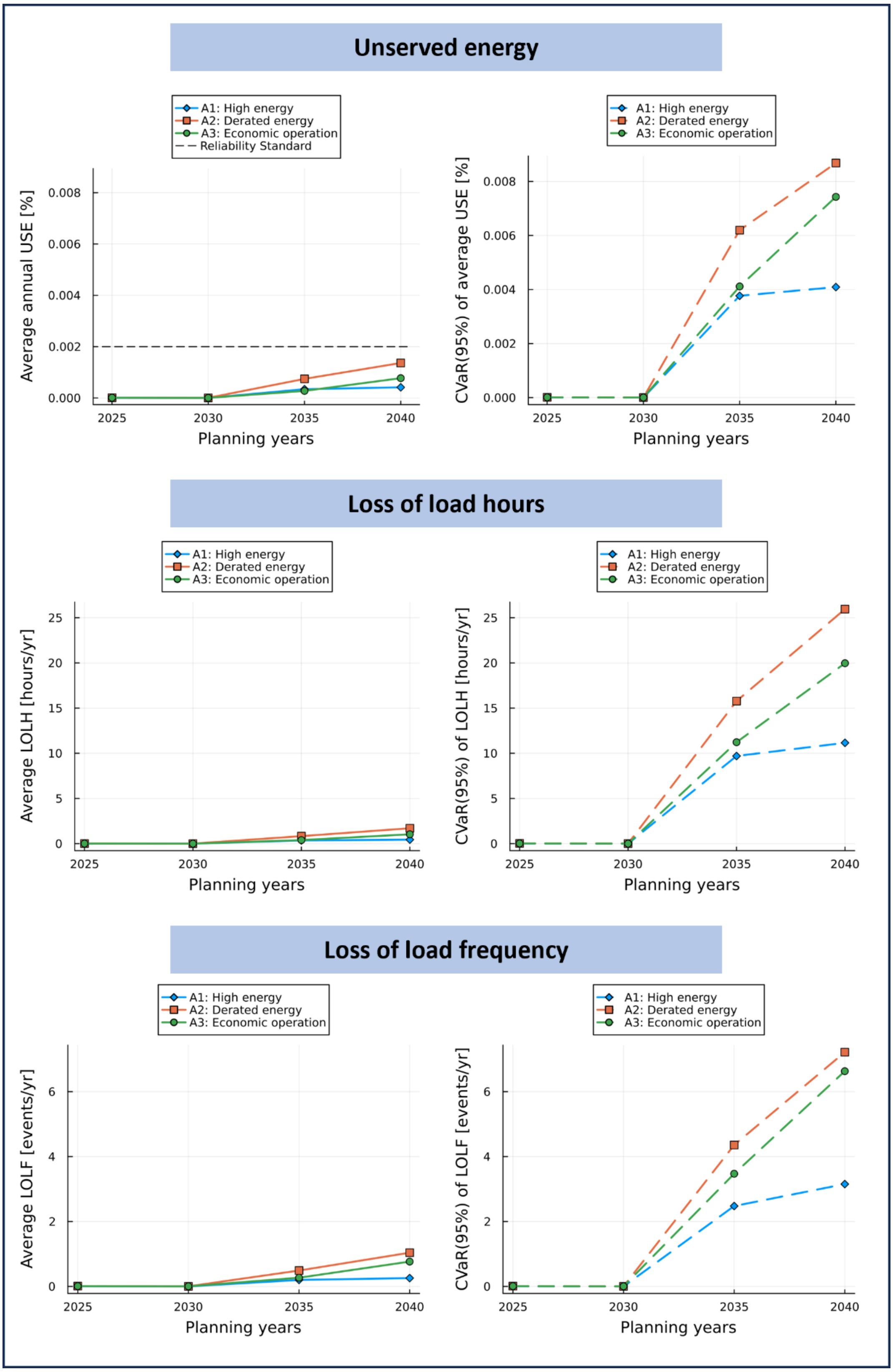

Figure 6.4: NEM-wide reliability risk measured across all weather-demand reference traces and weighted aligned with ESOO practices under different storage operation approximations and against metrics of unserved energy, duration and frequency.

When comparing the adequacy risk metrics across storage operation approximations and planning years, we can see an overall increase, especially post 2030. Across duration, frequency, and magnitude the tail risk rises stronger than the average, indicating that specific outage and weather conditions may especially drive the risk. Furthermore, the tail in duration may be especially large compared to the average, indicating that duration-based metrics may be unsuitable to capture the shift in risk as the system becomes dominated by storage and weather-based generation.

Further details can be uncovered by assessing the distribution of event level details in the following.

Event level risk details

Looking at the underlying load shedding events in detail across all weather-demand reference traces and planning years, we observe the results shown in Figure 6.5. Note that as these results show the distribution of all the measured events, these results assume all events as observed in the weather-demand reference years with the same weight (i.e. no weighting by demand level is applied).

Comparing the distribution of load shedding events across the planning years, we note an increase in numbers (i.e. frequency), as well as an increase in duration and magnitude of the events, which was also reflected in the metric level overview. This suggests that the NEM may face longer and larger USE events, particularly after 2030, as thermal generation is retiring.

While the operational approximation case of derated energy (orange) exhibits a greater frequency of tail events, there are a cluster of USE events in the economic operation case (green) with a significantly higher magnitude, particularly in the planning year 2040. However, the tail risk of both cases is of comparable magnitude (see Figure), which suggests that the annual tail is heavily influenced by a smaller number of larger USE events under the storage operation approximation of economic operation, which may not be able to capture under the derated operation approximation. This highlights how the uncertainty introduced by storage operation extends beyond overall metrics and may affect investment decisions: while shorter USE events may be well addressed by additional investments in storage, longer events may require investments in additional gas capacity or demand response.

On the other hand, this difference in underlying risk events also highlights *how tail events may potentially be addressed by storage operation interventions*, as the occurrence of these events is sensitive to the storage operational representation.

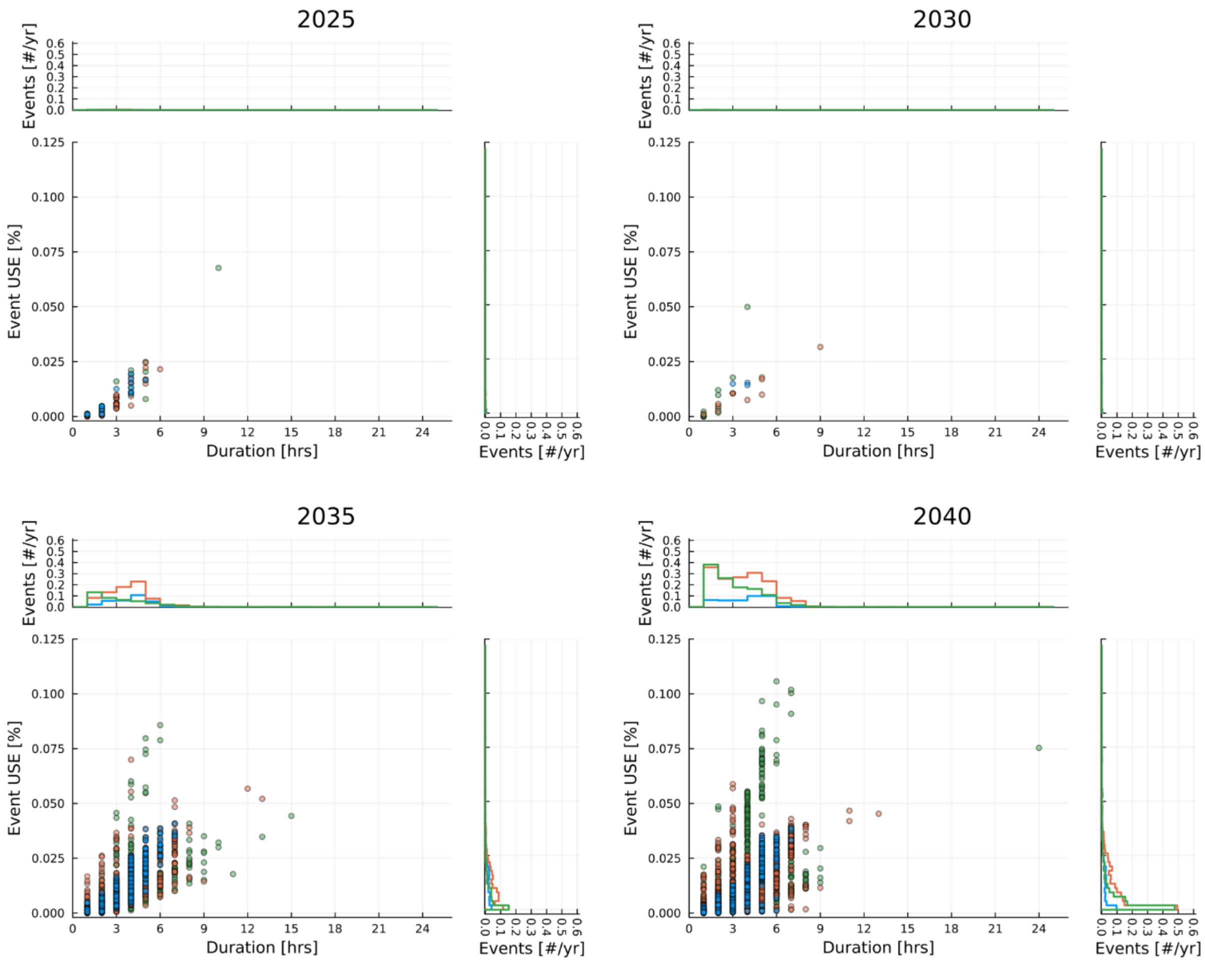

Figure 6.5: Details of unserved energy occurrences (USE events) across all weather-demand reference traces and storage operation assumptions.

Additionally, we consider the benefits of demand-side participation (DSP) coordination for reducing the observed adequacy risk occurrences. DSP is modelled as load reduction capacity with different corresponding price bands, as described in Section 5.4. We assume a compliance factor of 100% of the forecasted capacities and observe the results across all weather-demand reference years as shown in Figure 6.6.

While the distribution of the two cases is similar in the earlier planning years of 2025 and 2030, we observe that in the years when the system becomes dominated by weather-dependent generation and storage, the value of load reduction in critical periods through DSP is highly prominent. Especially *tail risk events are effectively reduced when considering the flexibility of reducing demand in critical periods*, in accordance with AEMO 2024 ISP forecast levels.

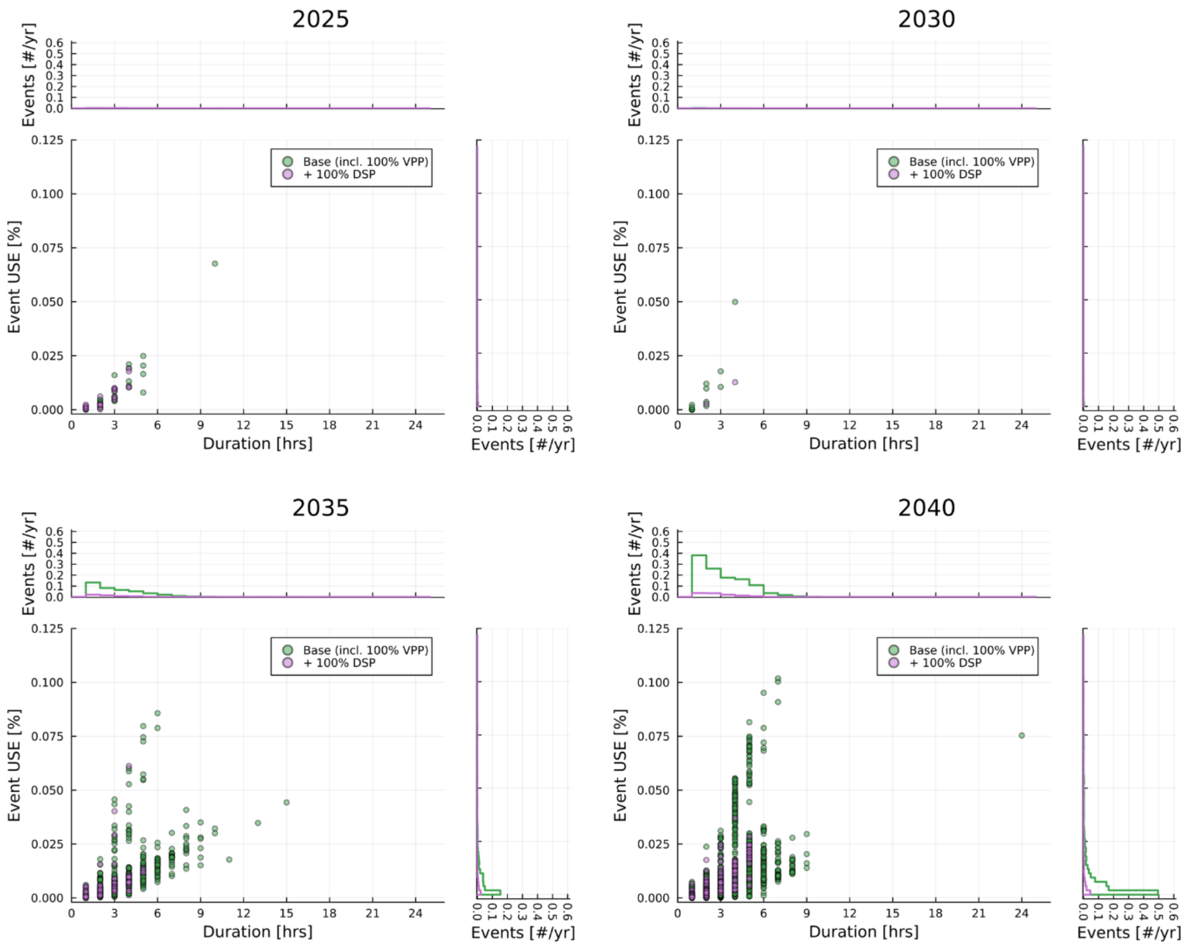

Figure 6.6: Details of unserved energy occurrences (USE events) in the NEM across all weather-demand reference traces under two different levels of DER coordination, based on the storage operation approximation of 'A3: economic operation'.

6.3.2 Assessing adequacy risk drivers and conditions

In the following we are investigating the specific system conditions and correlations that may serve as specific risk drivers, with the aim at informing planning and targeting operational mechanisms to support reliability.

Critical periods across the day

Figure 6.7 shows the start times of the critical risk events across the time of day, as the underlying resource mix changes, and storage becomes the main adequacy support. We observe that while in 2025 and 2030 the main start of risk periods is in the evening, the start of the events shifts across the day and to the morning peak times. However, a difference between the storage operation approximations is visible: The risk in the *high energy* and *derated energy* approximations is concentrated at the net-demand peak times in the morning and evening, while the risk in the *economic operation* case is starting also later at night due to the lower state of charge of storage units, and therefore the reduced ability of the system to respond. This shift in risk times may require *flexible operational mechanisms* to address changing risk periods under uncertain storage operation regimes.

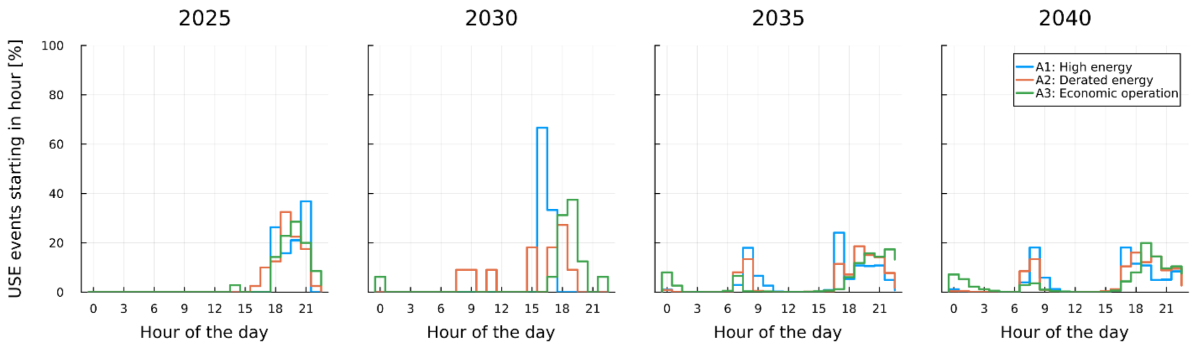

Figure 6.7: Distribution of start time of observed load shedding events across all weather-demand reference years, as well as under different storage operation approximations.

Demand levels

While varying demand across the day may serve as risk driver, the absolute magnitude has also traditionally been the key risk driver, as a thermal generation-based system may be capacity constraint especially in high demand hours. However, with increasing VRE penetrations, the relationship between high demand and adequacy risk may be increasingly weakening. The distribution of unserved energy events against the operational demand is shown in Figure 6.8. Since aggregated embedded storage is fully visible as VPP to the market in our simulation and is scheduled like utility scale storage, we are considering the underlying demand reduced by rooftop PV production, to get a better understanding of the demand conditions that the system and storage scheduling may face in critical periods.

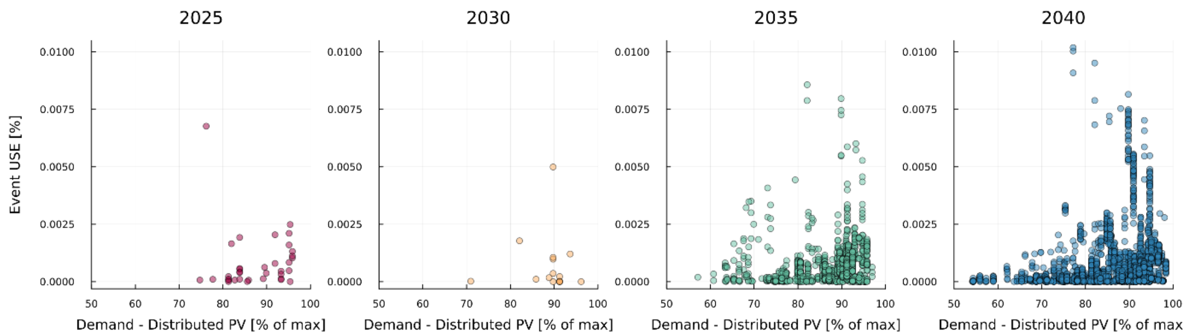

Figure 6.8: Distribution of event level unserved energy (USE) with respect to underlying demand minus distributed PV generation at the start of the event, under the economic operation storage approximation.

We observe that in the years 2035 and 2040, key reliability risk periods are still associated with periods of high demand (accounting for distributed PV) even as the system transitions away from thermal generation. This supports the traditional risk focus on preparing for the (net) peak periods and highlights the ongoing need to prepare and schedule the system for high demand periods. However, as thermal generation is retiring and storage operation defines system risk, an increasing number of USE events occur at lower levels of demand, occurring already as low as in 60% of the annual peak levels. This spread indicates that additional planning and operational measures may be required that can support reliability at various levels of demand.

VRE availability and storage state of charge levels

To understand what different storage operation approximations may reveal about adequacy risk drivers, we examine VRE availability and storage state of charge levels in the 8 hours before critical events. These pre-event hours are critical because they highlight the charging and discharging decisions of BESS across the system, as well as energy limitations that the whole system is facing in terms of VRE energy potential.

Figure 6.9 shows the distribution of risk events with recorded unserved energy in 2040 across all weather-demand reference years and under the three storage operation approximations introduced in chapter 50 with respect to residual demand (left) and to state of charge across the short- and medium duration storage units (right). Residual demand here is considered as the total NEM-wide demand, minus the NEM-wide VRE availability per hour.

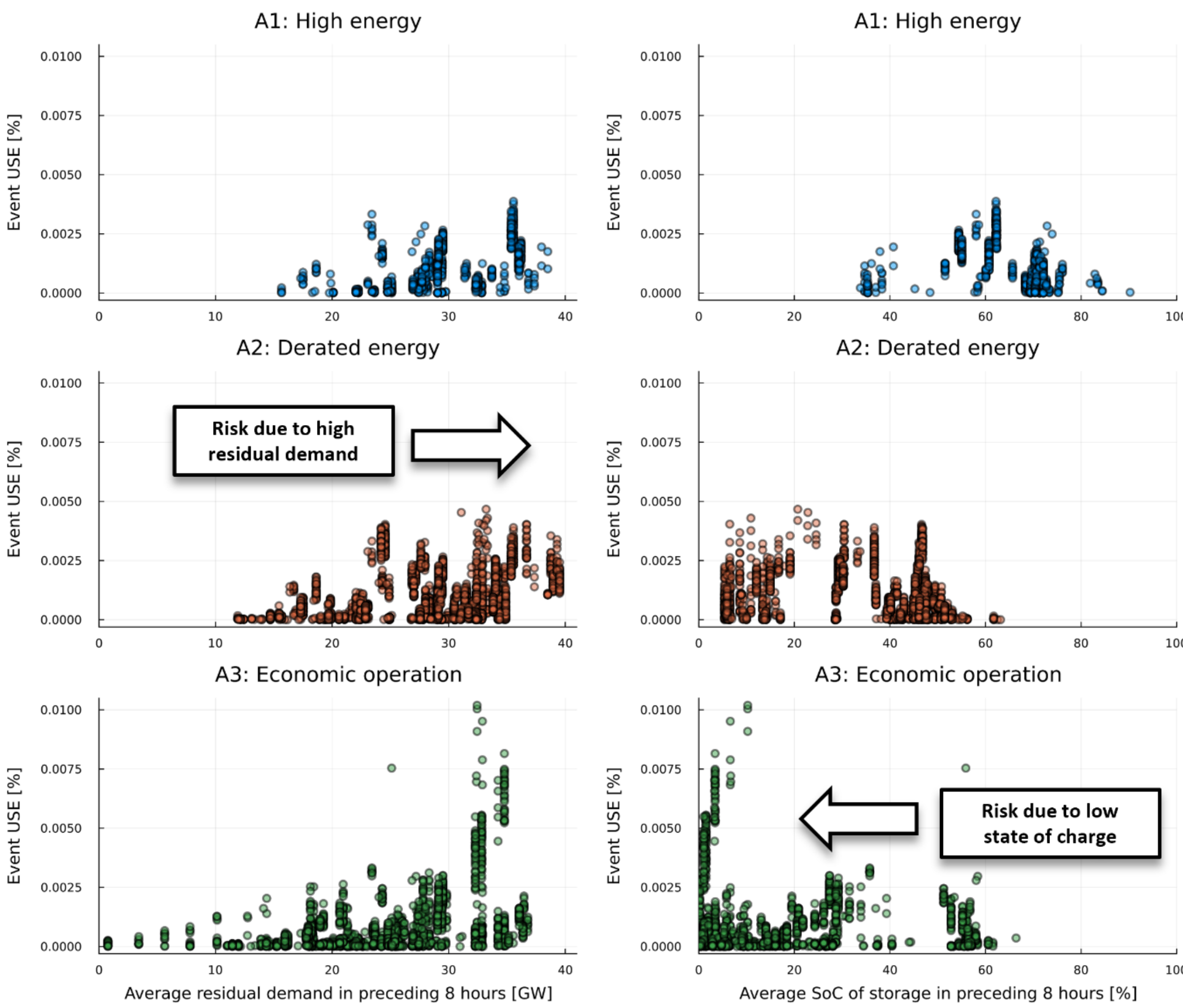

Figure 6.9: Distribution of risk events with recorded unserved energy (USE) in 2040 across the NEM under the three different storage operation approximations introduced in chapter 4. The average state of charge (SoC) of the storage units is calculated across all short- and medium duration storage as well as coordinated embedded units (in VPP). The magnitude of the event level USE is normalised by the total annual demand of the respective weather-demand reference year.

In line with Figure , we observe that the risk events recorded with storage approximation of “derated energy” are more concentrated compared to the approximation of economic operation. Additionally, a clear difference is emerging when comparing the risk events recorded by the different approximations (highlighted in the figure): While the events recorded under “derated energy” are concentrated around higher residual demand periods, the events from “economic operation” are stronger aligned with preceding lower state of charge periods.

This difference underscores a key takeaway from chapter 4, that adequacy assessments need to consider the dimension of storage operation uncertainty when evaluating a system defined by weather-dependent generation and storage. While all these approximations are characterised by limitations, a combination of storage operation approximation algorithms may be needed to identify all risk drivers and inform investment and operational measures.

6.3.3 Discussion on addressing the changing risk profile of the NEM

The above results warrant some key considerations regarding necessary planning and operational measures that should be taken for ensuring adequacy in the NEM post-2030, as thermal generation retires and is replaced by weather-dependent resources, complemented by storage.

Planning perspective

Considering required planning measures for ensuring adequacy across the next decades, it needs to be stressed that the ISP outlines a substantial level of investments to achieve the base case scenario. This includes approximately tripling VRE capacity (including distributed PV) between 2025 and 2040, alongside a massive buildout of storage exceeding 30 GW of storage in the form of utility storage or fully coordinated virtual power plants. These investments form the foundation upon which the adequacy outcomes presented in this analysis depend.

A key challenge in determining the optimal mix for planning investments is the uncertainty surrounding storage operation approximations. Rather than attempting to determine a single "correct" storage operation model, a more robust approach would be to calculate adequacy risk across multiple storage operation assumptions. This can provide a wider range of outcomes and may help identify investments that perform well for supporting reliability across different operational approximations. Additionally, demand response could be especially valuable for reducing this uncertainty, as it provides flexibility that is less dependent on perfect foresight or specific operational assumptions.

Beyond average adequacy conditions, reliability planning should facilitate DER coordination to prepare against tail risk driven by specific weather conditions. Enabling demand reduction (DSP) in those critical periods can improve system reliability massively (see Figure), reducing the need for cost intensive additional generation investments for tail risk events.

Measures on operational timescales

Complementary to investment considerations for resource adequacy, the results also highlight several operational options and requirements to address and ensure reliability in a changing NEM.

From the event level details, compare Figure , we observed a difference in tail risk events across the storage operation assumptions. While this highlights strong uncertainty and may potentially lead to reliability risk if left unaddressed, this divergence in event level details may also be seen as operational opportunity: Given that the size of the events changes purely from operational means – in contrast to different investments – operational measures such as interventions may provide a strong opportunity to prevent or limit tail risk events (e.g. this could shift the risk profile from approximation A3 towards the risk of A2).

Additionally, considering future risk drivers, there is an increasing need to consider flexible parameters to also capture non-peak demand periods in operational reliability measures. This should include for example support across the night or at low VRE periods. Also here, to identify the relevant periods, multiple different storage approximations may be required within the reliability assessment.

Economic and policy implications

There are economic implications of ensuring reliability in a system highly sensitive to storage operation. The intrinsic risk related to uncertain adequacy results increases system costs in two ways: either through increased levels of unserved energy, or through additional infrastructure investments required to hedge against this uncertainty. On the other hand, storage operation can be influenced to resemble the operation assumed in planning models. This introduces additional costs or revenue losses for storage operators, as they must forgo profit opportunities to support system reliability.

This creates the fundamental trade-off between cost of aligning storage operation with system reliability objectives, effectively giving away opportunity cost to reduce overall system cost. However, the different storage operation mechanisms may also be understood to represent distinct regulatory and market frameworks. Storage operation in the high energy and derated energy cases may correspond to system operation under a form of capacity mechanism framework, where storage may be subject to a form of minimum state of charge requirements unless called upon. In contrast, the economic operation case may reflect an energy-only market-based framework where storage responds primarily to price signals. These mechanisms may be changed through policy interventions, such as introducing capacity mechanisms or imposing operational constraints in form of the operational measures discussed above.

The presence of a capacity mechanism that explicitly influences storage operation could also provide another significant benefit: it would reduce the intrinsic uncertainty in storage operation modelling. Rather than storage behaviour being driven by complex heterogeneous market interactions under imperfect foresight, a capacity mechanism could constrain storage operation within more predictable bounds, making adequacy assessments more robust to operational assumptions. This suggests that policy design choices may influence both actual system adequacy and the confidence with which adequacy results may be interpreted.

6.4 Key findings

This chapter provided a comprehensive overview of the NEM reliability risk profile, as the underlying system resources change from a thermal-dominated to a weather-dependent, energy-limited resource mix, in line with the *2024 ISP Step Change optimal development path*. While the overall system is expected to meet the reliability standard across the considered planning years of 2025 to 2040, the underlying distribution of risk events is experiencing a shift which is sensitive to storage and system operation approximations and may exhibit increasing tail risk events. The following key points are emphasised:

- As the system becomes dominated by VRE and storage, the NEM may face **longer and larger load shedding events**, especially under storage behaviour aligned with *A3 economic operation* approximations. However, demand flexibility may significantly reduce the impact of these events.
- Tail events may be avoided by investments, increased DER coordination, **as well as storage operation interventions, as they are sensitive to storage operation assumptions.**
- Ensuring reliability in a future weather-dependent system while relying on energy-limited resources to shift energy requires addressing critical periods that may occur across various times of day, including late evening hours, and across a wider range of demand levels.
- There is **substantial potential for operational interventions**, given the significant differences in adequacy outcomes across storage operation approximations.
- The changing risk periods and drivers, as well as the sensitivity to storage operation may necessitate investments in control of flexible assets, as well as operational and policy changes that are able influence storage operation. However, such **measures should be complementary to, rather than replace, typical peak demand risk management**.
- Identifying risk periods to define investment and operational measures requires using more than one storage operation approximation as indicated in Figure 6.10. As storage operation may be inherently uncertain, **different storage operation algorithms may expose different risk drivers and risk periods in the system.**
- **Increased DER coordination, for example in form of price-sensitive demand reduction (DSP), can be effective for mitigating tail risk events and storage operation uncertainty** that may occur in NEM after 2030. Investments and policy promoting DER visibility and controllability may prove key for ensuring reliability even under low VRE conditions.

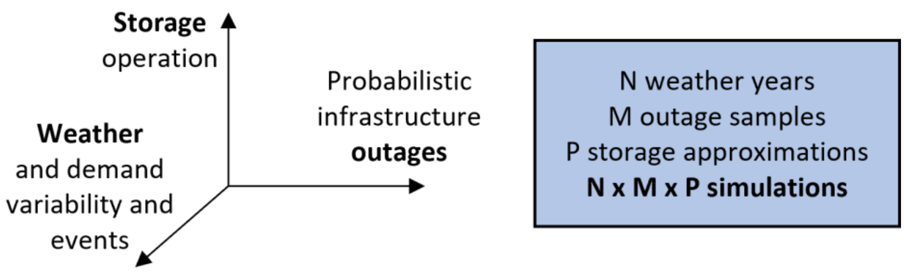

Figure 6.10: Stylised representation of dimensions of uncertainty fundamental for adequacy assessments in weather-dependent systems dominated by storage.

7 Resilience scenario modelling for power system planning

The primary purpose of a power system is to supply electricity to consumers. This requires adequate generation resources and secure network operation so that the system can maintain stability during and after disturbances. These requirements have long been addressed through reliability planning, which is built around generation adequacy and network security criteria. Separately, the concept of resilience has been discussed in the context of natural disasters, extreme events, and high-impact-low-probability (HILP) disruptions, recognising that some disruptions exceed what conventional reliability planning is designed to handle. While the two concepts are not new individually, their interaction becomes more relevant as power systems evolve. This chapter highlights the difference between reliability and resilience while highlighting the importance of incorporating resilience modelling as the systems transition to VRE-dominated system. A comparison of the two paradigms is provided in Table 7.1.

A power system planned under the reliability paradigm is designed to **perform consistently under foreseeable operating conditions**. This involves two core requirements: sufficient generation must be available to meet prevailing load demand, and the system must be capable of withstanding N-1 (or N-1-1 and N-2, where applicable) contingencies without instability or cascading outages. The underlying logic is that designing for credible disturbances and maintaining adequate reserves will allow the system to serve load reliably under normal conditions. Reliability planning is effective for credible contingencies but does not extend to events well beyond N-1 or N-2. On the other hand, natural disasters affect multiple facilities simultaneously in ways that are difficult to anticipate. It is neither practical nor economical to design a power system to withstand all such events.

Under the resilience paradigm, the system is expected to **mitigate the initial impact**, for example, limiting the scope of widespread blackout, and **recover as quickly as possible**. The resilience expectation may vary significantly depending on the time, nature, intensity, location of the natural disaster events that would result in different N-k extreme contingencies on the system. Rather than preventing all outages, the aim is to limit the extent of system degradation and restore normal operation as quickly as possible. Simply put, the goal is **to sustain critical system operation to enable quick recovery**.

7.1 Reliability and resilience definition from industry and standards bodies

The concept of reliability has been defined and refined across multiple international bodies over several decades. The International Council on Large Electric Systems (CIGRE) established an early definition in 1987, describing reliability as '*a measure of the ability of a bulk power system to deliver electricity to all points of utilization within accepted standards and in the amount desired*.' This was subsequently refined in 2002 to encompass two functional aspects, adequacy and security [2], [120]. By 2018, CIGRE updated the definition to include bidirectional power flow, reflecting the growing presence of distributed generation. Reliability was redefined as 'a measure of the ability of a power system to deliver electricity to all points of consumption and receive electricity from all points of supply within accepted standards and in the amount desired'[2], [120], [121]. It is worth noting that the 2018 update derives from the 1987 definition rather than the 2002 version.

The Institute of Electrical and Electronics Engineers (IEEE) adopted a probabilistic perspective in their now inactive standard, defining reliability as '*the probability that a system will perform its intended functions without failure, within design parameters, under specific operating conditions, and for a specific period of time*' [122]. A joint IEEE/CIGRE task force described it as '*the probability of its satisfactory operation over the long run … the ability to supply adequate electric service on a nearly continuous basis, with few interruptions over an extended time period*' [123].

The North American Electric Reliability Corporation (NERC) characterises reliability in terms of measurable outcomes. It describes reliability as '*the degree to which the performance of the elements of that system results in power being delivered to consumers within accepted standards and in the amount desired*', noting that reliability may be measured by the frequency, duration, and magnitude of adverse effects on consumer service [123].

The Australian Energy Market Operator (AEMO) defines reliability as '*the ability of the power system to supply adequate power to satisfy consumer demand, allowing for credible generation and transmission network contingencies*' [124], while the Australian Energy Market Commission (AEMC) describes it simply as ensuring '*there is enough capacity (generation, demand response and networks) to supply customers*'[125].

The concept of resilience, although newer compared to reliability, also has been defined and refined across multiple international bodies. IEEE defines resilience as '*the ability to withstand and reduce the magnitude and/or duration of disruptive events, which includes the capability to anticipate, absorb, adapt to, and/or rapidly recover from such an event*'[126], [127].

AEMO has drawn on several external frameworks in its planning documents. Earlier references cited the 2009 United Nations Office for Disaster Risk Reduction (UNDRR) definition, which described resilience as '*the ability of a system, community or society exposed to hazards to resist, absorb, accommodate to and recover from the effects of a hazard in a timely and efficient manner, including through the preservation and restoration of its essential basic structures and functions*'[128], [129], [130]. In the Integrated System Plan (ISP) context, AEMO adopted CIGRE's power-system-specific definition, describing resilience as '*the ability of a power system to limit the extent, severity, and duration of system degradation following an extreme event*'[131, p. 8], [132].

Table 7.1: Comparison of reliability and resilience definitions and characteristics, based on [133].

	Reliability	Resilience
AEMO Definition	The ability of the power system to supply adequate power to satisfy consumer demand, allowing for credible generation and transmission network contingencies.[124]	(using CIGRE Definition) The ability of a power system to limit the extent, severity, and duration of system degradation following an extreme event.[131], [132]
IEEE Definition	Reliability of a power system refers to the probability of its satisfactory operation over the long run. It denotes the ability to supply adequate electric service on a nearly	The ability to withstand and reduce the magnitude and/or duration of disruptive events, which includes the capability to

	continuous basis, with few interruptions over an extended time period.[123]	anticipate, absorb, adapt to, and/or rapidly recover from such an event.[126]
Contingencies Considered	Deterministic, Normal criteria: minimum N-1 and N-1-1 (with system restoration) Planned outages must be duly considered.	All contingencies from beyond normal criteria contingencies to selected extreme contingencies with probabilistic assessments
Performance expectation	No instability or cascading outages allowed	Partial or total system collapse is expected for certain events
Load levels	Peak and off-peak condition	Goal is to meet at least the critical load level
System restoration	Restoration is not modelled but is considered achievable, as only credible contingencies are considered	Challenging due to expected equipment impairment for certain events, dependence on other critical infrastructures, and the scale of the damage
Compliance	Mandatory for members systems in the NERC and ENTSO-E interconnections Mandatory within relevant regulatory framework worldwide	Challenging due to expected equipment for certain events or dependence on other critical infrastructures
Inter-dependencies between infrastructures	With appropriate consideration especially in system restoration	Must be duly considered, during and after event(s)

7.2 Resilience in transition to VRE-dominated system

As the system undergoes transition into a VRE-dominated system, the importance of considering resilience in the planning framework increases. VRE resources introduce characteristics that are not well captured by traditional reliability frameworks as they differ from thermal generators. Generation output of VRE plants depends on weather conditions rather than fuel availability, making it inherently variable and uncertain. Furthermore, VRE resources are distributed across multiple voltage levels and locations. This is in contrast with traditional synchronous generators that are often clustered and connected to high-voltage transmission networks. Another consideration is the behaviour of inverter-based control technology as it exhibits different dynamic behaviour compared to synchronous machines. Unlike synchronous machines, inverter-based resources are not electro-mechanically coupled with the system. Combined with the increase in weather-related events, both in severity and frequency, there is a growing need to better incorporate resilience towards extreme weather-related events into the planning framework. Some notable aspects of weather-related events that need to be better considered in the planning process are (i) the spatio-temporal behaviour of hazards, (ii) the multiple hazards simultaneously triggered by a single extreme weather event, and (iii) the occurrence of common mode effects of a single hazard across multiple asset types.

The characteristics of contingencies during weather-related events sit outside the scope of common reliability criteria via credible contingencies. Consider, for example, high ambient temperature across a wide area. Firstly, understanding the spatio-temporal behaviour gives us information that some regions experience more severe temperature during the day. With a system as large as the NEM, the far north and the south part of the NEM may exhibit different temperature profiles and peak at different times. Secondly, the compound of multiple hazards gives information that the high temperature might be followed by other hazards such as bushfire and heat dome. The bushfire can also produce smoke while the heat dome can produce downward wind, both increasing the outage rate of transmission lines over a wide area. Lastly, the common mode events due to high ambient temperature inform us that high ambient temperature not only reduces the capacity of the networks, but also reduces the power output and the capacity of wind turbines and solar panels.

Considering hazard characteristics with a proper consideration of plausible future extreme events will provide insights that cannot be obtained through conventional high N-k reliability studies. Conventional reliability studies assumptions do not capture the nature of weather-driven impacts as explained above. Traditional reliability metrics such as Loss of Load Expectation (LOLE) and deterministic security analysis are not well suited to characterising these risks. On the other hand, incorporating resilience modelling into power system planning does not replace reliability assessments. Rather, it extends the analytical framework to cover a wider range of risk scenarios. Reliability addresses performance under credible contingencies on typical days. Resilience addresses the system's ability to limit damage and recover when those contingencies are exceeded. Together, they provide a more complete basis for planning a system that is secure, stable, and robust as the energy transition continues.

7.3 A survey of extreme events in Australia

As explained before, designing resilience scenarios for planning frameworks requires an understanding of the hazard itself. To build this understanding, a survey of historical extreme events in Australia is conducted. This survey is not exhaustive but rather showcases hazards in Australia to better identify common drivers and the events related to those drivers. The survey is also used to better understand the impact of each hazard at the component or device level. A summary of the historical events grouped by their driver is provided in Table 7.2.

Table 7.2: Summary of reviewed historical extreme events in the NEM.

Hazard	*Driver*			
	Heat wave	***Windstorm***	***Hailstorm***	***Flash flood***
High Ambient Temperature	SA-02/17			
High Front Wind Speed	VIC-02/24	SA-09/16	NSW-10/24	
Smog	VIC-01/07			
Hail		SA-09/16	NSW-10/24	
Lightning	TAS-02/15	SA-09/16	QLD-11/25	
Flood		SA-09/16		QLD-02/22
Bush Fire	NSW-01/20			
Low Wind Speed	SA-02/17			
Drought	NSW-06/07			

VIC-01/07—Victoria Heat Wave and Smog Event (January 2007): Victoria experienced a prolonged heat wave followed by a bushfire in January 2007. The bushfire produced significant smoke that caused a line trip of the Dederang–South Morang 330 kV transmission line due to flashover. This event triggered the separation of New South Wales, Victoria, and South Australia due to a cascade of transmission line tripping[134]. The event is a useful example of how a tertiary hazard (smoke) can compound the secondary (bushfire) and primary (high ambient temperature) hazards that already impose stress on a power system.

NSW-06/07—New South Wales Drought (June 2007): A severe and prolonged drought during 2006–07 was later identified as the National Electricity Market's first major widespread shock to electricity financial markets. The drought reduced dam levels in the Snowy, Tasmania, and Victoria, reducing hydro generators' output and increasing their costs. Snowy Hydro, for example, was pumping water at high cost to deliver a third of its output. The drought also reduced the availability of coal plants. While some coal plants are air cooled and others use sea water, most coal plants in the eastern states use fresh water for cooling. In Queensland, water shortages reduced output by around 8 per cent. Wholesale prices in the NEM averaged around $70 per megawatt hour in the June 2007 quarter compared to around $25 at the same time the previous year[135] . Drought is a slow-onset, long-duration hazard driver whose system-wide impacts manifest through reduced generation availability and elevated wholesale electricity prices. Combined with other sudden hazards, drought could deliver even higher impacts to the system.

TAS-02/15—Tasmania Lightning (February 2015): On the summer day of 23 February 2015, lightning strikes on transmission infrastructure caused the simultaneous trip of the Gordon–Chapel Street No.2 transmission line and the Basslink interconnector. This disrupted power flows and required activation of the Fast Contingency Secondary Protection Scheme to maintain system frequency. AEMO invoked frequency control ancillary service constraints and directed Gordon Power Station to reduce generation to manage the increased FCAS requirements at that time [136]. While Tasmania itself experienced only moderate temperatures that day, the northern part of the NEM was experiencing high ambient temperatures. The incident demonstrates that lightning-driven transmission failures can occur independently of local temperature stress yet still affect a power system already under thermal strain elsewhere in the interconnected network.

SA-09/16—South Australia Black System (28 September 2016): A severe storm crossed South Australia on 28 September 2016, generating multiple tornadoes with wind speeds between 190 and 260 km/h alongside thunderstorms, hail, flooding, and intense lightning. Three separate 275 kV transmission lines tripped in quick succession, resulting in six voltage dips over a two-minute period. The resulting voltage dips triggered the protection systems of multiple wind farms, and around 456 MW of wind generation was lost. The Heywood interconnector then tripped, islanding South Australia from the rest of the NEM. The South Australian system could not sustain frequency on its own and collapsed within seconds, blacking out approximately 850,000 customers in South Australia. The same storm also produced widespread thunderstorms, damaging hail, and heavy rainfall. Significant localised flooding across parts of the state contributed to further infrastructure damage and failures. Restoration was also hampered by the persistence of severe weather throughout Wednesday 28 and Thursday 29 September. Although widespread thunderstorms affected mostly South Australia, the system led to significant rainfall over Victoria and southern New South Wales, where flooding subsequently continued after earlier rainfall events [137]. These events highlight how multiple hazards compound during a severe windstorm event.

SA-02/17—South Australia Heat Wave (February 2017): An intense heat wave swept across southern and eastern Australia in early February 2017. Area-average maximum temperatures reached 43.9 °C in South Australia on 8 February [138]. The extreme heat drove several compounding failures across South Australia's generation fleet. Thermal ratings of the Torrens Island B1 and B4 gas power plant units were reduced from 200 MW to 150 MW and 190 MW respectively. This event resulted in involuntary load shedding in South Australia, approximately 300 MW for 31 minutes on average, with some reports describing the outages last up to about 40-45 minutes. Two days later 10 February, New South Wales experienced area-average temperatures of 42.2 °C, again impacting thermal generation. The Eraring coal power plant reported a 340 MW capacity reduction, while the Liddell coal power plant was taken out of action entirely. These outcomes are consistent with the well-documented effects of high ambient temperature on thermal generators, where reduced cooling efficiency and derating can occur at high temperatures [139] or even increase their outage rate [140]. Wind output on 8 February also fell below the already-low forecast levels due to the heat dome, showing how high ambient temperature and low wind speed can act as co-occurring hazard drivers [141]. High ambient temperatures also reduce wind turbine capacity and output directly [142]. Rooftop PV solar generation, by contrast, was only slightly derated around 40 °C and in fact helped the system by shifting and reducing the afternoon demand peak [138]. According to several reports, significant PV power reduction does not occur until temperatures exceed approximately 50 °C [142], [143], [144].

NSW-01/20—New South Wales Black Summer Bushfire (January 2020): The 2019–2020 Black Summer produced catastrophic fire conditions across New South Wales and Victoria, driven by record extreme heat and strong winds. TransGrid's transmission network sustained direct physical damage from the bushfire, including scorched conductors, insulators, wooden poles, and crossarms. Indirect damage also occurred due to smoke-induced flashovers on high-voltage lines [145]. The heavy smoke also depressed PV solar generation over affected regions for extended periods. The event underscores that bushfire is not a standalone hazard but rather compounds with other hazards such as extreme heat, strong winds, and smoke to create a complex hazard environment that can inflict widespread damage on power system assets and disrupt generation.

QLD-02/22—Queensland Floods (February 2022): A large trough battered south-east Queensland for almost four days from late February 2022, bringing extreme rainfall and life-threatening flash floods. An area north of Biggenden recorded 423 mm of rain in 24 hours, with 389 mm falling in just four hours. The Mary River at Gympie was forecast to possibly exceed the major flooding levels last seen in February 1999. Emergency services responded to almost 1,000 events in a single day, including 41 swift-water rescues [146].

VIC-02/24—Victoria Windstorm (February 2024): On 13 February 2024, extreme heat and bushfires affected Victoria. When a cool change arrived in the early afternoon, it brought severe downdrafts that toppled six 500 kV transmission towers near Anakie at 14:08 [147]. At its peak, over 530,000 electricity customers were offline, and some customers remained without power for more than a week [148]. Earlier at approximately 12:35, Australia's largest wind farm at Stockyard Hill had disconnected due to a nearby grass fire. This wind farm outage turned out to help the system by reducing the transmission loading [147]. However, this event illustrates how extreme convective downdrafts can inflict catastrophic mechanical damage on even the transmission infrastructure, compounding high ambient temperature and bushfire hazards.

NSW-10/24—New South Wales Windstorm, Far West (October 2024): On the night of 16 October 2024, severe weather with high-speed winds and hail struck western New South Wales near Broken Hill. Seven transmission towers collapsed approximately 56 km south of the town, causing some outages in the town and nearby areas [149]. The event illustrates how extreme wind and hail can inflict mechanical damage on transmission infrastructure.

QLD-11/25—Queensland Giant Hailstorm (24 November 2025): On 24 November 2025, a long-tracked supercell thunderstorm moved approximately 1,400 km from northern New South Wales through south-east Queensland and north along the coast, finally dissipating near Mackay around 7:00 am on 25 November. The Bureau of Meteorology recorded 11 cm hail at Ferny Hills and Manly in Brisbane, with wind gusts of 107 km/h at Brisbane Airport and 100 km/h at Maroochydore. Additional reports cited hailstones up to 14–15 cm in suburbs including Gumdale, Chandler, and parts of Logan and Redlands. Power provider Energex reported over 150,000 customers without supply at the peak, with approximately 600 downed powerlines across the region. The event produced an estimated 525,000 lightning strikes. Hailstones of this size exceed the mechanical and impact loadings typically considered in the design of overhead network assets [150]. The co-occurrence of giant hail, destructive winds, and intense lightning in a single long-lived supercell illustrates the tail-risk posed by extreme convective storms where multiple hazards occur together over a wide area.

7.4 Research Questions

Following the above discussion, and to understand and represent the perspective of resilience within adequacy planning, we investigate the following research questions:

1. How may resilience scenarios be systematically parametrised?
2. How can a detailed parametrisation of a heatwave and a VRE drought, taken as specific, representative case studies, be conducted for the Australian east coast system, and which data requirements, methodological advancements, and considerations need to be performed to ensure an appropriate level of detail?
3. What may be the impact of explicitly considering resilience events and what are the implications for ensuring reliability in a future weather-driven Australian power system?

7.5 Representing resilience scenarios

In the following, we outline the methodological steps for developing, characterising, and implementing stress-test scenarios within reliability assessments for the Australian east-coast power system.

First, we present a general workflow, followed by the steps for a specific example of a heatwave based on the 2017 extreme event in South Australia, highlighting the complexity and considerations that are required to translate an abstract external stressor into parameter changes for resilience studies.

Furthermore, since weather-driven stressors may also arise within the power system itself through extended periods of low VRE availability, then we present considerations that may support explicit representation and assessment of a VRE drought within resilience studies.

7.5.1 Workflow for designing resilience scenarios for planning studies

To better incorporate resilience into planning studies, we propose a sequential workflow that is shown in Figure 7.1. This workflow is built around the following terms:

1. **Driver**: The underlying scenario that drives events and triggers outages (e.g., a heatwave).

2. **Trigger**: The instantaneous initiation of an event due to the driver (e.g., line outages triggered by downdraft winds).
3. **Event**: A condition that can be:
    a. lasting consequence of the driver (e.g., reduced line capacity),
    b. a direct result of a trigger (e.g., islanding), or
    c. a cascade from another event (e.g., under-frequency generator trip).

Their relationship between these terms is illustrated in Figure 7.2.

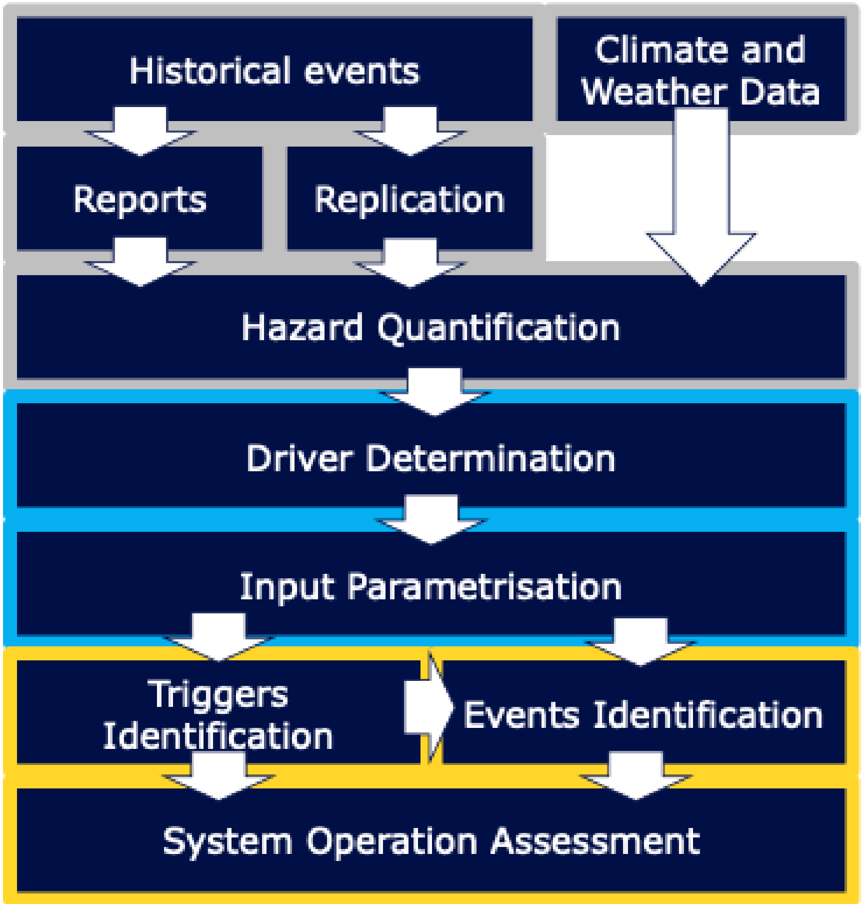

Figure 7.1 Overview of the proposed workflow for the design of scenarios to assess system resilience.

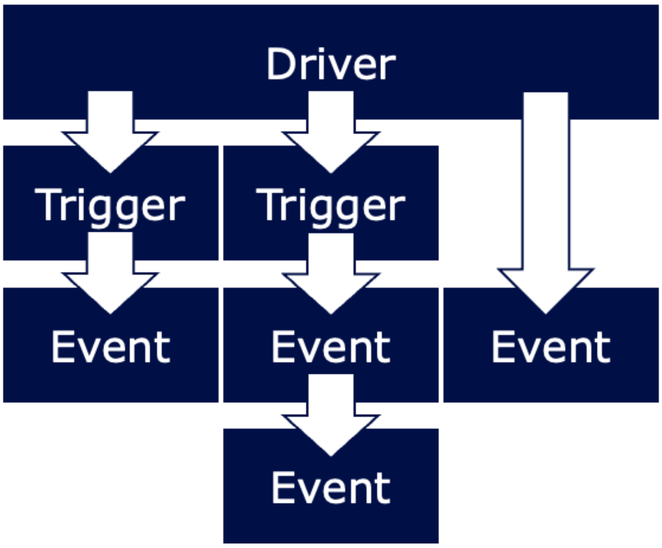

Figure 7.2: Relationship between a driver, trigger and events for the design of resilience scenarios.

The workflow for integrating system resilience under climate and weather event into a planning study can be grouped into three major parts. Those parts are (1) data collection and analysis, (2) simulation setup, and (3) modelling. In the following, we present these steps in more detail on a theoretical level, which is followed by a concrete example in the following section.

The first part of the workflow is built on **data collection and analysis**. We start this part by investigating historical contingency events across the east coast Australian power system. The main information sources for this process are event reports and replication studies. This process is used to better identify the drivers and relationships of those contingency events. The historical event investigation is presented in Section 7.3. We also examine historical and projected climate and weather data for the NEM. Based on historical events and available data, we conduct hazard quantification to better understand the risk of weather-related events for the power system. This process is presented in Section 7.5.2. This data collection and analysis process is then followed by a simulation setup process.

The **simulation setup process** consists of the driver or scenario determination and input parametrisation steps. The driver determination step involves selecting an appropriate driver or scenario used to generate weather-related triggers and events that will impact the system. The input parametrisation step then defines how the system responds to the selected driver. The parametrisation used in this report applies a direct parametrisation approach, informed by various reports, studies, nameplate specifications, standards, and previous research on the impact of weather events on devices in the power system. In this approach, we translate weather events such as high ambient temperature into device-level parameter changes such as the capacity and forced outage rate of lines. Thus, this process translates exogenous weather events into endogenous system parameters, which feed directly into the modelling process.

The last part of the workflow is modelling. In the **modelling step**, we determine which triggers and events are incorporated into the models. For example, we apply changes to the capacity of lines. These updated parameters are then passed to several open-source models developed for this project. This last step of power system assessment is conducted using SiennaNEM, SchedNEM, and PRASNEM. The output of this workflow is a quantitative assessment of power system behaviour under extreme weather events. These results can then be used to inform decision makers on how the future power system behaves under plausible extreme weather conditions.

7.5.2 Climate and weather data sources

Based on the risk rating matrix based on consequence and likelihood published by the Electricity Sector Climate Information (ESCI) project, heatwave-related events are assigned a major consequence rating (4/5) and a high likelihood rating (4/5) under future climate projections [151]. Although heatwaves are often discussed high-impact low-probability events, the ESCI rating suggests that their projected likelihood is high enough to warrant explicit consideration in future planning studies. These ratings position heatwave-related events as a critical focus area when assessing a future power system operability across NEM in the context of weather and climate hazards as external driver. The result of historical event reviews in Section 7.3 also align with the insight provided by the ESCI project. Based on this reasoning, the modelling example focuses on heatwave as the external weather and climate driver. The climate and weather data is then used to parametrise input data for system operation assessment.

Data required to create realistic future heatwave scenarios to model the impact of climate and weather conditions are collected from various sources. We collected high-resolution meteorological data from the European Centre for Medium-Range Weather Forecasts Reanalysis v5 (ERA5) [152], [153] and the Australian Community Climate and Earth System Simulator Coupled Model 2 (ACCESS-CM2) [154], [155], [156] with sufficient spatial granularity to represent realistic geographic variation across the NEM. The data from ACCESS-CM2 is part of a bigger international collaboration project called Coupled Model Intercomparison Project Phase 6 (CMIP6).

To simulate future climate and weather conditions, ERA5 and CMIP6 data are combined. This approach is chosen due to ERA5 having higher temporal granularity than CMIP6 but not providing any forecast data. The process begins with the selection of a historical hazard scenario or event. The merging process then generates a plausible future event by assuming that all climate and weather data in the historical data stay the same as in the future, except for the daily maximum and minimum temperatures. The corresponding historical temperature profile is then normalised based on its daily shape at every spatial point, from which a spatial and temporal profile is extracted. This profile is subsequently used to disaggregate future daily data into hourly data. In doing so, the methodology is able to replicate the shape of the temporal profile of a historical hazard scenario or event, scaled to reflect the severity of future conditions as projected under global warming.

To avoid introducing unintended artificial common mode effects into the simulations, the spatial and temporal granularity of the meteorological data are fully utilised. For the spatial granularity, each renewable zone is modelled as a mesh of components across its whole area of the renewable zone. The region boundaries are based on the indicative REZ boundaries of the 2024 ISP data. The resulting mesh of grid-scale solar and wind farms can be seen in Figure 7.3. This method is also applied to bus loads, using urban centres and localities data, to incorporate spatial granularity into the solar rooftop traces.

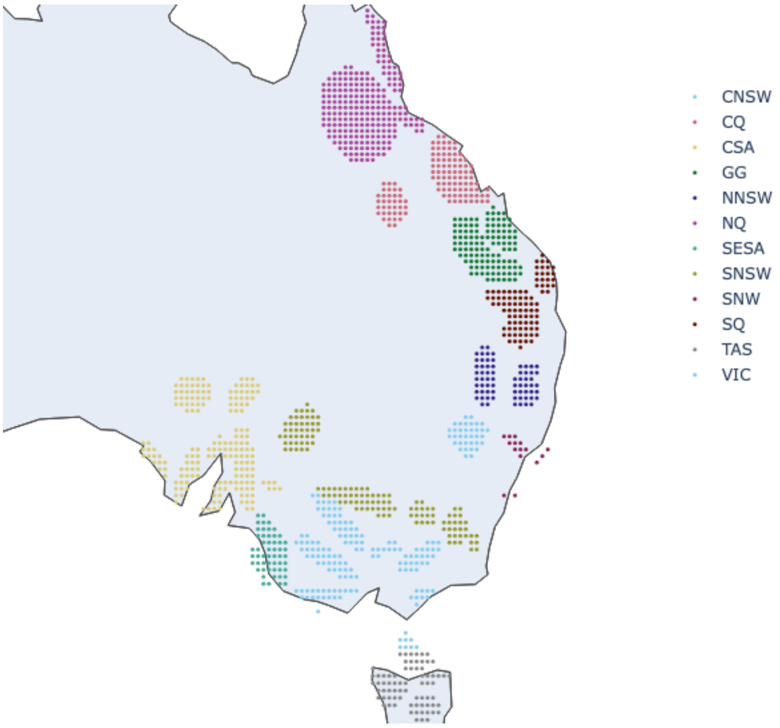

Figure 7.3: ERA5-aligned temperature measurement mesh points inside renewable energy zones, assigned to the nearest node in the 2024 ISP 12 bus network representation.

7.5.3 Parametrising a heatwave scenario

The workflow for parametrising a heatwave scenario into resilience modelling begins with collecting forecasted climate and weather data layers consisting of temperature and wind speed data. In this step, a spatial and temporal profile of how the heatwave event revolve is determined. This step is important to capture both spatial and temporal correlation to avoid introducing unintended artificial common mode effects, where multiple components unrealistically behave in the same way across different locations and times.

In this study, we seek to use, align with, and preserve the data provided in the 2024 ISP, including the demand and renewable energy traces. Demand under heatwave conditions is represented by selecting demand traces associated with historical heatwave periods contained within the reference traces. This selection process also ensures that renewable generation traces are selected from the same time window and operating conditions. By doing so, the analysis captures the heat-driven load that is inherently reflected in the demand traces, while preserving the characteristic behaviour of rooftop PV, wind, and solar generation under the same weather conditions. Maintaining this correlation is necessary to avoid constructing an internally inconsistent stress event, such as combining heatwave-driven derating with demand profiles that do not reflect heatwave conditions.

The next step required for performing resilience analysis is a component-level impact parametrisation. Through this, the spatial and temporal profile of the heatwave event from the data acquisition and curation step is used to construct system component data with associated climate and weather profiles. The geo-tagged system components are extracted from *AEMO ISP Inputs and Assumptions* data, with urban centres and localities as the secondary source for distributed solar geo-location data.

The forecasted climate and weather profiles of each component, combined with other system data and traces provided by AEMO, are used as inputs for parametric functions governing each component.

In this project, parameters of different types of system components are adjusted based on the climate and weather profiles. The considered impacts on the components are the thermal derating of transmission lines, thermal generators, wind turbines, and PV. The final output of the input parametrisation process is a set of components with new parametric profiles attached to each component. Thus, various system parameters become time-sequential data instead of static data. In the following, we outline the detailed parametrisations of those four component classes.

Transmission line thermal derating

In the publicly available 2024 ISP data, there is no explicit transmission line thermal capacity rating is provided. The input data of the 2024 ISP for transmission lines is their transfer capacity limit for forward and backward power flow direction. While several transmission lines are constrained by their thermal capacity, various lines are limited by other security-and stability-related constraints. Some lines are constrained by thermal capacity in one direction but not in the other direction. Furthermore, there are seasonal transfer capacity constraints that might not be enforced by thermal capacity but by the direction of power flow or generator commitments. To respect this information as much as possible, while integrating transmission line thermal capacity derating, the following considerations are applied. First, thermal capacity derating is only applied to corridors that are explicitly limited by the thermal capability of any components mentioned in the 2024 ISP data. Second, the base capacity value is based on summer transfer capacity while respecting the typical summer reference temperature of each area provided in the 2024 ISP. Third, a peak-demand transfer capacity limit is inferred from the temperature of the two buses connected by each transmission line. These considerations are applied for every line type in the 2024 ISP.

Furthermore, the transmission line thermal derating is categorised into three main groups based on their type, as follows:

1) direct-current subsea cable
2) direct-current underground cable
3) alternating-current overhead cable

For direct-current subsea cables, no thermal derating is applied as their capacity is not affected by ambient temperature based on 2024 ISP data. The direct-current underground cables are modelled using a constant linear derating of 12.5% capacity reduction per 1 °C starting from 38 °C, following 2024 ISP data. The alternating-current overhead cables are modelled mainly from the steady state heat balance model used by the NEM TNSPs [157]. The central principle of the transmission line derating is driven by the physical heat balance of the conductor where Joule heating capacity falls when ambient temperature rises, solar gain increases, or convective cooling weakens. For an overhead conductor at steady state, heat input equals heat output.

The conductor gains heat from electrical heating and solar heating, whereas it loses heat from convection to surrounding air and radiation to the sky and ground environment. This heat balance equation can be written as:

$$I^2 R_{\mathrm{ac}} + P_S = P_C + P_R \quad (1)$$

where I denotes the steady state line current and R_{ac} denotes the ac resistance of the conductor at the operating point. The P_S, P_C, and P_R denote the solar heat gain, wind convective cooling, and radiative heat loss. Rearranging Equation (1) for current gives the deterministic rating current (I_{DR}) as:

$$I_{\mathrm{DR}} = \sqrt{\frac{P_C + P_R - P_S}{R_{\mathrm{ac}}}} \tag{2}$$

For each line l, a set of mesh points (M_l) are generated along a straight line between two buses. For each time t, I_{DR} is calculated. By comparing the value of I_{DR} of each mesh points, a transmission line hot spot is identified. For different time t, the location of the hot spot of each line changes, depending on the interaction of P_S, P_C, and P_R on every mesh point of that time t. For all meshes m along line l and time t then we can get the deterministic rating current at the bottleneck point $\left(I_{DR}^{bot}\right)$ as follows:

$$I_{DR}^{bot} = \min_{m \in M_l}\left(I_{DR,m,l,t}\right) \tag{3}$$

where $I_{DR,m,l,t}$ denotes the deterministic rating current of the line based on the climate and weather data at mesh point m. This approach ensure that temporal and spatial granularity of climate and weather data are utilised. The correction factor for the transfer limit for each corridor l and time t is then can be formulated as follows:

$$C_{l,t} = \min\left(\frac{I_{DR,l,t}^{bot}}{I_{t,summer}}, 1\right) \tag{4}$$

where $I_{t,summer}$ denotes the line rated capacity during typical summer days derived from data available in the 2024 ISP.

Thermal generator thermal derating

The derating of thermal generator used in this study is based on the aggregate derating of direct ambient-air prime-mover derating, cooling-source heat rejection derating, and any other thermal derating functions into a single usable-capacity function for its simplicity [158], [159]. The focus of the thermal generator derating is to parametrisation is to determine the usable capacity remaining at each ambient temperature during a heatwave for given a generator's technology, cooling system, reference capacity, and heat-rate parameters. The usable capacity of thermal generator g at time t after heatwave parametrisation can be seen as follows:

$$P_{g,t}^{\mathrm{thermal,av}} = C_{g,t}^{\mathrm{thermal}} \overline{P}_g \tag{5}$$

where $P_{g,t}^{\mathrm{thermal,av}}$ and $\overline{P}_g$ denote the available and nameplate capacity, respectively, while $C_{g,t}^{\mathrm{thermal}}$ denotes the correction factor of the thermal generator.

In this study, the thermal derating model separates thermal generators into two modelling families. Once-through cooling (OLC) units are represented using the water loop model formulation, where usable capacity depends on intake-water temperature, water availability, and discharge-temperature limits. All non-once-through (nOLC) units are represented using a linear temperature-derating relationship with their constant parameter depending on the cooling used. In this study, the thermal generator derating due to ambient temperature is grouped into two groups as follows:

1) non-once-through cooling (nOLC) systems;
2) once-through cooling (OLC) systems.

The general correction factor formula of thermal generator with non-once-through cooling system $\left(C_{g,t}^{\text{nOLC}}\right)$ used in this study can be written as follows:

$$C_{g,t}^{\text{nOLC}} = \max(1 - \alpha \Delta T,\ 0) \tag{6}$$

where α denotes the linear derating coefficient and the ΔT denotes the change in temperature from the reference temperature. This linear derating model represents the aggregate derating from all components of the thermal generator. For a generator with an OLC system, the usable capacity of the thermal generator after heatwave parametrisation can be seen as follows:

$$P_{g,t}^{\text{thermal,av}} = \begin{cases} \min(1,\omega)\overline{P}_g, & T^* \leq T_{\text{health}} \\ \min(1,\omega)[1 - \alpha(T^* - T_{\text{health}})]\overline{P}_g, & T_{\text{health}} < T^* \leq T_{\text{risk}} \\ \min(1,\omega)\zeta \dfrac{\max\left(\overline{T}_{\text{outlet}} - T_{\text{eff}}, 0\right)}{\Delta\overline{T}}\overline{P}_g, & T^* > T_{\text{risk}} \end{cases} \tag{7}$$

where ω denotes the availability coefficient of cooling water intake, used as a proxy of water scarcity or drought parameter in [158], [159]. T^* and $\overline{T}_{\text{outlet}}$ denote the cooling water inlet temperature and the maximum allowed cooling-water outlet temperature, respectively. T_{health} and T_{risk} denote the healthy and risk inlet water cooling temperature threshold, respectively. The α denotes the linear derating coefficient, while the ζ denotes the scaling term for the collapse region. In this study a shutdown behaviour can occurs due to collapse caused by the ζ term even though there is no shutdown temperature as a hard limit for the generator operating regions. In this study, the value of T_{risk} is defined as:

$$T_{\text{risk}} = \overline{T}_{\text{outlet}} - \frac{1}{\omega}\Delta\overline{T} \tag{8}$$

where $\Delta\overline{T}$ denotes the required outlet-inlet temperature difference. The ζ term in this study is calculated as follows:

$$\zeta = \begin{cases} \omega[1 - \alpha(T_{\text{risk}} - T_{\text{health}})], & T_{\text{risk}} \geq T_{\text{health}} \\ \omega, & T_{\text{risk}} < T_{\text{health}} \end{cases} \tag{9}$$

Wind turbine thermal derating

Wind generation availability during a heatwave is represented as the interaction between two constraints:

1. Meteorological wind resource constraint, determined by wind speed and turbine power curves.
2. Thermal capacity constraint, determined by ambient temperature and equipment derating limits.

In this study, the meteorological wind resource constraint is extracted from AEMO 2024 ISP traces. For each wind turbine g and time t, the available power output of wind turbine after temperature derating $\left(P_{g,t}^{\text{wind,av}}\right)$ is defined as:

$$P_{g,t}^{\text{wind,av}} = \min\left(P_{g,t}^{\text{wind}}, C_{g,t}^{\text{wind}} \cdot \overline{P}_g\right) \tag{10}$$

where $P_{g,t}^{\text{wind}}$ and $\overline{P}_g$ denote the resource-limited output before thermal derating and rated capacity of each wind turbine g. The $C_{g,t}^{\text{wind}}$ denotes the wind turbine per-unit correction factor. This correction factor should be applied to capacity, not directly to the resource-limited wind output. The distinction provided in Equation (10) indicates that a thermal derating might not impact actual wind power output if the wind turbine only generates low power due to low wind speed, or $P_{g,s,t}^{\text{wind}} < C_{g,s,t}^{\text{wind}} \cdot \overline{P}_g$.

Since historical records often correlates hot days with weak wind conditions due to heat dome phenomenon, it is inherently in the weather profile that high ambient temperature may be less likely to coincide with high wind power output during heat wave event. This distinction supports a stronger reliability interpretation that heatwaves can affect wind through both low wind conditions and thermal operating limits, but these are separate mechanisms and should not be conflated. However, a long duration heatwave might last to early evening where it meets the common time of high wind power output, the temperature-adjusted capacity ceiling can bind and create a real reduction in available wind output.

In this study, the value of $P_{g,t}^{\text{wind}}$ and $\overline{P}_g$ are extracted from 2024 ISP, making the modelling fully respect 2024 ISP data and traces. Whereas the $C_{g,t}^{\text{wind}}$ for each wind turbine g and time t is calculated based on derating function as defined as follows:

$$C^{\text{wind}}(T^*) = \begin{cases} 1.0, & T^* < T_1 \\ 1.0 + \alpha_2(T^* - T_1), & T_1 \leq T^* < T_2 \\ C_2 + \alpha_3(T^* - T_2), & T_2 \leq T^* \leq T_{\text{stop}} \\ 0.0, & T^* > T_{\text{stop}} \end{cases} \tag{11}$$

Where T^* denotes the ambient temperature around the nacelle, the heavy box-like housing that sits at the top of a wind turbine tower behind the blades. The wind thermal correction factor is defined based on four piece-wise linear derating regions. The temperature boundaries between regions are defined by T_1, T_2, and T_{stop}, whereas the linear slope of the second and third region is defined by α_2 and α_3. The C_2 denotes the correction factor in the boundary between the second and third regions.

It is worth mentioned that some manufactures specify that a wind turbine operates with tower base located above 500 metre above sea level (masl) can only be operated up to the second region. In this study, a non-conservative value of tower base height under 500 masl is selected for all sites.

Since common ambient temperature only available for 2 metres above the surface temperature, a small adjustment is applied to approximate the nacelle-relevant or turbine-relevant ambient condition as follows:

$$T^* = T^{2\text{m}} + \Delta T \tag{12}$$

where $T^{2\text{m}}$ and ΔT denotes the 2 m near surface and adjustment temperature. A common value of ΔT for a location 100 m above ground is between -0.63 °C to -1.0 °C. In this study, a non-conservative adjustment of -1.0 °C is selected. Under hot, dry daytime conditions, reduced evaporative cooling can increase sensible heating near the surface, making the vertical temperature gradient steeper and causing the 2 m to 100 m adjustment to approach the dry-adiabatic value of approximately -0.98 °C per 100 m. Extremely hot and dry daytime conditions may produce stronger super adiabatic gradients than -1.0 °C per 100 m, but such gradients are highly dependent on the specific event and location [160]. Therefore, for extreme hot and dry daytime scenarios, an adjustment close to -1.0 °C is considered physically representative.

Photovoltaic thermal derating

The photovoltaic thermal derating used in this study is designed to respect 2024 ISP data and traces. The modelling is build based on the assumption that traces provided in the 2024 ISP data traces already experience thermal derating. Thus, the modelling of correction factor for solar traces needs to account the realistic non-derated trace and adjust it for future heatwave event. For each solar g and time t the available power output of a solar site after temperature derating $\left(P_{g,t}^{\text{solar,av}}\right)$ is defined as:

$$P_{g,t}^{\text{solar,av}} = C_{g,t}^{\text{solar,adj}} P_{g,t}^{\text{solar}} \tag{13}$$

where $P_{g,t}^{\text{solar}}$ denotes the solar power output trace before adjusted to future heatwave event. The $C_{g,t}^{\text{solar,adj}}$ denotes adjustment correction factor for solar power, and is defined as:

$$\begin{aligned} C_{g,t}^{\text{solar,adj}} &= \frac{C_{g,t_f}^{\text{solar}}}{\max\left(C_{g,t_h}^{\text{solar}}, \varepsilon\right)} \\ &\approx \frac{C_{g,t_f}^{\text{solar}}}{C_{g,t_h}^{\text{solar}}} \end{aligned} \tag{14}$$

where C_{g,t_f}^{solar} and C_{g,t_h}^{solar} denote the thermal correction factor of the solar module using forecast and historical temperature traces, respectively. For solar module, the terms correction factor is interchangeable with capacity factor as the power output of a solar module always defined by the temperature of the back of the module. The general capacity factor used in this study is based on Faiman model [161] as follows:

$$C_{g,t}^{\text{solar}} = 1 + \alpha\left(T_a + \frac{G_{\text{POA}}}{U_0 + U_1 v} - T_{\text{stc}}\right) \tag{15}$$

where α denotes the module power temperature coefficient. The T_a and T_{stc} denote the ambient and standard test conditions (STC) temperature. The parameters U_0 and U_1 denote the constant and wind-dependent heat-loss coefficients, respectively, while the v denotes the wind speed at module height. The G_{POA} denotes the plane-of-array irradiance. Its value depends on the irradiance components, solar zenith angle, solar azimuth angle, module surface tilt, module surface azimuth, and ground albedo. The utility-scale solar-farms in the REZ are modelled as single-axis tracking systems. For these systems, the tracker axis azimuth is optimised for each REZ mesh location, while the module surface tilt and module surface azimuth vary throughout the day according to the tracker geometry.

7.5.4 Parametrising a VRE drought scenario

Complementary to the identified hazards and detailed representation of the external stressor of an extreme heatwave as described above, there may also be an increasing exposure to intrinsic weather-related stressors in a highly weather-dependent system, specifically considering extended periods of low VRE availability [162], [163]. While adequacy assessments are typically based on historical weather reference years, the response of the system to explicitly introduced stressors may be required to understand the exposure to risk within the system itself. Additionally, this risk may be sensitive to imperfect storage operation and hence storage operational assumptions. Therefore, complementary to the heatwave representation, we investigate a methodology for representing VRE droughts and evaluate adequacy implications in a highly weather-dependent system.

The parametrisation of the VRE drought is based on the provided historical weather traces of the 2024 ISP input data and observed low VRE availability conditions, which are parametrised to intensify in duration. Specifically, to represent the impact of increasingly worse VRE droughts, we first identify the day with the highest residual demand and then iteratively increase the number of consecutive days that the system is exposed to these low-energy availability conditions. This data-driven approach is designed to provide a straightforward sensitivity analysis of VRE droughts as complementary resilience risk driver in an increasing energy-limited and weather-dependent system.

7.6 Case study parameters and parametrisation impacts

7.6.1 Representing the impact of a heatwave onto generators and lines

Based on the survey of historical extreme events in Australia, one of the heatwaves occurred in 2017, which is included in the underlying reference weather traces of the 2024 ISP. This historical heatwave included a load shedding event in South Australia on 8 February 2017 (SA-02/17). Based on the collected data from ERA5, the peak temperature in South Australia at that time was around 46.03 °C, then increasing to 48.27 °C and 48.76 °C on the 9 and 10 February, respectively. Even though the 10 February 2017 did not result in any reported load shedding, it is recorded as the hottest day in South Australia.

As heatwaves are projected to intensify and may present an increasingly strong external stress to the system, we are investigating the potential impact of an extreme heatwave under 2040 conditions, which includes increased maximum temperatures, based on the weather forecasts in the CMIP6 ACCESS-CM2 dataset. To understand the potential effect of the extreme heatwave on the future resource mix, we apply the derating parameters to the planning year 2040. Furthermore, we focus the resilience assessment to the months of January to March to better localise and isolate the effects of the heatwaves, while still allowing to capture implications across multiple weeks due to impacts on storage energy levels. We simulate the system risk under 1500 outage samples of generator and transmission infrastructure.

The ambient temperature at the location of all thermal generators across the NEM during the simulated heatwave is shown in Figure , aggregated by region.

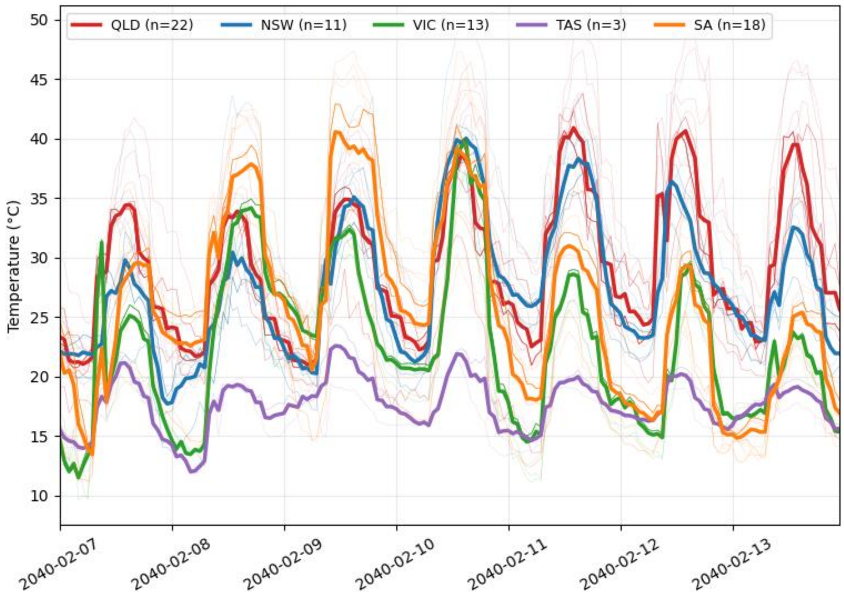

Figure 7.4: Ambient temperature at the location of all thermal generators across the NEM during the extreme heatwave in 2040 simulated in this resilience study.

The demand profile during 2040 underlying in this resilience study can be seen in Figure 7.5. The NEM-wide demand peak in the critical week occurs on the 10th and 11th of February, in line with the hottest days in the underlying temperature data.

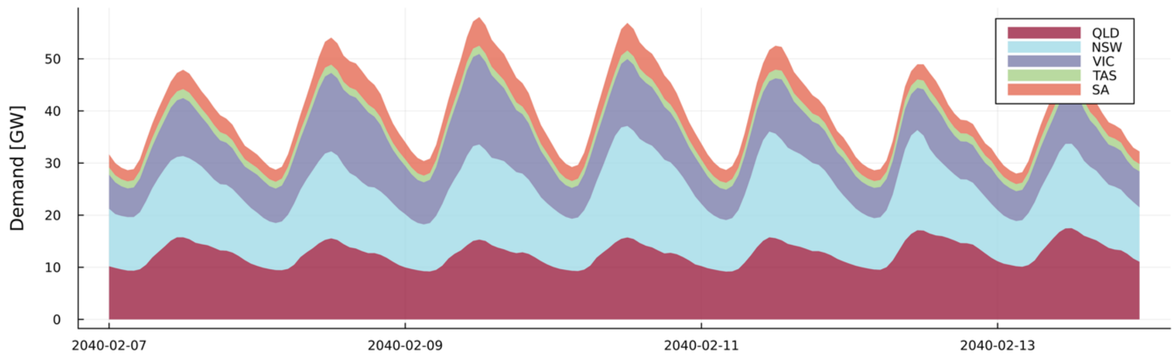

Figure 7.5: Demand traces of planning year 2040 based on the weather reference trace of 2017 with the demand level of POE 10%, as forecasted in the 2024 ISP Step Change scenario.

The derating of the generators in the system used in the resilience study grouped by state and generation types can be seen in Figure 7.6 and Figure 7.7, respectively. The derating of the transmission line forward and backward capacity can be seen in Figure 7.8.

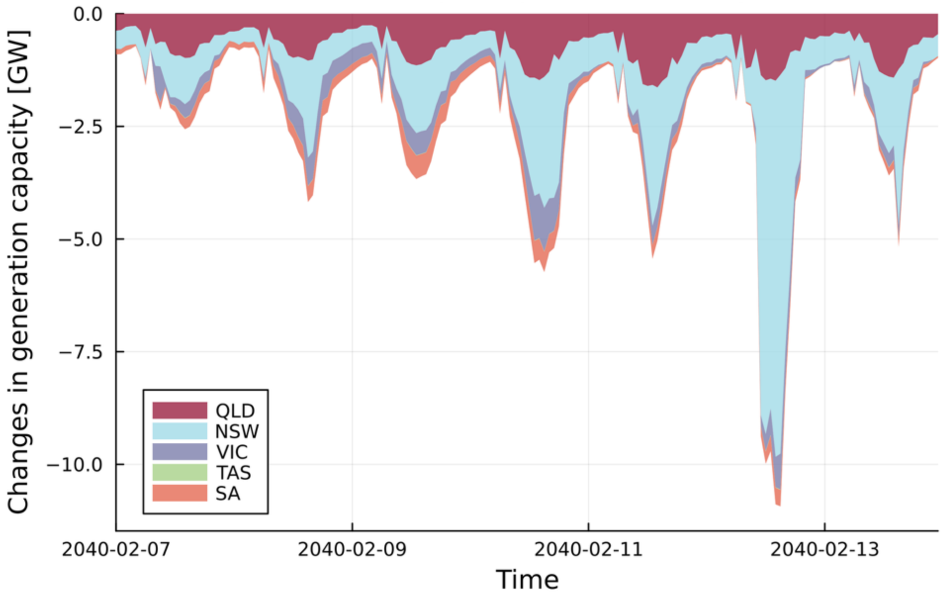

Figure 7.6: Changes in generation capacity in 2040 by states, as determined from the climate and weather data, the parametrisation, as well as the input reference traces.

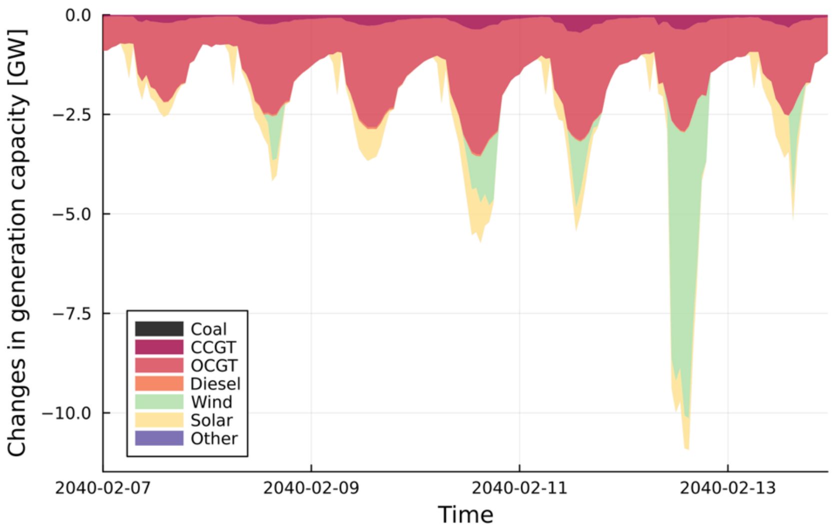

Figure 7.7: Changes in generation capacity driven by the extreme heatwave in 2040 by type of generation, as determined from the climate and weather data, the parametrisation, as well as the input reference traces.

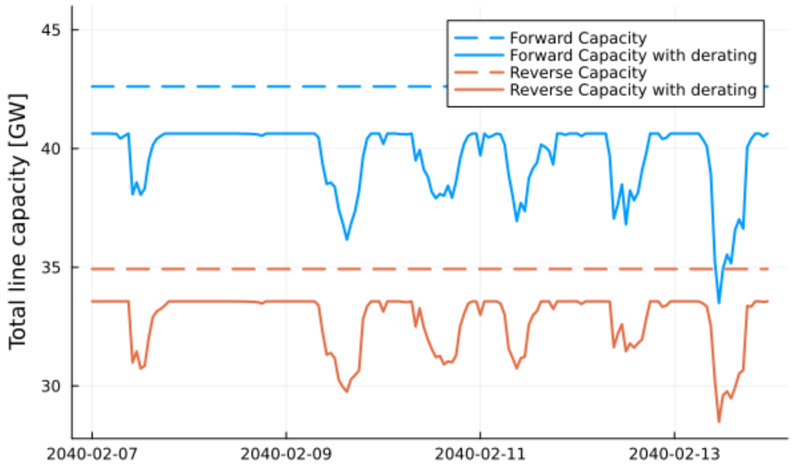

Figure 7.8: Impacts in transmission line forward and backward capacity driven by the extreme heatwave in 2040, as determined from the climate and weather data, the parametrisation, as well as the realised transmission line capacity.

7.6.2 Representing VRE droughts

The analysis for representing an extreme VRE drought is performed on the high VRE availability year used in the previous studies in chapter 4 and 5, which is based on weather reference year of 2019 and the demand profile of POE 50%. The residual demand (demand minus VRE availability) is shown in Figure 7.9, with the annual average of around -200 GWh per day, which highlights the overall high abundance of energy from VRE sources across the NEM. In this weather year, low VRE conditions are observed in the winter months, particularly in the southern states excluding Queensland, which is also described by AEMO in the 2024 ISP Appendix 4 [119].

We extend the day with highest residual demand to three consecutive days, representing a typical potential VRE lull in Australia [164], as well as to seven days to represent an extreme case of VRE drought, which may be unlikely to occur regularly but may expose structural risks. Note that these extended periods occur in a period of already low VRE availability (in winter), therefore the effects may be further compounded with surrounding high residual demand days and affect subsequent risk periods and events.

Furthermore, to isolate the effects of low VRE availability, we focus the adequacy assessment on the winter months of June until end of August and assume 50% state of charge of the long-duration storage units (deep storage and pumped hydro) at the beginning of the interval across the long-duration storage units in the system.

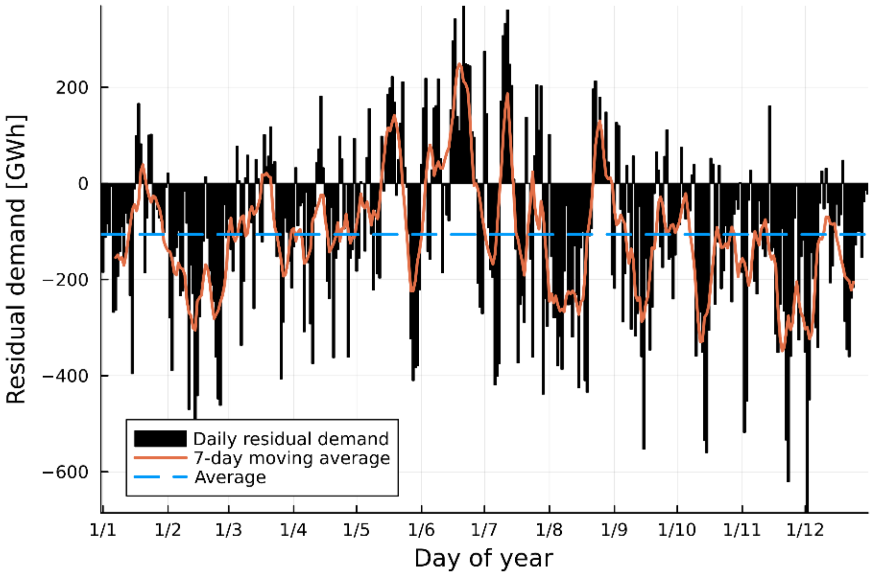

Figure 7.9: Daily residual demand of 2040, based on the reference weather year 2019 and the demand trace of POE 50%.

The reduced energy availability in 2040 can be seen in Figure 7.10. We note that five days after the original day with high residual demand (on 21/6/2024), there is another day with the VRE peak not exceeding demand even in the original underlying traces. This highlights the tight energy conditions in this winter period.

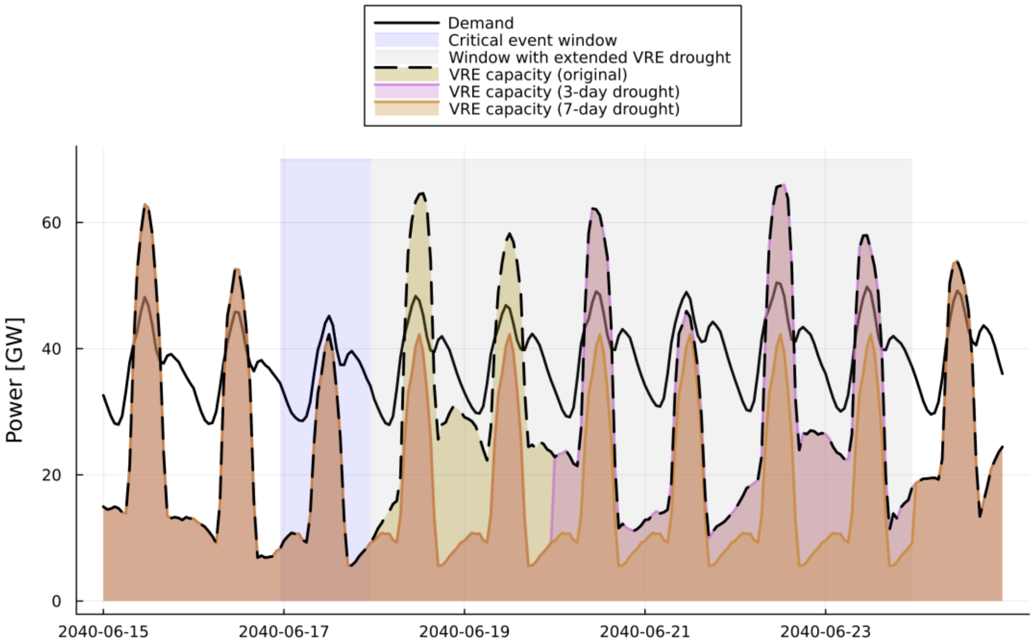

Figure 7.10: NEM-wide VRE availability and demand in 2040 under the two extended VRE drought levels. The missing VRE energy can directly be observed by comparing the total area of the VRE availability under the extended drought scenarios compared to the original availability

When extending the VRE drought across multiple days, we observe a decrease mostly in VRE availability in Tasmania and Victoria, see Figure 7.11, as the wind production in the subsequent days is suppressed. As the low VRE period is extended to seven consecutive days, an increasing amount of renewable generation in New South Wales is also reduced.

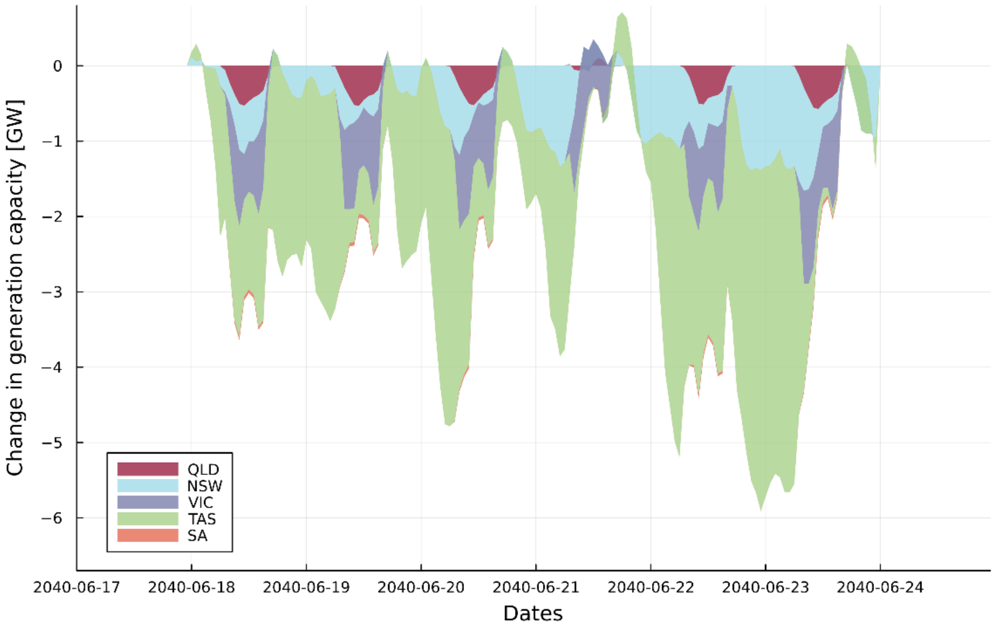

Figure 7.11: Change in VRE generation capacity in 2040 compared to the base case when extending the VRE drought day across the following consecutive days.

7.7 Insights and Results

In the following, we describe and present the implications of explicitly representing two extreme weather events within adequacy assessments: the exogenous stress of an extreme heatwave and endogenous stressor of an extreme VRE drought. We emphasize that the results aim at demonstrating how resilience studies may be integrated into reliability thinking, rather than attempting to represent the full resilience risk to the NEM. Additional details about the system operation in the two resilience events can be found in Appendix 0.

7.7.1 Impacts of an extreme heatwave

The results of the unserved energy event magnitude distribution in 2040 with the 2017 weather year trace with and without heatwave parametrisation are shown in Figure 7.12. It can be observed that even without any derating from incorporating climate and weather events into the system, the selected months in the 2017 weather year itself have an inherent risk of unserved energy events. By incorporating climate and weather events into the system, some components in the system experience derating as described in Section 7.6.1. When adding the heatwave derating, the system clearly experiences higher increase of the number and size of unserved energy events just by incorporating a single week of climate and weather data.

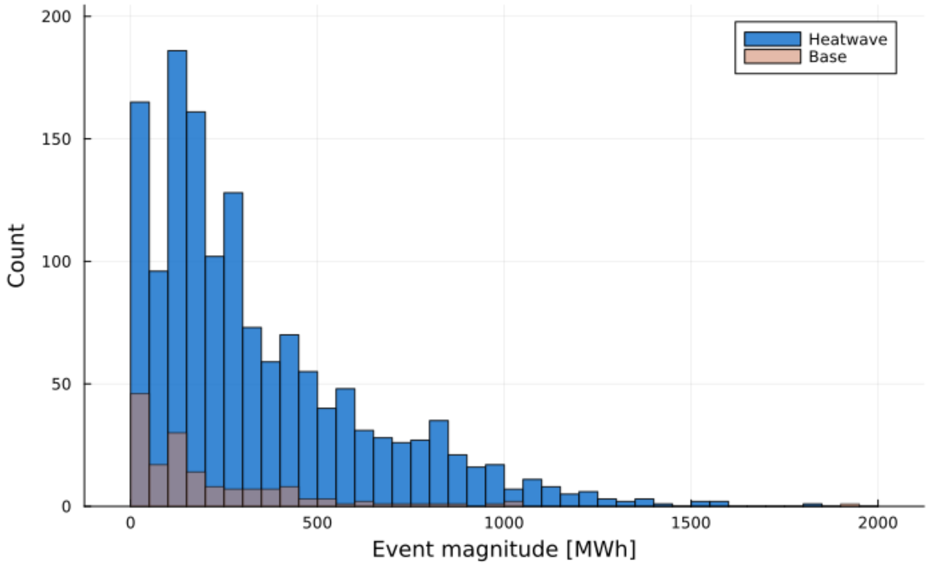

Figure 7.12: Event level magnitude distribution of unserved energy compared between without (base) and with heatwave system parametrisation in 2040 based on the 2017 reference weather year trace, binned at 50 MWh intervals.

This observed unserved energy from the adequacy assessment in Figure 7.12 may further be identified by region as shown in Figure 7.13, which clearly shows that the outage events in the three months of January to March 2040 are localised in two states, Queensland and South Australia. By incorporating the heatwave period, we further increase the stress to the system in those months, resulting in higher amounts of load shedding across sampled outages. This is clearly shown in Figure 7.13 as a sharp increase in total USE is observed in South Australia.

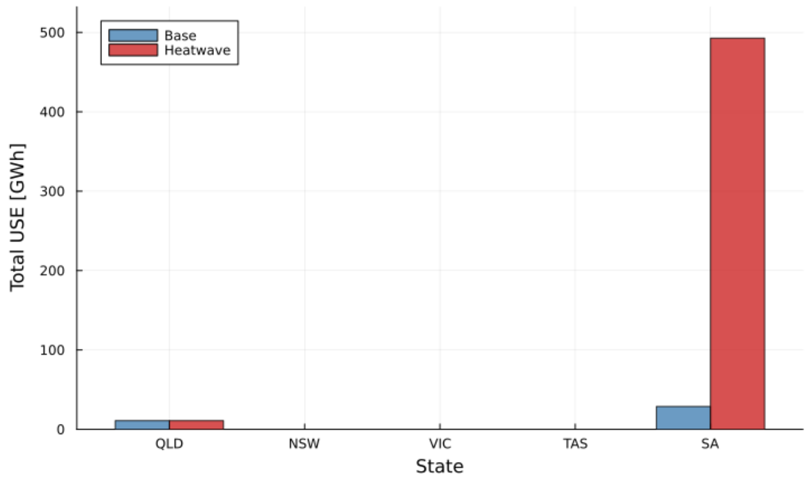

Figure 7.13: Comparison of unserved energy (USE) in GWh between the base case (without heatwave system parametrisation) and the heatwave-parametrised case, from January to March 2040, using the 2017 weather year trace

To better understand how the extreme heatwave drives the unserved energy risk, we decompose the heatwave impacts to system component categories. For each simulation, only one system component type is parametrised. The comparison of average USE among various system components parametrisations can be seen in Figure 7.14. We can observe that incorporating the derating of thermal generator results in the highest impact to average USE. This means that the system is more sensitive to reduced thermal capacity compared to reduced total energy during the day through VRE derating.

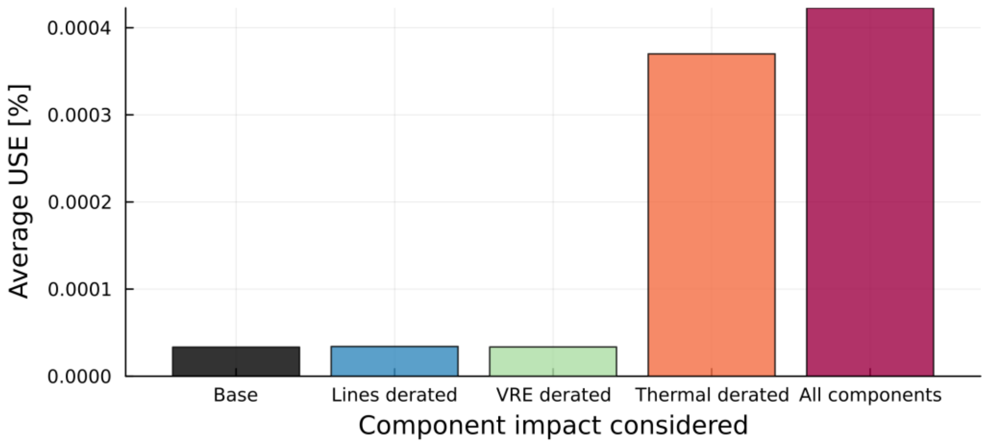

Figure 7.14: Average unserved energy (USE) in 2040 under scenarios with extreme heatwave impact on different components. USE normalised by total demand in simulation window (Jan – March).

Based on Figure 7.14, the heatwave reliability risk in the future NEM may be best understood as a critical-hour firming problem rather than a long-duration of energy drought problem. The issue is not whether the system has enough total energy during the heatwave, even for a multi-day's heatwave, but the issue is whether there is enough firm capacity available during the exact intervals when heat, demand, and resource availability create scarcity. Under this lack of available capacity, further derating of thermal generators poses a high risk to the system. This conclusion is also tied to the selection of the historical trace profile used. In this report, we use actual historical heatwave event profiles to fully capture the actual spatiotemporal patterns of heatwaves. Based on that profile, further reduction of available capacity greatly increases USE, while increasing storage capacity to shift available energy during the day greatly reduces USE.

To further characterize the risk introduced by the different component derating and identify relevant metrics to capture the specific risk of an extreme heatwave, we compare multiple average and tail metrics, as presented in Figure 7.15 below.

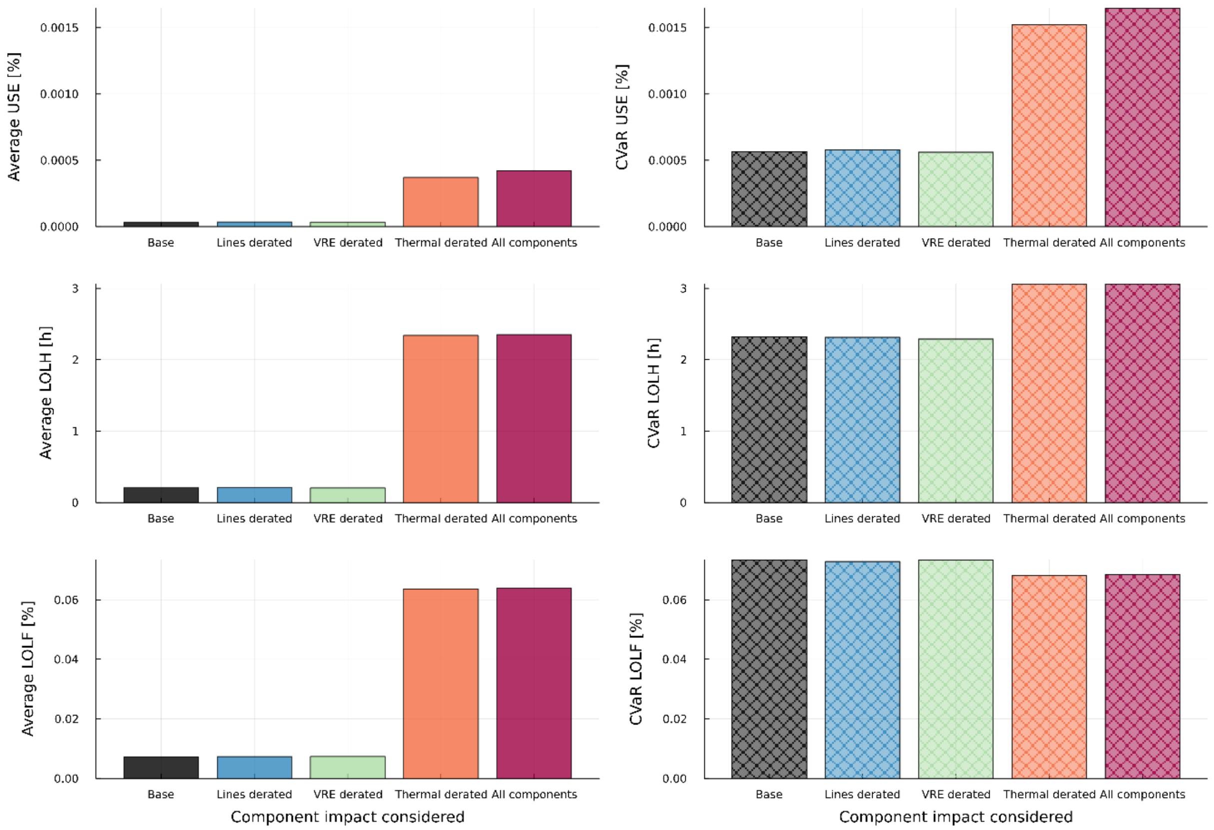

Figure 7.15: Comparison of NEM-wide average (left) and tail (right) metrics of unserved energy (USE), loss of load hours (LOLH) and loss of load frequency (LOLF) across 1500 outage samples for the extreme heatwave derating in 2040, under the storage operation approximation of economic operation. The Conditional Value at Risk (CvaR) is calculated with respect to the 95th percentile. The energy results are normalised for the three-month simulation period (January – March).

Comparing the results across the different average metrics, we observe an increase in energy, duration, and frequency of the average risk when considering thermal capacity derating and the parametrisation across all system component categories. Looking at the tail's metrics, we note that the extreme heatwave parametrisation increases tail events mostly with respect to energy, while the duration and frequency of the worst 5% of events (with respect to the underlying metric) only changing marginally. This comparison of different metrics gives the insight that CVaR USE as an energy-based metric is able to capture the tail risk of extreme hot-day events. On the other hand, CVaR LOLF and CVaR LOLH are not suitable to capture the tail risk of extreme hot-day events as the tail only marginally differs from the average.

The value of LOLH at Figure 7.15 informs that both the average and tail of the unserved event last for a short time during the peak hour. This insight also aligns with the historical event of the South Australian heatwave in 2017 that the load shedding only lasted up to 45 minutes as mentioned in Section 7.3. This suggests that an extreme heatwave increases the overall risk of the system, particularly the power needed in the narrow time window of peak load during a heatwave. The distribution of the number of event-hours of shortfall events per hour of the day is shown in Figure 7.16.

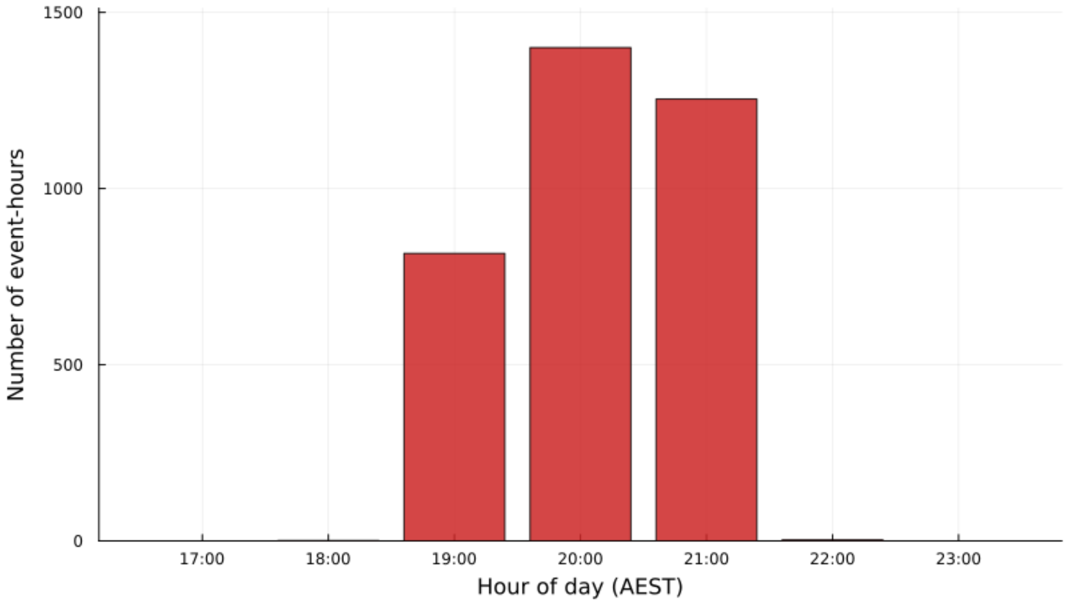

Figure 7.16: Distribution of the number of load shedding events occurring in critical hours of 8 Feb 2040 during the heatwave simulation.

When VPP coordination is considered to the system, the USE reduces to zero both in the base case and the extreme heatwave scenario as shown in Figure 7.17. This supports the interpretation that the heatwave reliability risk is concentrated in a small number of critical scarcity intervals, where increased energy storage capacity can relieve the shortfall. Sufficient energy remains available during the heatwave, so the increased storage capacity in form of VPP is able to shift this available energy to the critical scarcity intervals, see appendix 9A.6.

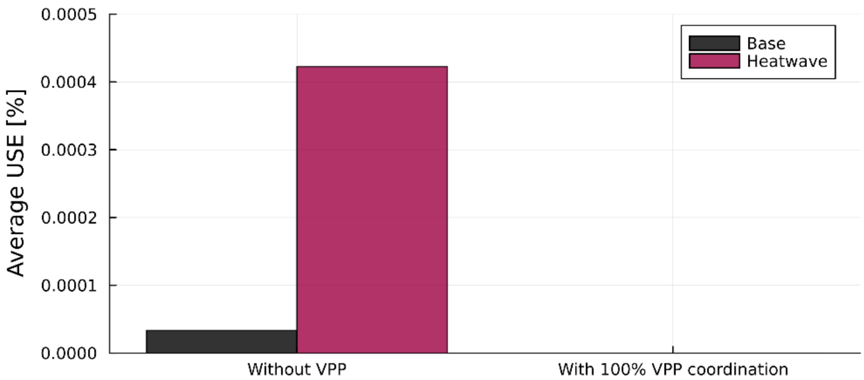

Figure 7.17: Average unserved energy (USE) of the heatwave simulation in 2040, comparing a sensitivity study with full VPP coordination capacity under the 'economic operation' approximation.

The results under increased VPP coordination should not be interpreted as showing that VPPs eliminate all heatwave reliability risk. In practice, the zero-USE outcome is conditional on the assumed extreme heatwave parametrisation, the assumed VPP capacity, availability, dispatchability, customer response, telemetry, and operational coordination. The insight therefore shifts the key planning question from whether consumer-side flexible capacity can reduce USE in principle to whether the assumed VPP or increased storage capacity can reliably respond and deliver power in the critical hours.

7.7.2 VRE drought impacts

Looking at the impact of the VRE drought onto the resource mix as thermal generation is retiring, we observe the NEM-wide average and tail unserved energy risk as seen in Figure 7.18.

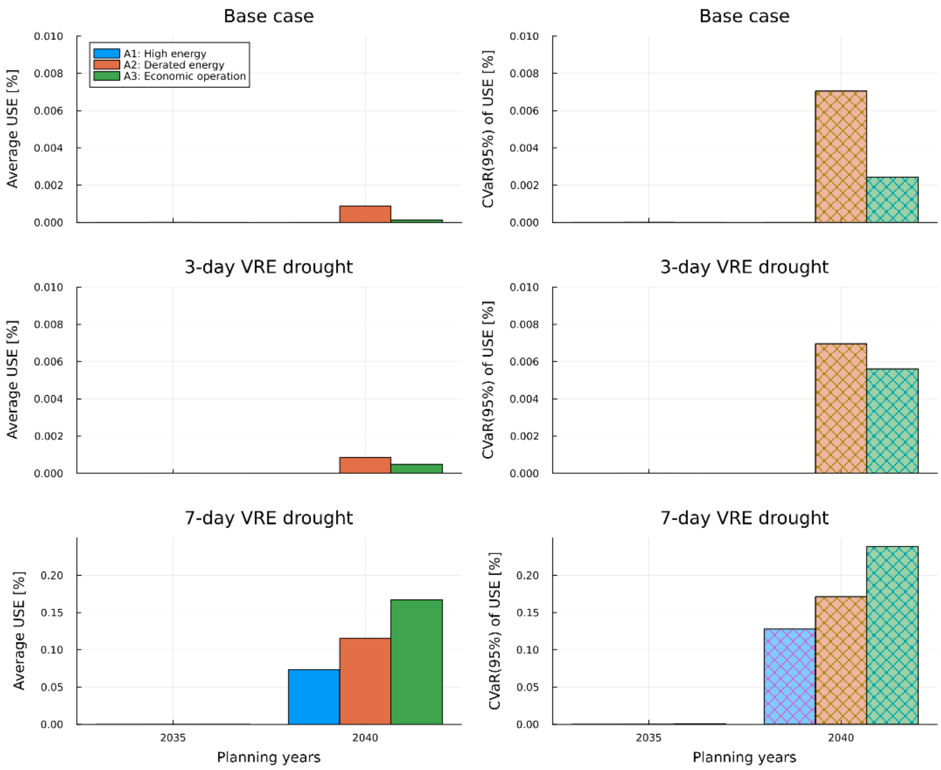

Figure 7.18: Average NEM-wide unserved energy risk (left) and NEM-wide tail risk (right) with increasing duration of VRE drought, under different storage operation assumptions. Note the different scale in the 7-day drought scenario. Unserved energy is normalised with respect to total demand in the simulated horizon (June – August).

First, the impact of the extended and extreme VRE drought only emerges significantly in the resource mix of 2040, indicating that the increase in storage uptake and thermal generation retirements results in a system that is highly exposed to weather risk as internal stressor. Furthermore, introducing a 3-day VRE drought explicitly does not change the overall average USE results significantly, however adding an extreme 7-day VRE drought increases the observed risk of unserved energy significantly.

While the increasing impact is expected as energy availability is reduced, there is a stark difference between the risk captured by the different storage operation assumptions: The high energy assumption does not show any adequacy risk in the studied scenario in the base case and 3-day drought both for average and tail risk, and only captures the extreme event risk. In contrast both the derated energy and economic operation approximations record a risk across the low VRE availability periods in the base case and with explicit 3-day VRE drought.

Capturing the impact of VRE droughts and periods of low energy availability may therefore be strongly sensitive to storage operation approximations, as the derated and economic operation approximations showcase increasing differences and only extreme lack of VRE availability are captured by high energy case.

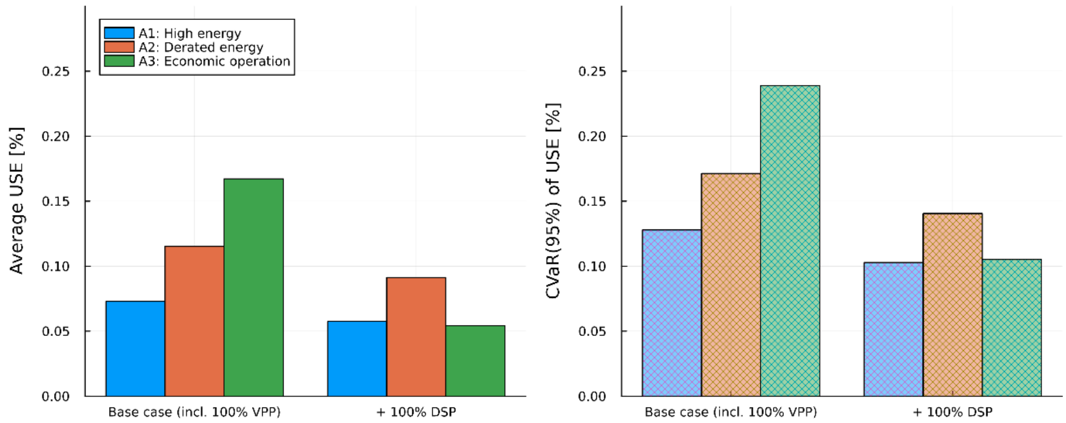

Figure 7.19: Average and tail NEM-wide unserved energy (USE) under the 7-day VRE drought scenario in 2040, comparing the base case with a sensitivity case with full compliance of demand side-participation (DSP). Unserved energy is normalised with respect to total demand in the simulated horizon (June – August).

However, when including demand response in the evaluation of the system resilience risk under the 7-day VRE drought scenario in 2040 (in the form of price sensitive DSP capacity as described in chapter 5), we observe a reduction in the sensitivity of the adequacy results across the storage operation approximations. Especially in the 'economic operation' case, the average and tail risk reduces significantly, again highlighting the potential and importance of enabling demand reduction in a weather-dependent power system, in line with the results presented in chapter 5 and 6.

7.8 Key findings

Based on the insights and findings in this chapter, we highlight the following key takeaways for addressing and parametrising weather-driven resilience scenarios for system planning.

- As weather-driven extreme event impacts increase due to climate change and power system weather dependency grows, **resilience studies can provide complementary insights to traditional adequacy assessment frameworks**.
- Four weather-related hazards affecting the Australian east coast power system were identified through historical event analysis: heatwaves, windstorms, hailstorms, and flash floods. These hazards may affect the system through multiple stressors, including temperature extremes, high wind speeds, and bushfires.
- The developed framework may provide guidance about hazard, stressor, and event definitions before identifying risk drivers and input parameters.
- As demonstrated on the example of a heatwave, **representing weather-related external stressors is highly complex, requiring** compromise **between model realism and computational feasibility.** A high number of system parameters are required to capture impacts realistically, while spatial granularity is needed to avoid unintended artificial common mode failures.

- **Heatwave events may present primarily a capacity constraint to the system.** Solar PV output remains relatively high during heatwaves, whilst wind generation is typically low. The system becomes especially sensitive to thermal generation outages during these periods, suggesting that increased system flexibility through storage may serve as an effective resilience measure.
- **Unlocking VPP coordination at system level can reduce USE during heatwaves.** When including additional storage capacity through VPP coordination, USE falls to zero in both the base case and the extreme heatwave scenario. This suggests that the modelled heatwave reliability risk is not primarily caused by insufficient energy availability, but by critical-hour capacity and flexibility constraints that may be resolved through increased DER coordination, underscoring the significant potential of demand side flexibility to hedge against tail risk events, as identified in chapter 5.
- Prolonged VRE drought events are critical to weather-dependent systems, posing an energy constraint to the system. **Storage operation approximations may have a large discrepancy on perceived VRE drought risk**, highlighting fundamental uncertainty about the severity and visibility of VRE drought events for system resilience in highly storage defined systems. Also in this resilience scenario, DER coordination (here considered in form of demand response (DSP)) may play a crucial role for reducing uncertainty and ensuring system resilience to endogenous weather stressors for the future Australian east coast power system.

8 Conclusions

This report presents a comprehensive assessment of resource adequacy, risk characterisation, and resilience in the Australian National Electricity Market as it transitions toward a system dominated by variable renewable energy, energy storage, and distributed energy resources. Through the development of open-source modelling tools, systematic analysis of storage operational uncertainty, evaluation of DER coordination, and stress testing under extreme weather scenarios, this research identifies fundamental shifts in how reliability risks manifest and must be managed in a weather-dependent, energy-limited power system.

The work performed for this report highlights the following key takeaways:

- **The NEM becomes sensitive to storage operation approximations post-2030.** As energy storage transitions from a supporting role to a dominant component of the resource mix, storage operational assumptions materially influence adequacy outcomes. The divergence between the high-energy, derated-energy, and economic-operation approximations grows substantially after 2030, with implications for both average and tail risk.
- **Storage operation assumptions impact the distribution of reliability events.** Different operational approximations produce events with different frequencies, durations, and timing. Storage behaviour uncertainty should therefore be treated as a distinct risk dimension alongside traditional outage and weather variability.
- **DER coordination, even at lower compliance levels, may be fundamental for ensuring reliability.** Partial DER coordination—including 25% EV load reduction, 50% VPP availability, or 50% demand-side participation—can deliver material adequacy benefits. Universal consumer participation is not necessarily required to realise system-level reliability improvements.
- **Demand response provides hedging against storage operation uncertainty and tail risk events.** Demand-side participation demonstrates particular value in reducing tail risk and narrowing the spread of adequacy outcomes across different storage operational assumptions. DSP should be treated as a strategic resource for managing storage operation uncertainty and preparing for critical periods of low VRE availability.
- **Adequacy risk may increasingly shift from capacity-constrained events during peak demand to energy-constrained events during periods of low renewable availability.** However, the specific timing, magnitude, and frequency of these events depend critically on storage operational assumptions.
- **Risk drivers extend beyond peak demand periods.** Reliability risks increasingly emerge during early morning, nighttime, and moderate-demand periods. Operational measures and investment strategies must address reliability across the full daily cycle, not just peak-demand management.
- **The sensitivity of adequacy outcomes to storage operation indicates opportunity for operational measures to ensure reliability.** While adequacy assessment outcomes and hence system planning faces increased variability, policy mechanisms may influence storage behaviour and reduce the intrinsic uncertainty in adequacy assessments, as well as system operation.

- **A comprehensive review of risk events and resilience framework has been developed for systematic studies.** Historical analysis of extreme weather events in Australia identified multiple hazard classes—heatwaves, windstorms, hailstorms, flash floods—and their compound effects on power system infrastructure. A systematic framework was developed to translate external weather drivers into endogenous system parameters for resilience stress testing and demonstrated on an extreme heatwave and a prolonged VRE drought.
- **Heatwave events may present primarily a capacity constraint rather than an energy scarcity problem.** Thermal generator derating emerges as the dominant risk driver, with greater impact than VRE or transmission derating alone. Resilience against heatwaves may be best addressed through flexible capacity (storage, demand response) and targeted operational measures during critical hours.
- **Extended VRE droughts beyond 3 days may be particularly sensitive to storage operation approximations, however increased levels of demand response may reduce uncertainty.** A 3-day VRE drought period did not increase resilience risk materially, however stress-testing the system against a 7-day VRE drought resulted in divergence across the storage operation approximations, which was able to be relieved by increased demand response (modelled as price-sensitive demand-side participation capacity bands).

This research further identified several crucial directions for future work on advancing resource adequacy and resilience assessments in weather-dependent power systems dominated by storage and DER:

- **Improving storage operational representation.** To reduce storage operation uncertainty, a better understanding of potential operational behaviours is needed. While the proposed framework presents an attempt to more accurately capture storage behaviour, actual operation of heterogeneous storage operators with various utility functions may be better captured by data-driven approaches, based on real world data.
- **Evaluating the economic implications of storage operation uncertainty**. Storage operation directly impacts its revenues, yet the uncertainty surrounding operational behaviour means that actual revenues remain unpredictable. Reduced revenues due to “imperfect” operation have been observed in the NEM [51], creating uncertainty about whether all projected storage investments will materialise. This investment uncertainty directly feeds back into system reliability outcomes, as the adequacy levels of this report depend on storage capacity being deployed as planned. Further research is needed to quantify the economic implications of storage operation uncertainty, how this influences investment decisions and, consequently, system reliability levels. **Formalising operational intervention measures.** System operators may employ various operational measures to support reliability, including minimum state-of-charge requirements, or strategic directions. These measures warrant systematic assessment within adequacy frameworks to understand their effectiveness and trade-offs. Formalising these interventions would enable evaluation of their contribution to reliability and identification of optimal operational policies across different system states.
- **Representing and evaluating distribution system constraints and buildout.** Whilst this research demonstrates that DER coordination can provide significant adequacy benefits, distribution system constraints (such as line and transformer limits) may restrict the ability to realise these benefits in practice. Investment into distribution system upgrades may therefore

be necessary to unlock DER coordination potential; however, this creates a trade-off between distribution-level investments and large-scale infrastructure investments. The optimal investment across these different system levels requires systematic evaluation to ensure reliability outcomes are achieved cost-effectively.

- **Extending resilience studies beyond heatwaves.** This work focused on heatwave and VRE drought resilience as case studies; however, the framework developed can be extended to other weather-related risk drivers identified in the historical analysis, including windstorms, hailstorms, and flash floods. Comprehensive resilience studies across multiple hazard classes would provide a more complete picture of weather-dependent risks and identify common or divergent mitigation strategies.

9 References

[1] Department of Climate Change, Energy, the Environment and Water (DCCEEW), “National Consumer Energy Resources Roadmap (CER Roadmap),” Commonwealth of Australia, Aug. 2025. [Online]. Available: https://www.dcceew.gov.au/energy/renewable/consumer-energy-resources

[2] CIGRE Working Group C1.27, *The future of reliability - Definition of reliability in light of new developments in various devices and services which offer customers and system operators new levels of flexibility*, 715, 2018. Accessed: Feb. 06, 2025. [Online]. Available: https://www.cigreaustralia.org.au/in-the-loop/in-the-loop-news/the-future-of-reliability-wg-c1-27/

[3] EPRI, “Resource Adequacy for a Decarbonized Future: A Summary of Existing and Proposed Resource Adequacy Metrics,” Palo Alto, CA, Apr. 2022. Accessed: Feb. 10, 2025. [Online]. Available: https://www.epri.com/research/products/000000003002023230

[4] R. Billinton and R. N. Allan, *Reliability Evaluation of Power Systems*, Second Edition. in SpringerLink Bücher. Boston, MA: Springer US, 1996. doi: 10.1007/978-1-4899-1860-4.

[5] ESIG, “Redefining Resource Adequacy for Modern Power Systems,” Reston, VA, 2021. [Online]. Available: https://www.esig.energy/resource-adequacy-for-modern-power-systems/

[6] M. Tillmanns, J. Schöttler, and A. Praktiknjo, “A review of probabilistic resource adequacy assessments in power systems: Methods, applications, and future challenges,” *Energy Policy*, vol. 209, p. 114924, Feb. 2026, doi: 10.1016/j.enpol.2025.114924.

[7] Australian Energy Market Operator (AEMO), “2025 Electricity Statement of Opportunities (ESOO),” Aug. 2025. Accessed: Sep. 03, 2025. [Online]. Available: https://www.aemo.com.au/energy-systems/electricity/national-electricity-market-nem/nem-forecasting-and-planning/forecasting-and-reliability/nem-electricity-statement-of-opportunities-esoo

[8] Australian Energy Market Operator (AEMO), “Forecasting Approach - Electricity Demand Forecasting Methodology,” Jul. 2025. [Online]. Available: https://www.aemo.com.au/energy-systems/electricity/national-electricity-market-nem/nem-forecasting-and-planning/forecasting-approach

[9] EPRI, “Resource Adequacy Philosophy: A Guide to Resource Adequacy Concepts and Approaches,” Palo Alto, CA, Dec. 2022. Accessed: Feb. 06, 2025. [Online]. Available: https://www.epri.com/research/products/000000003002024368

[10] R. N. Allan, A. M. L. Da Silva, A. A. Abu-Nasser, and R. C. Burchett, “Discrete Convolution in Power System Reliability,” *IEEE Trans. Rel.*, vol. R-30, no. 5, pp. 452–456, Dec. 1981, doi: 10.1109/TR.1981.5221166.

[11] G. Stephen *et al.*, “Clarifying the Interpretation and Use of the LOLE Resource Adequacy Metric,” in *2022 17th International Conference on Probabilistic Methods Applied to Power Systems (PMAPS)*, Manchester, United Kingdom: IEEE, Jun. 2022, pp. 1–4. doi: 10.1109/PMAPS53380.2022.9810615.

[12] ESIG, “New Resource Adequacy Criteria for the Energy Transition: Modernizing Reliability Requirements,” Reston, VA, 2024. [Online]. Available: https://www.esig.energy/ new-resource-adequacy-criteria

[13] C. J. Dent, N. Sanchez, A. Shevni, J. Q. Smith, A. L. Wilson, and X. Yu, “Resource adequacy and capacity Procurement: Metrics and decision support analysis,” *Proceedings of the Institution of*

Mechanical Engineers, Part A: Journal of Power and Energy, vol. 239, no. 1, pp. 199–209, Feb. 2025, doi: 10.1177/09576509241292100.

[14] G. Mantegna, Z. Huang, G. Van Caelenberg, B. Frew, M. Lynch, and M. O'Malley, "Electric grid reliability in an era of unprecedented uncertainty: a review of advances in electric sector resource adequacy assessment and planning," *IEEE Trans. on Enrgy Mrkts, Pol and Reg*, pp. 1–9, 2025, doi: 10.1109/TEMPR.2025.3640116.

[15] P. Mancarella, "Considerations in support of the 2022 Reliability Standards and Settings Review," The University of Melbourne, Briefing Note, Aug. 2022. [Online]. Available: https://www.aemc.gov.au/market-reviews-advice/2022-reliability-standard-and-settings-review

[16] P. Brito-Pereira, K. Bruninx, L. De Vries, P. Mastropietro, and P. Rodilla, "Future-proofed resource adequacy metrics: A model-based assessment of multi-metric vs. composite-metric reliability standards," *Sustainable Energy, Grids and Networks*, vol. 44, p. 101957, Dec. 2025, doi: 10.1016/j.segan.2025.101957.

[17] Elia, "2022-2032 Adequacy and flexibility study for Belgium," Brusseles, Belgium, 2021. [Online]. Available: https://www.elia.be/-/media/project/elia/shared/documents/elia-group/publications/studies-and-reports/2021/20210701_adequacy-flexibility-study-2021_en_v2.pdf

[18] L. Zhang, Y. Zhou, D. Flynn, J. Mutale, and P. Mancarella, "System-Level Operational and Adequacy Impact Assessment of Photovoltaic and Distributed Energy Storage, with Consideration of Inertial Constraints, Dynamic Reserve and Interconnection Flexibility," *Energies*, vol. 10, no. 7, p. 989, Jul. 2017, doi: 10.3390/en10070989.

[19] D. Stenclik *et al.*, "Quantifying Risk in an Uncertain Future: The Evolution of Resource Adequacy," *IEEE Power and Energy Mag.*, vol. 19, no. 6, pp. 29–36, Nov. 2021, doi: 10.1109/MPE.2021.3104076.

[20] A. Burdick, N. Schlag, A. Au, R. Go, Z. Ming, and A. Olson, "Lighting a Reliable Path to 100% Clean Electricity: Evolving Resource Adequacy Practices for a Decarbonizing Grid," *IEEE Power and Energy Mag.*, vol. 20, no. 4, pp. 30–43, Jul. 2022, doi: 10.1109/MPE.2022.3167572.

[21] Coordinator of Energy, "WA Power System Security and Reliability Standards Review," Government of Western Australia, 2026. [Online]. Available: https://www.wa.gov.au/government/document-collections/power-system-security-and-reliability-standards-review

[22] Australian Energy Market Operator (AEMO), "2023-24 Inputs, Assumptions and Scenarios," Sep. 2023. [Online]. Available: https://www.aemo.com.au/energy-systems/major-publications/integrated-system-plan-isp/2024-integrated-system-plan-isp/current-inputs-assumptions-and-scenarios

[23] G. Stephen, "Probabilistic Resource Adequacy Suite (PRAS) v0.6 Model Documentation," NREL/TP--5C00-79698, 1785462, MainId:35919, May 2021. doi: 10.2172/1785462.

[24] J. Bezanson, A. Edelman, S. Karpinski, and V. B. Shah, "Julia: A Fresh Approach to Numerical Computing," *SIAM Rev.*, vol. 59, no. 1, pp. 65–98, Jan. 2017, doi: 10.1137/141000671.

[25] C. Barrows *et al.*, *Sienna modeling framework*. Office of Scientific and Technical Information (OSTI), 2024. doi: 10.2172/2376836.

[26] M. Lubin, O. Dowson, J. D. Garcia, J. Huchette, B. Legat, and J. P. Vielma, "JuMP 1.0: recent improvements to a modeling language for mathematical optimization," *Math. Prog. Comp.*, vol. 15, no. 3, pp. 581–589, Sep. 2023, doi: 10.1007/s12532-023-00239-3.

[27] L. Zhang, T. Capuder, and P. Mancarella, "Unified Unit Commitment Formulation and Fast Multi-Service LP Model for Flexibility Evaluation in Sustainable Power Systems," *IEEE Trans. Sustain. Energy*, vol. 7, no. 2, pp. 658–671, Apr. 2016, doi: 10.1109/TSTE.2015.2497411.

[28] Bagen and R. Billinton, "Impacts of energy storage on power system reliability performance," in *Canadian Conference on Electrical and Computer Engineering, 2005.*, Saskatoon, SK, Canada: IEEE, 2005, pp. 494–497. doi: 10.1109/CCECE.2005.1556978.

[29] J. Twitchell, K. DeSomber, and D. Bhatnagar, "Defining long duration energy storage," *Journal of Energy Storage*, vol. 60, p. 105787, Apr. 2023, doi: 10.1016/j.est.2022.105787.

[30] P. Denholm, W. Cole, A. Frazier, K. Podkaminer, and N. Blair, "Storage Futures Study: The Challenge of Defining Long-Duration Energy Storage," NREL/TP-6A40-80583, 1832215, MainId:53972, Nov. 2021. doi: 10.2172/1832215.

[31] S. Gonzato, K. Bruninx, and E. Delarue, "The effect of short term storage operation on resource adequacy," *Sustainable Energy, Grids and Networks*, vol. 34, p. 101005, Jun. 2023, doi: 10.1016/j.segan.2023.101005.

[32] G. Stephen, T. Joswig-Jones, S. Awara, and D. Kirschen, "Impact of Storage Dispatch Assumptions on Resource Adequacy and Capacity Credit," in *2022 17th International Conference on Probabilistic Methods Applied to Power Systems (PMAPS)*, Manchester, United Kingdom: IEEE, Jun. 2022, pp. 1–6. doi: 10.1109/PMAPS53380.2022.9810584.

[33] F. Mohamad and J. Teh, "Impacts of Energy Storage System on Power System Reliability: A Systematic Review," *Energies*, vol. 11, no. 7, p. 1749, Jul. 2018, doi: 10.3390/en11071749.

[34] Ayesha, M. Numan, M. F. Baig, and M. Yousif, "Reliability evaluation of energy storage systems combined with other grid flexibility options: A review," *Journal of Energy Storage*, vol. 63, p. 107022, Jul. 2023, doi: 10.1016/j.est.2023.107022.

[35] R. Sioshansi *et al.*, "Energy-Storage Modeling: State-of-the-Art and Future Research Directions," *IEEE Trans. Power Syst.*, vol. 37, no. 2, pp. 860–875, Mar. 2022, doi: 10.1109/TPWRS.2021.3104768.

[36] Y. Zhou, P. Mancarella, and J. Mutale, "Modelling and assessment of the contribution of demand response and electrical energy storage to adequacy of supply," *Sustainable Energy, Grids and Networks*, vol. 3, pp. 12–23, Sep. 2015, doi: 10.1016/j.segan.2015.06.001.

[37] Y. Sun, B. Frew, S. Dalvi, and S. C. Dhulipala, "Insights into methodologies and operational details of resource adequacy assessment: A case study with application to a broader flexibility framework," *Applied Energy*, vol. 328, p. 120191, Dec. 2022, doi: 10.1016/j.apenergy.2022.120191.

[38] P. A. Dratsas, G. N. Psarros, and S. A. Papathanassiou, "Contribution of PV Generation With Embedded Battery Storage to Capacity Adequacy," *IEEE Trans. Sustain. Energy*, vol. 16, no. 2, pp. 1125–1138, Apr. 2025, doi: 10.1109/TSTE.2024.3505413.

[39] C. Byers and A. Botterud, "Additional Capacity Value From Synergy of Variable Renewable Energy and Energy Storage," *IEEE Trans. Sustain. Energy*, vol. 11, no. 2, pp. 1106–1109, Apr. 2020, doi: 10.1109/TSTE.2019.2940421.

[40] P. Hu, R. Karki, and R. Billinton, "Reliability evaluation of generating systems containing wind power and energy storage," *IET Gener. Transm. Distrib.*, vol. 3, no. 8, pp. 783–791, Aug. 2009, doi: 10.1049/iet-gtd.2008.0639.

[41] G. Liu and P. Mancarella, "Adequacy Assessment of Renewables-Dominated Power Systems with Large-Scale Energy Storage," in *2019 29th Australasian Universities Power Engineering*

Conference (AUPEC), Nadi, Fiji: IEEE, Nov. 2019, pp. 1–6. doi: 10.1109/AUPEC48547.2019.211877.

[42] S. Zachary, A. Wilson, and C. Dent, "The Integration of Variable Generation and Storage into Electricity Capacity Markets," *The Energy Journal*, vol. 43, no. 4, pp. 231–250, May 2022, doi: 10.5547/01956574.43.4.szac.

[43] G. Liu, M. Vrakopoulou, and P. Mancarella, "Capacity Credit Evaluation Framework of Wind, Solar and Pumped Hydro Storage Considering Generation Adequacy and Flexibility," in *2019 9th International Conference on Power and Energy Systems (ICPES)*, Perth, Australia: IEEE, Dec. 2019, pp. 1–6. doi: 10.1109/ICPES47639.2019.9105380.

[44] P. A. Dratsas, G. N. Psarros, and S. A. Papathanassiou, "A Real-Time Redispatch Method to Evaluate the Contribution of Storage to Capacity Adequacy," *IEEE Trans. Power Syst.*, vol. 39, no. 1, pp. 1274–1286, Jan. 2024, doi: 10.1109/TPWRS.2023.3243669.

[45] G. Liu, M. Vrakopoulou, and P. Mancarella, "Assessment of the Capacity Credit of Renewables and Storage in Multi-Area Power Systems," *IEEE Trans. Power Syst.*, vol. 36, no. 3, pp. 2334–2344, May 2021, doi: 10.1109/TPWRS.2020.3034248.

[46] A. Botterud, M. Korpas, and G. Tarel, "Price formation and long-term equilibrium in future electricity markets: the role of energy storage," *Powering the Future: Energy Storage in Tomorrow's Electricity Markets*, no. 140, Apr. 2024. [Online]. Available: https://www.oxfordenergy.org/publications/powering-the-future-energy-storage-in-tomorrows-electricity-markets-issue-140/

[47] N. Qi, P. Pinson, M. R. Almassalkhi, Y. Zhuang, Y. Su, and F. Liu, "Capacity credit evaluation of generalized energy storage considering strategic capacity withholding and decision-dependent uncertainty," *Applied Energy*, vol. 397, p. 126310, Nov. 2025, doi: 10.1016/j.apenergy.2025.126310.

[48] T. K. Shrestha and R. Karki, "Impact of market-driven energy storage system operation on the operational adequacy of wind integrated power systems," *Journal of Energy Storage*, vol. 32, p. 101792, Dec. 2020, doi: 10.1016/j.est.2020.101792.

[49] Australian Energy Market Operator (AEMO), "AEMO's contribution to the Certification of Capability Class 2 Technologies (CC2T) Review," Oct. 2025. Accessed: Oct. 27, 2025. [Online]. Available: https://www.wa.gov.au/government/document-collections/capability-class-2-technologies-review-working-group

[50] Matt Grover, "How the NEM BESS fleet is operating on peak days, and how to be a savvy operator," WattClarity. [Online]. Available: https://wattclarity.com.au/articles/2025/10/how-the-nem-bess-fleet-is-operating-on-peak-days-and-how-to-be-a-savvy-operator/

[51] Y. Yang, R. Dheerasekara, J. Whiting, and B. Vanderwaal, "Bridging the gap: Analysing differences between investment business case modelling and real-time operation for BESS," presented at the CIGRE Australia Conference, Sep. 03, 2025.

[52] O. J. Guerra, S. Dalvi, A. Thatte, B. Cowiestoll, J. Jorgenson, and B.-M. Hodge, "Towards robust and scalable dispatch modeling of long-duration energy storage," *Renewable and Sustainable Energy Reviews*, vol. 207, p. 114940, Jan. 2025, doi: 10.1016/j.rser.2024.114940.

[53] A. Prakash, A. Bruce, and I. MacGill, "The scheduling role of future pricing information in electricity markets with rising deployments of energy storage: An Australian National Electricity Market case study," *Energy Economics*, vol. 142, p. 108191, Feb. 2025, doi: 10.1016/j.eneco.2025.108191.

[54] G. Edwards, S. Sheehy, C. J. Dent, and M. C. M. Troffaes, “Assessing the contribution of nightly rechargeable grid-scale storage to generation capacity adequacy,” *Sustainable Energy, Grids and Networks*, vol. 12, pp. 69–81, Dec. 2017, doi: 10.1016/j.segan.2017.09.005.

[55] M. P. Evans, S. H. Tindemans, and D. Angeli, “Minimizing Unserved Energy Using Heterogeneous Storage Units,” *IEEE Trans. Power Syst.*, vol. 34, no. 5, pp. 3647–3656, Sep. 2019, doi: 10.1109/TPWRS.2019.2910388.

[56] S. Zachary, “Scheduling and dimensioning of heterogeneous energy stores, with applications to future GB storage needs,” *Energy Syst*, Apr. 2025, doi: 10.1007/s12667-025-00734-7.

[57] H. J. Kim, R. Sioshansi, E. Lannoye, and E. Ela, “Assessing the Capacity Value of Energy Storage That Provides Frequency Regulation,” *IEEE Trans. Power Syst.*, vol. 40, no. 3, pp. 2661–2673, May 2025, doi: 10.1109/TPWRS.2024.3501095.

[58] WECC, “Western Assessment of Resource Adequacy 2024,” 2024. [Online]. Available: https://feature.wecc.org/wara/

[59] M. Spilger, D. Schneider, and C. Weber, “Uncertainty characterization for generation adequacy assessments – Including an application to the recent European energy crisis,” *Energy Economics*, vol. 144, p. 108304, Apr. 2025, doi: 10.1016/j.eneco.2025.108304.

[60] I. Konstantelos and G. Strbac, “Capacity value of energy storage in distribution networks,” *Journal of Energy Storage*, vol. 18, pp. 389–401, Aug. 2018, doi: 10.1016/j.est.2018.06.002.

[61] S. Wang, N. Zheng, C. D. Bothwell, Q. Xu, S. Kasina, and B. F. Hobbs, “Crediting Variable Renewable Energy and Energy Storage in Capacity Markets: Effects of Unit Commitment and Storage Operation,” *IEEE Transactions on Power Systems*, vol. 37, no. 1, pp. 617–628, Jan. 2022, doi: 10.1109/TPWRS.2021.3094408.

[62] A. J. Conejo and C. Ruiz, “Complementarity, Not Optimization, is the Language of Markets,” *IEEE Open Access Journal of Power and Energy*, vol. 7, pp. 344–353, 2020, doi: 10.1109/OAJPE.2020.3029134.

[63] I. S. Jimenez, D. Ribó-Pérez, M. Cvetkovic, J. Kochems, C. Schimeczek, and L. J. De Vries, “Can an energy only market enable resource adequacy in a decarbonized power system? A co-simulation with two agent-based-models,” *Applied Energy*, vol. 360, p. 122695, Apr. 2024, doi: 10.1016/j.apenergy.2024.122695.

[64] J. Boegheim, “The challenge of imperfect foresight: Storage operation in a highly renewable NEM,” WattClarity. Accessed: Aug. 04, 2025. [Online]. Available: https://wattclarity.com.au/articles/2025/04/the-challenge-of-imperfect-foresight-storage-operation-in-a-highly-renewable-nem/

[65] H. Kim, R. Sioshansi, E. Lannoye, and E. Ela, “A Stochastic-Dynamic-Optimization Approach to Estimating the Capacity Value of Energy Storage,” *IEEE Trans. Power Syst.*, vol. 37, no. 3, pp. 1809–1819, May 2022, doi: 10.1109/TPWRS.2021.3110497.

[66] C. Füllner and S. Rebennack, “Stochastic Dual Dynamic Programming and Its Variants: A Review,” *SIAM Rev.*, vol. 67, no. 3, pp. 415–539, Aug. 2025, doi: 10.1137/23M1575093.

[67] ENTSO-E, “European Resource Adequacy Assessment - 2024 Edition - Appendix 2 - Methodology,” Brusseles, 2024. [Online]. Available: https://www.entsoe.eu/eraa/2024/

[68] ENTSO-E, “Winter Outlook 2025-2026,” 2025. [Online]. Available: https://www.entsoe.eu/outlooks/seasonal/

[69] National Energy System Operator (NESO), “Resource Adequacy in the 2030s,” Warwick, UK, Jul. 2025. Accessed: Sep. 25, 2025. [Online]. Available: https://www.neso.energy/about/our-projects/resource-adequacy

[70] Eirgrid, "All-Island Resource Adequacy Assessment," Ireland, 2025. [Online]. Available: https://www.eirgrid.ie/all-island-resource-adequacy-assessment

[71] Bundesnetzagentur Deutschland, "Versorgungssicherheit Strom Bericht 2025." [Online]. Available: https://www.bundeswirtschaftsministerium.de/Redaktion/DE/Publikationen/Energie/versorgungssicherheit-strom-bericht-2025.html

[72] Elia, "2026-2036 Adequacy and flexibility study for Belgium," Brusseles, Belgium, 2025. [Online]. Available: https://www.elia.be/en/electricity-market-and-system/adequacy

[73] ENTSO-E, "Transparency Platform." Accessed: Nov. 05, 2025. [Online]. Available: https://newtransparency.entsoe.eu/

[74] WECC System Performance Data Portal, "Actual and Projected Annual Capacity (GW) by Fuel." 2026. [Online]. Available: https://wecc-spdp-weccgeo.hub.arcgis.com/pages/generation-capacity

[75] NERC, "2024 Long-Term Reliability Assessment," 2024. [Online]. Available: https://www.nerc.com/pa/RAPA/ra/Pages/default.aspx

[76] PJM, "Effective Load Carrying Capability and Reserve Requirement Study," Oct. 2025. Accessed: Oct. 28, 2025. [Online]. Available: https://www.pjm.com/-/media/DotCom/planning/res-adeq/elcc/2025-pjm-elcc-rrs.pdf

[77] "Rencana usaha penyediaan tenaga listrik (RUPTL) 2025–2034. Electricity Supply Business Plan (RUPTL) 2025–2034," PT Perusahaan Listrik Negara (Persero), Jakarta, Indonesia, 2025. [Online]. Available: https://web.pln.co.id/statics/uploads/2025/06/b967d-ruptl-pln-2025-2034-pub-.pdf

[78] PLN, "Rencana Umum Ketenagalistrikan Nasional (RUKN)," 2024. Accessed: Oct. 28, 2025. [Online]. Available: https://gatrik.esdm.go.id/assets/uploads/download_index/files/28dd4-rukn.pdf

[79] Generadoras, "Chilean Power Generators Bulletin," 2026. [Online]. Available: https://generadoras.cl/centro-de-informacion/#boletin

[80] Ministerio De Energia, *MODIFICA DECRETO SUPREMO Nº 62, DE 2006, DEL MINISTERIO DE ECONOMÍA, FOMENTO Y RECONSTRUCCIÓN, QUE APRUEBA REGLAMENTO DE TRANSFERENCIAS DE POTENCIA ENTRE EMPRESAS GENERADORAS ESTABLECIDAS EN LA LEY GENERAL DE SERVICIOS ELÉCTRICOS E INTRODUCE MODIFICACIONES A LOS DECRETOS QUE INDICA*. [Online]. Available: https://www.bcn.cl/leychile/navegar?idNorma=1204012

[81] The Superpower Institute, "Open Electricity: NEM." [Online]. Available: https://openelectricity.org.au

[82] Ministerio De Energia, *MODIFICA LA LEY GENERAL DE SERVICIOS ELÉCTRICOS, CON EL FIN DE INCENTIVAR EL DESARROLLO DE LAS GENERADORAS RESIDENCIALES*.

[83] Australian Energy Market Operator, "2024 Integrated System Plan (ISP) for the National Electricity Market (NEM)," AEMO, Australia, Jun. 2024. Accessed: Feb. 24, 2025. [Online]. Available: https://aemo.com.au/energy-systems/major-publications/integrated-system-plan-isp/2024-integrated-system-plan-isp

[84] J. Caballero-Peña, C. Cadena-Zarate, A. Parrado-Duque, and G. Osma-Pinto, "Distributed energy resources on distribution networks: A systematic review of modelling, simulation, metrics, and impacts," *International Journal of Electrical Power & Energy Systems*, vol. 138, p. 107900, Jun. 2022, doi: 10.1016/j.ijepes.2021.107900.

[85] J. L. Mathieu *et al.*, “A New Definition and Research Agenda for Demand Response in the Distributed Energy Resource Era,” *IEEE Trans. on Enrgy Mrkts, Pol and Reg*, vol. 3, no. 3, pp. 324–339, Sep. 2025, doi: 10.1109/TEMPR.2025.3554734.

[86] Australian Energy Market Commission (AEMC), “Distributed energy resources.” [Online]. Available: https://www.aemc.gov.au/energy-system/electricity/electricity-system/distributed-energy-resources

[87] Australian Energy Market Operator (AEMO), “Fact Sheet: The National Electricity Market,” 2025. [Online]. Available: https://www.aemo.com.au/energy-systems/electricity/national-electricity-market-nem

[88] I. M. Alves, L. M. Carvalho, and J. A. Peças Lopes, “Modeling demand flexibility impact on the long-term adequacy of generation systems,” *International Journal of Electrical Power & Energy Systems*, vol. 151, p. 109169, Sep. 2023, doi: 10.1016/j.ijepes.2023.109169.

[89] D. Huang and R. Billinton, “Effects of Load Sector Demand Side Management Applications in Generating Capacity Adequacy Assessment,” *IEEE Trans. Power Syst.*, vol. 27, no. 1, pp. 335–343, Feb. 2012, doi: 10.1109/TPWRS.2011.2164425.

[90] K. Pacco, D. N. Viet, L. Weber, and A. Moser, “Modeling Demand Side Management in European Resource Adequacy Assessments,” in *2023 International Conference on Future Energy Solutions (FES)*, Vaasa, Finland: IEEE, Jun. 2023, pp. 1–5. doi: 10.1109/FES57669.2023.10183335.

[91] L. Efe, J. Ponoćko, and E. A. M. Ceseña, “Day-ahead Demand Side Management Optimisation Considering Payback Potential,” in *2024 4th International Conference on Smart Grid and Renewable Energy (SGRE)*, Doha, Qatar: IEEE, Jan. 2024, pp. 1–6. doi: 10.1109/SGRE59715.2024.10429011.

[92] P. Alstone *et al.*, “2025 California Demand Response Potential Study,” Lawrence Berkeley National Laboratory, Mar. 2017. [Online]. Available: https://lpdd.org/resources/report-2025-california-demand-response-potential-study/

[93] N. Z. Xu and C. Y. Chung, “Reliability Evaluation of Distribution Systems Including Vehicle-to-Home and Vehicle-to-Grid,” *IEEE Trans. Power Syst.*, vol. 31, no. 1, pp. 759–768, Jan. 2016, doi: 10.1109/TPWRS.2015.2396524.

[94] M. Á. Lynch, S. Nolan, M. T. Devine, and M. O’Malley, “The impacts of demand response participation in capacity markets,” *Applied Energy*, vol. 250, pp. 444–451, Sep. 2019, doi: 10.1016/j.apenergy.2019.05.063.

[95] N. Qi, L. Cheng, Y. Zhuang, Y. Zhou, Y. Zhang, and C. Zhu, “Reliability assessment and improvement of distribution system with virtual energy storage under exogenous and endogenous uncertainty,” *Journal of Energy Storage*, vol. 56, p. 105993, Dec. 2022, doi: 10.1016/j.est.2022.105993.

[96] I. B. Sperstad, M. Z. Degefa, and G. Kjølle, “The impact of flexible resources in distribution systems on the security of electricity supply: A literature review,” *Electric Power Systems Research*, vol. 188, p. 106532, Nov. 2020, doi: 10.1016/j.epsr.2020.106532.

[97] Y. M. Atwa, E. F. El-Saadany, M. M. A. Salama, R. Seethapathy, M. Assam, and S. Conti, “Adequacy Evaluation of Distribution System Including Wind/Solar DG During Different Modes of Operation,” *IEEE Trans. Power Syst.*, vol. 26, no. 4, pp. 1945–1952, Nov. 2011, doi: 10.1109/TPWRS.2011.2112783.

[98] K. Zou, A. P. Agalgaonkar, K. M. Muttaqi, and S. Perera, “An Analytical Approach for Reliability Evaluation of Distribution Systems Containing Dispatchable and Nondispatchable Renewable DG Units,” *IEEE Trans. Smart Grid*, vol. 5, no. 6, pp. 2657–2665, Nov. 2014, doi: 10.1109/TSG.2014.2350505.

[99] J. Andruszkiewicz, J. Lorenc, and A. Weychan, “Distributed generation as efficient measure to improve power generation adequacy,” *Archives of Electrical Engineering*, pp. 373–385, May 2019, doi: 10.24425/aee.2019.128274.

[100] Y. Zhou, M. Panteli, R. Moreno, and P. Mancarella, “System-level assessment of reliability and resilience provision from microgrids,” *Applied Energy*, vol. 230, pp. 374–392, Nov. 2018, doi: 10.1016/j.apenergy.2018.08.054.

[101] A. Khashei, M. G. Dozein, and R. Razzaghi, “DER tripping in distribution networks: Root causes and classification framework,” *Sustainable Energy, Grids and Networks*, vol. 43, p. 101824, Sep. 2025, doi: 10.1016/j.segan.2025.101824.

[102] C. De Jonghe, B. F. Hobbs, and R. Belmans, “Optimal Generation Mix With Short-Term Demand Response and Wind Penetration,” *IEEE Trans. Power Syst.*, vol. 27, no. 2, pp. 830–839, May 2012, doi: 10.1109/TPWRS.2011.2174257.

[103] W. C. Khoo, J. Teh, and C.-M. Lai, “Integration of Wind and Demand Response for Optimum Generation Reliability, Cost and Carbon Emission,” *IEEE Access*, vol. 8, pp. 183606–183618, 2020, doi: 10.1109/ACCESS.2020.3029273.

[104] A. Zerrahn and W.-P. Schill, “On the representation of demand-side management in power system models,” *Energy*, vol. 84, pp. 840–845, May 2015, doi: 10.1016/j.energy.2015.03.037.

[105] P. J. Wildstein, M. T. Craig, and P. Vaishnav, “Participant overrides can halve the reliability value of direct load control programs,” *Energy and Buildings*, vol. 299, p. 113606, Nov. 2023, doi: 10.1016/j.enbuild.2023.113606.

[106] R. Earle, E. P. Kahn, and E. Macan, “Measuring the Capacity Impacts of Demand Response,” *The Electricity Journal*, vol. 22, no. 6, pp. 47–58, Jul. 2009, doi: 10.1016/j.tej.2009.05.014.

[107] A. Bagchi, L. Goel, and P. Wang, “Generation Adequacy Evaluation Incorporating an Aggregated Probabilistic Model of Active Distribution Network Components and Features,” *IEEE Trans. Smart Grid*, vol. 9, no. 4, pp. 2667–2680, Jul. 2018, doi: 10.1109/TSG.2016.2616542.

[108] L. Xiao, K. M. Muttaqi, and A. P. Agalgaonkar, “Reliability assessment of modern distribution networks embedded with renewable and distributed resources,” *Electric Power Systems Research*, vol. 212, p. 108374, Nov. 2022, doi: 10.1016/j.epsr.2022.108374.

[109] G. Morales-España, R. Martínez-Gordón, and J. Sijm, “Classifying and modelling demand response in power systems,” *Energy*, vol. 242, p. 122544, Mar. 2022, doi: 10.1016/j.energy.2021.122544.

[110] L. P. Wagner, L. M. Reinpold, M. Kilthau, and A. Fay, “A systematic review of modeling approaches for flexible energy resources,” *Renewable and Sustainable Energy Reviews*, vol. 184, p. 113541, Sep. 2023, doi: 10.1016/j.rser.2023.113541.

[111] L. Göransson, J. Goop, T. Unger, M. Odenberger, and F. Johnsson, “Linkages between demand-side management and congestion in the European electricity transmission system,” *Energy*, vol. 69, pp. 860–872, May 2014, doi: 10.1016/j.energy.2014.03.083.

[112] M. Jansen, R. Gross, and I. Staffell, “Quantitative evidence for modelling electric vehicles,” *Renewable and Sustainable Energy Reviews*, vol. 199, p. 114524, Jul. 2024, doi: 10.1016/j.rser.2024.114524.

[113] H.-G. Kwag and J.-O. Kim, “Optimal combined scheduling of generation and demand response with demand resource constraints,” *Applied Energy*, vol. 96, pp. 161–170, Aug. 2012, doi: 10.1016/j.apenergy.2011.12.075.

[114] G. A. Lunde, E. V. Damm, P. A. V. Gade, and J. Kazempour, “Aggregator of Electric Vehicles Bidding in Nordic FCR-D Markets: A Chance-Constrained Program,” *IEEE Trans. Power Syst.*, vol. 40, no. 6, pp. 4648–4659, Nov. 2025, doi: 10.1109/TPWRS.2025.3558868.

[115] C. Brancucci, D. Cutler, and J. Jenkins, “Flexible Data Centers: A Faster, More Affordable Path to Power,” Camus, encoord, and Princeton ZERO Lab, Dec. 2025. [Online]. Available: https://www.encoord.com/resources/blog/flexible-data-centers-study

[116] H. Moring, S. Jang, N. Ozay, and J. L. Mathieu, “Nodal Operating Envelopes vs. Network-wide Constraints: What is better for network-safe coordination of DERs?,” *Electric Power Systems Research*, vol. 234, p. 110702, Sep. 2024, doi: 10.1016/j.epsr.2024.110702.

[117] Australian Energy Market Operator, “Draft 2026 Integrated System Plan (ISP),” AEMO, Australia, Dec. 2025. [Online]. Available: https://www.aemo.com.au/consultations/current-and-closed-consultations/draft-2026-isp-consultation

[118] Australian Energy Market Commission (AEMC), “National Electricity Market Reliability & Security Report FY2025,” May 2026. [Online]. Available: https://www.aemc.gov.au/market-reviews-advice/national-electricity-market-reliability-security-report-fy2025

[119] Australian Energy Market Operator (AEMO), “2024 Integrated System Plan - Appendix 4: System Operability,” Jun. 2024. [Online]. Available: https://www.aemo.com.au/energy-systems/major-publications/integrated-system-plan-isp/2024-integrated-system-plan-isp

[120] P. J. Palermo *et al.*, “The definition of reliability in light of new developments in various devices and services offering customers and system operators new levels of flexibility—summary of technical brochure 715,” in *2018 Grid of the Future Symposium*, USA: CIGRE US National Committee, 2018.

[121] G. Stephen, S. Tindemans, and Genevieve (Genna) de Mijolla, “Fundamentals of resource adequacy for modern power systems.” Jul. 2024.

[122] “The authoritative dictionary of IEEE standards terms, seventh edition,” *IEEE Std 100-2000*, pp. 1–1362, 2000, doi: 10.1109/IEEESTD.2000.322230.

[123] P. Kundur *et al.*, “Definition and classification of power system stability,” *IEEE Transactions on Power Systems*, vol. 19, no. 3, pp. 1387–1401, 2004, doi: 10.1109/TPWRS.2004.825981.

[124] Australian Energy Market Operator, “Power system requirements,” AEMO, Australia, Report Version 2.0 (24/07/2020), Jul. 2020.

[125] Australian Energy Market Commission, “NEM Reliability & Security Report FY2024,” AEMC, Australia, Report, Jun. 2025.

[126] A. Stankovic, “The definition and quantification of resilience,” IEEE, Technical Report PES-TR65, 2018. doi: 10.17023/K3V1-2H47.

[127] Bill Chiu *et al.*, “Resilience framework, methods, and metrics for the electricity sector,” IEEE Power & Energy Society, Technical Report PES-TR83, Oct. 2020. doi: 10.17023/x83h-mn15.

[128] Australian Energy Market Operator, “Building power system resilience with pumped hydro energy storage,” AEMO, Australia, Report, Jul. 2019.

[129] United Nations General Assembly, “Sendai framework for disaster risk reduction 2015-2030,” United Nations, New York, NY, USA, Report A/RES/69/283, Jun. 2015.

[130] United Nations International Strategy for Disaster Reduction, “2009 UNISDR terminology on disaster risk reduction,” UNISDR, Report, May 2009.

[131] Australian Energy Market Operator, “2020 ISP appendix 8: Resilience and climate change,” AEMO, Australia, Report Version 1.0, Jul. 2020.

[132] CIGRE Working Group C4.47, “Power system resilience: Definition, features and properties,” *CIGRE Science & Engineering*, 2019.

[133] N. D. Hatziargyriou, “Power system resilience against natural disasters.” Hong Kong, China, Jan. 2026.

[134] Australian Energy Market Operator, “Appendices to the 2018 integrated system plan,” AEMO, Report, 2018.

[135] L. Enright, “Drought national electricity financial market’s ‘first major shock.’” Australian Energy Regulator, Jun. 2007.

[136] S Darnell, “Trip of transmission lines in tasmania followed by the loss of basslink on 10 and 16 december 2014, and 23 february 2015,” AEMO, Power System Operating Incident Report, May 2015.

[137] Australian Energy Market Operator, “Black system – South Australia, 28 September 2016,” AEMO, Australia, Report, Mar. 2017.

[138] M. Ogge and H. Aulby, “Can’t stand the heat: The energy security risk of australia’s reliance on coal and gas generators in an era of increasing heatwaves,” The Australia Institute, Australia, Discussion Paper, Nov. 2017.

[139] C. L. Henry and L. F. Pratson, “Effects of environmental temperature change on the efficiency of coal- and natural gas-fired power plants,” *Environmental Science & Technology*, vol. 50, no. 17, pp. 9764–9772, 2016, doi: 10.1021/acs.est.6b01503.

[140] A. Sergio and F. P. Colelli, “Weather-induced power plant outages: Empirical evidence from hydro and thermal generators in Europe,” *Energy Economics*, vol. 148, p. 108549, 2025, doi: 10.1016/j.eneco.2025.108549.

[141] J. You, F. Yin, and L. Gao, “Escalating wind power shortages during heatwaves,” *Communications Earth & Environment*, vol. 6, no. 1, p. 245, Mar. 2025, doi: 10.1038/s43247-025-02239-8.

[142] Bureau of Meteorology, Commonwealth Scientific and Industrial Research Organisation, and Australian Energy Market Operator, “The impact of extreme heat on Variable Renewable Energy (VRE) generation.” 2021.

[143] J. Huang, B. Jones, M. Thatcher, and J. Landsberg, “Temperature impacts on utility-scale solar photovoltaic and wind power generation output over Australia under RCP 8.5,” *Journal of Renewable and Sustainable Energy*, vol. 12, no. 4, p. 046501, Aug. 2020, doi: 10.1063/5.0012711.

[144] E. Radziemska, “The effect of temperature on the power drop in crystalline silicon solar cells,” *Renewable Energy*, vol. 28, no. 1, pp. 1–12, 2003, doi: 10.1016/S0960-1481(02)00015-0.

[145] TransGrid, “Overview of 2019–20 bushfire damage to TransGrid’s network: Cost pass through application,” Australian Energy Regulator, Report, 2020.

[146] Australian Associated Press, “Savage weather batters south–east Queensland with deadly flash flooding escalating.” Feb. 2022. [Online]. Available: https://www.theguardian.com/australia-news/2022/feb/25/savage-weather-batters-south-east-queensland-with-deadly-flash-flooding-escalating

[147] B. Mountain, “Victoria’s power outage could have been far worse. Can we harden the grid against extreme weather?” Feb. 2024. [Online]. Available: https://www.9news.com.au/national/victorias-power-outage-could-have-been-far-worse-can-we-harden-the-grid-against-extreme-weather/3dda4008-c118-48c1-8958-e06d3cf57abd

[148] Network Outage Review Expert Panel, “Review into the transmission and distribution businesses operational response to the 13 february 2024 storms,” Victorian Department of Energy, Environment and Climate Action, Melbourne, Victoria, Interim Report, 2024.

[149] D. Lee, “Seven transmission towers collapse near Broken Hill overnight.” Oct. 2024. [Online]. Available: https://wattclarity.com.au/articles/2024/10/seven-transmission-towers-collapse-near-broken-hill-overnight/

[150] Coastwatch, “Record–breaking supercell storm hammers South–East Queensland.” Nov. 2025. [Online]. Available: https://coastwatch.com.au/articles/record-breaking-supercell-storm-devastates-south-east-queensland/

[151] Bureau of Meteorology, Commonwealth Scientific and Industrial Research Organisation, and Australian Energy Market Operator, “Electricity sector climate information (ESCI) project User Guide: Step 4 — evaluate all risks,” Electricity Sector Climate Information (ESCI) Project, 2021. [Online]. Available: https://www.climatechangeinaustralia.gov.au/en/projects/esci/esci-publications/esci-additional-resources/

[152] H. Hersbach *et al.*, “The ERA5 global reanalysis,” *Quarterly Journal of the Royal Meteorological Society*, vol. 146, no. 730, pp. 1999–2049, Jul. 2020, doi: 10.1002/qj.3803.

[153] Copernicus Climate Change Service (C3S), “ERA5: Fifth generation of ECMWF atmospheric reanalyses of the global climate.” Copernicus Climate Change Service Climate Data Store (CDS). [Online]. Available: https://cds.climate.copernicus.eu

[154] M. Dix *et al.*, “CSIRO-ARCCSS ACCESS-CM2 model output prepared for CMIP6 CMIP historical.” Earth System Grid Federation, 2019. doi: 10.22033/ESGF/CMIP6.4271.

[155] Rama Nemani / NASA, “NASA Earth Exchange Global Daily Downscaled Projections - CMIP6.” NASA Center for Climate Simulation, 2021. doi: 10.7917/OFSG3345.

[156] B. Thrasher, W. Wang, A. Michaelis, F. Melton, T. Lee, and R. Nemani, “NASA Global Daily Downscaled Projections, CMIP6,” *Sci Data*, vol. 9, no. 1, p. 262, Jun. 2022, doi: 10.1038/s41597-022-01393-4.

[157] Transmission Network Service Providers, “TNSP Operational Line Ratings,” TNSP, Mar. 2009. [Online]. Available: https://www.powerlink.com.au/sites/default/files/2018-01/TNSP%20Operational%20Line%20Ratings.pdf

[158] B. Wang, Y. Zhou, P. Mancarella, and M. Panteli, “Assessing the impacts of extreme temperatures and water availability on the resilience of the GB power system,” in *2016 IEEE International Conference on Power System Technology (POWERCON)*, Wollongong, NSW, Australia: IEEE, Sep. 2016, pp. 1–6. doi: 10.1109/POWERCON.2016.7754047.

[159] Y. Zhou, M. Panteli, B. Wang, and P. Mancarella, “Quantifying the System-Level Resilience of Thermal Power Generation to Extreme Temperatures and Water Scarcity,” *IEEE Systems Journal*, vol. 14, no. 1, pp. 749–759, Mar. 2020, doi: 10.1109/JSYST.2019.2938332.

[160] J. Yin, H. Gu, J. Huang, and M. Wang, “An investigation into the vertical structures of low-altitude atmosphere over the Central Taklimakan Desert in summer,” *Atmospheric Science Letters*, vol. 22, no. 9, p. e1042, Sep. 2021, doi: 10.1002/asl.1042.

[161] D. Faiman, “Assessing the outdoor operating temperature of photovoltaic modules,” *Progress in Photovoltaics*, vol. 16, no. 4, pp. 307–315, Jun. 2008, doi: 10.1002/pip.813.

[162] Peter Brook, “Dunkelflaute writ large - May 2024?,” Australian Energy Council. Accessed: May 26, 2026. [Online]. Available: https://www.energycouncil.com.au/analysis/dunkelflaute-writ-large-may-2024/

[163] Chris Gilbert, “It’s dark, it’s still – it’s dunkelflaute,” Energy Networks Australia. Accessed: May 26, 2026. [Online]. Available: https://www.energynetworks.com.au/news/energy-insider/2021-energy-insider/its-dark-its-still-its-dunkelflaute/

[164] Risk Frontiers, “Impact of climate change on VRE lulls,” Aug. 2025. [Online]. Available: https://asl.org.au/our-role/infrastructure-investment-objectives-report#panel2

[165] Australian Energy Market Operator, “Pre-dispatch procedure,” AEMO, Australia, Procedure Version 17 (03/06/2024), Jun. 2024.

[166] T. Gutierrez, *ParametricOptInterface*. [Online]. Available: https://github.com/jump-dev/ParametricOptInterface.jl

[167] Australian Energy Market Commission (AEMC), “AEMC updates market price cap for 2025-26.” Accessed: Feb. 28, 2025. [Online]. Available: https://www.aemc.gov.au/news-centre/media-releases/aemc-updates-market-price-cap-2025-26

[168] Australian Energy Market Operator, “Projected assessment of system adequacy (PASA).” 2025.

[169] Australian Energy Regulator (AER), “State of the energy market 2025 - Chapter 2 - National Electricity Market,” Aug. 2025. [Online]. Available: https://www.aer.gov.au/publications/reports/performance/state-energy-market-2025

[170] Vestas Wind Systems, “General specification: 2.0/2.2 MW V90/V100/V110 50/60 hz,” Vestas Wind Systems, Datasheet Document No. 0062-4191 V05, Feb. 2018.

Appendices

The following appendices are aimed at providing further details about the underlying modelling, as well as additional results. 9A.1 explains and lists key parameters and underlying assumptions of the simulations. This is followed by 9A.2, which details the mathematical modelling of the open-source Julia package *SchedNEM.jl* that was employed for the time-sequential modelling within the adequacy studies. 9A.3 provides further details about the adequacy assessment framework developed for this work, as well as calibration and scheduling results, and lists key differences between the scheduling engines of the underlying adequacy frameworks. 9A.4 provides a discussion on the impact and differences resulting from the unit commitment implementation. 9A.5 details assumptions and parameters of the extreme heatwave resilience case study, while 9A.6 presents further system operation results of the resilience impact case studies.

A.1 System details and parameters

A.1.1 Default settings and constraints

- 12 node sub-regional model as per ISP 2024
- Scheduling rolling horizon with 48h foresight and 24h steps, which is chosen in alignment with the pre-dispatch run horizon at AEMO that provides market participants with dispatch and price expectations for the next 16 - 40 hours [165].
- Because the workflow methodology relies on storage scheduling separate to outage sampling, we derate the storage discharging and charging capacity by its forced outage rate, instead of sampling the outages probabilistically.

A.1.2 Unit commitment details

An overview of the up/down time limits for the units that are applied in the modelling can be found in Table 0.1. These values are collected by *ParseISP.jl* from the ISP 2024 for all gas turbines as well as from the ISP 2018 for coal power plants.

Table 0.1: Generators with minimum up/down time limits that are considered within the modelling. The unit commitment constraints are applied for each unit within each generator separately.

Name	DUID	Fuel	Technology	Units	Up/Down Time [h]	Source
Bayswater	BW01	Coal	Black Coal	4	8	ISP18
Callide B	CALL_B_1	Coal	Black Coal	2	8	ISP18
Callide C	CPP_3	Coal	Black Coal	2	8	ISP18
Eraring	ER01	Coal	Black Coal	4	8	ISP18
Gladstone	GSTONE1	Coal	Black Coal	6	8	ISP18
Kogan Creek	KPP_1	Coal	Black Coal	1	8	ISP18
Loy Yang A Power Station	LYA1	Coal	Brown Coal	4	16	ISP18
Loy Yang B	LOYYB1	Coal	Brown Coal	2	16	ISP18
Millmerran	MPP_1	Coal	Black Coal	2	8	ISP18
Mt Piper	MP1	Coal	Black Coal	2	8	ISP18
Stanwell	STAN-1	Coal	Black Coal	4	8	ISP18
Tarong	TARONG#1	Coal	Black Coal	4	8	ISP18

Tarong North	TNPS1	Coal	Black Coal	1	8	ISP18
Vales Point B	VP5	Coal	Black Coal	2	8	ISP18
Yallourn W	YWPS1	Coal	Brown Coal	4	16	ISP18
Condamine A	CPSA	Natural Gas	CCGT	3	4	ISP24
Darling Downs	DDPS1	Natural Gas	CCGT	4	4	ISP24
Newport	NPS	Natural Gas	GFST	1	4	ISP24
Osborne	OSB-AG	Natural Gas	CCGT	2	4	ISP24
Pelican Point	PPCCGT	Natural Gas	CCGT	3	4	ISP24
Smithfield Energy Facility	SITHE01	Natural Gas	OCGT	2	6	ISP18
Swanbank E GT	SWAN_E	Natural Gas	CCGT	1	4	ISP24
Tallawarra	TALWA1	Natural Gas	CCGT	2	4	ISP24
Tamar Valley Combined Cycle	TVCC201	Natural Gas	CCGT	1	4	ISP24
Torrens Island B	TORRB1	Natural Gas	GFST	4	4	ISP24
Townsville Power Station	YABULU	Natural Gas	CCGT	2	4	ISP24
Yarwun Cogen	YARWUN_1	Natural Gas	CCGT	1	6	ISP18

A.1.3 Hydro modelling

Since hydro storages may be crucial for reliability in future, energy-limited systems, we obtain parameters of key large hydro reservoirs from additional sources. An overview of the default setting of the hydro parameters can be found in the table below. Note that we define the reservoir size based on the maximum discharge time that the specific generator would be able to run when full. This allows to utilise default values based on installed power capacity for units that are not explicitly defined.

Table 0.2: Hydro power parameter assumptions and default values within the adequacy modelling.

Region	Parameter	Sub-parameter	Value	Unit	Comment
TAS	reservoir_discharge_time_units[13]	Gordon (GORDON)	10000	h	Max capacity: 4700 GWh, with 450MW capacity = approx. 10000 h
		Poatina (POAT110)	20000	h	Max capacity: 6600 GWh, with 325MW capacity = approx. 10000 h
	reservoir_discharge_time_states	Tasmania (Region 4)	2000	h	Assed on total remaining storage capacity (3100 GWh and 1.4 GW capacity = 2000h)
	reservoir_initial_soc_units	Gordon (GORDON)	0.4	-	Average (2020 – 2026[14]): 1827 GWh => Approx 40%
		Poatina (POAT110)	0.3	-	Average (2020 – 2026): 1827 GWh => Approx 30%
	reservoir_initial_soc_states	Tasmania (Region 4)	0.6	-	Average (2020 – 2026): 1946 GWh => Approx 60%
	reservoir_discharge_time_units	Murray (MURRAY1) Tumut (UPPTUMUT)	2100	h	Approximated based on total Snowy Scheme values of average inflows (2800 GL), average production (4500 GWh), maximum active storage

[13] All values for Tasmania are from: Hydro Tasmania: *Energy in Storage*, https://www.hydro.com.au/water#energy_in_storage

[14] Note that the inflows in Tasmania were below average in the last two water years (https://www.economicregulator.tas.gov.au/Documents/25%204379%20Annual%20Energy%20Security%20Review%202024-25.PDF). Therefore, the average levels of storage are likely a conservative estimation.

					capacity (5300 GL) and 4.1 GW generation capacity[15]
		Bagong / McKay (MCKAY1)	300	h	Based on reports of the Kiewa Hydroelectric Scheme[16]: around 25-30 ML, with 80/320m head for McKay/Bogong, which accounts for approx. 87 GWh for 300 MW capacity
	reservoir_discharge_time_states	Victoria (Region 3)	200	h	Assume smaller reservoirs for the smaller hydro schemes
	reservoir_initial_soc_units	Murray (MURRAY1) Tumut (UPPTUMUT)	0.5		Approximation informed by Snowy Hydro reporting[17]
		Bagong / McKay (MCKAY1)	0.5		Approximation based on historical yearly levels[18]
	reservoir_initial_soc_states	Victoria (Region 3)	0.5		
Other regions	reservoir_discharge_time_other	-	200	h	Approximation based on VIC/TAS small hydro
	reservoir_initial_soc_other	-	0.5		
NEM	pumped_hydro_initial_soc	-	0.5		Assume similar storage behaviour to reservoir storage
	run_of_river_discharge_time	-	0	h	Amount of timesteps that the run-of-river can discharge at full capacity (e.g. 0 = no storage)
	run_of_river_discharge_efficiency	-	0.9	-	Assume 90% efficiency
	run_of_river_carryover_efficiency	-	1.0	-	Irrelevant when discharge time (reservoir size) is set to zero
	reservoir_discharge_efficiency	-	0.9	-	Assume 90% discharging efficiency
	reservoir_carryover_efficiency	-	1.0	-	Assume no losses in dams
	default_static_inflow	-	0.0	-	Hourly inflow if inflow trace is not found for hydro power station. Factor of grid injection power capacity.

To reflect the longer foresight that is typically employed when scheduling hydro power stations, we price any hydro discharge at the short-run marginal cost outlined in the AEMO ISP dataset (8.58 AUD/MWh) [83]. Furthermore, to avoid continuous discharge of reservoirs over the year, we add targets to the final state of charge of hydro reservoir stations to be equal greater than the initial state of charge within each optimisation run (for a discussion about this modelling implementation compared to other options we refer to [52]). We price any deviation from these targets just below the Value of Lost Load (VoLL), to allow usage of this water to prevent unserved energy, effectively keeping these reservoirs as last resort for long-duration VRE drought periods. Additionally, we price any water spillage within the model also just below the Value of Lost Load (VoLL) to avoid spillage of water from the inflows, while preserving feasibility of the optimisation model.

A.1.4 Transmission upgrades

To anticipate transmission buildouts within the base case scenario, we add several key anticipated and actionable transmission expansion projects to be online within the next years. An overview can be found in Table 0.3.

[15] See https://www.snowyhydro.com.au/generation/the-snowy-scheme/ and https://www.snowyhydro.com.au/generation/water/

[16] https://accounts.water.vic.gov.au/2022/local-water-reports/surface-water-by-river-basin/kiewa/

[17] See: https://www.snowyhydro.com.au/generation/water/

[18] https://accounts.water.vic.gov.au/2022/local-water-reports/surface-water-by-river-basin/kiewa/

Table 0.3: Transmission expansion projects considered in the base case.

Name	Dataset Name	Connecting Subregions	Increased Capacity Forward / Reverse [MW]	First Calendar Year in Service
HumeLink	NL_86_INV30	SNSW -> CNSW	2200 / 2200	2027
Sydney Ring North	NL_67_INV19	CNSW -> SNW	5000 / 0	2029
Gladstone Grid Reinforcement	NL_23_INV3	CQ -> GG	2600 / 500	2029
VNI	VNI North VNI South	SNSW -> CNSW VIC -> SNSW	2950 / 2590 1000 / 400	2030 2030
VNI West	NL_98_INV34	VIC -> SNSW	1935 / 1669	2030
New England REZ Transmission Link 1	NL_65_INV14	CNSW -> NNSW	3000 / 3000	2030
Marinus Link Stage 1	NL_109_INV35	TAS -> VIC	750 / 750	2031
Queensland SuperGrid South	NL_42_INV8	SQ -> CQ	3150 / 3150	2032
Marinus Link Stage 2	NL_109_INV36	TAS -> VIC	750 / 750	2033
QNI Connect	NL_54_INV0	NNSW -> SQ	1260 / 1700	2034
New England REZ Transmission Link 2	NL_65_INV15	CNSW -> NNSW	3000 / 3000	2034

A.2 SchedNEM.jl modelling details

SchedNEM.jl is an **economic dispatch unit commitment (ED-UC)** optimisation package for in *julia* [24], using JuMP [26] and the *ParametricOptInterface* [166]. It includes a rolling horizon setup and a transport network power flow formulation. The data structure is built upon the system model formulation in PRAS [23], with additional parameters imported from data files generated by *ParseISP.jl*. In the following, the detailed underlying model formulation is outlined. The source-code of the package is freely available at https://github.com/ARPST-UniMelb/SchedNEM.jl.

A.2.1 Parameters and variables

The parameters of the formulation can be seen in Figure 0.1. The decision variables and indices and sets are detailed in Figure 0.2.

1. General parameters
   - $D_{b,t}$ - Demand, bus b, time t [MW]
   - $\bar{P}_{g,t}$ - Max. power output, generator g, time t [MW]
   - $\underline{\mathrm{P}}_{g,t}$ - Min. power output, generator g, time t [MW]
   - $\bar{F}_i, \underline{\mathrm{F}}_i$ - Max. forward/reverse flow, interface i [MW]
2. Storage parameters
   - $\bar{P}_s^{\mathrm{Sch}}$, $\bar{P}_s^{\mathrm{Sdch}}$ - Max. charging/discharging power, storage s [MW]
   - $\bar{E}_s$ - Max. energy, storage s [MWh]
   - $e_{s,0}$ - Initial state of charge, storage s [MWh]
   - η_s^{Scarry} - Carryover efficiency, storage s [%]
   - $\eta_s^{Sdch/Sch}$ - Dis/charging efficiency, storage s [%]
3. Generator-Storage parameters
   - $\bar{P}_{gs}^{\mathrm{Sch}}$, $\bar{P}_{gs}^{\mathrm{Sdch}}$ - Max. charging/discharging power, generator-storage gs [MW]
   - $\bar{E}_{gs}$ - Max. energy, generator-storage gs [MWh]
   - $p_{gs,t}^{inflow}$ - External inflows, generator-storage gs [MW]
   - $e_{gs,0}$ - Initial state of charge, generator-storage gs [MWh]
   - $\eta_{gs}^{GScarry}$ - Carryover efficiency, generator-storage gs [%]
   - $\eta_{gs}^{GSdch/GSch}$ - Dis/charging efficiency, generator-storage gs [%]
4. Demand Response parameters
   - $\bar{P}_{dr}^{\mathrm{DRbrw}}$, $\bar{P}_{dr}^{\mathrm{DRpyb}}$ - Max. borrow/payback power, demand-response dr [MW]
   - $\bar{E}_{dr}$ - Max. energy, demand response dr [MWh]
   - $\bar{E}_{dr,T}^{\mathrm{maxBrwHrs}}$ - Max. energy borrowing activation within time-window T, demand response dr [h]
   - r_{dr} - energy interest, demand response dr [unitless]
5. UC and ramping parameters
   - $p_{g,0}$ - initial power output of generator g [MW]
   - $\mathrm{R}_g^{\mathrm{up/down}}$ - up/downward ramp limit, generator g
   - $\delta_{g,0}^{\mathrm{on}}$ - initial commitment status, generator g [binary]
   - $\delta_{g,\tau}^{\mathrm{stup}}$, $\delta_{g,\tau}^{\mathrm{shdw}}$ - startup/shutdown indicators at preceding time steps before simulation time $\tau < t$, generator g [binary]
   - $\mathrm{T}_g^{\mathrm{up/dn}}$ - Min. up/down times, generator g [h]
   - $\delta_{g,t}^{\mathrm{fail}}$ - failure indicator for generator g, time t [binary]
   - $\delta_{g,\tau}^{\mathrm{fail}}$ - failure indicators at preceding time steps before simulation time $\tau < t$
6. Cost parameters
   - c_g^{SRMC} - Short run marginal cost, generator g [$/MW]
   - c_g^{stup} / c_g^{shdw} - Startup/shutdown cost, generator g [$]
   - c^{Spen} - Penaliser, storage discharging [$/MW]
   - c^{GSpen} - Penaliser, generator-storage discharging [$/MW]
   - $c^{GSspill}$ - Spillage penalty for generator storage units [$/MW]
   - $c^{GSslack}$ - SoC target violation penalty for generator storage units [$/MWh]
   - c_{dr}^{DRact} - Activation cost, demand response dr [$/MW]
   - c^{Fpen} - Flow penalty across interfaces [$/MW]
   - VoLL_t - Value of Lost Load, time t [$/MW]

Figure 0.1: Parameters of SchedNEM.jl

Decision variables

- Power generation and flows
  - $p_{g,t}$ - Power output, generator g, time t [MW]
  - $p^{\mathrm{Sdch}}_{s,t}$, $p^{\mathrm{Sch}}_{s,t}$ - Dis/charging power, storage s, time t [MW]
  - $e^{\mathrm{S}}_{s,t}$ - state of charge, storage s, time t [MWh]
  - $p^{\mathrm{GSdch}}_{gs,t}$, $p^{\mathrm{GSch}}_{gs,t}$ - Dis/charging power, generator-storage gs, time t [MW]
  - $e^{\mathrm{GS}}_{s,t}$ - state of charge, generator-storage gs, time t [MWh]
  - $s_{gs,t}$ - spillage, generator-storage gs, time t [MW]
  - e^{slack}_{gs} - slack variable for final SOC constraint, generator-storage gs, time t [MW]
  - $p^{\mathrm{DRbrw}}_{dr,t}$, $p^{\mathrm{DRpyb}}_{dr,t}$ - demand response borrow/payback power, demand-response dr, time t [MW]
  - $e^{\mathrm{DR}}_{s,t}$ - state of charge, demand-response dr, time t [MWh]
  - $f_{i,t}$ - Power flow, interface i, time t [MW]
  - $LS_{b,t}$ - Load shedding, bus b, time t [MW]
- And further optional UC variables:
  - $\delta^{\mathrm{on}}_{g,t}$ - on/off variable for each generator g, time t [binary/unitless]
  - $\delta^{\mathrm{stup}}_{g,t}$, $\delta^{\mathrm{shdw}}_{g,t}$ - startup/shutdown indicator, generator g, time t [binary/unitless]
  - $\delta^{\mathrm{fail}}_{g,t}$ - failure indicator, generator g, time t [binary/unitless]

Indices and sets

- $b \in B$ - buses in the system
- $g \in G$ - generators in the system
- $s \in S$ - storage units in the system
- $gs \in GS$ - generator-storage units in the system
- $dr \in DR$ - demand-response units in the system
- $i \in I_b^{from}$, I_b^{to} - Interfaces from, to bus b
- $t \in T$ - Total amount of hours

Figure 0.2: Decision variables, as well as indices and sets of SchedNEM.jl

A.2.2 Objective function

We define the following costs, which include operational costs and penalties to represent more realistic behaviour.

Cost functions

Generators	$C_{\mathrm{gen,op}} = \sum_{t\in T}\left(\sum_{g\in G} c^{\mathrm{SRMC}}_g\, p_{g,t} + \sum_{g\in G} c^{\mathrm{stup}}_g\, \delta^{\mathrm{stup}}_{g,t} + \sum_{g\in G} c^{\mathrm{shdw}}_g\, \delta^{\mathrm{shdw}}_{g,t}\right)$
Demand	$C_{\mathrm{dem}} = \sum_{t\in T}\left(\sum_{dr\in DR} c^{\mathrm{DRact}}_{dr}\, p^{\mathrm{DRbrw}}_{dr,t} + \sum_{b\in B} \mathrm{VoLL}_t\, LS_{b,t}\right)$

Penalty functions

(Gen-)Storage	$C^{\mathrm{pen}}_{\mathrm{stor,op}} = \sum_{t\in T}\left(c^{Spen}\sum_{s\in S} p^{\mathrm{Sdch}}_{s,t} + c^{GSpen}\sum_{gs\in GS} p^{\mathrm{GSdch}}_{gs,t}\right)$
Flow	$C^{\mathrm{pen}}_{\mathrm{flow}} = c^{\mathrm{Fpen}}\sum_{t\in T}\left(\sum_{l\in I} f_{i,t}\right)$
Spill	$C^{\mathrm{pen}}_{\mathrm{spill}} = \sum_{t\in T}\left(c^{GSspill}\sum_{gs\in GS} s_{gs,t}\right)$
SoC Target Slack	$C^{\mathrm{pen}}_{\mathrm{slack}} = c^{GSslack}\sum_{gs\in GS} e^{\mathrm{slack}}_{gs}$

Figure 0.3: Cost and penalty functions included in the objective function.

Which are combined to the overall objective function:

$$\min \quad \left(C_{\mathrm{gen,op}} + C_{\mathrm{dem}} + C^{\mathrm{pen}}_{\mathrm{stor,op}} + C^{\mathrm{pen}}_{\mathrm{flow}} + C^{\mathrm{pen}}_{\mathrm{spill}} + C^{\mathrm{pen}}_{\mathrm{slack}}\right)$$

Figure 0.4: Objective function.

With the default parameters of:

Table 0.4: Default values and description of parameters used in the objective function.

Parameter	Sub-parameter	Default value	Comment
Value of Lost Load (VoLL)		20'300 AUD/MWh	As of 2025-26, determined by AEMC [167]. Discounted linearly across the optimisation horizon to 99% of its value to uniquely define storage operation in case of load shedding events (i.e. shift load shedding to the end of the optimisation if possible).
Storage discharging cost	BESS (c^{Spen})	0.1 AUD/MWh	Small penalty to avoid storage operation degeneracies in the presence of VRE curtailment.
	Hydro power (c^{GSpen})	8.58 AUD/MWh	See explanation in A.1.3 above.
Hydro operation penalty	Spillage penalty ($c^{GSspill}$)	80% of VoLL	See explanation in A.1.3 above. Incentivises hydro reservoirs to keep maintain its state of charge over the whole horizon if not needed for reliability response. However, stored hydro energy would be used to recharge BESS or other PHES before unserved energy events.
	SoC target slack penalty ($c^{GSslack}$)	80% of VoLL	
Cost of DSP reliability response band (c_{dr}^{DRact})		95% of VoLL	Only use DSP reliability response in case no other generation is used but make it possible to share DSP across subregions.
Transmission flow penalty (c^{Fpen})		0.1 AUD/MWh	Small penalty to contain unserved energy within primary subregion. Furthermore, this helps preventing unrealistic storage operation across subregions for minimal cost benefits.

A.2.3 Constraints

Power balance

The nodal power balance for each bus b and time t:

$$\begin{aligned}\sum_{g\in\mathcal{G}_b} p_{g,t} - \sum_{l\in I_b^{from}} f_{i,t} + \sum_{l\in I_b^{to}} f_{i,t} \\ + \sum_{s\in\mathcal{S}_b} p_{s,t}^{\mathrm{Sdch}} + \sum_{gs\in\mathcal{GS}_b} p_{gs,t}^{\mathrm{GSdch}} + \sum_{dr\in\mathcal{DR}_b} p_{dr,t}^{\mathrm{DRbrw}} \\ - \sum_{s\in\mathcal{S}_b} p_{s,t}^{\mathrm{Sch}} - \sum_{gs\in\mathcal{GS}_b} p_{gs,t}^{\mathrm{GSch}} - \sum_{dr\in\mathcal{DR}_b} p_{dr,t}^{\mathrm{DRpyb}} \\ = D_{b,t} - LS_{b,t}\end{aligned}$$

Figure 0.5: Nodal power balance constraint.

Technical limits

The technical limits of generators, storage units, generator-storage units, demand response units and lines:

$$
\begin{array}{ll}
\text{Generators} & \\
\underline{\mathrm{P}}_{g,t} * \delta^{\mathrm{on}}_{g,t} \leq p_{g,t} \leq \bar{P}_{g,t} * \delta^{\mathrm{on}}_{g,t} & \forall g \in G,\, t \in T \\
\text{Storage Units} & \\
0 \leq p^{\mathrm{Sch}}_{s,t} \leq \bar{P}_s & \forall s \in S,\, t \in T \\
0 \leq p^{\mathrm{Sdch}}_{s,t} \leq \bar{P}_s & \forall s \in S,\, t \in T \\
0 \leq e^{\mathrm{S}}_{s,t} \leq \bar{E}_s & \forall s \in S,\, t \in T \\
\text{Generator Storage Units} & \\
0 \leq p^{\mathrm{GSch}}_{gs,t} \leq \bar{P}_{gs} & \forall gs \in GS,\, t \in T \\
0 \leq p^{\mathrm{GSdch}}_{gs,t} \leq \bar{P}_{gs} & \forall gs \in GS,\, t \in T \\
0 \leq e^{\mathrm{GS}}_{gs,t} \leq \bar{E}_{gs} & \forall gs \in GS,\, t \in T \\
\text{Demand Response Units} & \\
0 \leq p^{\mathrm{DRbrw}}_{dr,t} \leq \bar{P}^{\mathrm{DRbrw}}_{dr} & \forall dr \in DR,\, t \in T \\
0 \leq p^{\mathrm{DRpyb}}_{dr,t} \leq \bar{P}^{\mathrm{DRpyb}}_{dr} & \forall dr \in DR,\, t \in T \\
e^{\mathrm{DR}}_{dr,t} \leq \bar{E}_{dr} & \forall gs \in GS,\, t \in T \\
\text{Lines} & \\
\underline{\mathrm{F}}_i \leq f_{i,t} \leq \bar{F}_i & \forall i \in I,\, t \in T
\end{array}
$$

Figure 0.6: Technical limits of generators, storage units, generator storage units, demand response units and lines.

Storage constraints

We add storage time coupling constraints:

$$
\begin{array}{lll}
e_{s,1} = \eta_s^{Scarry} e_{s,0} + \eta_s^{Sdch}\, p_{s,1}^{Sch} - \frac{p_{s,1}^{Sdch}}{\eta_s^{Sdch}} & & \forall s \in S \\
e_{s,t} = \eta_s^{Scarry} e_{s,t-1} + \eta_s^{Sch}\, p_{s,t}^{Sch} - \frac{p_{s,t}^{Sdch}}{\eta_s^{Sdch}} & \text{for } t = 2, \ldots, N & \forall s \in S
\end{array}
$$

Figure 0.7: Storage time-coupling constraints.

And for generator-storage units:

$$
\begin{array}{lll}
e_{gs,1} + s_{gs,1} = \eta_g s^{GScarry} e_{gs,0} + \eta_g s^{Sdch}\, p_{gs,1}^{Sch} - \frac{p_{gs,1}^{GSdch}}{\eta_{gs}^{GSdch}} + p_{gs,1}^{inflow} & & \forall gs \in GS \\
e_{gs,t} + s_{gs,t} = \eta_g s^{GScarry} e_{gs,t-1} + \eta_{gs}^{GSch}\, p_{gs,t}^{GSch} - \frac{p_{gs,t}^{GSdch}}{\eta_{gs}^{Sdch}} + p_{gs,t}^{inflow} & \text{for } t = 2, \ldots, N & \forall gs \in GS
\end{array}
$$

Figure 0.8: Generator-storage time-coupling constraints.

Additionally, we add the SoC constraints for generator-storage units when activated:

$$
e_{gs,N} \geq e_{gs,0} - e_{gs}^{\mathrm{slack}} + p_{gs,1}^{inflow} - p_{gs,2}^{inflow} \quad \forall gs \in GS
$$

Figure 0.9: SoC constraints for generator-storage units.

Demand response

The inflows in timesteps 1 and 2 are explicitly included to capture the step when all the SoC is coming from inflows in the first timestep to set a more realistic initial SoC – this is a workaround since PRAS does not support initial SoC yet.

For all demand response that is not allowed to “pre-charge”, we enforce limits on the energy SoC:

$$
0.0 \leq e_{dr,t}^{\mathrm{DR}} \quad \forall dr \in DR_{\mathrm{no\,pre-charge}}, t \in T
$$

Figure 0.10: Limits on the energy SoC of demand response units that are not allowed to "pre-charge".

And then ensure that energy conservation across timesteps (adjusted with the interest rate r_{dr}):

$$
\begin{array}{lr}
e_{dr,1} = (1+r_{dr})p_{dr,1}^{DRbrw} - p_{dr,1}^{DRpyb} & \forall dr \in DR \\
e_{dr,t} = e_{dr,t-1} + (1+r_{dr})p_{dr,t}^{DRbrw} - p_{dr,t}^{DRpyb} \quad \text{for } t = 2,\ldots,N & \forall dr \in DR
\end{array}
$$

Figure 0.11: Energy conservation across timesteps.

Additionally, we enforce maximum energy activation limits within each time-window T, as well as for the window including any previous borrowed energy:

$$
\begin{array}{lr}
\sum_{t\in t:t+T} p_{dr,t}^{DRbrw} \leq \bar{E}_{dr}^{\text{maxBrwHrs}}\, \bar{P}_{dr}^{\text{DRbrw}} & \forall dr \in DR \\
\sum_{t\in 1:T^{brwBefore}} p_{dr,t}^{DRbrw} + e_{dr}^{brwBefore} \leq \bar{E}_{dr}^{\text{maxBrwHrs}}\, \bar{P}_{dr}^{\text{DRbrw}} & \forall dr \in DR
\end{array}
$$

Figure 0.12: Maximum energy activation limits.

And enforce payback within the time horizon T if needed (not applied in this work):

$$
\sum_{t\in t:t+T} p_{dr,t}^{DRpyb} \geq (1+r_{dr}) \sum_{t\in t:t+T} p_{dr,t}^{DRbrw} \quad \forall dr \in DR
$$

Figure 0.13: Payback enforcement.

Generator constraints

We add the following ramping constraints:

$$
\begin{array}{lr}
p_{g,1} - p_{g,0} \leq \mathrm{R}_g^{\text{up}} + \underline{\mathrm{P}}_{g,1}\delta_{g,1}^{\text{stup}} & \forall g \in G \\
p_{g,t} - p_{g,t-1} \leq \mathrm{R}_g^{\text{up}} + \underline{\mathrm{P}}_{g,t}\delta_{g,t}^{\text{stup}} \quad \text{for } t = 2,\ldots,N & \forall g \in G \\
p_{g,0} - p_{g,1} \leq \mathrm{R}_g^{\text{dn}} + \underline{\mathrm{P}}_{g,1}\delta_{g,1}^{\text{shdn}} & \forall g \in G \\
p_{g,0} - p_{g,1} \leq \mathrm{R}_g^{\text{dn}} + \underline{\mathrm{P}}_{g,t}\delta_{g,t}^{\text{shdn}} \quad \text{for } t = 2,\ldots,N & \forall g \in G
\end{array}
$$

Figure 0.14: Generator ramping constraints.

And unit commitment constraints for all generators that have $\mathrm{T}_g^{\mathrm{up/dn}} > 0$ or $\underline{\mathrm{P}}_{g,t}$:

$$
\begin{array}{lr}
\delta_{g,t}^{\text{stup}} - \delta_{g,t}^{\text{shdw}} = \delta_{g,t}^{\text{on}} - \delta_{g,t-1}^{\text{on}} & \forall g \in G_{\text{UC}} \\
\delta_{g,t}^{\text{stup}} - \delta_{g,t}^{\text{shdw}} = \delta_{g,t}^{\text{on}} - \delta_{g,t-1}^{\text{on}} \quad \text{for } t = 2,\ldots,N & \forall g \in G_{\text{UC}} \\
\delta_{g,t}^{\text{stup}} + \delta_{g,t}^{\text{shdw}} \leq 1 & \forall t \in T, \forall g \in G_{\text{UC}},
\end{array}
$$

Figure 0.15: Unit commitment constraints.

And add minimum up/down time constraints:

$$
\begin{array}{lr}
\delta_{g,t} \geq \sum_{\tau=t-\mathrm{T}_g^{\text{up}}} \delta_{g,t}^{\text{stup}} & \forall t \in T, \forall g \in G_{\text{UC}} \\
\delta_{g,t} \leq 1 - \sum_{\tau=t-\mathrm{T}_g^{\text{dn}}} \delta_{g,t}^{\text{shdw}} & \forall t \in T, \forall g \in G_{\text{UC}}
\end{array}
$$

Figure 0.16: Minimum up/down time constraints.

If the generators are not affected by UC constraints, we assume the generator as available $\delta_{g,t}^{\text{on}} = 1\ \forall t \in T, \forall g \in G_{\text{no UC}}$.

With this we follow the formulation in [27]. For an exact solution, we may set all δ-parameters to binary, however for increased computational speed, we relax the parameters to be within [0, 1] and round the resulting on/off status. This allows to represent the capacity constraints that the system may face in greater detail than with economic dispatch alone.

A.3 Initial calibration results

To calibrate the underlying operational model that informs the resource adequacy assessments, we perform simulations based on the first planning year of the ISP data (2025) and the optimal development path trace (ODP 4006) for VRE and demand traces (with Probability of Exceedance (POE) of 10%, i.e. high demand). The calibration is structured to present the three main stages of the methodology, namely the (1) system scheduling, followed by the (2) outage sampling and simulation, and the (3) system response evaluation (see Figure 4.3). In the following the results of the three parts are discussed.

It should be stressed here that the aim is not to exactly replicate observed system dispatch, but to *establish a reasonable approximate system behaviour* that may provide a baseline for evaluating changes in resource mix, operational assumptions, and critical system conditions. While any reasonable effort has been made to ensure accuracy of the results, the conclusions of this report should be considered in light of the changes and trends observed rather than exact values.

A.3.1 System scheduling

The goal of the system scheduling stage is to determine an approximate system dispatch under expected conditions. This schedule is aimed at reflecting storage and DER operation, as well as unit commitment (UC) and ramping constraints through a least-cost market dispatch. This is implemented through a rolling horizon with 48h foresight and 24h steps, which is roughly aligned with the pre-dispatch horizon of 16h - 40h [168]. While an implementation of the UC model with binary variables is possible to capture the scheduling of units, we use a linearised implementation based on Zhang et al. [27] to increase speed while preserving reasonable accuracy.

Running the scheduling for the whole NEM for the target year 2025, we observe an energy production as presented in Figure 0.17. While Queensland, New South Wales, and Victoria are dominated by coal generation, South Australia is powered by renewable energy, and Tasmania by hydroelectric power generation.

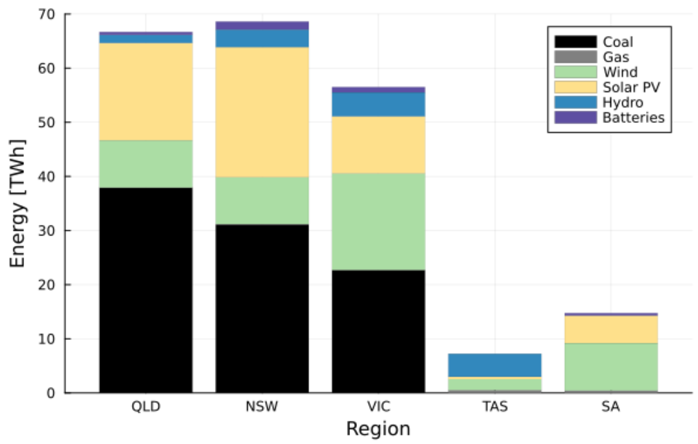

Figure 0.17: Energy production per state across the planning year 2025, based on the reference weather trace of the optimal development path (ODP), and the demand trace of POE 10%.

Furthermore, comparing regional imbalances, we observe the import and export flows in Figure 0.18. While Victoria and Queensland are net exporting regions, New South Wales, Tasmania, and South Australia are mainly importing energy across the year. This roughly aligns with expectations of the general resource mix, and observed in recent years [169].

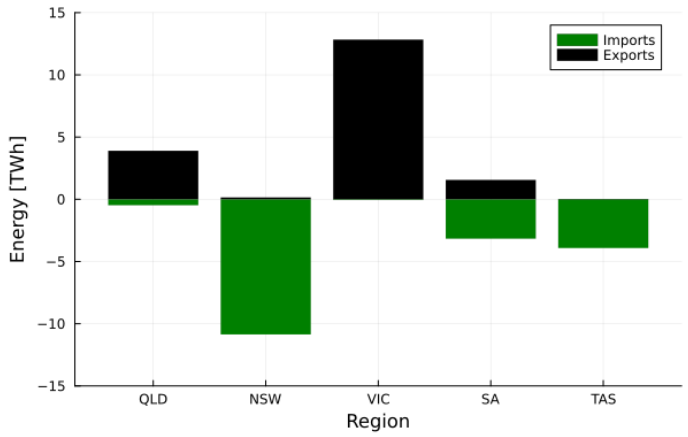

Figure 0.18: Import and export flows between regions in the NEM across the planning year 2025 and the underlying weather reference trace of the 2024 ISP optimal development path, obtained from the pre-dispatch with SchedNEM.jl.

To investigate and validate the unit commitment (UC) implementation, we run the scheduling for an artificial stress day with high demand ramp, reduced overall demand, and without wind generators. This leads to a scenario in which a larger number of commitment constraint generators is needed to meet the evening net-peak but would not be required in the low net demand periods during the day. The optimised schedules are presented in Figure , and the difference in UC and ramping behaviour of the coal units can be observed: In the schedule with ramping, a higher number of units is committed even during high PV availability, and less coal generation is scheduled in the evening, replaced by higher storage discharges. The commitment status of the individual units with commitment constraints during the same days is presented in Figure 0.19. Note that we assume generators as on at the start of the full simulation, therefore some units are turning off immediately in the first timesteps, however the unit commitment status is carried over within the rolling horizon framework, therefore following commitment decisions across the optimisation steps.

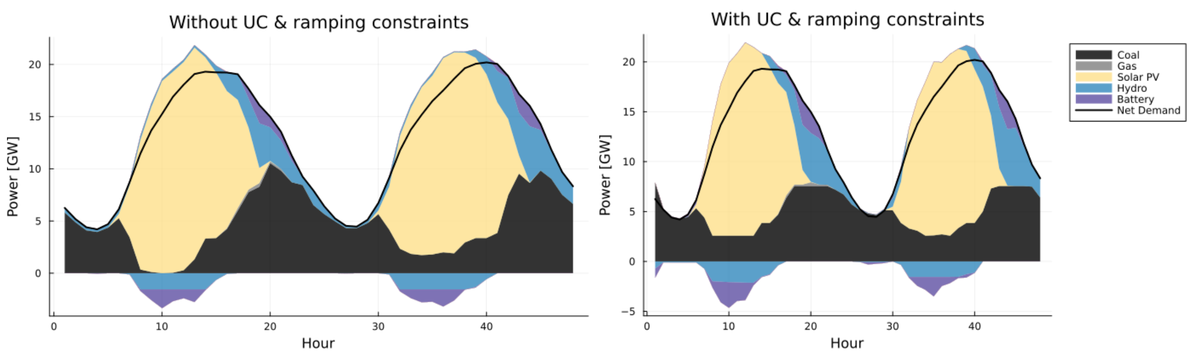

Figure 0.19: System schedule for a scenario with high demand ramp, reduced overall demand, and without wind generation to stress-test the unit commitment and ramping constraints.

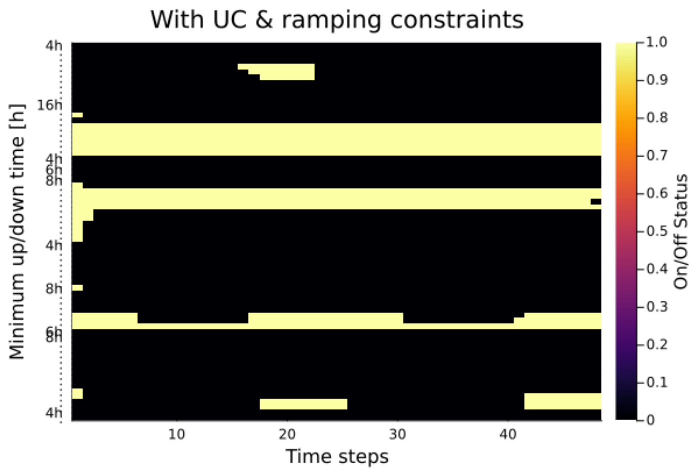

Figure 0.20: Commitment status of generators with up/down time constraints activated (see full list in appendix).

A.3.2 Sampling and recording of critical events

The aim of the second stage is to sample generator and line outages probabilistically and identify critical periods and configurations that may lead to unserved energy, given the schedule determined in stage one. This is done by using the PRAS internal sampling and simulation engine and the forced outage rate (FOR) and mean time to repair (MTTR) from the AEMO ISP datasets, see Table 0.5Table 0.5. The correlation of the sampled FOR compared with the input can be found in Figure 0.21.

Table 0.5: Generation and transmission outage parameters as inputs to the outage sampling, ordered by FOR.

Technology	Type / Name	Forced Outage Rate [%]	Mean Time To Repair [h]
Generation	VRE (PV and Wind)	0.0% *	N/A
Transmission	*All other lines*	0.0% **	N/A
Transmission	Murraylink (HVDC)	0.07%	12.40
Transmission	Heywood (HVAC)	0.09%	7.80
Transmission	QNI (HVAC)	0.19%	14.50
Generation	BESS	1.84% ***	N/A
Generation	Hydrogen-based	2.0%	22.00
Generation	CCGT + Steam Turbine	5.04%	61.19
Generation	Hydro	5.11% ***	N/A
Transmission	Basslink (HVDC)	5.39%	213.90
Generation	Black Coal NSW	6.31%	157.62
Generation	Black Coal QLD	6.75%	185.00
Generation	OCGT	7.21%	111.73
Generation	Brown Coal	7.75%	90.05
Generation	Small peaking plants	9.58%	150.20

*Outages of VRE are included within the traces provided by AEMO.

** Outages of transmission lines not explicitly mentioned are considered not material for interregional flows by AEMO and no data is provided in the ISP.

*** The FORs of BESS and hydro units are applied as capacity derating, due to the scheduling in stage one before the outage sampling.

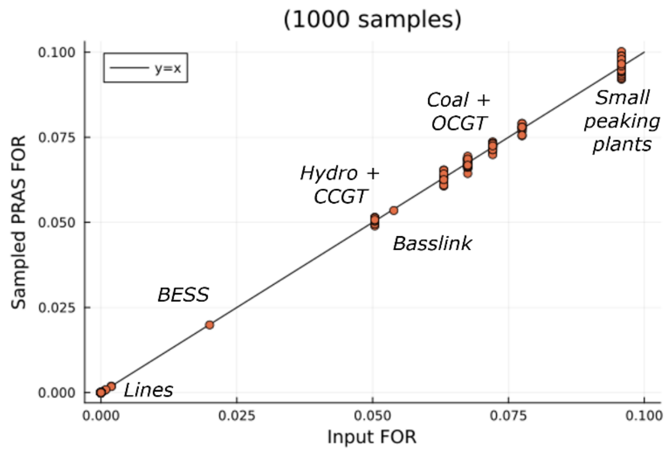

Figure 0.21: Validation of sampled forced outage rate (FOR) from PRAS results compared to the input parameters. Values close to the line correspond to high alignment of the input values with the sampling results.

Furthermore, since the key goal of the second stage is to record critical hours across the samples, we test the recording for a two-day horizon and one sample with reduced generation capacity (exclude any VRE generation). The result can be observed in Figure , which highlights that stage two successfully records the hours and magnitude of shortfalls of the committed and available generation against the net demand. These times are the critical periods in which the schedule of generation, storage and DER in combination with the sampled outages would result in unserved energy. These results are then passed on to stage three, which evaluates the actual system response (including storage redispatch, generator ramping, and demand response).

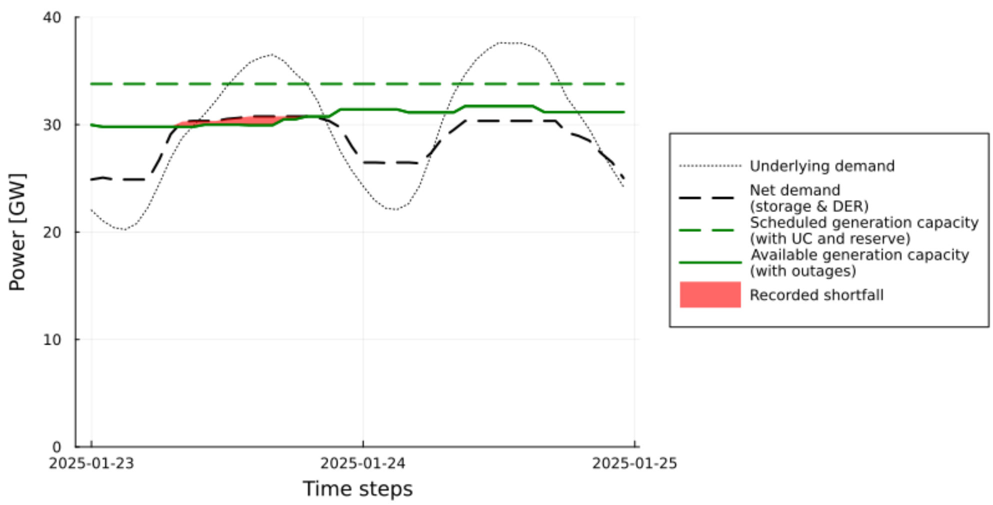

Figure 0.22: Example of a shortfall recording of PRAS, for a scenario without VRE capacity.

A.3.3 Response simulation

The third step of the methodology is included to simulate the response of the system to outages of infrastructure that would result in unserved energy with the original schedule. This builds upon the results from stage one and two to identify critical periods. In the following, we show an example of the workflow, considering a critical period and outage combination that leads to unserved energy in New South Wales (NSW). Figure 0.23 shows the system pre-dispatch of units and demand connected to the four sub nodes in NSW for two critical days in 2025. No unserved energy is recorded in this first stage as all units are assumed operational.

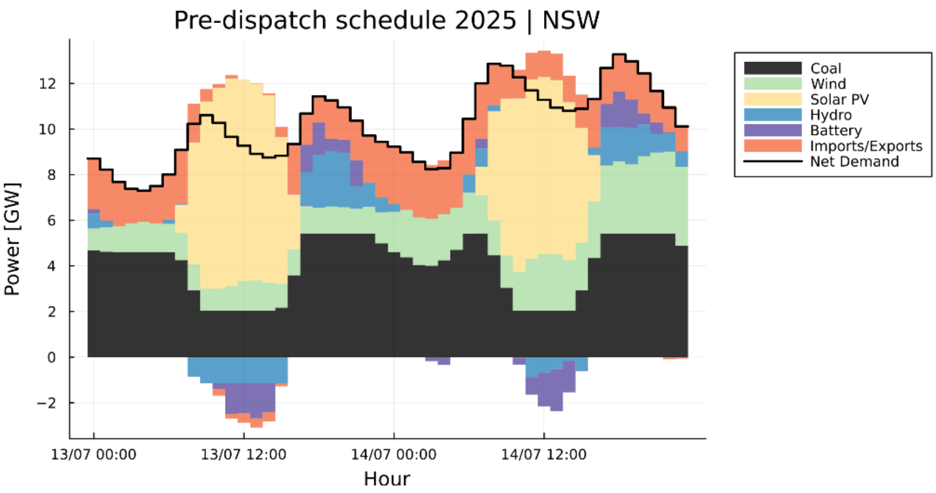

Figure 0.23: Pre-dispatch schedule for the NSW sub-nodes determined by SchedNEM.jl in the first stage.

After running the outage sampling with PRASNEM, a specific sample resulted in the unavailable scheduled capacity as shown in Figure 0.24. Therefore, the system schedule including flexible and committed units cannot maintain reliability anymore (given that storage units and commitment is fixed to the pre-dispatch schedule). The resulting dispatch is shown in Figure 0.25.

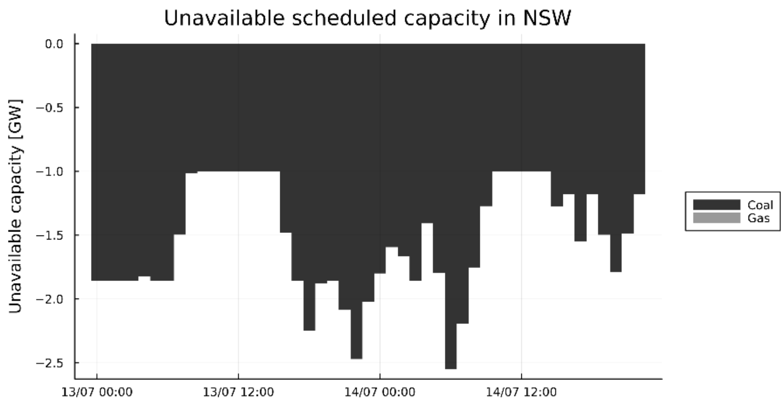

Figure 0.24: Scheduled capacity unavailable in the NSW sub-nodes, resulting change in missing capacity.

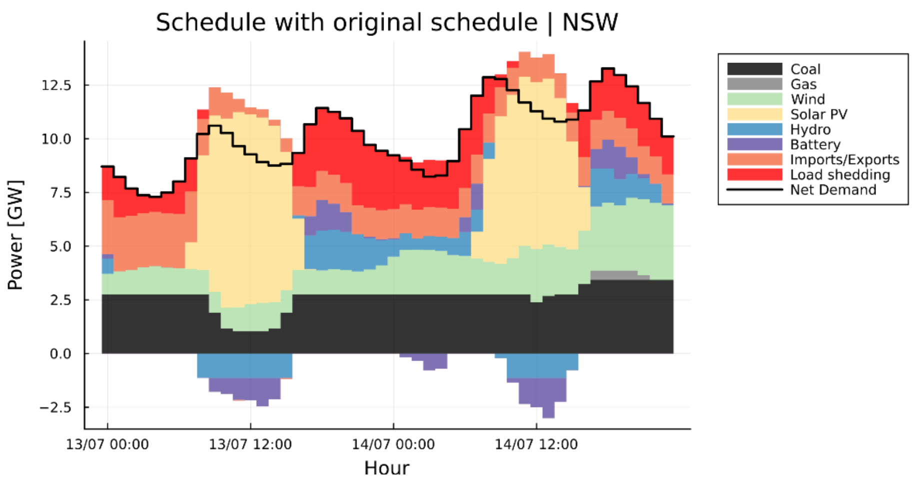

Figure 0.25: System operation under original schedule, including reserve dispatch of all committed units.

However, to assess the adequacy risk correctly, system response needs to be considered. The resulting schedule can be seen in Figure 0.26. We note an increase in gas generation, as well as slight increase in storage dispatch to relieve the forced outages of the coal generators, however a small amount of unserved energy is remaining in the evening hours of the first day. Note that this situation is observed with the resource mix of 2025, particularly in the planning years 2035 and 2040, the redispatch is dominated by storage operation.

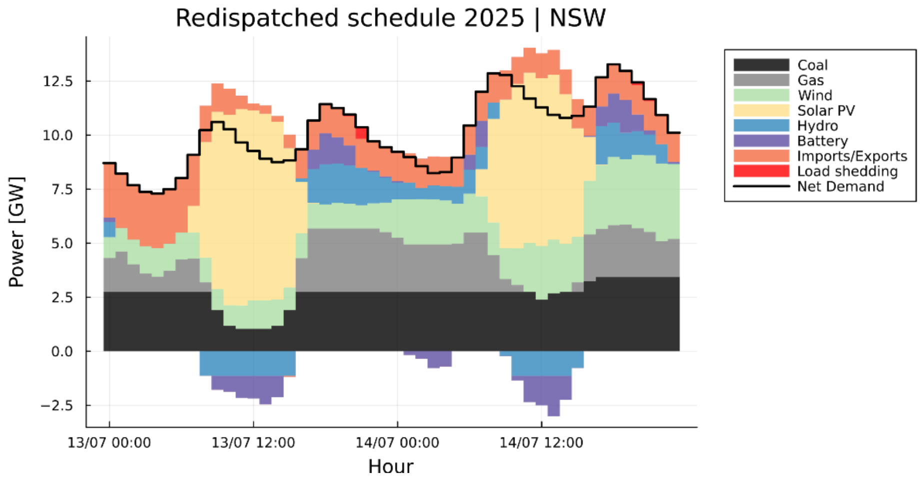

Figure 0.26: System schedule after redispatch, allowing storage units and commitment constraint units to respond to the unavailable capacity.

A.3.4 Key scheduling differences in between PRAS and SchedNEM

While *SchedNEM.jl* and *PRAS* both have internal dispatch engines, there are multiple differences that may lead to different schedule outcomes and in turn influence reliability results, especially in the case of small sample numbers. As *PRAS* is optimised for computational efficiency, dispatch follows heuristics without intertemporal constraints. *SchedNEM.jl* captures storage arbitrage and unit commitment across the whole optimisation horizon, however, at the expense of longer run-times. An overview of key differences can be found in Table 0.6.

Table 0.6: Key differences in operational detail in the scheduling of SchedNEM.jl and PRAS.

	SchedNEM.jl	**PRAS**
Storage and hydro discharge	Optimised to minimise cost. Energy limits for hydro discharge apply (see appendix)	Discharge after all generator dispatch, prioritise by descending discharge duration length (time-to-go [55]), i.e. unit with longest time-to-go discharged first. However, in the presence of multiple units with the same sizes and energy levels, the dispatch may be suboptimal due to integer rounding. Discharging storages for shortfalls multiple nodes away may be limited if using default PRAS (adjusted in PRAS fork in *ARPST-UniMelb GitHub repository*).

Storage and hydro charge	Optimised to minimise cost	Charged as soon as possible without causing load shedding. Prioritised by ascending time-to-go [55]. Charging from generation multiple nodes away may be limited if using default PRAS.
Unit commitment	Considered with linear relaxation	Not considered
Demand response activation	Optimised with cost bands for the whole horizon (i.e. may displace storage to avoid load shedding later)	After all storage and hydro is dispatched (non-anticipatory)
Demand response reliability band maximum energy activation limit	Enforced as constraint to limit total borrowed energy within window	Enforced via maximum payback time for demand response within window

These differences in dispatch again highlight the uncertainty related to operation of a system with energy-limited resources. As described in chapter 2, while a traditional adequacy assessment in a thermal generation dominated system was based on capacity margins, simplifying system operation, the introduction of storage and demand side resources requires a detailed handling and understanding of system operational approximations.

A.4 Impact of unit commitment formulation on adequacy results

Results from scenarios *A1: High energy* and *A2: Derated energy* are based on the PRAS dispatch engine, whilst results from *A3: Economic operation* are from the framework developed for this work. Whilst the dispatch algorithms differ in storage operation, other differences are assessed to isolate the key drivers of adequacy outcomes.

One key parameter distinguishing the two approaches is that PRAS omits unit commitment (UC) constraints, whilst the developed framework (SchedNEM.jl) includes a full linearised UC and ramping formulation. However, as shown in Figure , removing the unit commitment constraints from SchedNEM does not materially change the results, indicating that storage operation is the key risk driver resulting in the difference in adequacy risk between the two frameworks.

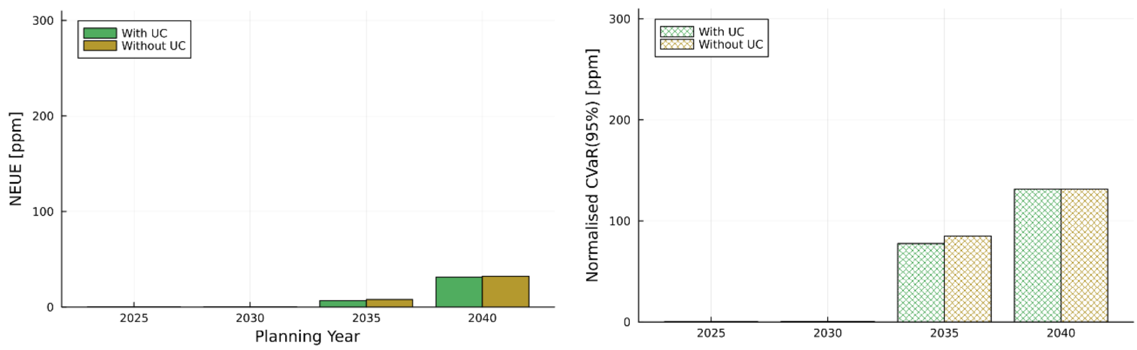

Figure 0.27: NEM-wide average risk (left) and tail risk (right) from purely supply-side resources (no DER), considering 500 outage samples and two reference weather years with high and low average VRE availability. Both formulations are based on the operation framework "A3: Economic operation". Note that 100 ppm = 0.01%.

In fact, removing unit commitment and ramping constraints may even increase unserved energy risk marginally. This is because unit commitment constraints may generally increase energy production by thermal, non-energy-limited generators during critical periods, which may lead to higher state of charge of storage units and therefore greater availability for discharge when needed. The absence of these constraints therefore removes a mechanism that may support adequacy during critical events.

A.5 Extreme Heatwave Assumptions and Parameters

This appendix provides further details on the assumptions and parameters used in the parametrisation of extreme heatwaves. These assumptions and parameters are not intended to replicate exactly actual system behaviour during extreme heatwave events, but rather to provide insight into how extreme events can be incorporated into system planning. Furthermore, some parameters are inherently proprietary. While reasonable efforts have been made to ensure the accuracy of the modelling, the conclusions of this report should be interpreted with reference to the observed changes and trends rather than the exact values.

9.5.1 Climate and weather data sources

The characteristics of the data from ERA5 and CMIP6 are summarised in Table 0.7.

Table 0.7: Weather and climate data sources.

Name	*Source*	*Type*	*Variable*	*Short Description*	*Spatial Resolution*	*Temporal Resolution*
ERA5	CDS	Historical	2m_temperature	Near-surface air temperature	0.25° lat/lon	Hourly
			ssrd	Surface solar radiation downwards		
			10m_u_component_of_wind, 10m_v_component_of_wind	Horizontal wind components at 10 metres above the surface, eastward and northward components		
CMIP ACCESS-CM2	NASA	Forecast SSP2-4.5	tasmin, tasmax	Daily minimum and maximum near-surface air temperature	0.25° lat/lon	Daily

The ERA5 data is obtained from the Copernicus Climate Data Store (CDS). It is a historical dataset with a spatial resolution of 0.25° latitude/longitude, equivalent to approximately 25 km. The temporal resolution is hourly, consistent with the requirements of subsequent operation and resource adequacy modelling. ERA5 is a historical reanalysis product that is physically consistent as a reconstruction of past atmospheric conditions constrained by real-world observations.

The CMIP6 ACCESS-CM2 data are obtained from NASA. Unlike ERA5, it is a forecast trace under a moderate global warming trajectory (SSP2-4.5), where the Earth warms by roughly 2–3.5 °C by 2100. The data are downscaled from ACCESS-CM2 output to a finer spatial resolution of 0.25° latitude/longitude, equivalent to approximately 25 km, by NASA. Since the data is provided with daily granularity, it cannot be used directly for generating hourly system parameters in the future. An example daily maximum temperature distribution provided by CMIP6 ACCESS-CM2 dataset can be seen in Figure 0.28.

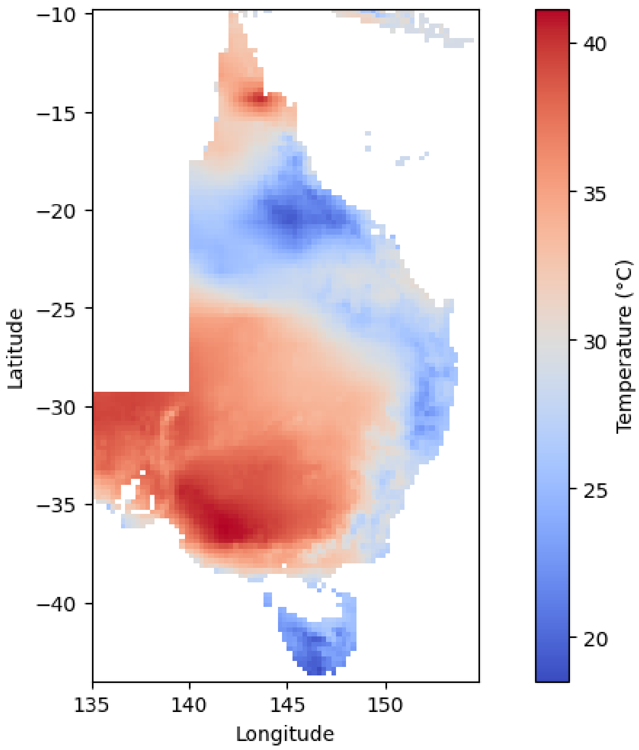

Figure 0.28: Forecasted ambient temperature from NASA CMIP6 ACCESS-CM2 with scenario SSP2-4.5.

The horizontal wind can be calculated using the eastward and northward components available on ERA5 data as follows:

$$v_{10} = \sqrt{v_{u,10}^2 + v_{v,10}^2} \tag{16}$$

where v_{10} denotes the horizontal wind speed at 10 m, while the $v_{u,10}$, and $v_{v,10}$ denote the eastward and northward components.

9.5.2 Transmission line assumptions and parameters

The derating of a transmission line is very sensitive with assumption of the characteristic of the cable. From equation (4), the correction factor of a transmission line is defined by $I_{DR,l,t}^{bot}$. This value is highly sensitive of transmission line used. The convective cooling P_C variable is also sensitive with wind direction across the lines, thus require line orientation data. Since those values are not available in the 2024 ISP, some assumptions are used. In this study, the wind direction is assumed to be always optimal direction for cooling, that is 90°. The relationship between wind speed, temperature, and line thermal correction factor across various spatio-temporal points is shown in Figure 0.29. The dashed line is based on the reference temperature and wind speed. We can clearly see that the main driver of transmission line derating is weak wind speed at the bottleneck point of the line during moderate to high ambient temperature.

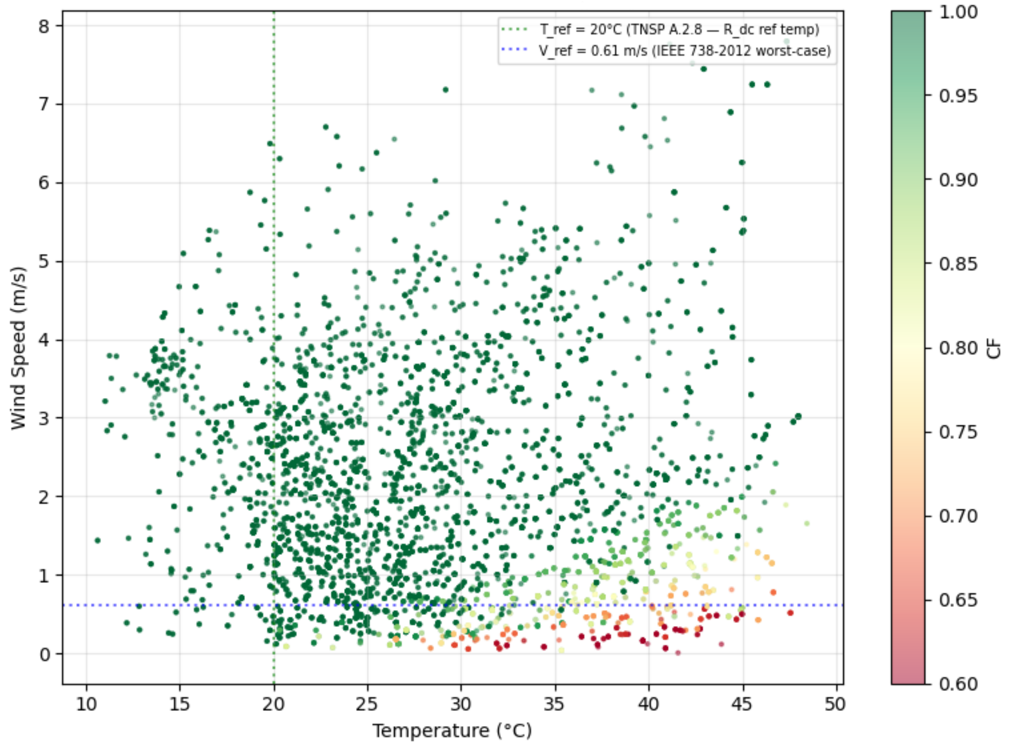

Figure 0.29: Relationship between wind speed, temperature, and line thermal correction factor across various spatio-temporal points. The green dots indicate a slight derating while red dotes indicate a more severe derating.

Following the document from NEM TNSPs, the line heat balance can be calculated by calculating each of the components, that is solar heat gain, wind convective cooling, radiative cooling, and line resistance.

The first component is solar heat gain. Since solar heat gain only exist during daylight, a solar altitude needs to be calculated. The solar altitude can be calculated as:

$$H_S = \sin^{-1}[\sin(\delta_s)\sin(\varphi) + \cos(\delta_s)\cos(\varphi)\cos(\omega_S)] \tag{17}$$

where H_S, δ_s, and ω_S denote the solar altitude, declination, and hour angle, respectively. The φ denotes the latitude coordinate of the line mesh point. The δ_s can be calculated using:

$$\delta_s = 23.45°\sin\left(360°\frac{284 + N}{365}\right) \tag{18}$$

where N denotes the day of year. The ω_S can be calculated using:

$$\omega_S = \omega_{SR} - 15°T_S \tag{19}$$

where the ω_{SR} and T_S denote the sunrise hour angle and solar time since sunrise. The ω_{SR} can be calculated using:

$$\omega_{SR} = \cos^{-1}[-\tan(\delta_s)\tan(\varphi)] \tag{20}$$

The T_S can be calculated using:

$$T_S = T_{actual} - \left(12 - \frac{\omega_{SR} + \lambda - 150°}{15} + 0.223\right) \tag{21}$$

The solar altitude is then can be used to approximate beam irradiance as:

$$I_{B0} = \frac{1280\sin(H_S)}{\sin(H_S) + 0.314} \tag{22}$$

where I_{B0} is the beam irradiance. Combined with solar altitude, the beam irradiance can be used to approximate diffuse irradiance as:

$$I_d = (570 - 0.47I_{B0})\big(\sin(H_S)\big)^{1.2} \tag{23}$$

The solar heat gain is then can be calculated using:

$$P_S = \alpha_s D\left[I_{B0}\left(\sin(\eta) + \frac{\pi F}{2}\sin(H_S)\right) + \frac{\pi}{2}I_d(1+F)\right] \tag{24}$$

where α_s and F denote solar absorptivity and albedo, where their values are set to 0.8 and 0.2, respectively. The D denotes line conductor. As stated in TNSP document, when conductor azimuth angle is not known or varies significantly along the line, the worst-case assumption is used, making the value of $\sin(\eta)$ equal to 1. Also following the document, equation regarding solar heat gain is computed internally from time and location, not using measured or forecasted solar irradiance to account the worst-case scenario of clear sky scenario. The line parameter D denotes the diameter of the transmission line, parametrised together with line parameters assumption.

The second component is wind convective cooling. Several steps are needed to calculate the convective cooling power. In this study, air thermal conductivity and kinematic viscosity at film temperature are approximated using:

$$\lambda_f = 2.42 \times 10^{-2} + 7.2 \times 10^{-5} T_f \tag{25}$$

$$\nu_f = 1.32 \times 10^{-5} + 9.5 \times 10^{-8} T_f \tag{26}$$

where λ_f and ν_f denote the air thermal conductivity and kinematic viscosity. The T_f denotes the film temperature. The film temperature is calculated using:

$$T_f = \frac{T_C + T_A}{2} \tag{27}$$

The Grashof number (Gr) in this study is calculated using:

$$Gr = \frac{D^3 g(T_C - T_A)}{(T_f + 273)\nu_f^2} \tag{28}$$

where g denotes the gravity. The T_C and T_A, denote the design conductor and ambient temperature.

The Prandtl number in this study is approximated as:

$$Pr = 0.715 - 2.5 \times 10^{-4} T_f \tag{29}$$

The natural-convection Nusselt number is calculated as:

$$Nu_{nat} = A(GrPr)^m \tag{30}$$

where A and m follows:

$$\begin{cases} A = 0.85, m = 0.188, & GrPr \leq 10^4 \\ A = 0.48, m = 0.250, & GrPr > 10^4 \end{cases} \tag{31}$$

The equivalent effective vertical component of wind-speed is then approximated using:

$$V_z = \frac{\nu_f}{D}\left(\frac{Nu_{nat}}{0.641}\right)^{1/0.471} \tag{32}$$

Combined with horizontal component of wind speed from climate and weather data, the effective wind speed can be calculated using:

$$V_{eff} = \sqrt{V^2 + V_z^2} \tag{33}$$

The effective wind angle (ϕ) and effective Reynolds number $\left(Re_{eff}\right)$ than can be calculated using:

$$\phi = \cos^{-1}\left(\frac{V\cos\psi}{V_{eff}}\right) \tag{34}$$

$$Re_{eff} = \frac{V_{eff} D}{\nu_f} \tag{35}$$

where ψ denotes the wind angle of attack. The convective cooling power is then can be calculated using

$$P_C = \pi \lambda_f (T_C - T_A) B \left(Re_{eff}\right)^n [0.42 + C(\sin\phi)^P] \tag{36}$$

Where the forced-convection coefficients (B, n) and wind-angle coefficients (C, P) are selected from:

$$\begin{cases} B = 0.641, n = 0.471, & Re_{eff} \leq 2650 \\ B = 0.048, n = 0.800, & Re_{eff} > 2650 \end{cases} \tag{37}$$

$$\begin{cases} C = 0.68, P = 1.08, & 0^\circ \leq \phi \leq 24^\circ \\ C = 0.58, P = 0.90, & 24^\circ < \phi \leq 90^\circ \end{cases} \tag{38}$$

Since the conductor span azimuth or direction is varied along the simplified 12 bus mode, the best-case assumption of the wind angle of attack of $\psi = 90^\circ$ is used, resulted on $\phi = 90$. This means that the convective cooling simplifies to:

$$P_C = \pi \lambda_f (T_C - T_A) B \left(Re_{eff}\right)^n \tag{39}$$

The third component is radiative cooling. For the radiative cooling, the temperature used is in Kelvin. The design conductor and ambient temperature in Kelvin can be calculated using:

$$T_{C,K} = T_C + 273.15 \quad (40)$$

$$T_{A,K} = T_A + 273.15 \quad (41)$$

The sky and daylight ground temperature in Kelvin can be approximated using:

$$T_{D,K} = 0.0552\left(T_{A,K}\right)^{1.5} \quad (42)$$

$$T_{G,K} = T_{A,K} + 5 \quad (43)$$

Then, the radiative cooling can be calculated using:

$$P_R = \pi D\sigma\varepsilon\left[\left(T_{C,K}\right)^4 - 0.5\left(T_{G,K}\right)^4 - 0.5\left(T_{D,K}\right)^4\right] \quad (44)$$

where ε denotes the conductor emissivity.

The fourth component is line resistance. The ac resistance can be approximated from a dc resistance. The dc resistance at the design conductor temperature is calculated as:

$$R_{dc} = R_{dc,20}[1 + \alpha_R(T_C - 20)] \quad (45)$$

where $R_{dc,20}$ denotes the dc resistance at 20 °C, while α_R denotes the resistance temperature coefficient. The skin effect is approximated using:

$$k_s = \sum_{i=0}^{4} a_i X^i \quad (46)$$

$$X = \sqrt{\frac{f}{R_{dc}}} \quad (47)$$

where f denotes the ac frequency. The ac resistance is then can be calculated using:

$$R_{ac} = \frac{R_{dc}k_s}{1000} \quad (48)$$

where the division by 1000 converts resistance from ohm/km to ohm/m to make the unit in the international system format.

From the equations defining the steady-state heat balance of the transmission line, it is evident that the results are highly sensitive to the assumptions and parameters. It should be stressed that the aim is not to replicate exactly how transmission line derating occurs in the NEM during extreme heatwaves, but to provide an example of how line parametrisation under heatwaves can be incorporated into a planning study. Regardless, the conductor thermal parameters used in this study, presented not as a gold standard but as an example, are provided in Table 0.8. For existing lines, the T_{ref} values used are the highest typical summer temperature at either end of the line, based on the 2024 ISP data.

Table 0.8: Conductor thermal parameters

Symbol	Description	Value

D	conductor diameter	0.02862 m
$R_{dc,20}$	dc resistance at 20 °C	0.0674 ohm/km
α_R	resistance temperature coefficient	0.00403 /°C
T_C	design conductor temperature	75 °C
ε	emissivity	0.8
α_s	solar absorptivity	0.8
V_{ref}	reference wind speed	0.61 m/s
T_{ref}	reference ambient temperature	20 °C

9.5.3 Thermal generators assumptions and parameters

In this study, assumptions based on geo-location data and generator name are used. The cooling water intake availability coefficient is then assumed to reflect abundant and robust water availability, with $\omega = 2$ corresponding to seawater cooling, for all generators with OLC system near a coastline. The thermal generator derating parameters for all generators used in this study can be seen in Table 0.9.

Table 0.9: Thermal generator derating parameters.

Cooling Group	T_{ref}	α	T_{health}	$\overline{T}_{\text{outlet}}$	$\Delta\overline{T}$	Name	Type
nOLC	25	0.32	10			Kogan Creek; Millmerran	Coal
nOLC	25	0.32	10			Bayswater; Callide B; Callide C; Loy Yang A; Loy Yang B; Mt Piper; Stanwell; Tarong; Tarong North; Yallourn W	Coal
OLC	25	0.35	15	35.0	10.0	Eraring; Gladstone; Vales Point B	Coal
nOLC	25	0.92	15			Angaston; Lonsdale; Mt Stuart; Port Lincoln GT; Port Stanvac 1; Snapper Point; Snuggery	Diesel
OLC	25	0.65	15	35.0	10.0	Newport; Torrens Island B	GFST
nOLC	15	0.92	15			Bairnsdale; Barcaldine; Barker Inlet; Bell Bay Three; Bolivar; Braemar; Braemar 2; Colongra; Dry Creek; Hallett; Jeeralang A; Jeeralang B; Kurri Kurri; Ladbroke Grove; Laverton North; Mintaro; Mortlake; Oakey; Quarantine; Roma; Smithfield; Somerton; Tallawarra B; Tamar Valley Peaking; Uranquinty; Valley Power	OCGT
nOLC	15	0.94	10			Darling Downs	CCGT
nOLC	15	0.94	10			Condamine A; Swanbank E	CCGT
OLC	15	0.97	15	35.0	10.0	Osborne; Pelican Point; Tallawarra; Tamar Valley CC; Townsville PS; Yarwun Cogen	CCGT

9.5.4 Wind turbine assumptions and parameters

In this study, the value of the wind parameters used can be seen in Table 0.10. These parameters are based on Vestas [170]. To account for dry adiabatic conditions that might occurs during extreme hot and dry days in the future, an ambient temperature adjustment of $\Delta T = -1.0$ °C around the nacelle is applied.

Table 0.10: Wind turbine thermal derating parameters.

Parameter	T_1	T_2	T_{stop}	α_2	α_3

Value	30 °C	40 °C	45 °C	-0.00909 /°C	-0.10909 /°C

9.5.5 Photovoltaic thermal assumptions and parameters

In this study, two types of solar generators are used with their parameters shown in Table 0.11. The grid-scale PV is modelled as single-axis tracker with tracker axis azimuth optimised for each site.

Table 0.11: Solar PV thermal parameters.

Group	U_0	U_1	T_{stc}	α	Albedo	Module/Axis Tilt	Module/Axis Azimuth
Grid-scale	25	6.84	25	-0.0024 /°C	0.20	0°	*
Rooftop	15	3.00	25	-0.0024 /°C	0.25	23°	0°

In this study, the effective wind speed hitting the module is calculated from horizontal wind speed as follows:

$$V = V_{10m}\left(\frac{2}{10}\right)^{0.16} \tag{49}$$

A.6 Operational details of resilience events

In the following, we show the system operation in the critical resilience event periods added as stressors to the 2040 system.

Figure 0.30 shows the system dispatch in South Australia in the critical two days, indicating the capacity constraint in the evening of the 8th of February, which may be relieved by additional investments into storage capacity or DER coordination.

Figure 0.31 displays the stored energy in all BESS storage units across the different VRE drought scenarios, including the scenario of doubled short-duration storage capacity.

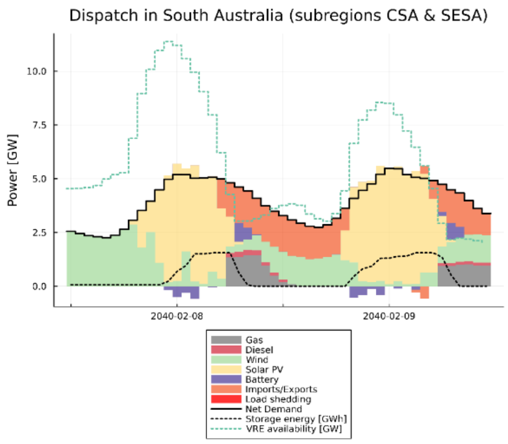

Figure 0.30: System dispatch of the two sub nodes in South-Australia with SchedNEM.jl across the most critical days under the heatwave event without outages. The most critical period is in the evening hours of the 8th of February, where the region is relying on imports and all available thermal generators.

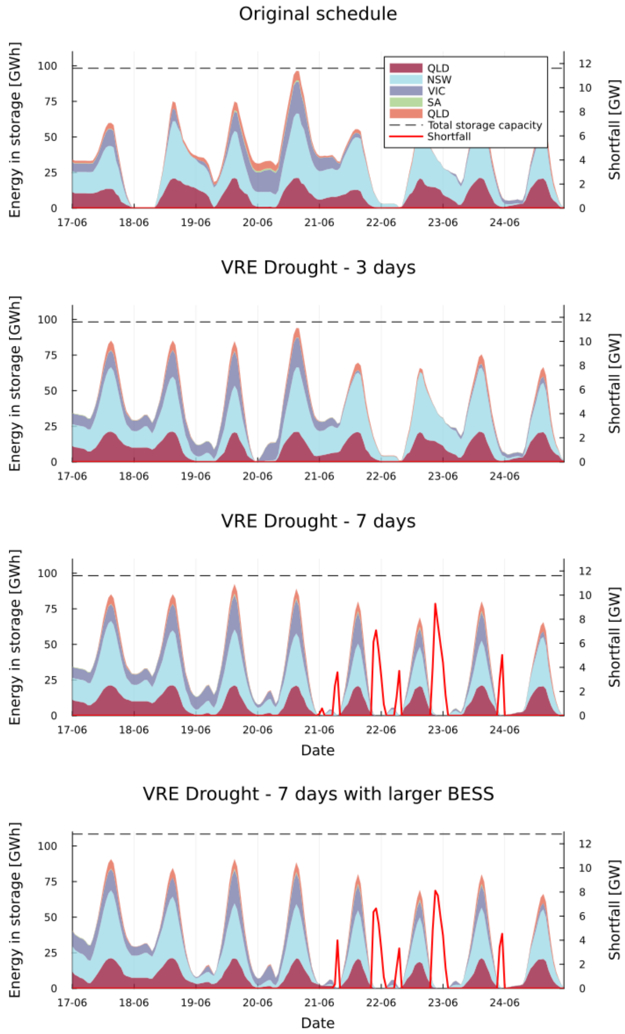

Figure 0.31: Stored energy schedule across all BESS and VPP units as scheduled by SchedNEM.jl with rolling horizon of 48h window and 24h timesteps, under the two extended VRE drought length events, as well as with increased short-duration BESS energy capacity.